The contractile properties of fibroblasts derived from Dupuytren's nodules and cords and the effects of TGF-β_1 stimulation.

Marcus Bisson MRCS

2003

A thesis submitted to the University of London

for the degree of

Doctor of Medicine (M.D.)

The RAFT Institute of Plastic Surgery

The Leopold Muller Building

Mount Vernon Hospital

Northwood

Middlesex

UK

&

The Tissue Repair & Engineering Centre

The Institute of Orthopaedics

The Royal National Orthopaedic Hospital

Stanmore

Middlesex

UK

BIBL.
LONDON.
UNIV.

UMI Number: U602858

UMI

Dissertation Publishing

UMI U602858

ProQuest

Abstract

Dupuytren's disease is a common fibroproliferative disorder with digital flexion deformities causing disability. Two forms are apparent clinically, nodules and cords.

Transforming growth factor beta-1 (TGF-β_1) has been implicated in Dupuytren's disease development. Myofibroblasts are prevalent in nodules and may be the source of cell-mediated contraction, which combined with matrix remodelling causes tissue shortening.

The hypothesis was that nodule and cord derived fibroblasts have differing contractile properties; have inherently altered tensional homeostasis and responses to mechanical stimuli.

It was found that nodule cultures contained significantly greater numbers of myofibroblasts, identified using immunohistochemical staining, than cord or carpal ligament.

A culture force monitor model was used to study the contractile properties of fibroblasts in culture. Mean peak force generated at 20hrs was significantly greater in nodule cells, than cord, whilst carpal ligament generated minimal force. There was a failure of force to plateau before 20hrs in Dupuytren's cells, possibly representing delayed tensional homeostasis.

Responses to increased tension were investigated by subjecting gels to four uniaxial overloads. Dupuytren's cells, particularly nodule fibroblasts, exhibited an unexpected increased contractile response to the first overload.

TGF-β_1 stimulation caused a significant upregulation of myofibroblasts in Dupuytren's cells to 25%; it also caused an increase in contraction profiles, with elevated mean 20hr force. Greatest stimulation occurred early in contraction, 2hr gradients increasing by 250 % in nodule fibroblasts.

After overloading greater contractile responses were observed in the first post-overload period and these persisted to subsequent overloads after TGF-β_1 stimulation. Flexion deformities in Dupuytren's disease occur due to shortening of the affected matrix. The abnormal contractile properties and altered tensional homeostasis in resident cells that we have found may be central to this. TGF-β_1 stimulation upregulated myofibroblast differentiation in Dupuytren's cells and exacerbated the abnormal contractile properties and responses to loading. Clinical relevance is discussed.

This thesis is dedicated to my wife.

Acknowledgements

Declaration of originality

I declare that the laboratory research for this thesis is original and that the ideas were developed in conjunction with my supervisor and advisors.

I performed the experiments myself with the guidance and technical assistance of the scientific staff at The RAFT Institute, Mount Vernon Hospital and the Tissue Repair and Engineering Centre, Stanmore.

Table of Contents

Common Abbreviations Used:

α-SMA	Alpha Smooth Muscle Actin
CFM	Culture Force Monitor
DMEM	Dulbecco's Modified Eagle Medium
DMSO	Dimethylesulphoxide
ECM	Extra Cellular Matrix
FCS	Foetal Calf Serum
FITC	Flourescein Iso-Thio-Cyanate
FPCL	Fibroblast Populated Collagen Lattice
NGM	Normal Growth Media (see appendix I for composition)
PBS	Phosphate Buffered Saline
PI	Propidium Iodide
TBS-T	Tris Buffered Saline with Tween(see appendix I for composition)
tCFM	Tensioning Culture Force Monitor
TGF-β_1	Transforming Growth Factor beta one

LIST OF FIGURES

CHPATER 3

Section 1

Section 2

Section 3

14

Section 4

Section 5

Section 6

Section 7

Section 9

CHAPTER 4

LIST OF TABLES

Thesis Introduction

This thesis will focus on the understanding of cellular events within diseased fascia in primary Dupuytren's disease, which lead to clinically problematic flexion contractures. A second aspect of this study will be the differentiation between the cellular properties of nodules and cords in primary Dupuytren's disease.

Hypothesis:

It is hypothesised that in Dupuytren's disease the fibroblasts have different characteristics from normal fibroblasts and the physical shortening of fascial tissue fabric is a result of the complex interaction between:

a) Upregulation of myofibroblast phenotype

b) TGF-β_1 stimulation (a profibrotic cytokine) and

c) Mechanical forces that result in altered cell mediated contraction and subsequent matrix shortening.

The literature review begins with a general appraisal of Dupuytren's disease, examining the history, epidemiology and proposed aetiological factors as well as the surgical anatomy and current therapeutic options. Subsequently an evaluation of literature specific to the focus of the thesis is undertaken, concentrating on current theories of contracture formation, cell mediated contraction, tensional homeostasis and factors that influence these processes. The currently published differences between nodules and cords will also be presented.

In order to tackle the overall hypothesis of contracture formation, a series of experiments have been conducted in order to answer specific questions. It was important that only primary cases were chosen to exclude any influence of prior surgery.

Primary Dupuytren's tissue was divided into regions of nodule and cord, from which specific cell cultures were established.

- Does the myofibroblast phenotype and the differences encountered between nodules and cords in tissue, persist into fibroblast cultures? This justifies the subsequent use of specific nodule and cord cultures in investigating responses to TGF-β_1 stimulation and the contractile properties. **Chapters 3.1, 3.2 and 3.3.**

- Do Dupuytren's fibroblasts display enhanced contractility, and, are there contractile differences between nodule and cord fibroblasts? **Chapter 3.4**

- Are fibroblast responses to mechanical stimulation altered in Dupuytren's disease? **Chapter 3.5**

- Does the pro-fibrotic growth factor, TGF-β_1, up-regulate both myofibroblastic phenotype and matrix contraction in either nodule fibroblasts or cord fibroblasts or both? **Chapters 3.6, 3.7.**

- Does TGF-β_1 act in synergy with mechanical stimulation to cause exacerbation of abnormal cellular responses? **Chapter 3.8.**

At each stage experimental comparisons will be drawn with fibroblasts from non-Dupuytren's disease tissue but of a similar, upper limb, fascial origin.

Discussion will centre around the observed differences between the properties of nodule and cord fibroblasts and the way in which altered contractile properties might lead to a propensity for the Dupuytren's fibroblasts to effect an excessive shortening of the 3D matrix. This would have direct implications clinically for the mechanism of fascial tissue fabric shortening, and thus generation of contractures.

Additionally an explanation for the high rates of recurrence following corrective surgery for Dupuytren's contracture will be proposed and possible reasons why the continuous elongation techniques for contracture correction result in rapid recurrence if not accompanied by fasciectomy.

Chapter 1

Review of the Literature

Chapter 1
Review of the Literature

1   Dupuytren's Disease

1.1   The History of Dupuytren's Disease

Thickening of the palmar fascia of the hand which progresses to cause digital contraction is most often referred to by its eponymous name, Dupuytren's disease gained from the remarkable nineteenth century French surgeon Baron Gauillaume Dupuytren. He presented a case of the disease at what has now become a famous lecture in 1831, however this was not the earliest description of the condition by several centuries.

Felix Plater a Swiss surgeon from Basel wrote of an affliction to a stone mason's hand in 1614 where the ring and little fingers had become contracted. Referring to the tendons he wrote, *"They contracted and in so doing were loosed from the bonds by which they are held and became raised up, as two cords forming a ridge under the skin. These two fingers will remain contracted and drawn forever."* It can be seen that Plater believed the condition to be one of the flexor tendons rather than the more superficially situated fascia, however this description is thought to be the earliest record in the surgical literature of Dupuytren's disease (Elliot, 1988).

The disease was no doubt present in the population well before this and people have postulated that the "Papal Hand of Benediction" seen in early Christian imagery was adopted because one of the Popes of the time suffered with Dupuytren's contracture. It is unlikely that a single pope would be influential enough to spread such symbolism related to a condition of his own hand and this gesture probably originated even earlier in history, as a Roman sign (Elliot, 1999).

The true anatomical nature of Dupuytren's disease was elucidated by Henry Cline senior, who dissected two hands affected by the condition in 1777 (the year of Dupuytren's birth). It was clear to him that the cause of the observed contractures was thickening and shortening of the palmar fascial fibres and, furthermore, that division of these allowed immediate return of extension. Cline lectured with Sir Astley Cooper in

23

London and Cooper continued this practice with Henry Cline junior when his father retired. They continued to describe the anatomy of the disease and it's treatment by palmar fasciotomy in the early part of the nineteenth century.

Baron Gauillaume Dupuytren was chief surgeon at the Hotel Dieu in Paris. He was considered the greatest surgeon in France by many at that time and was indeed surgeon to both Louis XVIII and Charles X. He was referred a patient with the disease in 1831 from a neighbouring hospital and following successful treatment by palmar fasciotomy he went on and delivered his lecture in December of that year. Using a patient with the condition and anatomical specimens he described the morphology, history, clinical signs and differential diagnosis before proceeding to perform his method of open fasciectomy. The lecture was reported verbatim in the French medical press at the time and repeated several times over the ensuing years. Despite much debate and some criticism Dupuytren's name stuck such that the condition bears it to this day.

1.2 Epidemiology of Dupuytren's Disease

A number of population studies have been carried out to determine the prevalence of Dupuytren's disease with significant variations between geographical locations and native ethnicity. Mikkelson (1972) found the overall prevalence in Norwegian men to be 9.4% and in women 2.8%, with the disease being bilateral in 59% and 43% respectively. There was a large increase in prevalence starting from the fifth decade in life in men and from the mid-sixties in women. By the eighth decade the ratio of men to women with the disease had fallen to 1:2 (Mikkelson, 1990). Gudmundsson et al (2000) studying a sample of the Reykjavik population found a similar pattern (overall prevalence 19.2% in men, 4.4% in women), whilst in the United Kingdom, Early (1962) found the prevalence in men to be 4.2% and in women 1.4%. In a group of nursing home residents in Scotland, Lennox (1993) found the disease in 21% of women and 39% of men over sixty years of age, whilst Carson and Clarke (1997) found an incidence of 13.75% of elderly ex-service men.

There are also well-documented cases in blacks, Indians, Asians and Japanese (Yost, 1955, Su, 1970, Zaworski, 1979, Haeseker 1981 and Mitra and Goldstein 1994, Gonzalez et al, 1998, Egawa et al, 1990, Srivastava et al, 1989).

1.3 Aetiology of Dupuytren's Disease

Since Baron Dupuytren and others noted the disease in "laborious people" many apparent associations and related factors have been proposed although the underlying cause of Dupuytren's disease remains unclear. It is likely a combination of such factors or events is ultimately responsible for disease development.

1.3.1 Alcohol

Several studies have been undertaken in an attempt to confirm the classic association of alcohol and Dupuytren's disease. Both Wolfe *et al* (1956) and Atalli *et al* (1987) found a higher incidence of Dupuytren's disease in alcoholics than in controls. Other studies however (Rafter *et al* 1980, Houghton *et al* 1983) found no statistically significant increase in alcoholism in patients with Dupuytren's disease and opinion remains divided on the importance of this as an aetiological factor.

1.3.2 Genetics

In view of the observed racial variations in Dupuytren's disease it would be unsurprising for there to be a genetic basis to the condition. Ling (1963) suggested the disorder was autosomal dominant and that there was variable penetrance, whilst others have also suggested an autosomal dominant mode of inheritance (Reviewed by Burge, 1999). It may merely be the case that a genetic predisposition is inherited with a multitude of other environmental or patient factors combining to manifest the disease (Ragoowansi *et al*, 2001).

1.3.3 Smoking

The association between smoking and Dupuytren's contracture is often blurred by the common coexistence of alcohol intake, however Burge *et al* (1997) found a strong link with smoking and a more modest association to alcohol intake. An *et al* (1988), in contrast to an earlier study by Fraser-Moodie (1976), demonstrated a significant difference in the smoking habits of patients operated on for Dupuytren's disease compared with controls.

1.3.4 Convulsive Disorders

The link between Dupuytren's disease and epilepsy was first reported in 1941 by Lund and subsequently supported by Skoog (1948) and Early (1962), who in addition found a higher increase in Dupuytren's disease in those with severe epilepsy. More recently Arafa *et al* (1992) found an increase in the incidence of Dupuytren's disease in epileptic patients compared with a control group, however this only reached significance in those over the age of 50.

1.3.5 Diabetes

Several studies have demonstrated an increased prevalence of Dupuytren's disease in diabetic patients (Machtey, 1997; Larkin and Frier, 1986; Heathcote *et al*, 1981; Arkkila, 1996) one group finding a rate of 43% in diabetics compared with 18% in the controls (Noble *et al*, 1984). One study has also correlated diabetic retinopathy with Dupuytren's suggesting a combined role of the microangiopathy as a causative factor (Pal *et al*, 1987).

1.3.6 Occupation

Early surgeons investigating and describing Dupuytren's disease often came across the condition in manual workers; indeed Skoog (1963) has suggested micro-ruptures of the palmar fascial fibres following repeated minor trauma as a possible aetiology. A recent epidemiological study by Gudmundsson *et al* (2000) found the disease to be more common in men with occupations where they worked primarily with their hands and often outdoors. Other studies have strongly refuted the theory that occupation type itself is causative. Early (1962) found no difference in the prevalence of Dupuytren's disease between two groups of workers at a single factory, one group being manual workers the other office staff. Furthermore no increase in Dupuytren's has been demonstrated in professional sportsmen who experience repeated significant stresses over the course of their careers (McFarlane, 1991). Currently there is no accepted link between Dupuytren's disease and occupation; indeed the sudden cessation of activity is thought to be more significant by one author (Heuston, 1962).

1.3.7 Injury

Whilst occupation is considered not to be associated with the onset of Dupuytren's disease the effect of a single injury is more contentious. Many cases of the condition have been reported to occur after a single insult ranging from forearm fractures (Stewart *et al*, 1985) to direct local trauma (Gordon and Anderson, 1961; Clarkson, 1961). McFarlane and Shum (1990) reviewed 309 patients of whom a close association could be made with a single insult in 6%. They pointed out, that the delineation needs to be made between Dupuytren's disease and scar tissue. They conclude that single insults may occasionally lead to Dupuytren's or progression of existing disease but it is likely this is in predisposed individuals and it is impossible to conclude a causal relationship unless relatively young.

1.3.8 Rheumatoid Arthritis

Arafa *et al* (1984) found a significantly lower incidence of Dupuytren's in the rheumatoid patients. The reason for this is not clear, however arthritis treatment such as steroids was one postulated cause.

1.4 The Morphology of Dupuytren's Disease

1.4.1 Histology

The microscopic appearances of Dupuytren's disease were described by Meyerding *et al* in 1941. They noted the highly cellular areas within active nodules as well as a relative decrease in adipose tissue and adnexal structures. There was an increase in capillaries and lymphocytic infiltration. Luck proposed a classification of the disease in 1959 based on the histological appearance of the disease and its activity and related this to his surgical intervention. He divided the disease into three stages. **Proliferative** was characterised by the active fibrous nodule where the lesion was highly cellular but arranged in a disorganised fashion. The collagen content was low. The **involutional** phase tissue was also cellular but the fibroblasts were beginning to align themselves, presumably in response to tensional forces, and more collagen was also being laid down along these axes. Finally the **residual** stage is characterised by highly organised, virtually acellular dense connective tissue. Luck postulated that diseased tissue would

begin as a nodule and progress through all three stages before leaving only fibrous cords.

1.4.2 <u>Surgical Anatomy</u>

The abnormal tissue that develops in Dupuytren's disease does so from defined anatomical structures that together make up the palmar and digital fascia. The non-diseased fascia is believed to have a functional role despite some authors' view that it is a vestigial structure (Reviewed by Caughell and McFarlane in Dupuytren's Disease, 1990). It supports the palmar skin, protecting against shearing and compressive forces as well as retaining the deeper structures and the bony framework of the hand. The normal anatomy is shown in fig. 1.1 and has both a longitudinal and transverse component. As the digit is reached aggregations of fascial fibres condense to form defined "ligaments" or bands (fig. 1.2). In the diseased state thickening, hypertrophy, shortening and merging of these bands lead to pathological cords with intervening nodules (fig. 1.3). The pattern of these cords and their origin from normal bands has been studied by several authors (McFarlane, 1974; McGrouther, 1982; Rayan, 1999). The cords displace nearby tissues and lead to specific joint contractures depending on their position. Table 1.1 summarises the effects and origin of diseased cords.

Natatory Ligament

Adipose tissue in Triangular Space

Pretendinous bands

Palmaris Longus Tendon

Distal Commisural Ligament from 1st Web Space

Proximal Transverse Palmar Ligament

Proximal Commisural Ligament from 1st Web Space

Palmar Cutaneous Branch of Median N.

Insertion of Abductor Pollicis Brevis
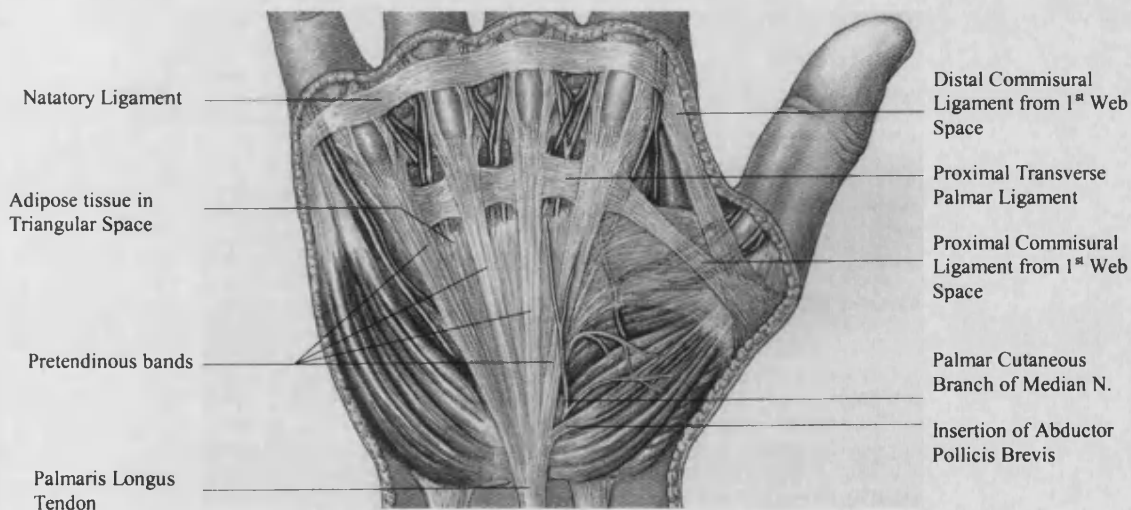
Figure 1.1. The Normal Anatomy of the Palmar Fascia. Transverse and longitudinal Aggregations of the normal palmar fascia are labelled. (Adapted from Anatomy by Tubiana, in Dupuytren's Disease, 2000)

Diseased Cord	Band of Origin	Effect
Pretendinous cord	Pretendinous band	MCPJ contracture
Central cord	Central fibrofatty tissues	PIPJ contracture
Lateral cord	Lateral digital sheet	DIPJ contracture
Spiral cord	Grayson's ligament, Clelands ligament , Lateral digital sheet, Pretendinous band	MCPJ contracture PIPJ contracture Displacement of neurovascular bundle
Natatory cord	Natatory ligament	Decreased abduction

Table 1.1. The pathological cords encountered in Dupuytren's disease, their normal anatomical origin and their primary effect.
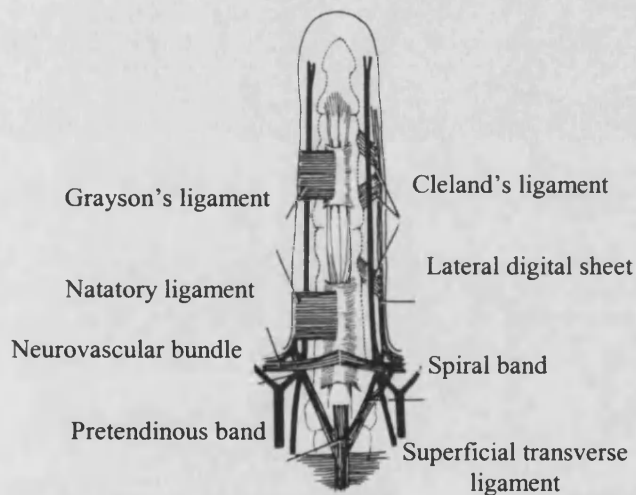
Figure 1.2. The Normal Anatomy of the Distal Palmar and Digital Fascia.
The structural elements of the normal fascial complex that become involved in Dupuytren's disease are labelled.
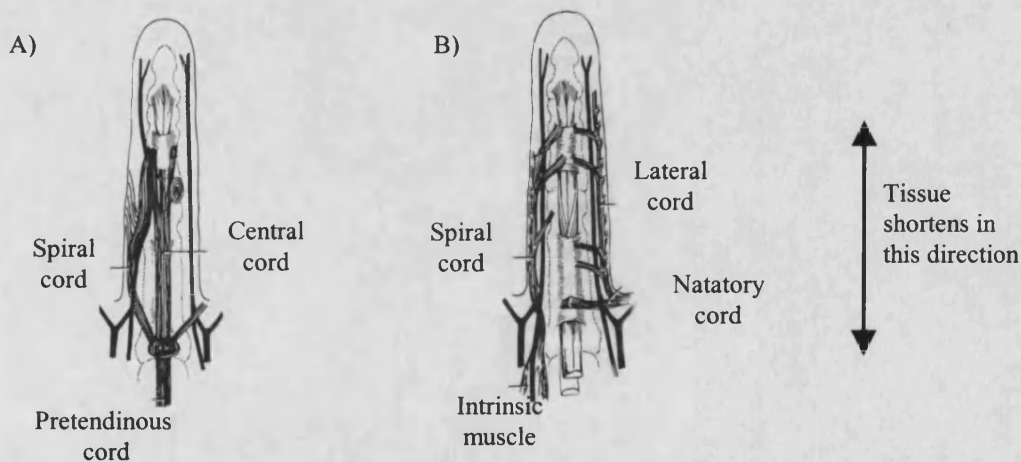
Figure 1.3. The Anatomy of the Pathological Cords That Develop in Dupuytren's Disease. A) Diseased fascia associated with pretendinous cords. B) Diseased fascia not associated with pretendinous cords. Taken from McFarlane (1974).

A detailed knowledge of the pathological anatomy and its variations prepares the surgeon when operating to both achieve his goal of removing affected fascia in order to straighten the digit and avoid damage to structures such as digital nerves and arteries which become intimately bound and displaced within the fibrous tissue.

1.5 Treatment of Dupuytren's Contracture of the Hand

Advances in the understanding of cellular processes involved in Dupuytren's disease have as yet failed to translate into new therapeutic options for Dupuytren's disease. Currently the mainstay of treatment remains surgery, however over the last several decades the results of surgery have improved, with less complications and better functional outcomes (Jabaley, 1999).

1.5.1 <u>Surgical Treatment</u>

Surgical **fasciotomy,** first described by Cline and then Dupuytren (Elliot, 1999), is still performed in selected cases, for example elderly patients with cords causing metacarpolphalangeal joint contractures. Bryan and Ghorbal (1988) reported it to be useful for initial correction at this joint but that this correction was unlikely to be maintained in the long term.

Fasciectomy comprises of varying degrees of resection of the Dupuytren's tissue. Segmental aponeurectomy (Moermans, 1991; Andrew and Kay, 1991) achieves a similar result to fasciotomy, whilst limited or regional fasciectomy removes the macroscopically abnormal fascial tissue. Radical fasciectomy where the resection extends into normal fascia in an attempt to limit recurrence or extension is no longer in favour.

Irrespective of the degree of resection the disease cannot be cured, with extension and recurrence being commonplace. **The aim of surgery, therefore, is to correct the deformity with the least complications and best chance of avoiding recurrence.** Recurrence appears to increase with time elapsed since surgery. In Mantero *et al*'s series from 1983 of 600 patients (Reveiwed by Leclercq, Results of Surgical Treatment in Dupuytren's Disease 2000) there was a 43% recurrence rate between the third and fifth post-operative years, but this rose to 77% in those patients who were followed for up to 30 years. Leclercq's own review of a series of Tubiana's patients confirmed this

pattern with a final value of 66% in those followed for more than ten years. Norotte *et al* (1988) similarly reported a 71% recurrence rate whilst Adam and Loynes (1992) found a lower rate of recurrence of 34% although the mean follow up was only 3.4 years. The open palm technique described by McCash (1964) also failed to provide superior results despite less early complications, with Schneider *et al* (1986) experiencing a 32% recurrence and 48% extension rate at 5 years following this technique.

The only procedure that has consistently shown improved results in terms of recurrence is **dermofasciectomy** and full thickness skin grafting of the defect (Leclercq, C., Recurrent Dupuytren's Disease, Presentation at British Society for Surgery of the Hand Meeting Nov 2002). Hueston first noted reduction of recurrence beneath Wolfe grafts in 1962 (Hueston, 1962) and went on to apply this technique for treatment of recurrent disease (Hueston, 1984). Others have found recurrence beneath grafts to be very infrequent (Brotherstone *et al*, 1994, Kelly and Varian, 1992) and Hueston now recommends dermofasciectomy as the primary procedure for younger patients with a strong diathesis (1985) although this does not prevent extension of disease in adjacent areas.

1.5.2 Splinting

Splinting of Dupuytren's contractures has been employed for centuries however James and Tubiana stated in 1952 (quoted by Leclercq, Hurst and Badalamente in Dupuytren's Disease 2000) that when applied discontinuously splints are ineffective. In this respect to prevent contracture progression a patient would be required to wear a permanent splint, itself an unacceptable impairment. As such it is generally accepted that pre-operative splinting alone is not useful in the management of Dupuytren's disease (Abbott *et al*, 1987).

Messina and Messina (1993) have however introduced the concept of continuous elongation of the Dupuytren's contracture as an adjunct prior to surgical intervention. They apply a bony fixed continuous elongation device (TEC), which can be gradually lengthened at 2mm per day to straighten severely flexed digits. Initial results of this technique have been encouraging (Citron and Messina, 1998) however it is reported that once traction is removed recurrence of contracture deformities is very rapid if

fasciectomy is not performed. Examination of the stretched fascia by light and electron microscopy revealed uniform orientation of collagen fibrils (Brandes *et al*, 1994) and biochemical evaluation of the tissue by Bailey *et al* (1994) revealed an increase in MMP levels, explaining the apparent remodeling without fiber rupture.

Other authors have now begun to adopt this technique, or modifications of it, to facilitate surgery in patients with severe contractures (Hodgkinson, 1994).

1.5.3 Other Non Surgical Treatments

Many non-operative treatment modalities have been attempted to halt or reverse Dupuytren's disease but with variable and often limited short-term value. Local radiotherapy for Dupuytren's disease was used by Keilholz *et al* (1996) with some success. Another study however by Weinzierl *et al* (1993) demonstrated no difference in the disease natural history after 7 years. In view of this and the potential side effects of radiotherapy in what is a benign disease, this treatment modality has not gained acceptance.

Weinzierl *et al* (1993) also looked at the 3-year results of treatment with DMSO, which again failed to alter the course of Dupuytren's disease. Similarly vitamin E was found to be ineffective (Richard, 1952).

Steroids have been employed with variable success (Reviewed by Leclercq, Hurst and Badalamente in Dupuytren's Disease 2000), Ketchum (1983) reporting resolution of nodules following intralesional triamcinolone injection. Meek *et al* (1999) proposed that this useful action of steroids was due to their anti-inflammatory role.

Enzymatic fasciotomy is currently on trial as a therapeutic option in the USA (Badalamente and Hurst, 2000), although degradation of collagen using pharmacological agents such as trypsin or pepsin has been proposed for some time (Reviewed by Leclercq, Hurst and Badalamente in Dupuytren's Disease, 2000).

1.6 Clinical Picture

Dupuytren's disease often presents as a small firm swelling within the palm of the hand or base of a finger, although the pattern is very variable (Skoog, 1963; McFarlane, 1991; Leclercq, 2000 in Dupuytren's Disease). This early "nodule" can remain static for several years, or progress rapidly, the reason for differences in behaviour being unclear. Clinically Dupuytren's diseased tissue can be divided into nodules or cords (Rayan, 1999), which as described above, broadly correspond to the histological stages of Dupuytren's disease. As described above (section 1.4.1) Luck proposed that nodules were the early active lesions with disease progressing and eventually burning out when nodules became replaced or degenerated into more quiescent cords. This natural history of Dupuytren's disease is currently favoured by many authors (Rayan, 1999) and it follows that there could be crucial differences in the characteristics and behaviour of cells from these two regions which may influence our understanding and future treatment of the condition.

One of the key aspects of this thesis was to study any differences between the characteristics of cells derived specifically from Dupuytren's nodules or Dupuytren's cords. This has been a relatively untapped avenue of research with some investigators looking at "Dupuytren's disease" tissue as a whole, making no differentiation between cords and nodules, or, more frequently simply concentrating on nodules.

It is not usually the presence of diseased tissue, which causes problems for the patient, although large nodules can be uncomfortable; however with disease progression flexion deformities of the digits occur. It is these flexion deformities, or contractures, which can cause significant disability for patients. Despite the large amount of research that has been undertaken into Dupuytren's disease and advances in the cell and molecular biology of this condition the actual mechanism by which contractures occur remains unclear (Kloen, 1999). Currently it is believed that the diseased tissue physically shortens (Brickley-Parsons, 1981) rather than folding or actually contracting (by matrix elements sliding along one another). It is proposed that this shortening results from a combination of two processes (Reviewed by Glimcher and Peabody, Collagen organization in Dupuytren's Disease, 1990) with nodules and cords together forming a "contractile unit".

Firstly

Cell mediated contraction of the matrix.

> Resident diseased fibroblasts, possibly those with a contractile phenotype (myofibroblasts), pull on the matrix that they are attached to causing it to shorten.

And Secondly

Continuous Matrix Remodelling.

> The extra cellular matrix of most tissues undergoes constant turnover, however this remodelling may be increased in Dupuytren's disease and thus it could fix the matrix in the shortened state brought about by cell mediated contraction (Reviewed by Flint and Poole, Contraction and contracture in Dupuytren's Disease, 1990).

Neither process alone could bring about sufficient changes to induce macroscopic tissue shortening, however by a continuous cycling of the two processes it can be seen that a minute step wise shortening of the diseased tissue could be achieved. This fixed shortened tissue on the volar aspect of a digit prevents full extension of the finger and hence the flexion deformities.

In addition to cellular differences between nodules and cords, this thesis concentrates on the cell mediated contraction aspect of Dupuytren's disease. The contractile cell phenotype (the myofibroblast), has been studied, as has the mechanism of contraction using a collagen lattice contraction model, and finally the role of a specific growth factor, TGF-β_1, thought to be involved in fibrosis.

1.7   The Myofibroblast.

In 1971 Gabbiani *et al* described a specialized type of fibroblast within granulation tissue. This had many features in common with smooth muscle cells both at the light and electron microscopic level. They proposed its role in the contraction observed in wound healing. Subsequently Gabbiani and Majno (1972) showed that cells found in nodules from Dupuytren's Disease were phenotypically similar and so hypothesized that this cell, the myofibroblast, was responsible for the tissue contraction leading to the

contractures seen in Dupuytren's. Myofibroblasts have also been identified in Peyronie's disease and contracted breast capsule tissue with Ariyan, *et al* (1978) proposing that this cell was the common denominator in all fibrocontractive disorders.

It has been shown that alpha smooth muscle actin (α-SMA) is present in the myofibroblast as opposed to normal fibroblasts and this can be detected by immunohistochemistry (Skalli *et al*, 1986, Schurch *et al*. 1984, Foo *et al*. 1992). Using these techniques myofibroblasts have been confirmed in Dupuytren's tissue and also a difference noted in their relative proportions in the three stages of the disease. Luck (1959) divided the disease into proliferative, involutional and residual phases and the myofibroblast appears more prominent in the proliferative nodule phase (Tomasek et al. 1995). Myofibroblasts were not demonstrated in Dupuytren's cord tissue by VandeBerg et al (1982) or Badalamente *et al* (1983), whilst Pasquali-Ronchetti *et al*, (1993) found a few myofibroblast phenotype cells in a single cord sample. In this respect there are similarities with wound healing where myofibroblasts are numerous in the hypercellular granulation tissue but disappear in the maturing scar tissue (Darby *et al*. 1990).

There has been much debate over the actual origin of the myofibroblast. Suggestions have included differentiation from fibroblasts, smooth muscle cells or vascular endothelial cells. Rayan *et al* (1994) showed that when grown in culture normal palmar fibroblasts developed stress fibres akin to the actin microfilaments seen in myofibroblasts. Myofibroblasts with α-smooth muscle actin positive intracellular fibres can also be induced in normal cultured fibroblasts by TGF-β (Desmouliere *et al*, 1993). Detailed cytoskeletal investigation has shown certain cells stain for limited types of intermediate cytoskeletal proteins. These appear to be involved in cellular architecture rather than generating forces. Fibroblasts express vimentin, whereas smooth muscle cells express either only vimentin or vimentin and desmin. Like granulation tissue myofibroblasts, the majority from Dupuytren's tissue express only vimentin, however in some patients there is expression of both (Schurch *et al*. 1990). From the above it seems likely that the majority of Dupuytren myofibroblasts originate from transformed fibroblasts.

A comprehensive review by Tomasek *et al* (2002) suggests that fibroblasts, given an appropriate stimulus, differentiate first into protomyofiboblasts that demonstrate intracellular stress fibres. Subsequently, differentiated myofibroblasts develop, characterised by the presence of α-SMA intracellular microfilaments. It may require combined stimuli such as a stiff matrix and TGF-β to maximally induce α-SMA (Arora *et al*, 1999). **This is a particularly important point in relation to the work that has been carried out here where not only have myofibroblasts been under investigation but stimulation with both external loading and TGF-β has been studied.**

1.8 The Extracellular Matrix

Cells exist within a complex three-dimensional environment, the extracellular matrix, which provides support, protection and a means of interconnection. It consists of a network of connective tissue fibres such as collagen and elastin contained within a ground substance of various macromolecular proteins, proteoglycans and hyaluronates. The composition varies depending on tissue type and in certain disease processes. The extracellular matrix is a dynamic milieu, thought to be in constant turnover even within such apparently stable tissues such as bone and cartilage (Flint and Poole, 1990 in Dupuytren's Disease). This is controlled by the cells within the matrix, which are responsible for production of the constituent parts as well as enzymes, the matrix metalloproteinases (MMPs) that act to break it down.

1.8.1 Collagen

Collagen comprises a large percentage of the extra cellular protein and currently more than 19 collagen molecules have been formally identified. Type I collagen is the most prevalent and ubiquitous (Prockop & Kivirikko, 1995) and is the major fibrillar collagen forming highly stable and mechanically strong collagen fibres.

Collagens are synthesised primarily by fibroblasts and myofibroblasts in the same way as other proteins, via transcription of the DNA into mRNA and the translation of this by ribosomes into protein (reviewed by Kivirikko, 1993).

Collagen amount is regulated by a number of factors, which together form a balance between production and breakdown. Proliferation of the fibroblast or myofibroblast population can cause an increased synthesis, thus factors such as TGF-β can have a fibrotic effect. Collagens are degraded by one of two mechanisms, either an intracellular pathway which degrades procollagen, or an extracellular process, which is mediated by the MMPs.

1.8.2 The Extracellular Matrix in Dupuytren's Disease

There have been specific biochemical changes identified in the extracellular matrix of Dupuytren's disease tissue. Brickley-Parsons *et al* (1981) using a number of techniques compared collagen characteristics in the diseased fascia and non-diseased fascia of patients with Dupuytren's disease and fascia from patients free of Dupuytren's. They demonstrated a significantly increased level of total collagen as well as increased hydroxylysine content and an increase in the number of reducible cross-links. Collagen type III, virtually absent in normal palmar fascia, was seen to comprise up to 40% of total collagen in diseased tissue. These changes are very similar to collagen characteristics encountered in embryos, healing wounds or newly synthesized collagens. The investigators hypothesized that this was due to a reparative response in the diseased tissue resulting from an increased turnover of collagen. They proposed that the shortening of contracted tissue was a result not of collagen folding or pleating but continuous remodeling, leaving a shorter section of matrix. Other studies have also demonstrated an increased type III collagen content using a range of techniques (Bailey *et al*, 1977, Bazin *et al*, 1980, Gelberman *et al*, 1980 and Menzel *et al*, 1979). Murrell *et al* (1991) confirmed this increased type III/I collagen ratio in cell cultures, proposing this to be a function of cell density not cell type, as Dupuytren's and control fibroblasts behaved similarly. This is in contrast to other studies where total collagen production was greater in Dupuytren's cells than controls (Delbruck and Schroder, 1983), which is of significance, by demonstrating that cellular differences observed in tissue are maintained in tissue culture. This was also established by previous studies in our laboratory (Bulstrode, N., MD Thesis, 2001).

Changes in other constituents of the extra cellular matrix have been reviewed by Delbruck and Gurr (in Dupuytren's Disease, Biology and treatment, 1990). There is an increase in overall glycosaminoglycan content in palmar fascia, occurring in a stepwise manner from apparently normal fascia to fascia adjacent to bands and nodules, to bands and finally greatest amounts in nodules. Dermatan sulphate and chondroitin sulphate are the main contributors to the increase. Water content is elevated in Dupuytren's tissue (Bazin et al, 1980) however another glycosaminoglycan, hyaluronate, is found in smaller amounts than normal palmar fascia (Flint et al, 1982).

Several of these studies (Bazin et al, 1980, Brickley-Parsons et al, 1981) have demonstrated that the characteristic changes in the extracellular matrix outlined above also occur in apparently uninvolved fascia of patients with Dupuytren's disease, all be it to a lesser extent. This suggests the condition may result from a global change within the palmar fascia and explains the often multifocal and recurrent nature of the disease.

Few studies have looked at the role of MMPs in Dupuytren's disease. Tarlton et al (1998) correlated increases in MMP 2 levels with the load applied to fresh tissue strips. Subsequently Prajapati et al (2000) demonstrated complex changes in MMP activity after cyclical loading regimens applied to dermal fibroblasts in a culture force monitor model

1.9 Growth Factors

There are many growth factors and cytokines produced both locally and from the general circulation that have possible roles in Dupuytren's disease either by stimulation of cellular proliferation, contraction or production of extracellular matrix. Many of these have been studied by observing their effects on Dupuytren's fibroblasts in vitro, either as monolayer cultures or in fibroblast populated collagen lattices.

Platelet derived growth factor (PDGF) has been studied in Dupuytren's disease by Badalamente et al (1992). They found co-localisation of this with myofibroblasts in the densely cellular areas corresponding to proliferative and involutional stages of the disease. They hypothesized that this finding was consistent with many of the known actions of PDGF, such as increased protein synthesis and reorganisation of cytoskeletal

components, leading to its possible role in the aetiology of Dupuytrens disease. The same group of workers (Badalamente *et al*, 1988) have also localised the vasoactive prostaglandins, PGE_2 and $PGF_{2\alpha}$ to myofibroblasts in sections of Dupuytren's nodule, hypothesising that they play a role in cell contractility.

The effects of interferon-α_{2b} (INF-α_{2b}) on fibroblast populated collagen lattices have been investigated by Sanders *et al* (1999). This anti-fibrogenic cytokine produced by leukocytes lead to a significant reduction in the contraction of FPCLs using both control palmar fascia and Dupuytren's fibroblasts.

Alioto *et al* (1994) studied a panel of growth factors and their effect on proliferation and protein synthesis in Dupuytren's and normal palmar fascia fibroblasts. Basic fibroblast growth factor (bFGF) and PDGF were both found to stimulate fibroblast proliferation in Dupuytren's and control cells. TGF-β_1 had no significant effects, however, it was a powerful stimulator of both collagen and non-collagen synthesis.

Dupuytren's fibroblasts have been found to express b-FGF and have high affinity receptor sites for this factor (Lappi *et al*, 1992; Gonzalez *et al*, 1992). Baird *et al* (1993) demonstrated a significantly increased expression of b-FGF in Dupuytren's nodule tissue compared with controls using RT-PCR as well as higher expression of Interleukins 1α and 1β and TGF-β.

TGF-β and bFGF have also been implicated in the pathobiology of Dupuytren's disease by Berndt *et al* (1995) who found localisation of TGF-β_1, TGF-β_2, bFGF and fibronectin RNA in proliferative areas of disease using in-situ hybridisation. They also found accumulation of TGF-β_1 and TGF-β_3 protein in surrounding normal tissue, hypothesising the diffusion of these growth factors causing activation of previously uninvolved fibroblasts.

1.9.1 Transforming Growth Factor β

One of the most widely investigated groups is the Transforming Growth Factor-β family. These related polypeptide trophic factors, which have diverse cellular functions, have three isoforms, TGF-β_1, TGF-β_2 and TGF-β_3. They are believed to play central roles in many fibrotic conditions (Border and Noble, 1994). It is thought that these cytokines control tissue repair processes in response to injury or insult, both initiating and turning them off (Bennett and Shultz, 1993). TGF-β_1 for example can function as an agonist or antagonist of cell proliferation depending on other factors but consistently stimulates extracellular matrix and collagen deposition (Reed *et al*, 1994) as well as regulating the action of other cytokines. Hence if the delicate balance is altered excess scarring or fibrosis can develop.

TGF-β_1 has been shown to increase proportions of myofibroblasts expressing α-smooth muscle actin in both *in-vivo* wounds and *in-vitro* fibroblast cultures (Desmouliere *et al*, 1993,Yokozeki *et al*, 1997). Tumour necrosis factor did not induce the same changes and the authors concluded TGF-β_1 to be important in regulating α-smooth muscle actin expression in wound healing and fibrocontractive diseases.

In addition to the studies outlined above, Badalamente *et al* (1996) demonstrated widespread immunohistochemical staining of Dupuytren's specimens for TGF-β_1 in all stages of the disease but not of TGF-β_2 in residual stage disease specimens. They further investigated TGF-β effects on fibroblast cell culture proliferation, finding an increased proliferation of Dupuytren's fibroblasts in response to TGF-β_1, TGF-β_2 and combined TGF-β_1 + TGF-β_2.

Kloen *et al* (1995) demonstrated three forms of TGF-β_1 receptor (I, II and III) with an increased expression of type II receptors in Dupuytren's fibroblasts compared with controls. They also found a consistent mitogenic response of fibroblasts in culture to exogenous TGF-β_1, again to a greater extent in Dupuytren's cells. Interestingly when combined with epidermal growth factor (EGF), there was a synergistic response to TGF-β_1 in Dupuytren's cell proliferation but this was only additive in control fibroblasts, suggesting they may be more susceptible to growth factor stimulation.

Work in this laboratory has confirmed the positive proliferative effects of TGF-β_1 on Dupuytren's fibroblasts and the upregulation of myofibroblast differentiation in these cell cultures (Jemec *et al*, 2000). TGF-β_1 has also been found to significantly increase both collagen and non-collagen protein synthesis in fibroblast cultures from Dupuytren's and control tissue (Bulstrode, MD Thesis, 2001).

TGF-β_1 has been shown to increase cellular contraction in FPCLs seeded with dermal fibroblasts (Montesano and Orci, 1988) and Dupuytren's fibroblasts (Vaughan *et al*, 2000). In a stressed relaxed model seeded with Dupuyten's fibroblasts, Vaughan *et al* (2000) showed a corresponding increase in α-smooth muscle positive cells preceded by an independent increase in other stress fibres, fibronexus adhesion complexes and fibronectin fibrils. These processes however, were reversed or unstable if TGF-β_1 was withdrawn.

The investigation into growth factors and cytokines and their involvement in the processes controlling the development or progression of Dupuytren's disease is an exciting area. Experiments are potentially difficult or time consuming and an *in-vitro* study can never recreate the complex milieu of interactions and feedback loops present in the patient. This avenue, however, may provide the key to understanding the cellular events leading to Dupuytren's contracture.

1.10 Cellular Contraction

In vivo cells exist within a dynamic environment where tension and loading play a part in the alignment, morphology and function. Elsdale and Bard (1972) demonstrated that fibroblasts acquired phenotypic appearances more like those observed *in vivo* when cultured in collagen matrices rather than as monolayers. Tomasek and Hay (1984) later investigated the processes involved in this reacquisition of the *in vivo* bipolar shape, concluding that both microfilaments and microtubules were involved through a series of four stages. Elsdale and Bard also observed that fibroblast populated collagen lattices (FPCLs) shrunk or contracted and subsequently Bell *et al.* (1979) used this as a model to study reorganization in wound contraction. Although other models of cell contraction

have been developed such as wrinkling of two dimensional silicone membranes (Hurst, et al, 1986) or deformable substrates (Wrobel et al, 2002), the 3D FPCL remains the most widely applied. Since Bell's work, several authors have used 3-dimensional FPCLs to study the contractile properties of many cell types and in varying species, including rabbit tendon and synovial fibroblasts, (Khan et al, 1998) human dermal fibroblasts (Stopak and Harris, 1982;Tingstrom et al, 1992; Eastwood et al, 1994, 1996 and 1998), rat dermal fibroblast (Levinson et al, 2001, Shreiber et al, 2001), dog periodontal fibroblasts (Kasugai et al, 1990) and human lung fibroblasts (Yokozeki et al, 1997; Mio et al, 1996). These collagen gels have traditionally been tethered, free floating or initially tethered and released at a set time point to float freely (stress-relaxed gels). Usually circular, the change in diameter of floating gels was used as a semiquantitative measure cellular force generation.

Collagen lattice contraction has been shown to be a cell-mediated process with increasing contraction occurring as more cells are seeded and no contraction if cells are left out. It is also serum dependent (Tomasek et al, 1992; Rayan and Tomasek, 1994, Brown et al, 2002) and related to the initial collagen concentration of the gels seeded (Bell et al, 1979; Zhu et al, 2001); and hence lattice stiffness.

The actual mechanism however is debated. Tomasek et al (1992) have suggested that there are different processes taking place between early rapid contraction in stress-relaxed gels, that they quantified, compared with the slow contraction over several hours or days seen in free floating collagen gels. Grinnell has reviewed these mechanisms of gel contraction (1994). Free floating lattice contraction has been proposed to be the result of cellular motile activity (Harris et al, 1981, Stopak and Harris, 1982) rather than typical smooth muscle type contraction. As such this has been termed "tractional remodelling" and was elegantly demonstrated by Ehrlich and Rajaratnam (1990) in different free-floating models. It has been demonstrated that the myofibroblast phenotype increases in tethered gels but not in free-floating gels (reviewed by Tomasek et al, 1999). Indeed Tomasek et al (1992) demonstrated the loss of stress fibres only 10 minutes after release of tethered gels and the contraction of stress-relaxed lattices is thought to occur in a similar fashion to the cell contraction seen in smooth muscle cells via a sliding actin-protein interaction (Guyton and Hall, 1996). Additionally the degree of contractility has been directly correlated with the level of

myofibroblast phenotype cells or α-SMA present (Tomasek *et al*, 1995; Hinz *et al*, 2001). Further evidence for two separate contractile mechanisms in the free floating and stress-relaxed collagen lattice models has come from Grinnell *et al* (1999) demonstrating different kinetics after addition of specific agonists and blocking agents.

Several studies have also demonstrated that collagen gel contraction is enhanced by a variety of cytokines such as Lysophosphatidic Acid (LPA) and PDGF (Reviewed by Grinnell, 2000). TGF-β_1 in particular, exhibits stimulatory effects on collagen lattice contraction (Reed *et al*, 1994, Montesano and Orci, 1988) although the exact mechanism or combination of mechanisms behind this effect remains unclear as increased contraction occurs in both free floating and stress-relaxed models. Grinnell and Ho (2002) demonstrated that in tethered lattices, increased contraction following TGF-β_1 stimulation corresponded with α-SMA elevation, however there also appeared to be a direct agonist effect of TGF-β_1 which was seen in free floating lattices where myofibroblasts fail to develop.

1.10.1 A Quantitative Model to Investigate Cell Contraction

With the early circular FPCL experiments only a semi-quantatative analysis of cellular contraction forces could be made, however recent advances have employed the use of highly sensitive force transducers attached to the gels in a friction free floating environment. This allows measurement of the actual forces involved for a given number of cells. Kasugai *et al* (1990) using this type of set up concluded that the force generated by dog periodontal fibroblasts was sufficient to be responsible for tooth eruption, whilst Delvoye et al (1991) measured the force generated by dermal fibroblasts. Kolodney and Wysolmerski (1992) noted the rapid dissipation of a measured force after the addition of cytochalasin D suggesting the cytoskeleton is essential for force generation. Subsequently Eastwood (1994) developed the culture force monitor (CFM) along similar lines which has been further refined to apply programmed cycles of force to FPCLs, called the tensioning culture force monitor (tCFM). Using these machines an accurate, reproducible, real time measurement of cellular forces within 3 dimensional collagen lattices has become available, as well as a means of studying responses to changes in the tensional environment. This has allowed several striking insights into the mechanism behind cellular force generation.

The same group (Eastwood *et al*, 1996) demonstrated three phases in dermal fibroblast contraction with most of the force being developed in the first phase from 0 to 7 hours. Subsequently in phase 2 there was a plateauing of force, which was then usually maintained in phase 3. By correlating the contraction profiles obtained with cell morphology they were able to determine that most of the force generated in the initial phase of contraction correlated with cellular attachment and locomotion. In other words this was equivalent to the tractional remodelling described above.

Brown *et al* (1996), after studying the effects of various cell cytoskeletal disrupters on a CFM model, proposed that microtubules act as an intracellular frame, counteracting the pulling force of microfilaments, maintaining a degree of cell morphology, and maintaining an intracellular tensional equilibrium.

Using the tCFM, Eastwood *et al* (1998) were able to determine that dermal fibroblasts aligned themselves along the lines of isometric force within a high aspect ratio collagen gel. Conversely in a low aspect ratio gel, the same cyclical loading regimen where the lines of stress were minimal, produced no cellular alignment. It appears therefore that fibroblasts are able to perceive an external load on the matrix in which they reside and are stimulated to modify their orientation accordingly, in order to shield themselves from further loading. This explains the cellular alignment in loaded structures such as tendons and ligaments.

1.10.2 Tensional Homeostasis

It has been known for some years that various cell types respond to tension or loading, however recently Brown *et al* (1998) demonstrated dermal fibroblasts exhibit tensional homeostasis. Using a fibroblast populated collagen lattice (FPCL) model, attached to a tensioning culture force monitor they confirmed the presence of an endogenous cell mediated tension as previously described (Eastwood *et al*, 1996). Subsequently various loading regimens were applied. The FPCLs showed a rapid endogenous cellular response to loading or unloading of the opposite direction, so that the overall tension tended to return towards the previously established baseline (see figure 1.4). The cells in this way were protecting themselves from excessive tensional variations. The mechanism by which this homeostasis occurs is as yet unclear. Some authors have suggested a cyclic AMP secondary messenger system in response to mechanical

stimulus (He and Grinnell, 1994). Others have suggested stretch induced intracellular calcium ion flux (Arora *et al*, 1994), whilst Chiquet-Ehrismann *et al* (1994) have demonstrated that control of the elevated levels of the extracellular matrix protein tenascin-C under stressed conditions, is regulated at the transcriptional level. This indicates that the cellular perception of tension can affect many levels of the cells behaviour.
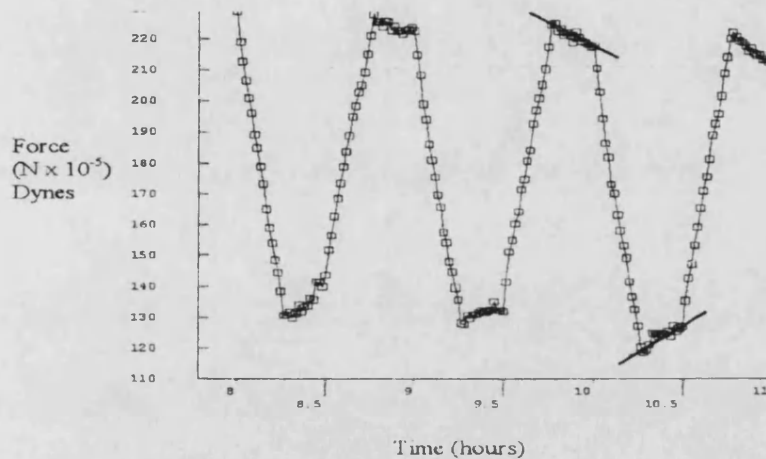
Figure 1.5. Section of a Contraction Profile with Tensional Homeostasis Being Displayed. The cellular responses seen at the troughs and peaks of this trace, where external forces have been increased or decreased, show a tendency to contract or relax in the opposite way to the force that has just been applied. This causes the overall trend in force produced by the cells (indicated by the solid lines) to return the system to a stable equilibrium. (Taken from Brown *et al*, 1998)

1.10.3 Contraction in Dupuytren's Disease

In Dupuytren's Disease cellular contraction and force have been examined in relation to the myofibroblast activity as well as the response to potential therapy. Rayan and Tomasek (1994) demonstrated an equivalent degree of contraction between dermal fibroblasts and Dupuytren's fibroblasts using a stress-relaxed model and that the contraction was dependent on an intact actin cytoskeleton. In contrast to this Tarpila *et al* (1996) found a lesser degree of contraction in Dupuytren's nodule fibroblasts compared with dermal fibroblasts, although they used a free floating collagen gel model and late stage nodule fibroblasts. Sanders *et al* (1999), looked at contraction of stress-relaxed FPCLs in response to interferon-α_{2b}. Both control and Dupuytren fibroblasts demonstrated a reduction in contraction however there was not a consistent difference between the two groups with 2 of 3 Dupuytren's strains being more contractile than matched controls. Jemec (1999, MD Thesis) showed a reduction in cellular contraction after the application of 5-flurouracil (5-fu) to Dupuytren's fibroblasts using a culture

force monitor. This was seen to occur both with pre treatment for 5 minutes and application of 5-fu to the FPCL itself. Several other pharmacological agents or trophic factors have been investigated with respect to their effect on Dupuytren's fibroblast contraction. Rayan *at al* (1996) demonstrated that lysophosphatidic acid (LPA) was a potent agonist of cell contraction using a circular FPCL, stress-relaxed model. They also noted that this effect was partially abrogated by the addition of prostaglandins E_1 or E_2 as well as by calcium channel blockers. Once again TGF-β_1 has been shown to enhance collagen lattice contraction by Dupuytren's fibroblasts in a stress-relaxed model (Vaughan *et al*, 2000).

The role of mechanical factors in the genesis of Dupuytren's disease has long been debated. Early descriptions of the condition, for example by Dupuytren himself and others (Elliot, 1999) noted the condition in manual workers, however since this time many opposing views have been proposed. Heuston (1990) disputes the role of occupation or injury as a cause, unless in the presence of the "Diathesis". Flint (1990) supports Skoog's theory (1963) and suggested that partial rupture of the palmar fascial fibres may lead to an alteration in distributed forces. He proposes that this lack of continuing uniaxial tension stimulates the processes leading to the Dupuytren's nodule.

There are also anecdotal reports (Skoog, 1963; Flint and Poole, 1990 in Dupuytren's Disease) that continuous physical attempts to overcome the disease by stretching affected fingers causes rapid development of thickened contracture tissue, whilst Messina and Messina (1993) have shown that, although contractures can be overcome by dynamic extension splinting techniques the flexion deformities will rapidly recur if splinting is withdrawn.

Interestingly other authors who have simply released tension in Dupuytren's contractures by fasciotomy or segmental aponeurectomy have observed softening or regression of the disease (Moermans, 1981; Andrew and Kay, 1991).

1.10.4 Transmitting the cellular force

Although the myofibroblast has been repeatedly implicated in Dupuytren's tissue contraction, thus being the possible means by which clinical contractures occur, it has only been recently that a mechanism for the transmission of this cellular force to the surrounding matrix and adjacent cells has been identified.

Cells appear to be linked to the surrounding extra-cellular matrix components as well as to each other via physical interconnections. The trans-membrane molecule integrin has been proposed as this crucial bond (Magro, 1995), and the close membrane association between matrix fibronectin filaments and intracellular actin microfilaments surrounding a $\beta 1$ integrin molecule has been termed the fibronexus. Tomasek and Haaksma (1991) have demonstrated such fibronexi in Dupuytren's contracture tissue proposing them to be the dominant means of transferring cell-mediated force to the matrix in the disease.

Interestingly Halliday *et al* (1994) using immunohistochemical techniques localised two fibronectin isoforms to Dupuytren's nodules but showed minimal signal in residual stage disease or normal palmar fascia.

The integrin molecule by its connection to the extracellular matrix is thought to transmit forces to the intra-cellular cytoskeleton and possibly directly affect protein production (D'Addario *et al*, 2001) by mechanotranscriptional coupling. Filamin A, an actin cross-linking protein that protects cells from applied forces, has been shown to increase in response to tension.

Furthermore Burridge (1981) has suggested that tight cellular adhesion to the matrix is fundamental to the formation of intracellular stress fibres and the subsequent generation of force.

Transforming Growth Factor β_1 has been shown to increase the specific integrin $\alpha 2\beta 1$, which has also been correlated with the degree of collagen gel contraction (Riikonen *et al*, 1995). This was in a free floating model and the increase in $\alpha 2\beta 1$, which enables cell – type I collagen interaction, was proposed to mediate the mechanism of increased gel contraction following TGF-β_1 stimulation. In contrast to this Brown *et al* (2002), using the culture force monitor, found that the temporal relationship of increased integrin expression by TGF- β_1 stimulation was inconsistent with the point where contraction was increased.

1.11 Summary

As can be appreciated from the discussion above there is no current widely accepted non-surgical therapy for Dupuytren's disease. Surgical results have improved, however rates of recurrence and extension of the disease remain high. A solution to the problem of Dupuytren's treatment is only likely to occur through gaining a deeper understanding of the cell and molecular biology involved in this condition. Several advances have been made in recent years, with the identification of myofibroblasts, the implication of growth factors such as TGF-β_1, and delineation of matrix changes in Dupuytren's disease. None of these findings have yet led to therapeutic progress. A single causative factor has not been identified and the mechanisms behind the development of the most disabling aspect of the condition, flexion contracture, remains poorly defined.

In this thesis it is intended to investigate further the mechanisms behind the shortening of Dupuytren's fascia that is thought to lead to flexion contracture development. By comprehending the way in which this occurs one may be better placed to develop and deliver a therapy to prevent this most troubling aspect of Dupuytren's Disease.

Additionally by defining differences between nodule and cord fibroblast phenotypes and behaviour it could be possible to obtain an enhanced understanding of the natural history of Dupuytren's disease and even enable an evidenced based strategy for targeting specific areas of the condition.

THE HYPOTHESIS:

In Dupuytren's disease there is an interaction between an increased myofibroblast phenotype, TGF-β_1 and mechanical stimulation that results in altered cell mediated contraction and hence the physical shortening of fascial tissue fabric.

Chapter 2

Materials and Methods

2. Materials and Methods

2.1. Cell Culture

Dupuytren and control carpal ligament fibroblasts were established in culture following local ethical committee approval (Number EC2001-21). Dupuytren's disease tissue was obtained from excised specimens at routine fasciectomy. Carpal ligament was selected as control tissue and excised from the incised free edge of the carpal ligament at routine carpal tunnel decompression. These patients showed no evidence of Dupuytren's disease. Several previous investigators have used carpal ligament cells as non-diseased fibroblasts for comparison with Dupuytren's disease derived cells (Badalamente *et al*, 1988, Rayan and Tomasek, 1994; Tomasek and Rayan, 1995, Halliday *et al*, 1994). Cell lines established are detailed in appendix I.

All cell culture work was carried out in sterile class II laminar airflow hoods, (HERA Safe, No. HS 12, Heraeus Instruments, Hanau, Germany) and flasks maintained in Heraeus (No. BB16, Heraeus Instruments) incubators kept at 37^0C, humidified and with a CO_2 concentration of 5%.

2.1.1. Processing of Tissue and Establishment of Cell Cultures

Fresh tissue was obtained from the plastic surgery theatres wrapped in a saline soaked sterile swab. Dupuytren's tissue excised at fasciectomy was selected to include at least one clinical nodule and a length of pathological cord identified where possible per-operatively. All tissue was obtained from patients undergoing **primary procedures** for Dupuytren's disease; **no recurrent** cases were included. When cleaned of surrounding fatty and loose connective tissue the specimen would often resemble a "drumstick" shape (figure 2.1). This tissue was sectioned longitudinally with one half being fixed in 10% formal saline for histology and the other half being used to establish cell cultures. An explant method was used to establish cells in culture with two lines obtained from each specimen, one from the nodule and one from the cord (figure 2.2). Tissue from these regions was macerated using a

sterile scalpel and forceps, which had been previously sterilized in 70% Industrial Methylated Spirits (IMS) and allowed to air dry. It was placed on the base of a T25 tissue culture flask (No. 690-160, Greiner Labortechnik, greiner bio one, Germany.) and allowed to adhere for 2 minutes. It was bathed in normal fibroblast growth medium (NGM, see appendix II for composition) and incubated until fibroblasts were observed migrating from the specimen. At this point the media was changed and then further media changes were carried out on every third or fourth day thereafter. Cells were passaged into T75 tissue culture flasks (No. 658-170, greiner bio one.) once an expanding monolayer was seen spreading from the tissue specimen.

Carpal ligament tissue was explanted in exactly the same way, but without separation into selected zones.
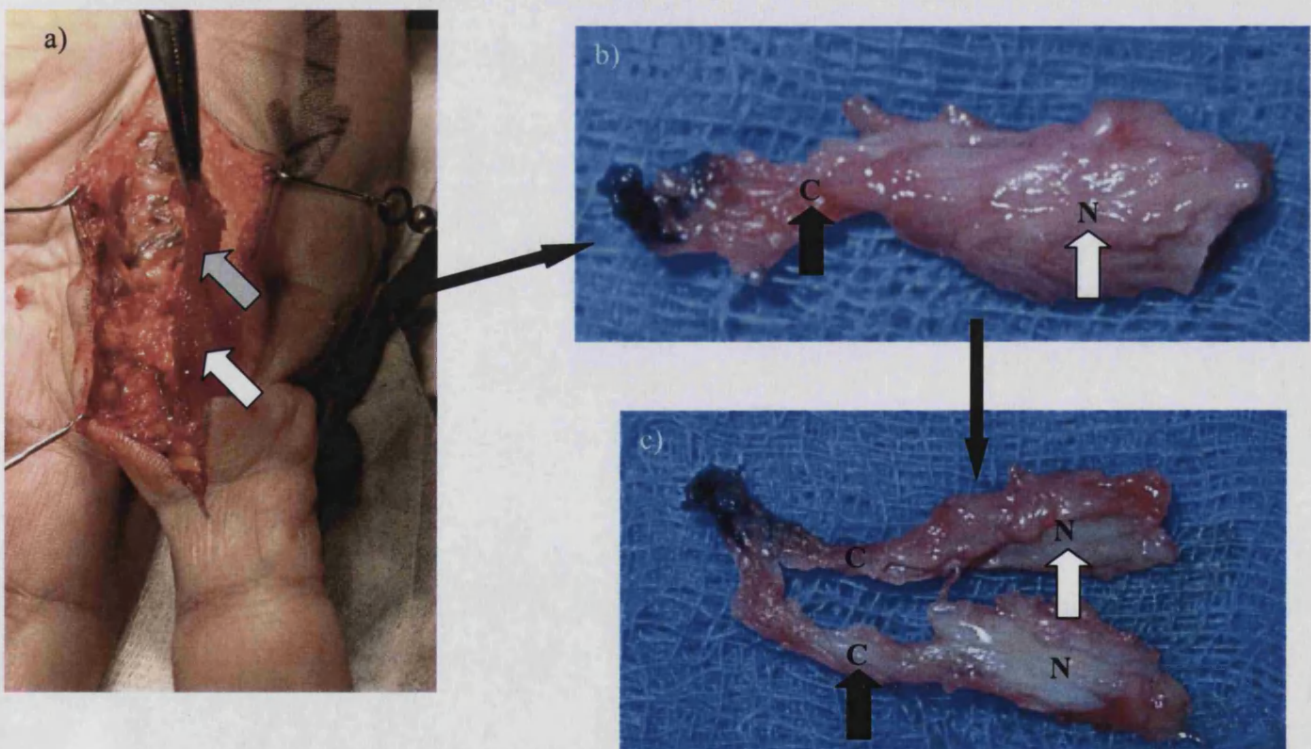
Figure 2.1. A Typical Dupuytren's Disease Specimen.
a) Dupuytren's disease tissue being excised from a patient undergoing routine primary fasciectomy. b) The defatted specimen illustrating macroscopically identifiable regions of nodule (N, white arrow) and cord (C, black arrow). c) The specimen bisected longitudinally. The inked end of the specimen allows orientation of the specimen throughout processing

2.1.2. <u>Routine Propagation of Cell Cultures</u>

Cells were passaged just prior to confluence by splitting 1:3 in T75 tissue culture flasks. Culture medium was aspirated and the cell monolayer washed with 10ml phosphate buffered saline w/o calcium and magnesium and w/o sodium bicarbonate (PBS) (No. 14190-094, Gibco, Paisley, Scotland). This was aspirated and 1ml of 1:10 trypsin : versene (see appendix II for formulation) solution was added. The flask was incubated for 5 minutes and then agitated to obtain a single cell suspension. The trypsin solution was neutralized with 10ml of culture medium (containing 10% Foetal Calf Serum which neutralises the trypsin) and the resulting suspension was then centrifuged at 1000rpm for 5 minutes. The supernatant was discarded and the cell pellet resuspended in 30mls of culture medium.

Ten millilitres of solution was distributed to each of three T75 cell culture flasks. These were incubated as previously described. Cells used were all at or below passage 5 in an attempt to limit any dedifferentiation of the fibroblast population.
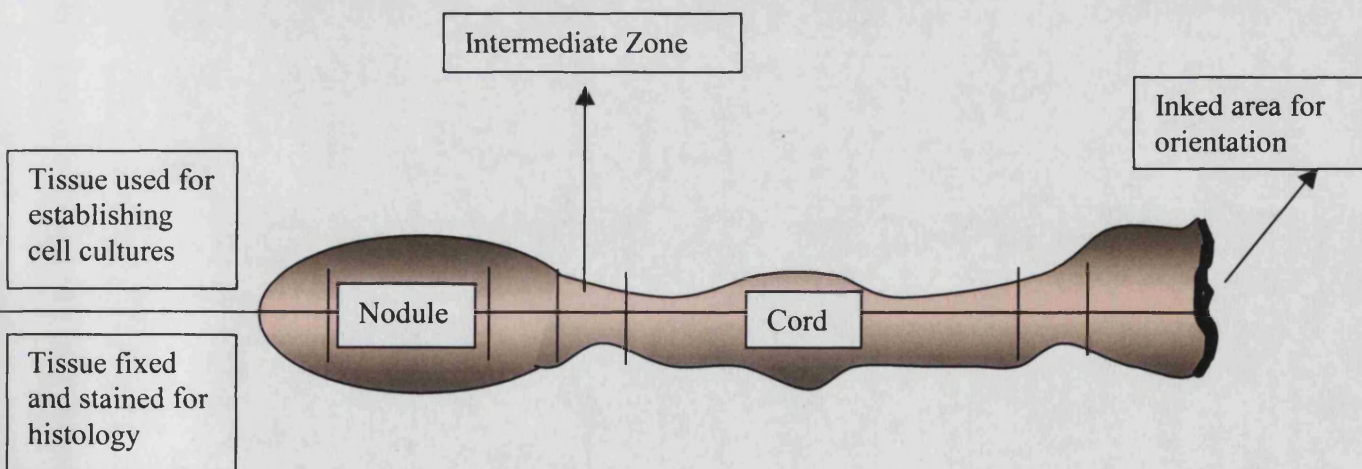
Figure 2.2 Diagram of a "drumstick" shaped specimen of Dupuytren's tissue. It was processed by sectioning longitudinally as indicated. Half was used for establishing separate zonal cell culture lines, the second half processed for histology.

2.1.3. Cryopreservation of Cells

Cells were stored once established in culture by freezing. A cell suspension obtained after trypsinisation of the monolayer, described above, was centrifuged at 1000rpm for 5mins to obtain a cell pellet. The supernatant was discarded and the pellet resuspended in 2ml of a solution of 10% DMSO (Dimethylesulphoxide, No. D2650, Sigma Chemical Company, Poole, Dorset) and 90% foetal calf serum (No. 10106-169, Gibco). 1ml was dispensed into each of two cryovials labelled with cell line, passage and date. They were wrapped in tissue paper as insulation and then frozen in a -80^0C freezer. The tissue paper allowed a gradual decrease in temperature during the freezing. Once frozen, samples were transferred to liquid nitrogen for long-term storage.

2.1.4. Raising Cells from Frozen

Cryovials were thawed rapidly in a water bath at 37^0C. The cell suspension was transferred to a 15ml Falcon tube and 10ml of NGM was slowly added whilst swirling gently. The resulting suspension was centrifuged at 1000rpm for 5mins and the cryopreservation containing supernatant aspirated and discarded. The cell pellet was suspended in 10ml of NGM and dispensed into a T75 flask for incubation.

2.1.5. Determination of Cell Number and Viability

For many experimental protocols specific numbers of viable cells were required. Cells were counted using a haemocytometer (improved Neubaur) and stained with Trypan Blue to determine viability. An aliquot of 50μl of a well-mixed cell suspension was diluted 1 in 2 with 50μl of Trypan Blue (0.4%, No. T8154, Sigma.) and then drawn between the haemocytometer and cover slip by capillary action. This was examined under an inverted phase contrast microscope (Olympus CK2, Olympus Optical Co., Japan.) where dead cells were seen to stain darkly with the Trypan Blue as live cells pump out the dye. The number of viable cells contained within 1 large grid of the haemocytometer was counted and this

repeated in 3 further grids. The mean cell number of all 4 was taken and multiplied by 2 (the dilution factor) and then by 10^4 to give the cell density (Viable cells/ml).

2.2. Histology

The fixed specimens of Dupuytren's tissue were embedded in paraffin blocks with a known orientation maintained by inking of one edge of the sample. This allowed accurate identification of the areas corresponding to those where cell cultures were established from, under light microscopy. Representative sections of the embedded tissue were cut and stained with haematoxylin and eosin. Paraffin blocks were sectioned at 4 μm using a Reichert-Jung Microtome (Leica Instruments, Germany) and were mounted on glass slides (No. 00210, Snowcoat Extra; Surgipath, St. Neots, Cambs.). Sections were dewaxed by bathing in xylene (No. 202-422-2, Genta Medical, York, UK) for 10 minutes and were then rehydrated through bathing in a series of ethanol (Hayman Ltd, Essex, UK) dilutions, from 100% then 90%, 70% then to tap water. The sections were stained in Harris Haematoxylin (No. 31945S, BDH, Poole, Dorset, UK.) and Eosin (1% solution; 1034197, BDH) by firstly immersing the slides in Haematoxylin for 1 minute. They were then washed well under running tap water before immersion in eosin for 1 minute. After a further washing sections were dehydrated through the alcohols, cleared and mounted using DPX (No. M81330/C, DiaCheM, London, UK.) and 22 X 30 mm cover slips (Menzel-glazer). Examination at x 100 and x 200 magnification (Zeiss Axioscope 20, Carl Zeiss, Germany) allowed confirmation of histological differences in the regions used for different cell culture zones. These broadly corresponded to Luck's 1959 classification. The "Nodule" zone was highly cellular with disorganized architecture and minimal collagen deposition correlating to the proliferative phase (fig. 3.1.1.). The "Cord" was relatively acellular with large amounts of parallel, longitudinally aligned collagen representing the residual phase (fig. 3.1.2.). The area between these two extremes was more variable, generally less cellular and more organized than nodular tissue. (fig. 3.1.7.) In order to quantify these differences, digital images were captured of nodule and cord regions at x20 magnification using the microscope and Leica DC200 mounted camera and software (Leica DC Viewer, Leica Microsystems-Ltd, Heerbrug, Switzerland). Three images of each area from all specimens were taken and a grid of known area was overlaid onto the image using Adobe Photoshop

(version 5.0.2. Adobe Systems Ltd.). The number of cell nuclei in the grid was then counted for each image and a mean obtained for each cell line, nodule and cord.

Mean cellularity was compared between nodule and cord and significance determined using a paired student's t-test (Sigma Stat 2.0, Jandel corps.).

2.3. Staining of Tissue Sections for α-Smooth Muscle Actin

Tissue sections similar to those used for standard H & E histology were stained for the presence of α-Smooth Muscle Actin in order to identify myofibroblasts within the specimens obtained. Paraffin blocks were sectioned at 4 μm using a Reichert-Jung Microtome and mounted on glass slides (Snowcoat Extra; Surgipath, St. Neots, Cambs.). Antigen retrieval was performed by steaming the slides for 10 minutes in 400 mls of preheated Tris HCl buffer, pH 9.0, in a steamer (No. 48870, Morphy Richards). This provided the optimal conditions for maintaining sections on the slide, which was found to be problematic with other methods of antigen retrieval. The "steaming" method was found to be as effective on positive control sections (tonsil or intestine sections) when tested against the standard, in house antigen retrieval method of 15 minutes microwave treatment in citrate buffer (pH 6.0).

Two methods were used to identify α smooth muscle actin within tissue sections of both Dupuytren's disease and carpal ligament (see figure 2.3). The first employed an immunohistochemical technique using the streptavidin alkaline phosphatase method, which provides a striking contrast for positive and negative reactions and was not confused with endogenous tissue pigment. The second method employed an immunoflourescent technique allowing visualisation of positive staining under ultraviolet light.

In the first method endogenous alkaline phosphatase was blocked by a 20 minute incubation in a bath of 20% acetic acid solution and then sections were washed in running tap water for 2-3 minutes. Prior to ringing the sections with a hydrophobic wax pen (No. H-4000, Vector Laboratories, Peterborough, UK), they were placed in a bath of 50 mM Tris buffered saline (pH 7.6). Sections were then placed in a flat bed humidification tray for all

subsequent applications of immunoreagents. Between reagent application, slides were rinsed off with a wash bottle containing TBS + T (see appendix II) before being placed in a slide rack and put in a fresh bath of TBS + T on a magnetic stirrer (No. 13135, Stuart Scientific, UK). This wash step was crucial in order to reduce background staining.

Sections were incubated with one drop of Avidin D blocking solution (Avidin Biotin Blocking Kit SP200, Vector Laboratories, Peterborough, UK.) for 15 minutes. This was flicked off and briefly rinsed with TBS + T after which one drop of the Biotin blocking solution was applied for 15 minutes (Avidin Biotin Blocking Kit SP200, Vector Laboratories). Sections were again briefly washed with TBS + T. Following this 100 μl of 1:5 normal rabbit serum (Vector S5000) diluted in Dako Chemmate antibody diluent (Dako S2022, Dako, Ely, UK) was applied to each slide for 30 minutes.

Excess rabbit serum was flicked off the slides and 100 μl of anti-α smooth muscle actin antibody (anti- α SMA; No. A2547, clone 1A4, Sigma) diluted 1:5000 was applied overnight at 4 °C. Negative controls used were either diluent only or a mouse IgG serum (No. 1-2000,Vector) substituted for the anti- α SMA at an equivalent dilution. Numerous test sections were performed which showed no reaction using either control, and subsequently Chemmate diluent was used alone as a negative control.

After a wash step with TBS + T, 100 μl of biotinylated rabbit anti-mouse antibody (Dako E0354), diluted 1:200 in Dako Chemmate diluent, was applied for 30 minutes. After washing in TBS + T, 100 μl of streptavidin alkaline phosphatase (Vector SA5100) diluted 1:200 in Dako Chemmate diluent was applied for another 30 minutes. After a further wash in TBS + T, Vector Red substrate (Vector Alkaline phosphatase substrate, SK5100) made up in 200 mM Tris HCl (pH 8.2) was applied for 10 minutes so that α SMA staining appeared bright pink. The intensity of the chromagen was checked under the microscope prior to washing the slides in running tap water for 2 – 3 minutes. Nuclei were counterstained blue with Harris's haematoxylin for 10 – 30 seconds, differentiated and then blued in water. Sections were subsequently dehydrated, cleared and mounted in permanent DPX mountant.

Immunohistochemical Method

Immunofluorescence Method

Antigen Retrieval
slides steamed for 10 minutes in 400 mls of preheated Tris HCl buffer, pH 9.0

endogenous alkaline phosphatase blocked
20 minute incubation in 20% acetic acid

running tap water for 2-3 minutes

bathe in 50 mM Tris buffered saline (pH 7.6)

Sections ringed and placed in a flat bed humidification tray

one drop of Avidin D blocking solution 15 minutes

Excess solution flicked off slides

one drop of Biotin blocking solution 15 minutes

Excess solution flicked off slides

100 μl of 1:5 normal rabbit serum diluted in Dako Chemmate antibody diluent 30 minutes.

Excess solution flicked off slides

anti-α smooth muscle actin
100 μl of 1:5000 overnight at 4 °C.

rabbit anti-mouse antibody
100 μl biotinylated of 1:200 in Dako Chemmate diluent 30 minutes

Vector Red substrate in 200 mM Tris HCl (pH 8.2) 10 minutes

running tap water for 2-3 minutes

Nuclei counterstained
Harris's haematoxylin. Slides dehydrated and mounted in DPX

Wash step with TBS + T

anti-α smooth muscle actin
100 μl of 1:5000 overnight at 4 °C.

FITC conjugated rabbit anti-mouse secondary antibody
100 μl of 1:400
+
propidium iodide 1:60
30 minutes.

slides mounted in DABCO and stored at −20 °

Figure 2.3. A flow diagram illustrating the two methods of staining for α SMA.

In the second immunofluorescent method, antigen retrieval was followed simply by the primary antibody (anti- α SMA) at a dilution of 1:5000. Then after a wash step in TBS + T a FITC conjugated rabbit anti-mouse secondary antibody (No. F0232, Dako) was applied at a dilution of 1:400 with propidium iodide (40μg/ml No. P-14170, Sigma) 1:60 dilution for 30 minutes. Following another wash step the slides were mounted in DABCO (Sigma, see appendix II) and stored at –20 °C.
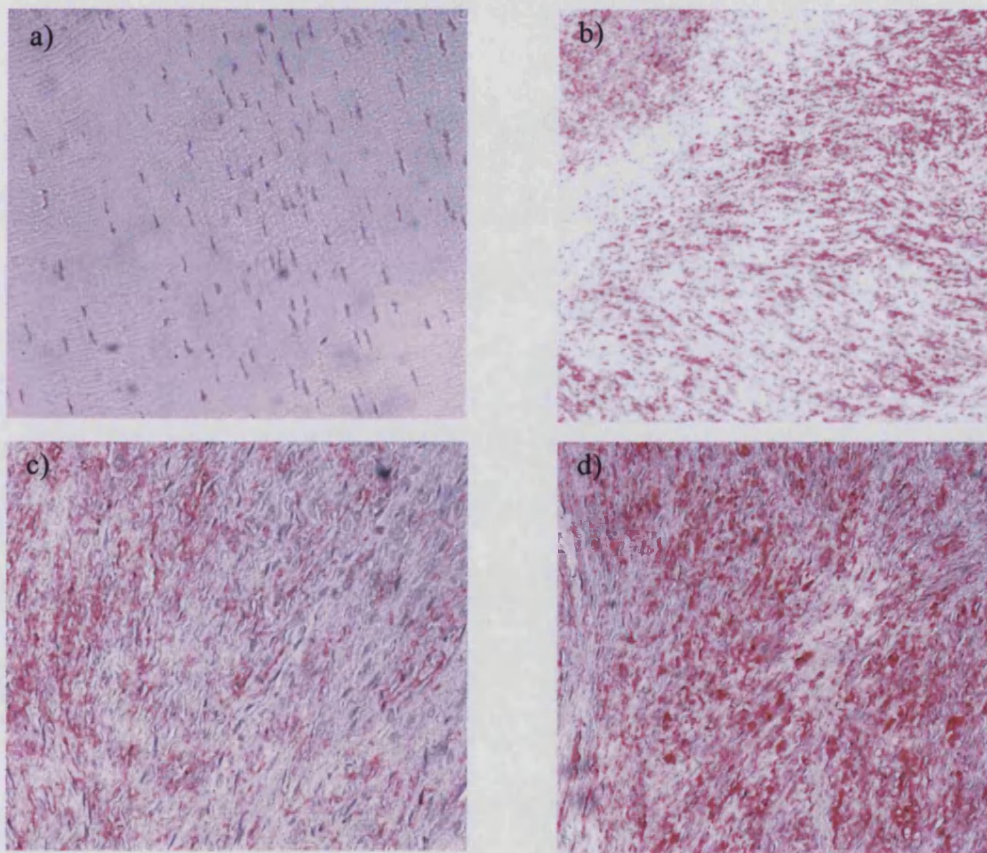
Figure 2.4a-d) Representative sections demonstrating the grading of positive staining for α SMA using the streptavidin alkaline phosphatase method. a) represents negative staining (-). b to d represent increasing levels of positive staining (+, ++ and +++ respectively)

Streptavidin alkaline phosphatase stained sections were viewed under a light microscope (Zeiss Axioscope 20) and sections of nodule and cord and carpal ligament were graded for the presence of positive staining for α SMA. As shown in figure 2.4.a "-" indicated no positive staining. Increasing levels of positive staining were represented by "+", "++" and "+++" respectively (figure 2.4.b to 2.4.d) allowing a semi quantitative (although subjective) assessment of the level of α SMA staining and hence myofibroblasts present in tissue sections.

The immunoflourescent method was used as a comparison to see if better visualisation of weakly positive areas could be obtained. Both methods were found to be equivalent.

2.4. Cultured Fibroblast Immunohistochemistry

2.4.1. Staining of Fibroblast Cultures for α-Smooth Muscle Actin

Six well plates (No. 657-160, Cellstar, Greiner bio one) were prepared with (24mmx24mm) glass cover slips in the bottom of each well. These were first soaked in alcohol and air-dried. Into each well were seeded 80,000 cells and these incubated with 2mls of normal fibroblast growth medium per well at 37^0C, 5% CO_2. For each cell line this was repeated in three wells. The media was aspirated and changed at twenty-four hours. At four days the cells on the glass cover slips were fixed by aspirating the growth media and bathing each in 2mls of ice-cold methanol at -20^0C for 30 minutes. Each cover slip was then removed and air-dried with the cell-coated side uppermost. Once dry the cover slips were mounted on labelled glass microscope slides using DPX mountant (DiaChem) again with the cell layer uppermost. The slides were stored at -20^0C in the dark until they were to be stained.

To stain the slides they were defrosted for 15 minutes and a ring drawn on each cover slip around the cells using a wax pen (Vector). They were washed three times in phosphate buffered saline (PBS, see appendix II for composition) and then laid out on a metal flat bed humidification staining tray. To each cover slip was added 100μl of mouse

monoclonal anti α-smooth muscle actin antibody (anti- α SMA; No. A2547, clone 1A4, Sigma) at 1 in 1000 dilution with PBS. The tray was covered and left for one hour. The antibody was washed off using Tris Buffered Saline with Tween (TBS-T, see appendix II for composition) and then the slides were washed three times in PBS. The secondary antibody, a FIT-C rabbit anti-mouse monoclonal antibody (No. F0232, Dako), was made up at a 1 in 400 dilution in PBS mixed with propidium iodide at a 1in 50 dilution as a nuclear counterstain. 100μl of this solution was added to each cover slip and again covered and left for 50 minutes. The antibody was washed off using TBS-T and then the slides were washed three times in PBS. One drop of DABCO (appendix II) was placed on each cover slip and a second 24x40mm cover slip placed over this.

The slides were examined under ultraviolet light using a FITC filter where nuclei appeared red due to the counterstain and α-smooth muscle actin fluoresced green. Images of three random areas from each cover slip were captured using a Zeiss Axioscope 20 microscope with a Leica DC200 mounted camera and software (Leica DC Viewer) so that a total of nine fields were obtained for each cell line (each one having been done in triplicate). For each field the total numbers of cells were counted as were the total number of cells staining positively for α-smooth muscle actin. A mean percentage of these positive myofibroblasts was calculated for each cell line and results for nodule, cord and control carpal ligament were compared.

Statistical analysis of the results was performed using a student's t test. (Sigma Stat.)

2.4.2. Myofibroblast Content of Cell Cultures Treated with TGF-β

The same experimental procedure was carried out as in section 2.4.1. with 80,000 cells again being seeded on sterilised and air dried cover slips in six well plates. They were allowed to settle and adhere for 24 hours in normal fibroblast growth media and then the media changed as above but this time substituted for 2 ml of TGF-β_1 (No. 240-B R&D Systems, Minneapolis, MN. USA) supplemented normal growth media at a concentration of 2ng per ml. The cover slips were fixed in ice-cold methanol at 4 days for 30 minutes and air-dried before being placed on glass microscope slides, attached with DPX mountant.

They were frozen at $-20°C$ for storage and then stained for α-smooth muscle actin and myofibroblast proportions determined in exactly the same way as in section 2.4.1.

2.5. The Culture Force Monitor

This is a novel experimental device for quantitative analysis of forces produced by cells in a three-dimensional collagen lattice, which was developed at University College London (Eastwood *et al*, 1994), and is now based at the Tissue Repair and Engineering Centre (TREC), at the Royal National Orthopaedic Hospital, Stanmore, Middlesex.

It consists of a collagen lattice seeded with the cells to be examined, suspended in a well containing growth media (figure 2.5). The well is actually a standard size created by a defect in a silicone elastomer mould (see appendix III) placed within a 10 cm petri dish. The collagen gel floats between two floatation bars, one attached to a fixed point and the other to a sensitive force transducer which has previously been calibrated in dynes (see appendix IV for calibration method). The force transducer is attached to a desktop computer (Akhter, Pentium PC; 48MB RAM; Windows 95 operating system) which records one reading of the force across the system every second in real time. The petri dish sits on a base stage, similar to that of a microscope mounting stage, with a micrometer calibrated wheel allowing accurate, unidirectional movement of the system towards or away from the force transducer. The whole apparatus is kept at constant temperature, CO_2, and humidity within an incubator (Galaxy S, Wolf Laboratories).
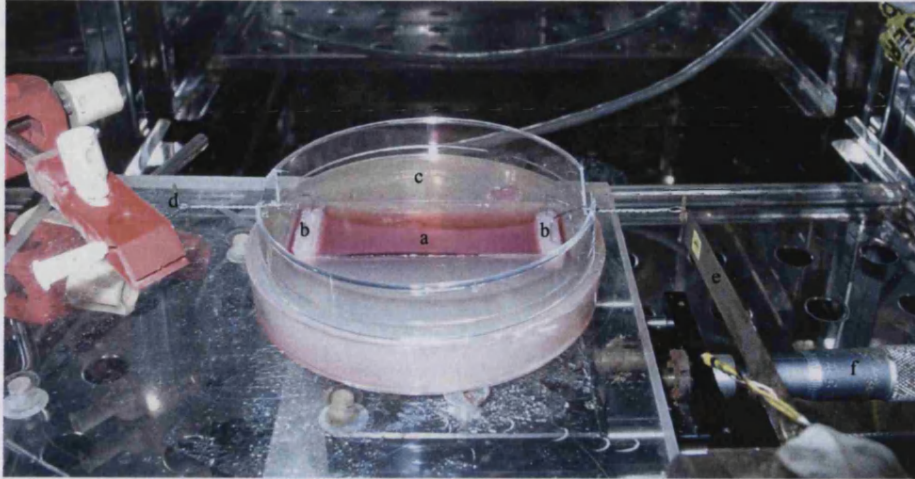
Figure 2.5. The Culture Force Monitor Set Up.
The collagen lattice (a) is suspended between two floatation bars (b) attached to "A" frames. It floats within a well of fixed dimensions in a silicone elastomer mould (c), which is filled with growth media. One "A" frame is attached to a fixed point (d), whilst the other is attached to the force transducer (e). The force transducer is connected to a desktop computer. The apparatus sits on a moveable microscope mounting stage, which can be moved towards or away from the force transducer by the micrometer wheel (f).

2.5.1. Preparing the Fibroblast Populated Collagen Lattice

The cells to be used were grown to 80 – 90 % confluence in a T225 cell culture flask (Corning, cat No. 431081, Corning inc. NY.). In general two flasks were required to provide sufficient cells at this density. The monolayer was washed twice with PBS and the cells were then trypsinised off of the flask using 5ml of trypsin/versene solution (1 in 9 dilution). Once in suspension the trypsin was neutralised with normal growth medium and then the cells were centrifuged at 1000rpm for 5 minutes. The supernatant was discarded and the cells resuspended in 5ml of normal growth media. Cell counting and viability confirmation was then carried out as per section 2.1.5. and the cells were centrifuged once more. The cell pellet was resuspended in normal growth media depending on the viable cell number to reach a concentration of one million viable cells per 100μl of media.

Meanwhile the mould and floatation bars for the culture force monitor gel were prepared. The bars (see appendix III for dimensions) were checked for symmetry and correct height relative to the mould. They were then immersed in alcohol to sterilise them and left on a sterile petri dish to air dry. Pre autoclaved moulds (see appendix III for dimensions and composition) were fitted into 10cm petri dishes (No. 8-0402, Nalgene, Nalge Company, Rochester, New York) and these sealed with 1ml of collagen gel mixture. To do this, one millilitre of collagen prep (2.3 mg/ml in 0.6% acetic acid; No. 60-30-810, First Link UK Ltd.) was added to 100µl of 10x MEM (No. 21430-012, Gibco) and mixed by swirling. This was then neutralised using 1M NaOH (No. 301674M, BDH, made up in distilled water) in a drop wise fashion until the solution just changed to a deep pink colour from the initial yellow. This was pipetted into the mould at the interface between its sidewalls and the base of the petri dish and left in an incubator at 37 ^{0}C to solidify.

The main collagen gel was prepared in a similar manner using 6ml of collagen prep mixed with 700µl of MEM. The solution was neutralised using first 5M NaOH and then with 1M NaOH again until the colour change is just observed. The liquid was mixed by swirling and 1ml of the solution was quickly dispensed into the lattice of each bar. Five million fibroblasts were then seeded into the remaining solution by adding 500µl of the cell suspension prepared above and mixed trying to avoid bubbles. The bars were placed at each end of the mould well and the gel poured between them and very gently agitated to fill the remaining space before it started to set. This was placed in an incubator at 37°C to solidify using an inverted 9cm petri dish base, with windows cut out to accommodate the bar arms, as a protective lid (see figure 2.6.).
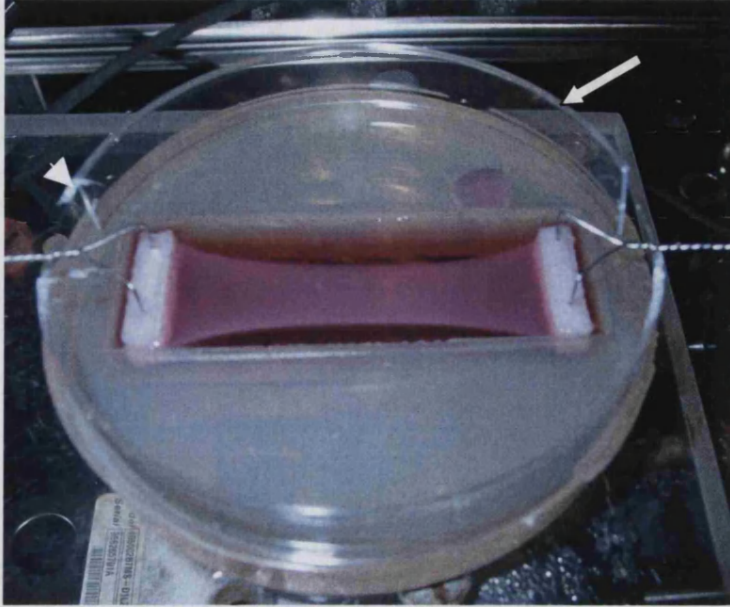
Figure 2.6. A Close Up View of the Collagen Lattice Within the Mould.
The collagen lattice has contracted, indicated by the concave long edges. It is floating freely in the well so that there is no friction on the system and even small changes in force can be accurately measured. The lid (arrow), made out of an inverted 9cm petri dish base, can be see sitting on top of the mould. Windows have been cut out of each side of the lid (arrow head) to allow the "A" frames to extend through.

2.5.2. Setting up the Fibroblast Populated Collagen Lattice on the Culture Force Monitor

Once set the fibroblast populated collagen lattice was floated in 25ml of normal growth media. A sterile needle was used to free the edge of the gel from the mould walls and the floatation bars gently moved inwards to release them. The gel then floated to the surface between the buoyant bars. The gel was then transferred to the culture force monitor situated within a humidified incubator at 37°C, and 5% CO_2. The eye of one bar was place over the fixed strut of the culture force monitor as the petri dish was placed on the mounting stage. The stage was moved in towards the measuring arm until the other bar could be hooked onto it and the system gently altered until the gel, bars and arms were aligned and floating free with no friction. (see figure 2.6) The lid was replaced and the force transducer

64

measured a voltage corresponding to the displacement of the measuring arm. The system was linked to a desktop computer with software (LabVIEW VI, National Instruments) recording one measurement every second, converting the voltage reading into a force measurement in dynes using a pre determined calibration factor (see appendix IV for method of CFM calibration). Thus a real time graph of the force across the system was generated. At initial set up the force at equilibrium was set at zero and subsequent changes were observed over the following 24 hours with readings once a second.

2.5.3. Basic Contraction Profile Determination and Method Development

Once the fibroblast populated collagen gel was set up in a satisfactory way the incubator was closed and data recording begun after 5 minutes of equilibration. The whole system was maintained at 37°C and 5% CO_2 for the duration of the experiment. The gel was left to contract for between 20 and 24 hours producing a contraction profile for each cell line studied as the attached desktop computer recorded one force reading every second for the duration of the experiment. This data was converted to a mean reading per minute at the end of the experiment using a DOS macro program and then analysed using Microsoft Excel software (Microsoft corporation).

The CFM has been used to extensively study contractile properties of dermal fibroblasts, both human and rat derived, and is currently being extended to investigate other cell types. Few people, however, have used the apparatus to study fibroblasts derived from Dupuytren's tissue and none have examined carpal ligament tissue. The methods of collagen gel preparation and set up on the machine are technically demanding with a steep learning curve and it was therefore important to ensure the technique was reliable and reproducible once it had been mastered.

AIM

To establish the reliability and reproducibility of the culture force monitor in this operator's hands and its applicability to the cell types of interest for study.

METHOD

To confirm the reliability of the method once learned, a standard dermal fibroblast cell line was used initially to allow comparison with previously published data.

Subsequently to confirm the reproducibility of the technique within the cell lines of interest several experimental runs were carried out repeating the same cell lines on three or more occasions. One Dupuytren's nodule, one Dupuytren's cord and two carpal ligament derived fibroblasts cell lines were examined in this way.

The relative paucity of contraction within carpal ligament cell lines, and in some Dupuytren's cord cell lines, raised the question of cell viability within the collagen gels over the 24-hour study period. Contraction may have been poor because of significant cell death within the population of fibroblasts seeded into the collagen gel. Had this preferentially occurred in certain cell types or lines, such as carpal ligament it would invalidate their use. A series of viability (Fluck *et al*, 1998) assays were therefore performed using four separate cell lines from each tissue type, nodule, cord and carpal ligament. Collagen lattices were set up in the same way as detailed above. They were left to contract for twenty-four hours. At this time the collagen gel was removed from between the floatation bars and placed intact into a 15 ml falcon tube containing a 5 ml solution of collagenase-D (5mg collagenase-D, No. 1 088 866, Roche Diagnostics, Mannheim, Germany, in 10 ml of Phosphate Buffered Saline without sodium bicarbonate, No. 14040-091, Gibco Life Technologies, Paisley Scotland; containing 50 mg of Bovine serum albumin, No. 11018-017, Gibco.). The tube was placed into a warmed shaker (Innova 4000, Incubator Shaker, New Brunswick Scientific) at 37°C for approximately 1hour until the collagen gel had completely dissolved. The cells now in suspension were centrifuged at 1000rpm for 5 minutes to pellet them and the collagenase solution was aspirated. The pellet was resuspended in 5 ml of Phosphate Buffered Saline with Mg^{2+} and Ca^{2+} and the percentage of viable and dead cells was calculated by staining with trypan blue and counting as described in Chapter 2.1.5.

RESULTS

Figure 2.7 displays graphically the contraction profiles of a standard dermal fibroblast cell line repeated on two occasions. The pattern is typical of that described in the literature for dermal fibroblasts (Eastwood *et al*, 1994 and 1996). There is an initial rapid contraction (arrow head), which is plateauing by between 8 and 15 hours. Subsequently until the end of the 24-hour experiment there is an extended steady state plateau stage (solid arrow).

The force generated is 126.9 dynes at 20 hours with the contraction profile gradient at this point (The rate of change of the force expressed in dynes per minute) being zero.
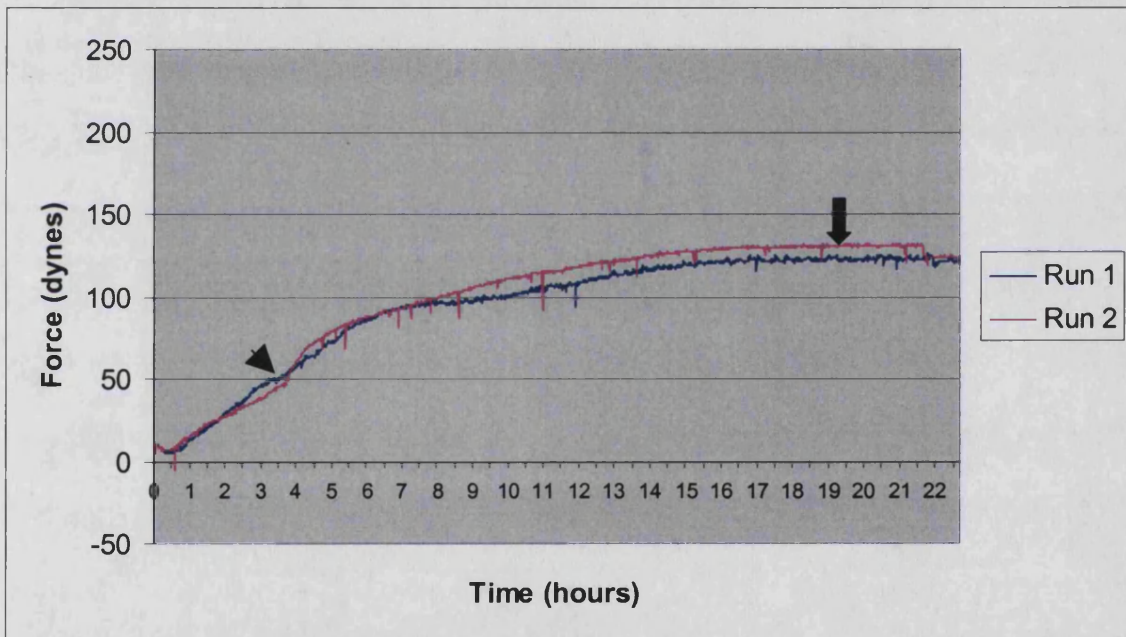
Figure 2.7. Contraction profiles of a single dermal fibroblast cell line repeated on two occasions. Five million viable fibroblasts were seeded into a 5 ml collagen lattice in each case and the force measured on the culture force monitor over 20 hours. The arrowhead indicates the point at which there is a rapid contraction, which eventually reaches a plateau phases (arrow).

Reproducibility for the cell lines of interest was then investigated. Figure 2.8 shows three contraction profiles obtained from the same Dupuytren's nodule cell line. There was some initial early phase variation in the trace obtained, especially on repeat 2 (arrow) however; subsequently the traces are virtually identical. This is illustrated by the mean trace shown in figure 2.9 with standard deviations displayed at hourly intervals.
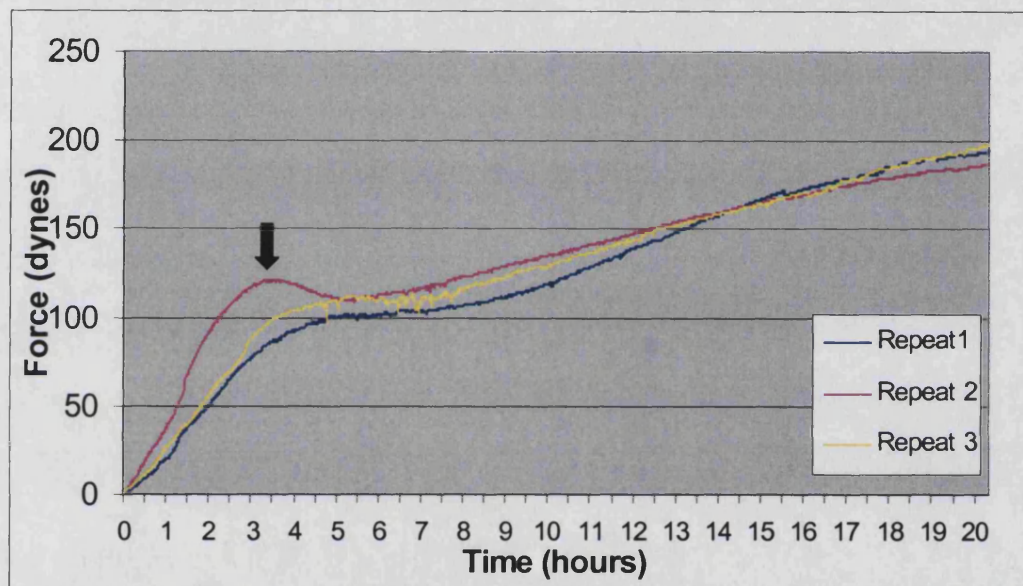
Figure 2.8. Contraction profiles of a single Dupuytren's nodule cell line repeated on three occasions. Runs were matched for cell number (5 million viable fibroblasts) and passage. Note some minor early phase variability (arrow) before the traces become nearly identical.

Mean force at 20 hours was 191 dynes SD ± 5.1 dynes. A similar mean trace for three experiments using a single poorly contracting cord cell line matched for passage number is illustrated in figure 2.10. Error bars again represent the standard deviations with the mean 20 hour force being 68 dynes SD ± 3.0 dynes. A single carpal ligament derived fibroblast cell line was then studied on four occasions, illustrated in figure 2.11 as a mean trace over 20 hours +/- standard deviations. Mean force generated at 20 hours was only 36.07dynes SD ± 14.5 dynes with a rate of change of force at this point of 0.002 dynes per minute.
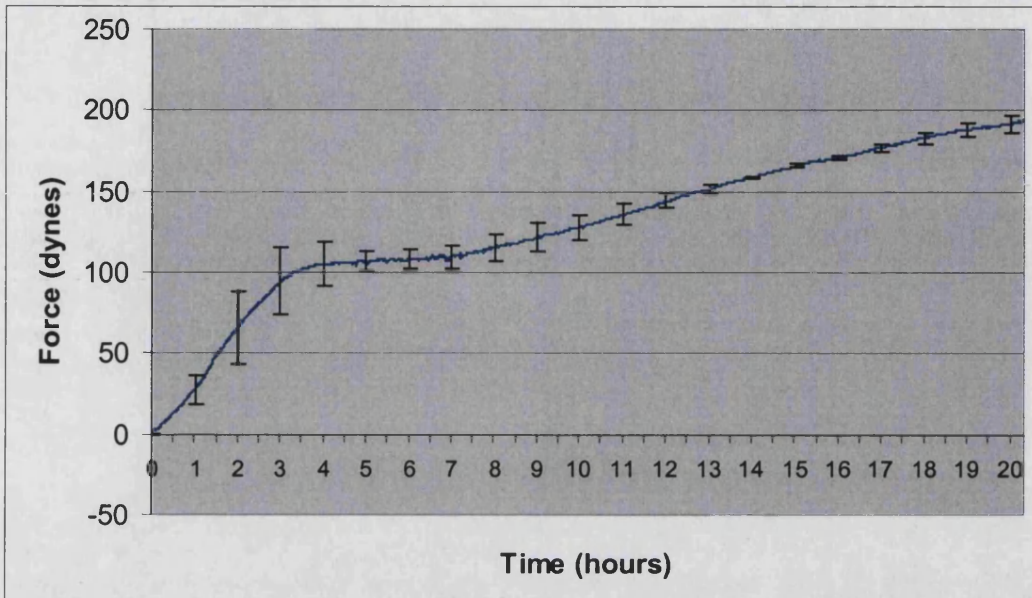
Figure 2.9. The mean contraction profile of a single nodule cell line repeated three times. 5 million viable fibroblasts were seeded into 5 ml collagen lattices. Cells were matched for passage. The error bars represent the standard deviations at hourly intervals.
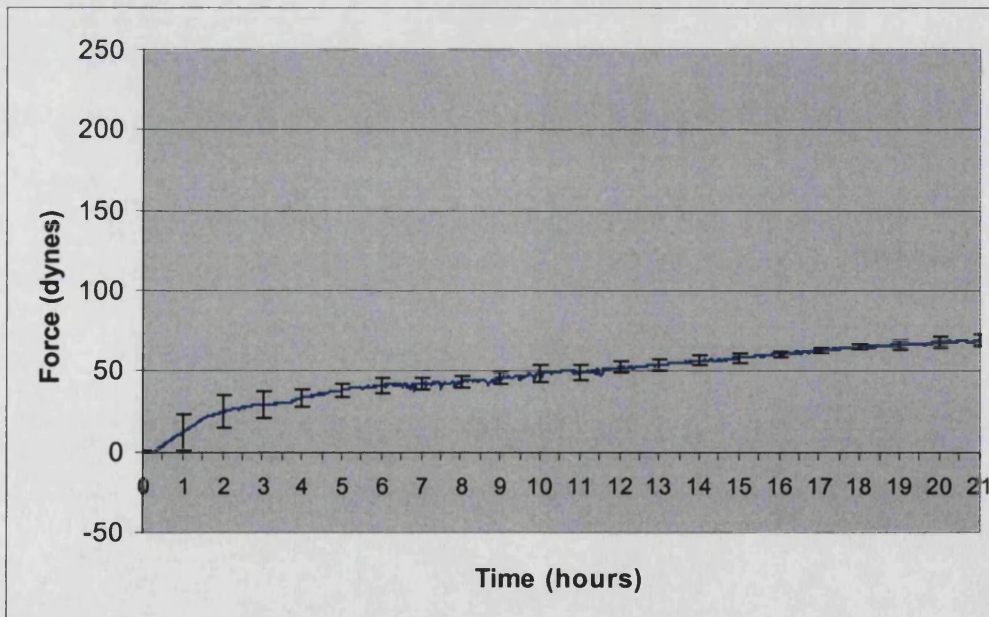
Figure 2.10. The mean contraction profile of a single cord cell line repeated three times. 5 million viable fibroblasts were seeded into 5 ml collagen lattices. Cells were matched for passage. The error bars represent the standard deviations at hourly intervals.
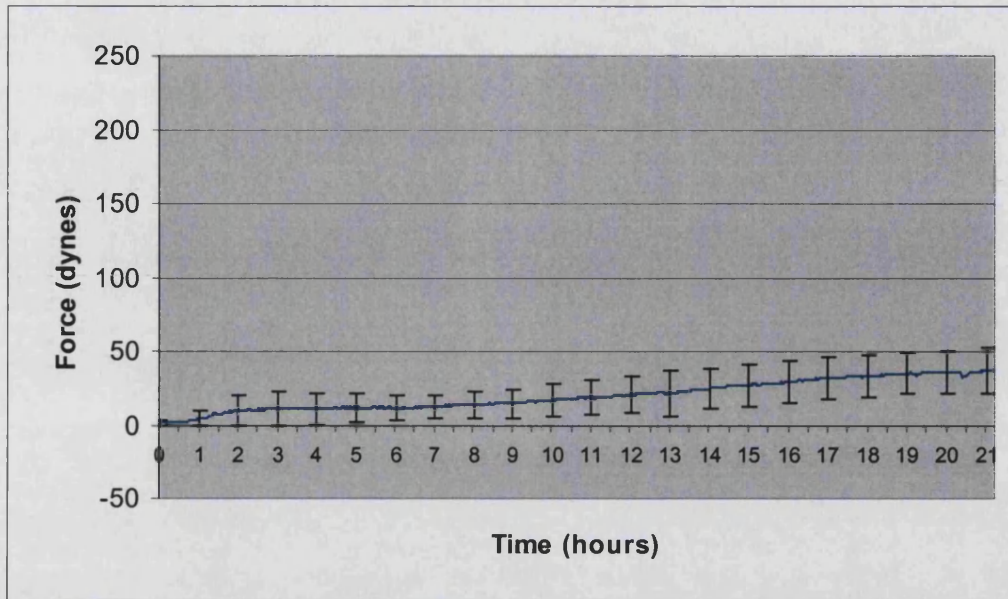
Figure 2.11. The mean contraction profile of a single carpal ligament cell line repeated four times. 5 million viable fibroblasts were seeded into 5 ml collagen lattices. The error bars represent the standard deviations at hourly intervals. (Note: viability > 90%)

This significant lack of force generation by this cell line was surprising and thus the reproducibility experiment was repeated with a second carpal ligament cell line, illustrated in figure 2.12. The trace is displayed as a mean value over time for three repeats of the same cell line +/- standard deviations. Mean force generated at 20 hours was 41 dynes SD ± 7.1 dynes. Again this was low compared with other cell types investigated here and in the literature. Figure 2.12 shows the percentage of viable cells remaining in 5 ml collagen lattices seeded with 5 million cells and left to contract over 24 hours. In all cell types the number of viable cells was high, above 90%, and there is no significant difference in viability between the three groups. Any variation in contraction profiles seen between cell types therefore cannot be attributable to differential cell death in the 3D lattice.
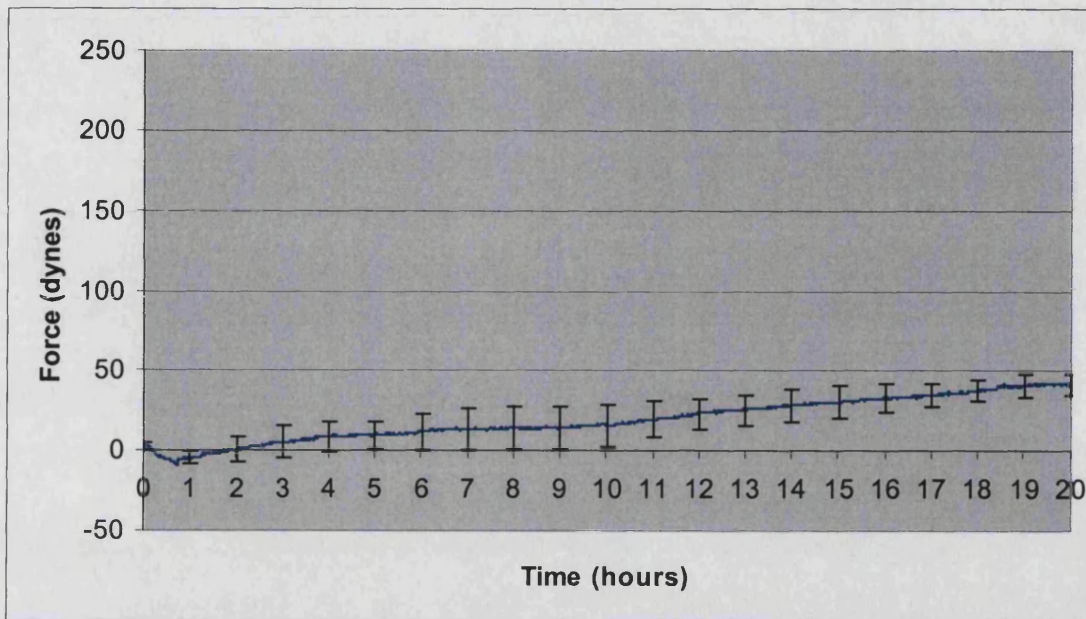
Figure 2.12. The mean contraction profile of a different single carpal ligament cell line to figure 2.11. repeated three times. 5 million viable fibroblasts were seeded into 5 ml collagen lattices. The error bars represent the standard deviations at hourly intervals. (Note: viability >90%)
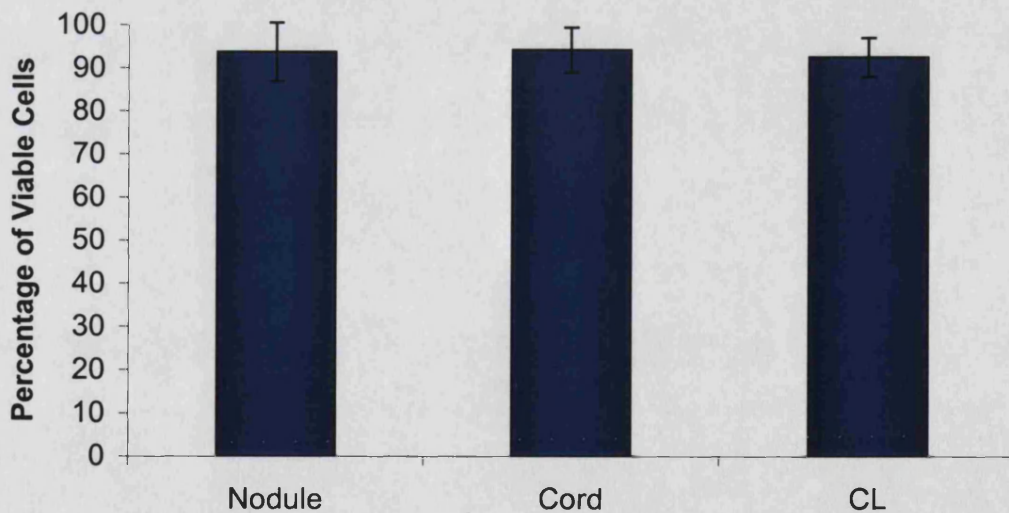
Figure 2.13. The mean percentage of viable cells extracted from collagen lattices at 24 hours from nodule cord and carpal ligament cell lines (CL). In all cases n=4. Note that there is high cell viability with no significant cell death at 24 hours and there is no significant difference between groups.

71

DISCUSSION

Initial experiments on the culture force monitor using collagen gels seeded with a dermal fibroblast cell line conformed with previously published literature regarding this type of cell both in the pattern of the trace obtained and in the absolute force values measured.

Eastwood *et al* (1996) described three phases of contraction seen in dermal fibroblasts populated collagen lattices using the CFM. The first phase up to 8 hours was characterised by rapid generation of force, and by observing changes in cell morphology, they determined this to be due to cell attachment and locomotion within the collagen gel. The second phase between 8 and 15 hours showed a plateauing of force and the subsequent third phase was where a steady state was reached and the contractile forces of the cells balanced the resistance within the matrix.

The initial studies here with a single dermal fibroblast cell line corresponded well with these observations demonstrating all three phases. The methods therefore appear reliable in my hands.

The true plateau only seemed to occur just at 15 hours with continued force generation up to this point. Previous reports of the amount of force generated by dermal fibroblasts using this model vary somewhat (Eastwood *et al*, 1996, Eastwood *et al*, 1994; Brown *et al*, 1998) ranging from 20 to 56 dynes per million cells, but our data falls within this range, peak force being 125 and 131 dynes respectively for the two repeats, or 25 and 26.2 dynes per million cells.

From these two experiments alone the technique appeared reproducible however it was important to confirm this in the cell lines to be investigated. The Dupuytren's nodule and cord cell line repeats experiments gave very consistent results with low standard deviations indicating little variability between runs (figures 2.9 and 2.10) and hence good reproducibility.

Results from the carpal ligament fibroblast cell line were intriguing, as they were not expected to produce so little force. Most cells investigated and published in the literature to date produce at least a moderate contractile force equivalent to that of a dermal fibroblast. The results however were reproducible, with near 100% cell viability, with a similar pattern of trace through all repeats and small standard deviations. A second cell line was examined because of the unexpected finding, but again consistently generated minimal force over the time period studied.

Bell *et al* (1979) demonstrated that collagen gel contraction was proportional to the number of cells seeded into the lattice. Our study of cell viability at 24 hours confirmed that the differences seen in contractile properties at this early stage were not due to differential cell death within the collagen gels and hence altered cell numbers.

SUMMARY:-

- It has been demonstrated that the method employed for using the culture force monitor by this operator is reliable, reproducing results similar to those previously published for dermal fibroblasts.

- The results are reproducible within single cell lines of the types to be used in the subsequent investigations with low standard deviations.

- The differing contraction profiles observed between cell types and specifically the paucity of contraction in carpal ligament and some Dupuytren's cord cell lines are not due to differential cell death within the collagen lattices.

Having confirmed the reliability using dermal fibroblasts and obtaining comparable results to published reports, and establishing the reproducibility of the experimental model, the subsequent experimental data could be interpreted as a true representation and not due to variability in the system. The basic contraction profiles of 9 Dupuytren's nodule, 10 Dupuytren's cord and 4 control carpal ligament cell lines were then studied. The mean contraction profile for each type of cell line was calculated using Microsoft Excel (Microsoft corporation.). The mean force generated at 20 hours and the mean gradient of the contraction profile at 2 hours and 20 hours after set up was also calculated. The gradient was determined by measuring the rate of change in force between either 1 and 2 hours or 19.5 and 20.5 hours respectively and expressed as dynes per minute. Thus the "two hour" gradient was calculated as the force measured at 2 hours minus the force at 1 hour, divided by 60 (minutes) to obtain a value in dynes per minute. A similar method was used to obtain the "twenty hour" gradient using the force value at 20.5 hours minus that at 19.5 hours and dividing by 60. A positive value indicated an increasing gradient whilst a negative value represented a falling slope. Statistical analysis of the data was performed using the students-t test utilising the Sigma Stat. Software Package.

2.5.4. System Overloading

At the end of recording the basic contraction profile each collagen gel was serially overloaded on the system. This was achieved by rapidly hand turning the micrometer wheel on the CFM mounting stage by 30 micrometers leading to an increase in longitudinal, uniaxial tension on the gel of around 20 to 25 dynes. The system was then left for 30 minutes to record the response to this rapid loading. The procedure was repeated a further three times so totalling four rapid overloads and four 30-minute "post overload" responses. The experiment was terminated at this point and the gel taken off and processed (Section 2.5.6.)

2.5.5. Addition of TGF-β_1

After basic contraction profiles and overloading data were collected for the cell lines as detailed above, the effects of pre-treatment with Transforming Growth Factor-β_1(TGF-β_1, R & D Systems) were investigated. Fibroblast cultures to be studied were again grown in T225 tissue culture flasks and when judged to be three to four days from sub-confluence

the media was changed and the cells then incubated with normal growth media supplemented with TGF-β_1 at the same concentration as used for 2D myofibroblast stimulation, 2ng per ml. The fibroblasts were then used after three days incubation in this media (No further media changes were carried out) for preparation of the FPCL. The collagen gels were set up in exactly the same way as described above and TGF-β_1 was not included in the growth media used in gel manufacture or subsequent gel floatation and nutrition. In this way the fibroblasts were merely pre-treated with TGF-β_1.

Collagen gel set up on the CFM and measurement of the resulting contraction profiles was performed in an identical fashion to non pre-treated fibroblasts and the same parameters were calculated for comparison. At between 20 and 24 hours the FPCLs were also serially overloaded four times and the post overload responses measured. Finally the gels were removed from the CFM and processed as described in the following section.

2.5.6. Removal and Processing of Gels from the CFM

At the conclusion of each experimental run the data was saved and the fibroblast populated collagen lattice removed from between the bars. As illustrated in figure 2.14 it was cut in two, and half was snap frozen in liquid nitrogen before being stored at -80^0C. The media was also kept and frozen as aliquots in case subsequent analysis was thought to be of use. The other half of gel was processed in order to study its morphology. It was rapidly fixed by immersion in 10% formal saline (see Appendix II for formulation) and then left for 24 hours. At this point the gel was washed thoroughly in PBS and stored in a bijou tube at 4^0C before subsequent staining for light microscopy or immunohistochemical staining for α-smooth muscle actin fibres.

2.5.7. <u>Staining Fibroblast Populated Collagen Lattices for Light Microscopy</u>

Basic cellular morphology within FPCLs run on the culture force monitor was assessed by staining with Toluidene blue. One quarter of each gel was soaked in a 1% solution of Toluidene blue (No. G298, Gurr's Ltd, London, UK) for 15 seconds and then washed thoroughly with three changes of PBS. It was then observed under light microscopy (Zeiss Axioscope 20). Digital images were taken and comparisons made between Dupuytren's nodule, cord and carpal ligament cell lines.

2.5.8. <u>Staining Fibroblast Populated Collagen Lattices for α-Smooth Muscle Actin</u>

To assess myofibroblast content and orientation within the collagen gels small rectangular sections of the gel previously fixed and stored in PBS at 4^0C were cut. The position of origin within the gel was noted as this has a bearing on the lines of stress and hence cellular orientation (Eastwood *et al*, 1998). In each case a portion from the middle of the gel was used but additionally some pieces from the delta zones were stained in selected cell lines (see figure 2.14.).

The segment of gel to be stained was soaked in ice-cold methanol in a Universal container on an orbital shaker (Luckham R100 Rotatest Shaker) for 1hr to permeabilise the cells. The gel was then washed with three changes of PBS for a further 1hr again on the orbital shaker.

The gel was placed in a well of a 24 well plate. It was incubated overnight in the dark at 4^0C bathed in 500μl of the primary antibody, a mouse monoclonal anti α-smooth muscle actin antibody (Sigma) at 1in 1000 dilution in PBS. A second piece of gel to be used as a negative control was placed in a separate well and incubated in the same way with only 500μl of PBS.

The following morning the gels were transferred to separate universal containers and washed with three changes of PBS on an orbital shaker for a total of 40 minutes.

They were then placed in another well of the 24 well plate and each incubated with 500µl of the secondary antibody solution covered in foil on orbital shaker for 1hr. The secondary solution was a FITC conjugated rabbit anti-mouse monoclonal antibody (Dako) at 1 in 400 dilution in PBS with Propidium Iodide at 1 in 50 dilution as a nuclear counterstain.

Finally the gels were again washed with three changes of PBS for 1hr in a Universal container wrapped in foil to keep them in the dark and prevent degradation of the fluorescence.

The pieces of gel were placed on a glass slide, two drops of DABCO (see appendix II for composition) added and then covered with a cover slip for viewing. Stained pieces of gel were viewed under ultraviolet light on a microscope at x 200 and x 400 magnification. Myofibroblasts positive for α-smooth muscle actin demonstrated intra cellular fibres that fluoresced bright green. Negative cells showed a red nucleus with diffuse pale red or orange cytoplasmic staining.

Delta zone: stained in
a selection of gels

Stained with
Toludine blue

Snap Frozen in
LN$_2$

Section stained for α-
smooth muscle actin
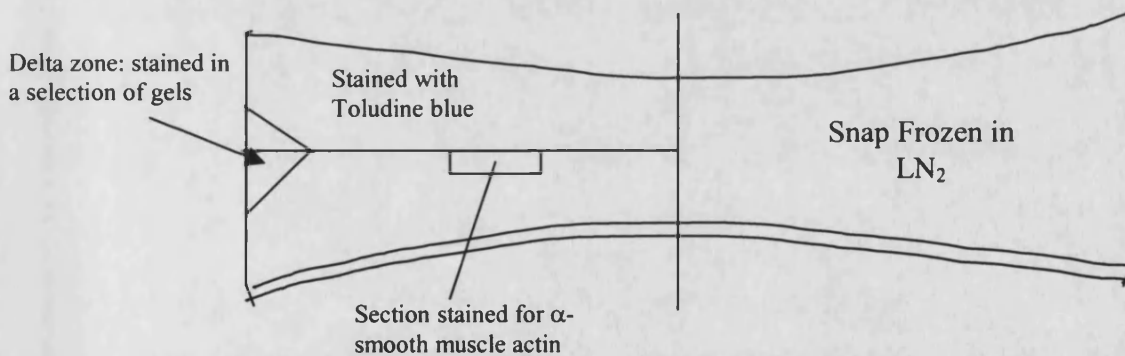
Figure 2.14. Processing of CFM gel at termination of runs.
Diagram indicating the whole collagen gel at the conclusion of experimental runs and the fate of different regions of the gel.

2.5.9. <u>Assessment of Cell Alignment within Collagen Gels</u>

A broad observation was made that there appeared to be morphological and orientation differences between the contractile Dupuytren's cell lines and the relatively non-contractile controls. It was therefore decided to attempt to analyse and quantify cell orientation within the gels stained for α-smooth muscle actin. Two methods were devised and tested initially

in 6 nodule cell lines and 6 gels seeded with carpal ligament fibroblasts (4 different cell lines, 2 repeated). Digital images of the stained gels were captured at x 400 magnification, using a Zeiss Axioscope 20 microscope with a Leica DC200 mounted camera and software (Leica DC Viewer, Leica Microsystems-Ltd). By focusing in a specific plane a 2D slice of the gel was captured and these were studied using image analysis software (UTHSCSA Image Tool).

By correct orientation of the rectangular piece of gel on the microscope slide the overall orientation of the whole gel and its long axis was known. The first method required the long axis of the all of the cells in focus to be drawn through them. The angle of this from the longitudinal gel axis was calculated from the slope of the line (figure 2.15a). The mean angle of orientation of the in focus cells was then calculated for each gel. A value of 0^0 would suggest perfect alignment along the gels long axis whilst an angle of 90^0 would suggest an orientation at right angles with the standard deviations giving an indication of the variability of the alignment.

The second method examined cell body height utilising the theory that aligned cells are spindle shaped as are the cell bodies themselves. Fibroblasts aligned with the long axis of the gel will therefore have shorter cell body heights when measured in this plane compared with more stellate cells or fibroblasts aligned at right angles to the axis of the gel (see figure2.15.b). The mean cell body height of cells in focus was determined for each gel and the overall means for each cell type then compared.

The first method was considered to be more reliable and applicable to the characteristic to be quantified (see chapter 3.9) and this was therefore applied to all other cell types in the study with the alignment of 6 Dupuytren's nodule, 5 Dupuytren's cord, 4 Carpal Ligament, 5 TGF-β_1 stimulated nodule, 5 TGF-β_1 stimulated cord and 4 TGF-β_1 stimulated carpal ligament cell lines being investigated.

Orientation of the
collagen gel

Orientation of the
collagen gel
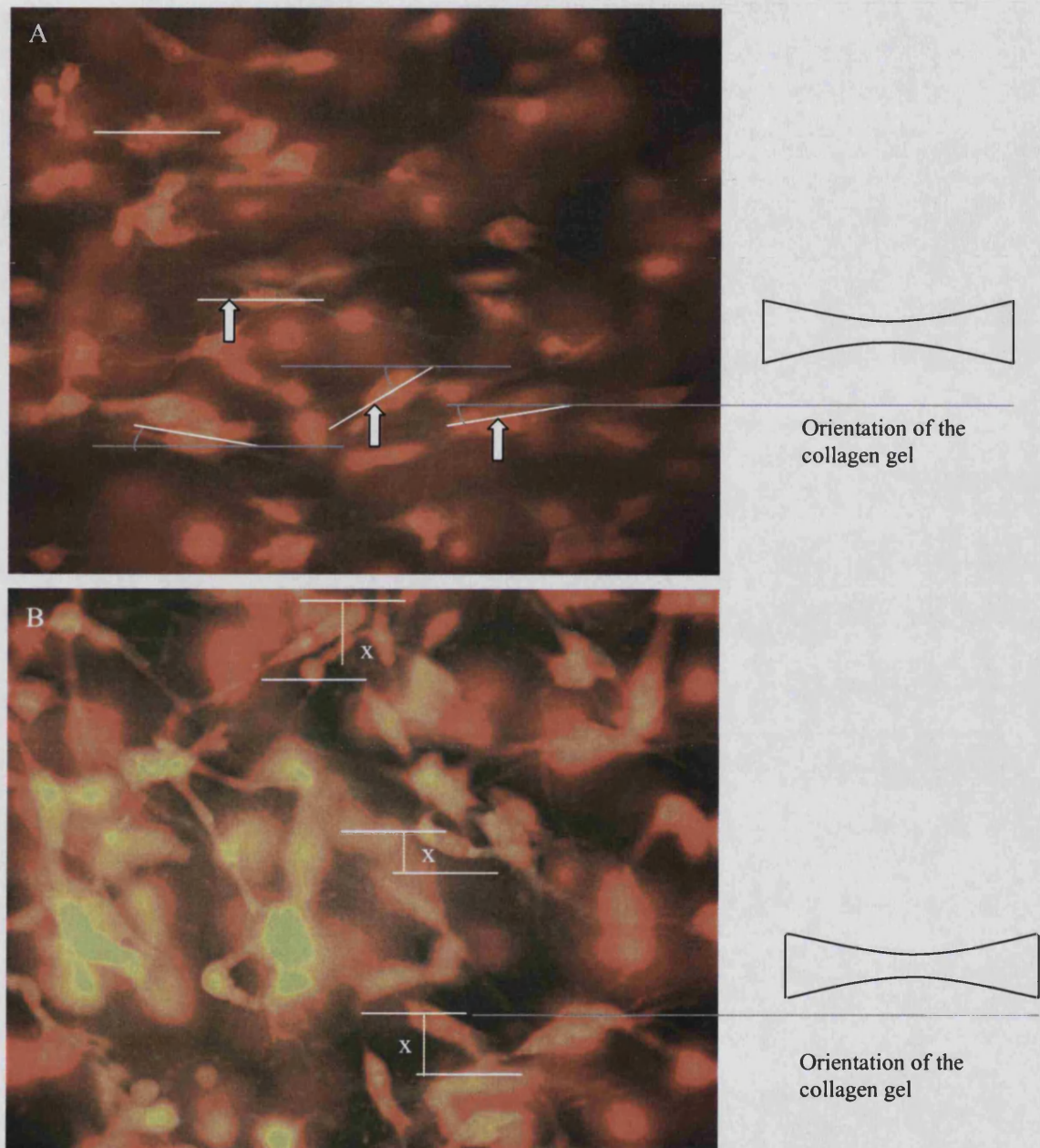
Figure 2.15. Methods Tested for Determining Degree of Cellular Orientation Within a Collagen Lattice. A) Indicates how the long axis was drawn through all the fibroblasts in focus within a random field (arrows). With the orientation of the collagen gel as a whole known, the relative angle of each cells long axis from that of the gel's long axis could be determined by measuring the slope of the lines (arrows). B) Illustrates the second method of measuring the relative height of fibroblast cell bodies (represented by distance x) at right angles to the orientation of the long axis of the whole gel.

Chapter 3

Results

3. Results

3.1. Histological assessment of clinically defined Dupuytren's nodules and cords

3.1.1. Introduction

Dupuytren's disease tissue has certain characteristic features when examined histologically depending upon the area that is observed. Luck (1959) classified these into proliferative, involutional and residual stages. Proliferative disease is highly cellular, randomly organised and the hyperplastic appearance can even be such as to confuse lesions with fibrosarcoma (Enzinger and Weiss, 1995). The involutional phase has increased fibroblast alignment although it is still cellular. The residual stage is relatively acellular with thick bundles of collagen, which are orientated with the lines of stress. It resembles the appearance of tendon.

The features of proliferative and involutional stages of disease are found in clinical nodules whereas the cords are tendon like both in gross macroscopic appearance and their residual stage histological appearance. Mayerding *et al* (1941) did note variable cellularity within the lesions and MacCallum and Hueston (1962) considered there to be only two phases of disease activity although these could intermingle even within a single lesion.

Although the above authors have undertaken descriptive studies of the histological appearances related to disease stage, no quantification of the appearances were carried out. This has only been done in a single previous study by Murrell et al (1989) and, as with many other studies, no differentiation was made between primary and recurrent disease and sample numbers were small. It was crucial for the purposes of subsequent experiments in this thesis to be able to say with confidence that clinically determined nodules and cords could be accurately differentiated.

3.1.2. <u>Aim</u>

To **quantify** differences in cellularity of excised Dupuytren's disease tissue categorized on the basis of macroscopic features as nodule or cord.

3.1.3. <u>Materials and Methods</u>

Specimens from routine fasciectomies for Dupuytren's disease were delineated as nodule or cord as outlined in section 2.1. Samples were only used from primary operations for Dupuytren's disease, patients with recurrent disease being excluded. After bisecting the specimens longitudinally as described in chapter 2.1.1, one half of each, containing areas of both cord and nodule, was fixed in 10% formal saline for histological assessment. These fixed specimens were wax embedded and representative sections through the sample taken and stained with haematoxylin and eosin using the standard protocol detailed in 2.2. Sections were examined at x400 magnification and the number of cell nuclei counted in three random areas in each of the nodule and cord regions. The area size (0.04mm^2) was chosen because a 0.2mm x 0.2mm square grid fitted comfortably into a high power field when the image was digitally captured. This was done for n=10 fasciectomy samples. The cord and nodule cellularity was compared using a paired students t-test.

3.1.4. Results

Nodules were generally highly cellular with a random organisation of cells and extra cellular matrix (figure 3.1.1.). Some regions of nodule were seen to contain "nests" of densely packed cells (figure 3.1.4). Other areas did show some reduction in cellularity often with a corresponding increase in alignment and thickening of interspersed collagen and other extra cellular matrix (figure 3.1.5). The cords were markedly hypocellular (figure 3.1.2) with very thick parallel-orientated collagen fibres. Between these the cells were small, thin and elongated, and aligned along the same axis as the collagen bundles. Despite the constant morphology found in the cords there were occasionally small areas within the cord where a nest of hypercellularity could be seen (figure 3.1.3).
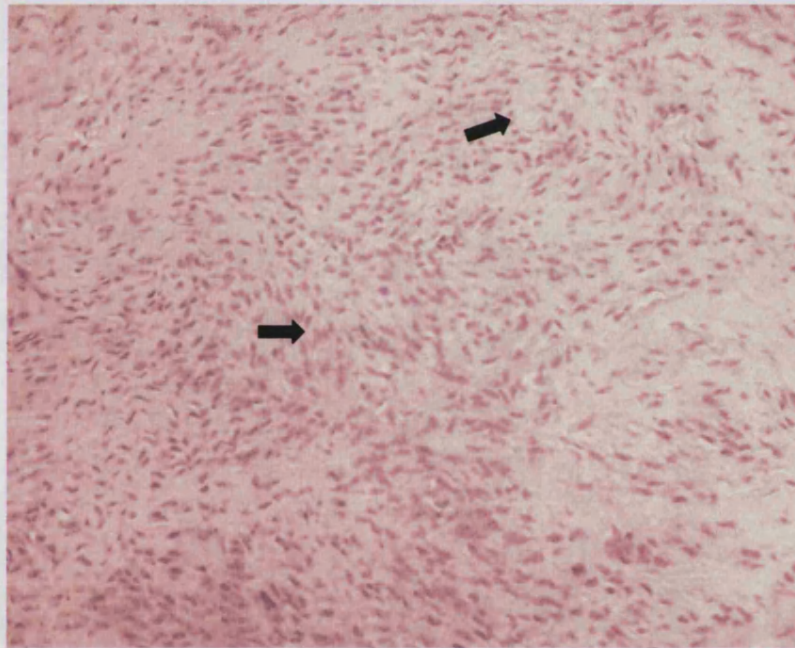
Figure 3.1.1. Typical histological appearances of an area defined as nodule stained with H and E at x 200 magnification. The cellular tissue displays a lack of organisation and alignment, as seen by swirls of cells (arrows).
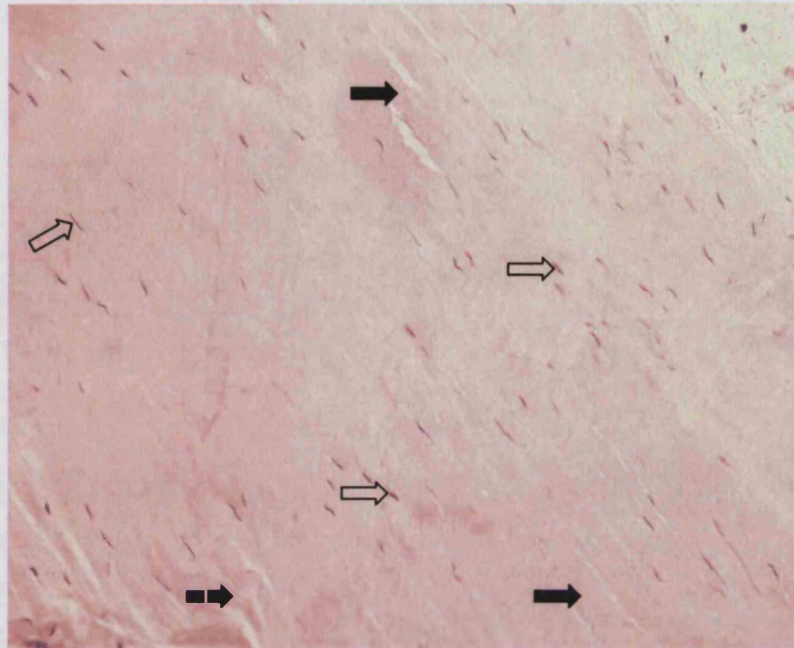
Figure 3.1.2. Typical histological appearances of an area defined as cord stained with H and E at x 200 magnification. The specimen is relatively acellular with thick parallel-aligned collagen bundles (solid arrows) surrounding the elongated cells (open arrows).
Note: At the same magnification the difference in cellularity between nodule in Fig 3.1.1 (highly cellular and unaligned) compared to the appearances here of cord (hypocellular and aligned)
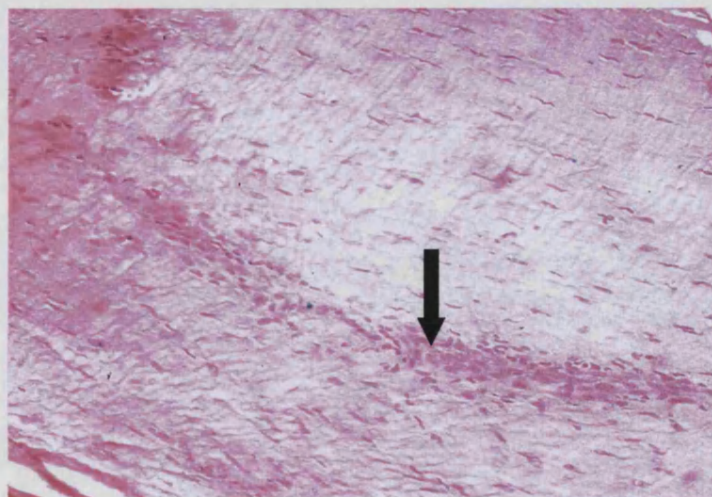
Figure 3.1.3 Histological appearances of a hypercellular focus within a cord. An area within a well-defined cord where a nest of hypercellularity (arrow) is evident within the surrounding uniform, collagen rich tissue.

Figure 3.1.6 shows the mean cellularity of ten nodules and cords specimens from separate patients all with primarily operated disease. Nodule cellularity was 105.61 cells per $0.04mm^2 \pm 52.4$ (Range 38-242 cells per $0.04mm^2$). Mean cord cellularity was only 36% of this at 38.5 cells per $0.04mm^2 \pm 20.3$ (Range 10-155 cells per $0.04mm^2$). The differences observed were statistically significant $p<0.01$. Despite the broad spectrum of patients from which the diseased tissue was excised the cellularity indexes within nodules or cords were remarkably similar with relatively narrow standard deviations despite some overlap of the ranges. This may be particularly pertinent to primary disease rather than recurrence. Recurrent disease may contain more variable features, often with less clear differentiation of nodules and cords than is encountered in primary, previously un-operated disease. This heterogeneous, macroscopic appearance may reflect an equally heterogeneous fibroblast population so obscuring important differences between nodule and cord.
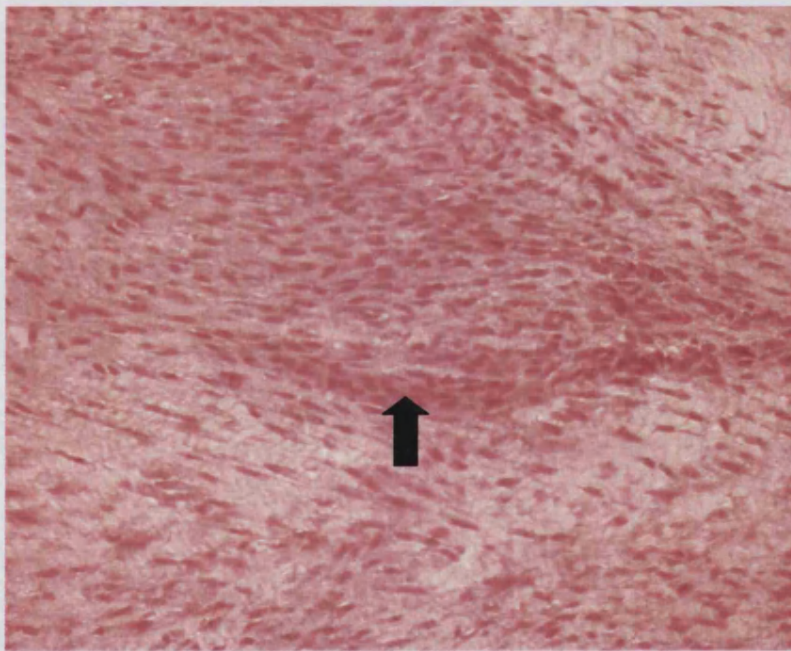
Figure 3.1.4. An area of nodule at x 400 magnification stained with H and E illustrating a "nest" of densely packed cells (arrow).
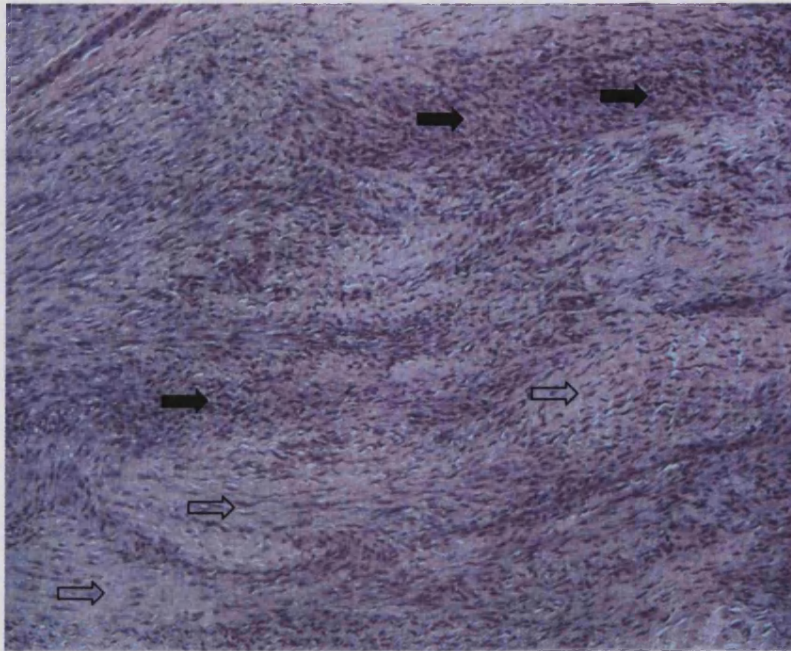
Figure 3.1.5. An area of nodule at x 200 magnification stained with H and E illustrating mixed areas of high cellularity (solid arrows) surrounding more organised collagen rich regions (open arrows).
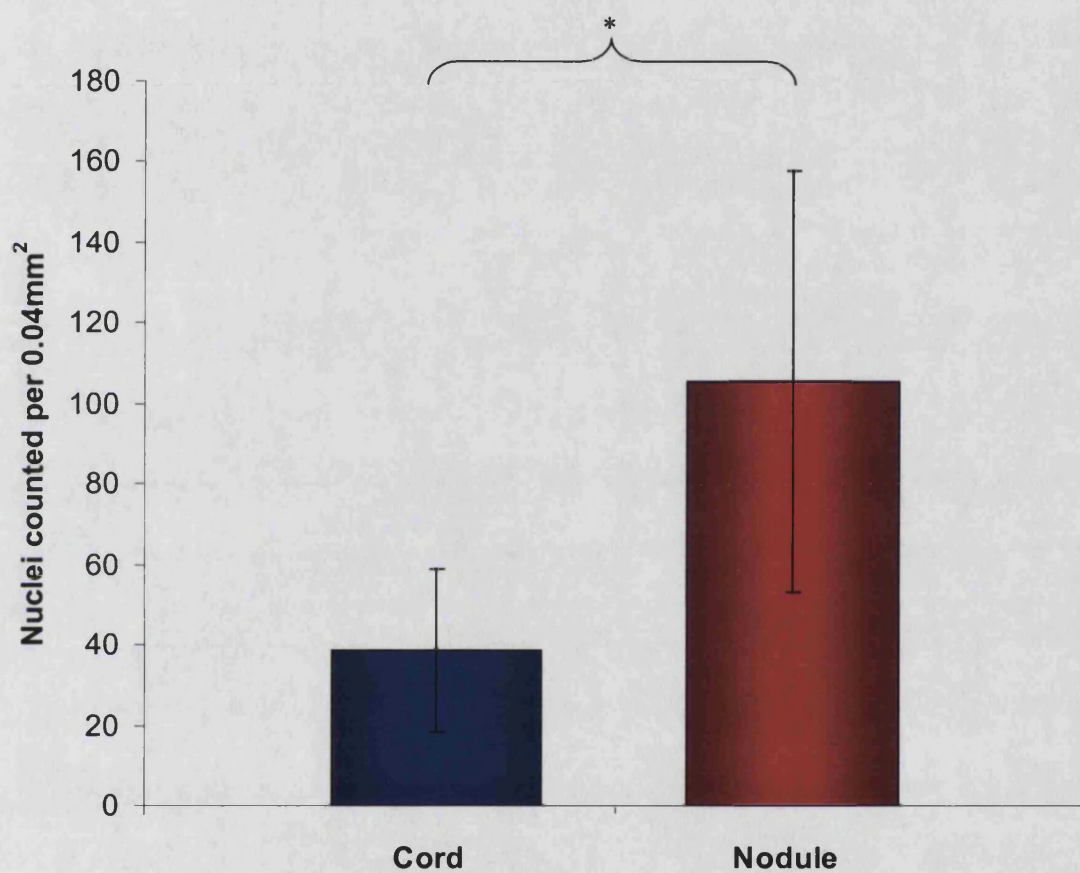
Figure 3.1.6. The mean cellularity of Dupuytren's disease tissue comparing regions defined clinically as nodule and cord. The error bars represent the standard deviations between n=10 fasciectomy specimens, expressed as nuclei counted per $0.04mm^2$.

* $p < 0.01$. The cellularity of regions defined clinically as Dupuytren's nodule are significantly more cellular than those defined as Dupuytren's cord.

3.1.5. Discussion

The findings presented here agree well with previous published descriptions of the histology from various regions of Dupuytren's disease tissue. The majority of literature regarding Dupuytren's disease histology to date has been descriptive, detailing the microscopic appearances and relating them to the clinical features of the disease or the area of the specimen from which the section originated (Meyerding *et al*, 1941; Luck, 1959; Larson *et al*, 1960; Reviewed by Shum, 1990).

In order to study specific nodule or cord cell cultures, those areas that appear to be macroscopically well defined nodules or cords have been determined clinically. The histological appearance of these regions has then been quantified by determining their cellularity. The nodules correspond to the proliferative stage disease described by Luck (1959) being highly cellular and relatively disorganised. The cords were sparsely populated by cells, which were elongated and arranged parallel to thick bundles of collagen (figure 3.1.3), Luck's residual stage. He also described an involutional stage where again there was high cellularity but the cells were beginning to align with the lines of stress. These areas were difficult to define accurately, occasionally being seen within nodules but often only in part or at the edge of a well defined nodule.

As noted by Meyerding (1941) and later by MacCallum and Hueston (1962) a degree of variability was seen in the histological appearances especially within nodules, often regions of increased cellularity merging with or occurring within, less populated regions (figure 3.1.5). These were probably the areas Luck referred to as involutional. If sections were examined progressively from a nodule to a cord in continuity one was often able to observe a transition encompassing all three of Luck's stages, from proliferative to involutional and finally residual (illustrated in figure 3.1.7). McCann also noted this in 1993.

Murrell *et al*, 1989 also calculated cell density in Dupuytren's disease sections, finding 4060 fibroblasts per mm^2 in nodule areas and 835 per mm^2 in cords. If the results presented here are multiplied by 25 to express them as cells per mm^2 then there is a very good agreement in the cord results at 962.5 cells per mm^2. The result for nodule is somewhat different to that found by Murrell *et al*, at only 2640 cells per mm^2, 65% of their value. The standard errors are also less than those stated by Murrell, however the overall range does extend to well above their mean cell density and it may be that selection or definition variability are enough to account for the differences observed.

It is remarkable that despite high n numbers (n=10) the range of cellularity and thus standard deviations are tight for both nodule and cord indicating a marked degree of consistency in the histological features of primary Dupuytren's disease nodules and cords.

In this study nodules may have included less "nests" of intense cellularity or more areas of collagen bundles where cells became less abundant. Furthermore tissue samples were all obtained from primary fasciectomies for Dupuytren's disease. Murrell does not state in his methods if specimens were obtained from primary operations, patients with recurrent disease or a mixture. They could have found a much higher cellularity in patients with recurrent disease where there may have been increased activation and proliferation of fibroblasts within aggressive nodules. Recurrent disease may represent a different spectrum of Dupuytren's disease to that investigated here. By restricting specimens to primary disease throughout this and the subsequent study the aim is to gain an insight into Dupuytren's disease in its pure form, not altered by intervention and excision.

By calculating the cellularity of the clinically defined regions of nodule and cord and not including the intermediate areas, it has been possible using histological examination to statistically prove that the regions labelled nodule are quantitatively different from those labelled cord.

Given this fact it was possible in the following experimental studies to define the cellular characteristics of fibroblasts established in culture specifically from nodule or cord.
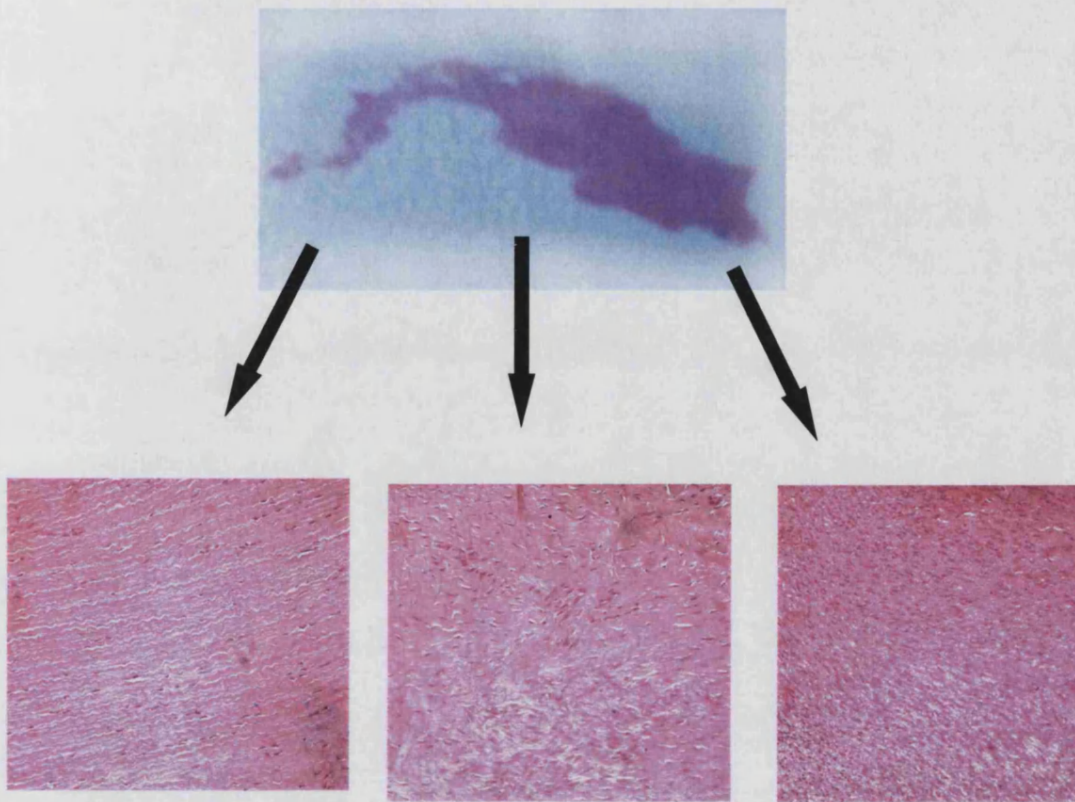
Figure 3.1.7. The transition of histological appearances in a single specimen of Dupuytren's Tissue. Hypercellular nodule tissue is seen on the right panel, which mixes into intermediate zone tissue shown in the centre panel. This is less densely populated with cells and collagen alignment can be seen starting to appear. This finally transforms into cord tissue with few cells between thick parallel collagen bundles seen in the left panel.

SUMMARY

- Regions of Dupuytren's disease defined clinically as nodule and cord were different with nodule being three times more cellular then cord when quantified histologically.

- By detailed observation and quantification of tissue from primary cases of Dupuytren's disease it has been possible to identify classically described regions but detail the changes seen across the spectrum of appearance more precisely.

3.2. Myofibroblast Phenotype in Tissue Sections Cut from Specimens of Dupuytren's Nodules, Cords and Control Carpal Ligament

3.2.1. Introduction

The myofibroblast is a specialised cell type so called because of its similarities with both fibroblasts and aspects of smooth muscle cells (Gabbianni *et al* 1971, Shultz and Tomasek, 1990 in Dupuytren's Disease). These cells have been implicated in wound healing and specifically granulation tissue contraction, many features of which are analogous to those encountered in Dupuytren's disease (Gabiani and Majno, 1972). These cells contain numerous intra-cellular microfilaments a key feature of which is their positive staining for alpha smooth muscle actin (α-SMA). This is currently the most reliable method for identifying differentiated myofibroblasts (Tomasek *et al*, 2002). The actual origin of these cells has been the subject of much debate, one that remains not fully resolved. Most authors however, believe them to be transformed fibroblasts (Shultz and Tomasek, 1990), and they appear to play a central role in fibrotic and wound healing processes (Walker *et al*, 2001). They have been linked to increased production of collagen and ECM (Petrov *et al*, 2002, Serini and Gabbiani, 1999) as well as being involved in cell contraction and motility. From these features it is clear that they are likely to be important in Dupuytren's disease both in terms of the excess collagen deposition and in the contractures observed as disease progresses. Indeed many authors have identified myofibroblasts in Dupuytren's nodules (Vande Berg *et al*, 1984; Pasquali-Ronchetti *et al*, 1993; Badalamente *et al*, 1983). They have, however only been reported once in cord specimens by Pasquali-Ronchetti *et al* (1983) in one patient. As outlined in chapter 1.6 contractures are thought to occur partly as a result of cell-mediated contraction causing matrix shortening. Collagen gel contraction has been correlated with the presence of myofibroblasts or α-SMA (Tomasek and Rayan, 1995 and Hinz *et al*, 2001) thus it is clear that myofibroblasts may be crucial in Dupuytren's contracture development. Although this cell phenotype has been identified in regions of Dupuytren's tissue its presence has not been quantified. Having determined a significant difference in cellularity between regions defined as nodule and cord from Dupuytren's fasciectomy specimens, it was desirable to investigate the prevalence of the myofibroblast phenotype within these areas.

3.2.2. Aim

To determine the frequency of cells demonstrating the myofibroblast phenotype in regions of Dupuytren's tissue defined as nodule and cord.

3.2.3. Materials and Methods

Sections of Dupuytren's tissue were cut from paraffin blocks as described in section 2.2. Similar sections of carpal ligament tissue specimens were used as comparisons. Antigen retrieval was found to be optimal using a steaming method to prevent lifting of the fibrous material. The sections were stained for alpha-smooth muscle actin (α-SMA) (Skalli et al, 1986) using the two different methods detailed in section 2.3. The first employed a routine Streptavidin Alkaline Phosphatase method and a vector red final substrate enabling visualisation of positive cells using light microscopy where a dark red colour was observed within the cell cytoplasm. The second method was similar until the final stages when a FITC conjugated secondary antibody was used so that positive cells fluoresced green under ultraviolet light. A weak Harris's haematoxylin counterstain was used in all sections to stain nuclei pale blue, and negative controls (where no primary antibody was included) were used for each. Sections of tonsil and intestine were used in each run as positive controls, although most sections contained blood vessels which acted as internal positive control regions. The staining was carried out on a total of sixteen Dupuytren's specimens each with previously clinically defined areas of nodule and cord. Three carpal ligament samples were also studied.

3.2.4. Results

Both methods of staining for α-SMA yielded similar results neither appearing to be superior to the other. Representative areas of nodules using both methods are shown in figures 3.2.1 and 3.2.2 at x 200 magnification. The positive staining myofibroblasts are generally clustered in areas of high cellularity and are easily identifiable adjacent to regions of non-staining cells where only the pale blue counterstained nuclei can be seen.
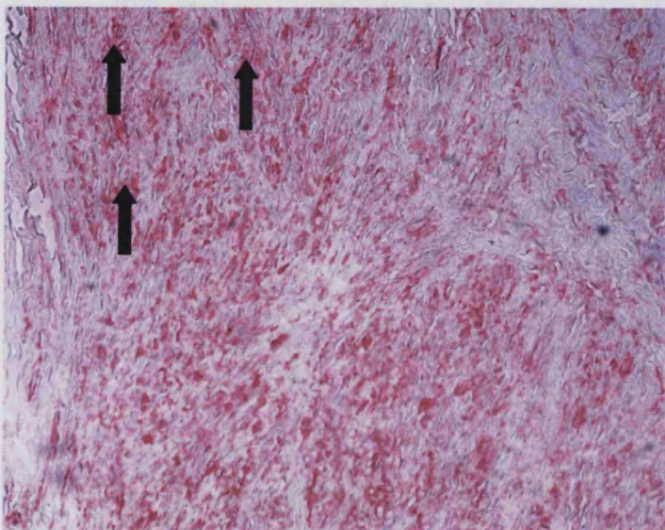
Figure 3.2.1. Section of Dupuytren's nodule stained for α-SMA using alkaline phosphatase and vector red final substrate method at x 200 magnification. There is widespread positive red staining of most of the cells within this field. This is especially strong in the upper left corner (arrows)
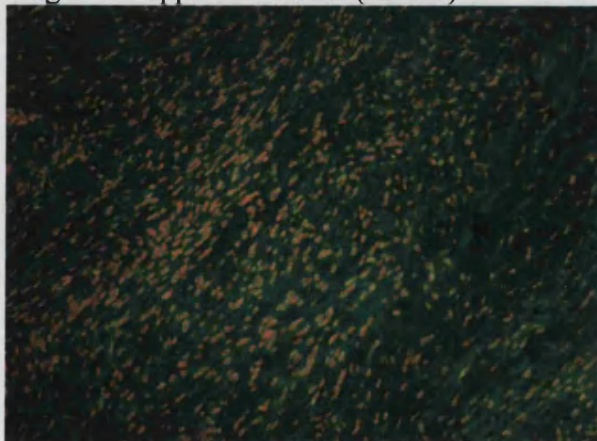
Figure 3.2.2. Similar section of Dupuytren's nodule as above stained for α-SMA using a FITC conjugated secondary antibody viewed under uv light at x 200 magnification. There is again widespread positive green staining of most of the cells within this field.

At higher power (x 400) the positive staining can be seen very clearly and is observed to localise around the cell nuclei often towards the periphery of the cytoplasm (figure 3.2.3). Not all areas of high cellularity contained myofibroblasts (figure 3.2.4); indeed 3 of the nodules contained no identifiable α-SMA positive staining cells.
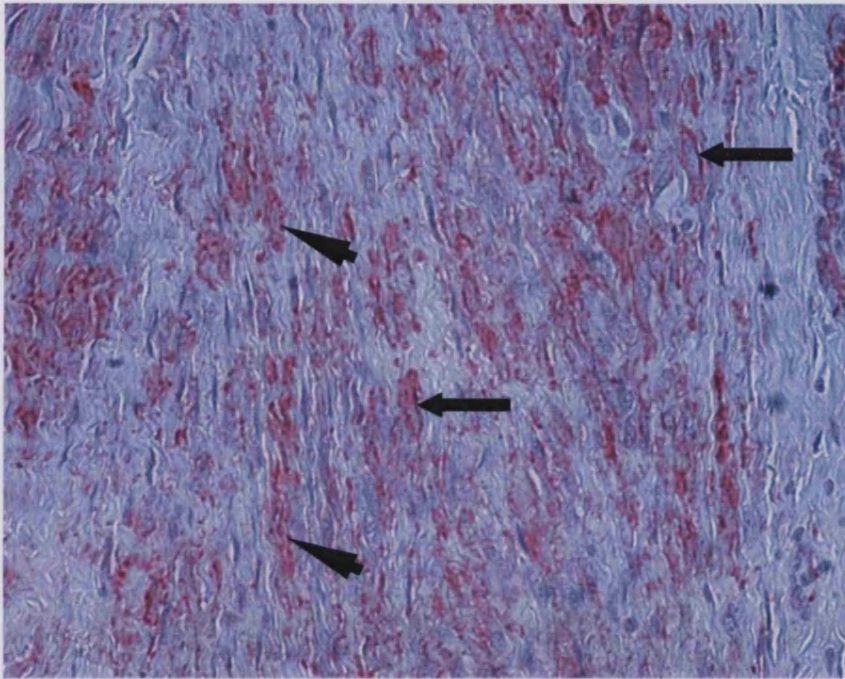
Figure 3.2.3. Section of Dupuytren's nodule stained for α-SMA using alkaline phosphatase and vector red final substrate method at x 400 magnification. At this higher power the distribution of the positive red staining is evident localised within the cytoplasm surrounding cell nuclei. It appears as longitudinal filaments (solid arrows) or dense circles (arrow heads) depending on whether actin fibres have been sectioned along their length or transversely.

Regions defined as cord with sparse fibroblast numbers and thick parallel orientated collagen bundles as described in section 3.1.4, contained virtually no positive staining cells using either method. Figures 3.2.5 and 3.2.6 illustrate this at x 200 magnification. In three of the specimens, however there were regions within the area defined as cord that were more cellular, as noted in standard histology (section 3.1.4) and it was in these regions that some myofibroblasts were identified. This is illustrated in figure 3.2.7 where obvious cord type morphology is interrupted by a highly cellular focus that stains intensely for α-SMA.
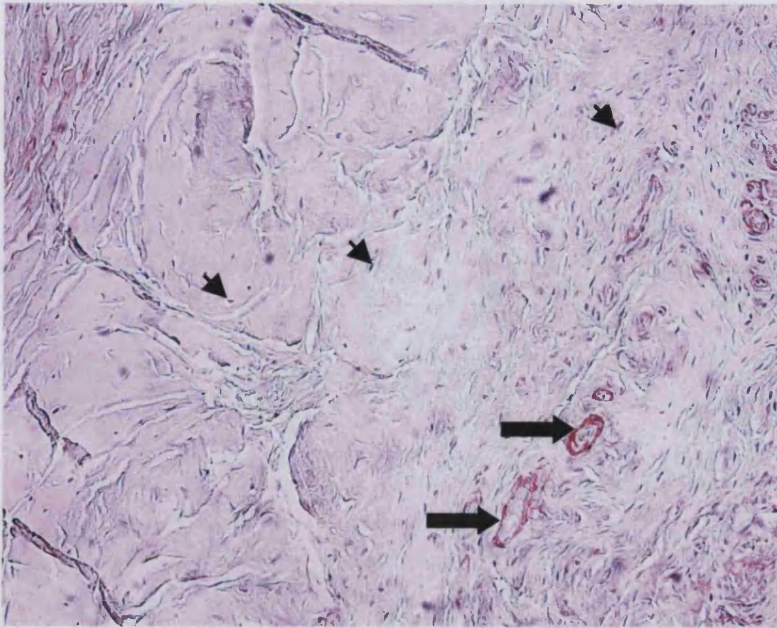
Figure 3.2.4. Section of Dupuytren's nodule stained for α-SMA using alkaline phosphatase and vector red final substrate method at x 200 magnification. Note in this specimen (As in 3 out of 16 specimens) there is no positive red staining despite the high cellularity (cell nuclei shown with arrow heads). Vascular smooth muscle cells however have stained positively around blood vessels (arrows)

Figure 3.2.5. Section of Dupuytren's cord stained for α-SMA using alkaline phosphatase and vector red final substrate method at x 200 magnification. There is no positive red staining of cells within this field. (cell nuclei shown with arrow heads)

95
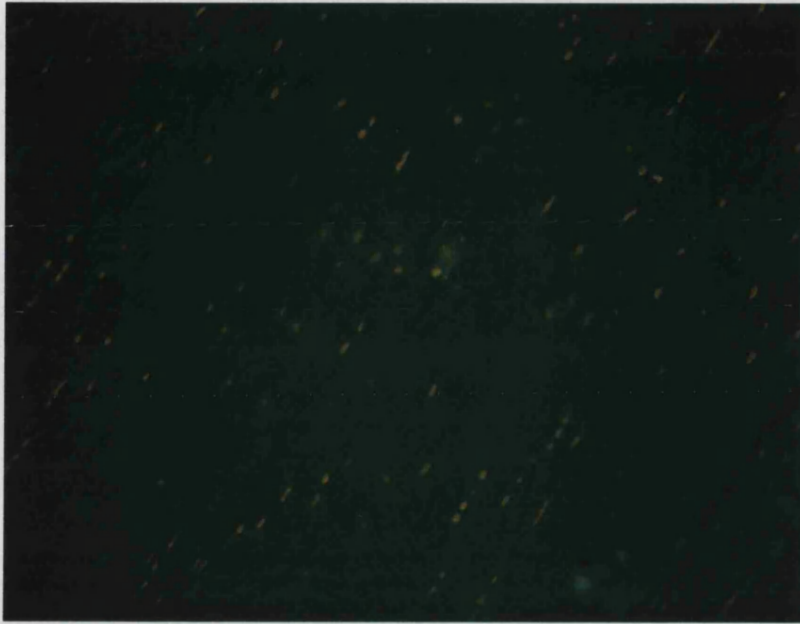
Figure 3.2.6. Section of Dupuytren's cord stained for α-SMA using a FITC conjugated secondary antibody viewed under uv light at x 200 magnification. There is again no positive staining.
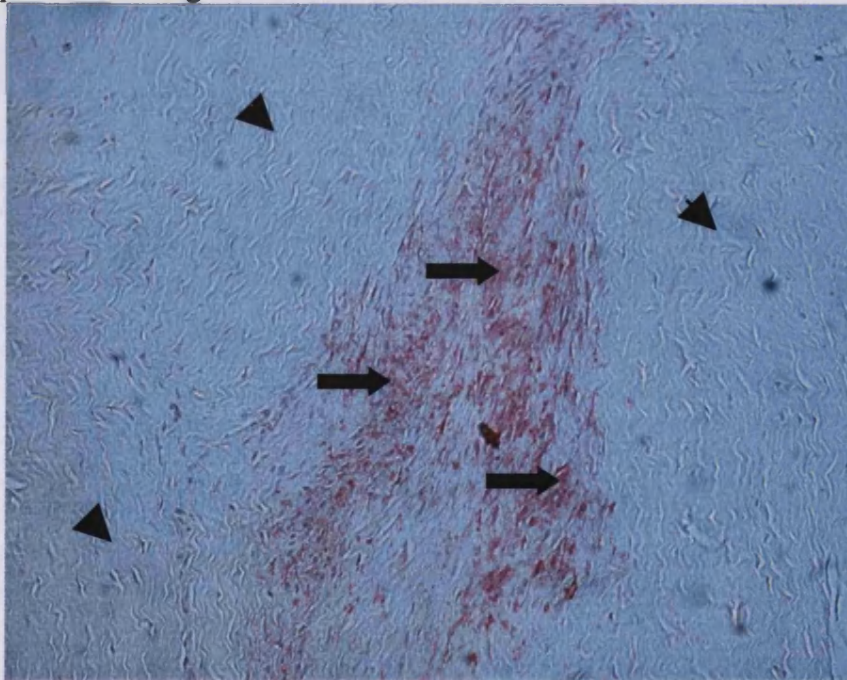
Figure 3.2.7. Section of Dupuytren's cord stained for α-SMA using alkaline phosphatase and vector red final substrate method at x 200 magnification showing a "nest" of densely positive staining myofibroblasts (arrows). This is completely encircled by more typical sparsely populated cord tissue, negative for α-SMA (arrow heads).

Carpal ligaments were uniformly negative for α-SMA as shown in figure 3.2.8. Table 3.2.1 summarises the results, indicating the distribution of nodules and cords that stained positively for α-SMA. A grading system has been used indicating the degree of positive staining in each section. This is illustrated in figure 2.3. in the methods section, where no positive staining is represented by a 0, rising to +++ where there is intense widespread staining. The overall percentage of positive staining nodules, cords and carpal ligaments is displayed graphically in figure 3.2.9. with the bar chart divided to indicate the level of positive staining.

Sample Dupuytren's	Nodule	Cord	Carpal Ligament	
1	++	+	1	0
2	0	-	2	0
3	+++	-	3	0
4	+++	+	Total Positive	0
5	+++	++		
6	+++	-		
7	+	-		
8	+	-		
9	+	++		
10	+++	-		
11	+	-		
12	0	-		
13	+++	-		
14	+++	-		
15	-	-		
16	++	-		
Total Positive	13	4		

Table 3.2.1. Summary of the results of staining for α-SMA in 16 Dupuytren and 3 Carpal Ligament specimens. The level of positive staining is indicated by the legend (+, ++ or +++) see Chapter 2.3 for method of determination.

97
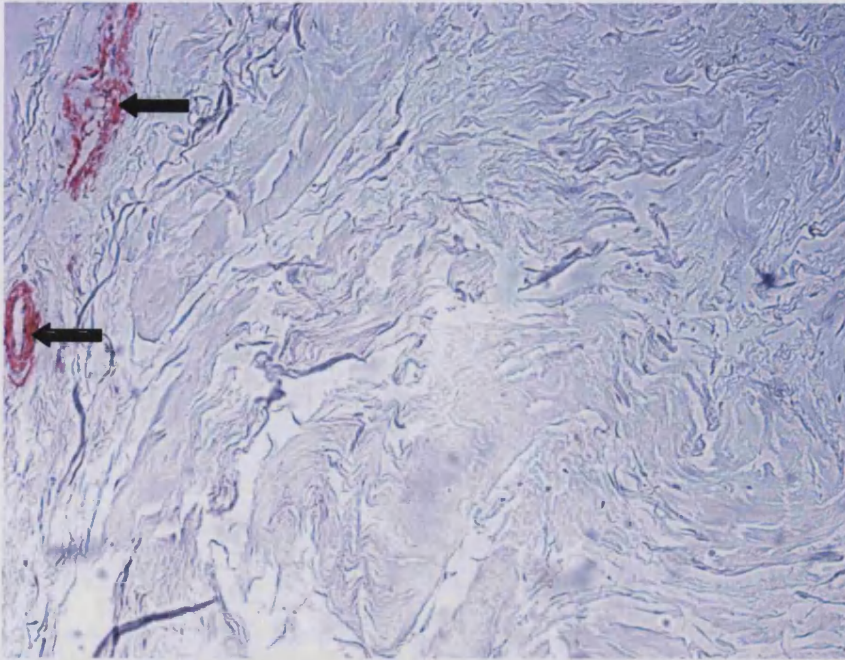
Figure 3.2.8. Section of carpal ligament stained for α-SMA using alkaline phosphatase and vector red final substrate method at x 200 magnification. There is no positive red staining of within this field except for the smooth muscle cells surrounding two blood vessels in the top left corner (arrows).
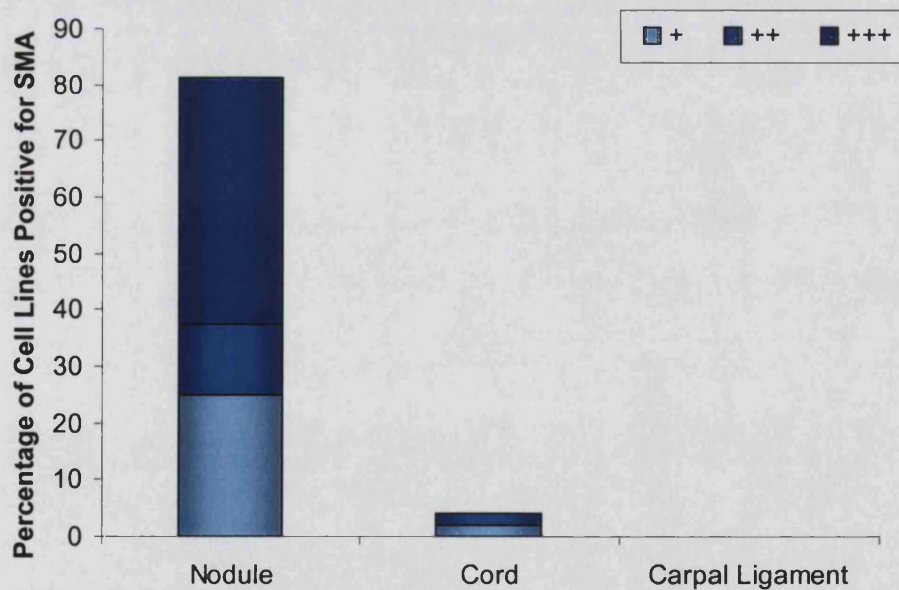
Figure 3.2.9. Histogram showing the percentage of specimens of Dupuytren's disease nodule and cord and control carpal ligament where positive staining for α-SMA was identified. The level of positive staining is indicated by the legend (+, ++ or +++). Note that more than half of the positive nodules were graded as +++, compared with none of the cords.

3.2.5. Discussion

Several authors have used immunohistochemical staining by means of a monoclonal antibody against α-SMA to identify myofibroblasts. Benzonana et al (1988) identified cells positive for α-SMA in a range of pathological tissues including Dupuytren's nodules and found these to correlate with the presence of non-muscle myosin. Darby et al (1990) found it transiently expressed in experimental wound healing.

Others have specifically studied Dupuytren's disease, with Bernt et al (1994) finding the co localisation of laminin and fibronectin with regions positive for α-SMA in Dupuytren's nodules. McCann et al (1993) using a similar method to the one utilised here, found myofibroblasts present in the dermis overlying Dupuytren's tissue as well as in the hypercellular diseased fascia. They did not find positive staining in hypocellular fibrous regions, but failed to delineate regions as nodules or cords.

Having separated Dupuytren's specimens clinically into nodule and cord the findings here, of myofibroblast phenotype cells appearing prominently within Dupuytren's nodules are consistent with those of several other authors. Badalamente et al (1983) examined the ultrastructural features of Dupuytren's disease tissue, identifying myofibroblasts by the presence of nuclear and cytoplasmic indentations, well-developed rough endoplasmic reticulum and bundles of 60 to 80 Å intracellular microfilaments. All of the 21 nodules they examined contained myofibroblasts but these were not identified in the cords. They found a positive reaction for ATPase (adenosine triphosphatase) localised to the myofilaments within cells in nodules and correlated this to the residual clinical contracture following surgery. Thus they related the myofibroblast activity in the nodules with clinical outcome and possible recurrence. Gelberman et al (1980) have also related the presence of myofibroblasts in excised Dupuytren's specimens with the recurrence of disease.

Vande Berg *et al* (1984) found a lack of myofibroblasts within Dupuytren's cords, again using ultrastructural studies, confirming their findings from a previous study (Vande Berg *et al*, 1982) when they analysed the relationship of overlying skin to nodules and cords. In both studies not all nodules investigated demonstrated cells possessing the myofibroblast phenotype, in keeping with the results here. This was also found by Pasquali-Ronchetti *et al* (1993), although in contrast to others, they found only five out of fifteen nodules to contain myofibroblasts. They are however the only authors to note the presence of myofibroblasts within cords, all be it in a single specimen. This is consistent with the findings presented here where 3 of the samples defined as cords were seen to contain myofibroblasts.

By grading the degree of intensity of positive staining an attempt has been made to quantify the level of myofibroblasts in these tissue specimens. It is accepted that this is a subjective and semiquantitative method, however it is interesting to note the differences in intensity between nodules and cords where positive staining is encountered. More than half of the nodule specimens were graded "+++" whereas none of the positive staining cords reached this score.

By careful observation of the distribution of positive cells using α-SMA staining it has been possible to document the fact that these myofibroblasts occur where there are regions of cords with increased cellularity, **which has not been stated before**. These foci of increased cellularity are often completely surrounded by more typical cord tissue, appearing like microscopic "nodules". With the demonstration of myofibroblast phenotype cells within these, it is interesting to speculate upon the origin and role of these regions.

Luck (1959) and others (Hueston in Dupuytren's Disease, 1990) proposed that nodules progress to residual cords, in which case these foci could be the last remnants of such a nodule. Alternatively the focus could represent the reactivation of Dupuytren's tissue within a residual stage cord surrounding an area of microtrauma (McGrouther, Dupuytren's disease in Methods and Concepts in Hand Surgery, 1986) or microvessel angiopathy (Pal *et al*, 1987). It could be destined to develop into a new, large macroscopic

nodule. Physical shortening of the resident contractile phenotype cells would pull directly on the surrounding cords leading to clinical contractures.

The lack of positive staining cells for α-SMA in carpal ligament tissue was not unexpected, as there is no functional reason for the presence of myofibroblasts. Normal mesenchymal tissue has been shown to be generally negative for α-SMA (Benzonana *et al*, 1988) and myofibroblasts appear only to be prevalent in normal organs where a high degree of remodelling is required (Desmouliere and Gabbiani, 1994). Furthermore Pasquali-Ronchetti *et al* (1993) also failed to demonstrate myofibroblasts in control normal palmar fascia or clinically unaffected fascia from patients with Dupuytren's disease.

SUMMARY:-

- Eighty one percent of Dupuytren's disease nodules contained widespread positive staining for myofibroblasts in contrast to cords. More than half of these positive nodules were graded at "+++".

- Contrary to most previous reports, cells exhibiting the myofibroblast phenotype were found to be present in 25% of cord specimens. By examination of the distribution of these it is clear they occur in hypercellular foci within the substance of established cords.

No other authors have previously reported the presence of the myofibroblast phenotype in cord tissue to this extent.

3.3. Myofibroblast Phenotype in Two-Dimensional Cell Cultures From Dupuytren's Nodules, Cords and Control Carpal Ligament

3.3.1. Introduction

As has been outlined in chapter 3.2.1 the myofibroblast is thought to play a central role in the pathogenesis of Dupuytren's disease and contracture formation. Dupuytren's fibroblasts grown *in vitro* have been shown to contain a proportion of α-SMA positive cells (Vande Berg *et al*, 1984), however a clear comparison of myofibroblast quantities has not been made between specific nodular derived and cord derived cell cultures. This gap in the current knowledge of Dupuytren's disease and the myofibroblast phenotype is addressed in this chapter.

Furthermore, having demonstrated that there are quantifiable differences in the presence of myofibroblasts in Dupuytren's nodule and cord tissue, if these differences persist into specific cell cultures from the two regions, then separating cultures in this way is a valid means of investigating cellular differences in subsequent experiments.

3.3.2. Aim

To prove that the cell phenotype persists from tissue into fibroblast culture by determining the percentage of myofibroblast phenotype cells in cultures derived specifically from Dupuytren's nodules and cords (and to compare these to control fascial fibroblast cultures derived from carpal ligament.)

3.3.3. Materials and Methods

Eighty thousand cells in established cultures from nodules, cords and carpal ligaments were seeded onto sterilised 22mm x 22mm cover slips in 6 well plates as detailed in chapter 2.4. After incubation for four days the cells were fixed on the cover slips and then stained for alpha smooth muscle actin using the immunohistochemical protocol in chapter 2.4. Nuclei were counterstained with propidium iodide allowing cells negative for α-SMA to be identified. The numbers of α-SMA positive fibroblasts were counted in three random microscope fields at x 200 magnification for each cover slip. Each cell line was examined

in triplicate. The percentage of cells with a myofibroblast phenotype was calculated, as determined by positively stained intra cellular microfilaments, see figure 3.2.1. The results were compared using the Student's t-test.

3.3.4. Results

Figure 3.2.1 illustrates a positively stained myofibroblast at high power (x 400 magnification). Bright green staining intracellular microfilaments are clearly seen throughout the cell with the nucleus counterstained red. Negative stained cells are seen at the periphery of the image. Figure 3.2.2 shows a typical field at x 200 magnification for nodular derived cells. There are scattered positively stained myofibroblasts throughout the field. Figure 3.2.3 shows a similar field from cord-derived cells, whilst figure 3.2.4 is from carpal ligament cells. In both there is a virtual absence of cells positive for alpha smooth muscle actin. Often when cells were found to be positive the staining, although still located along microfilaments, was noticeably weaker than in nodule cells.
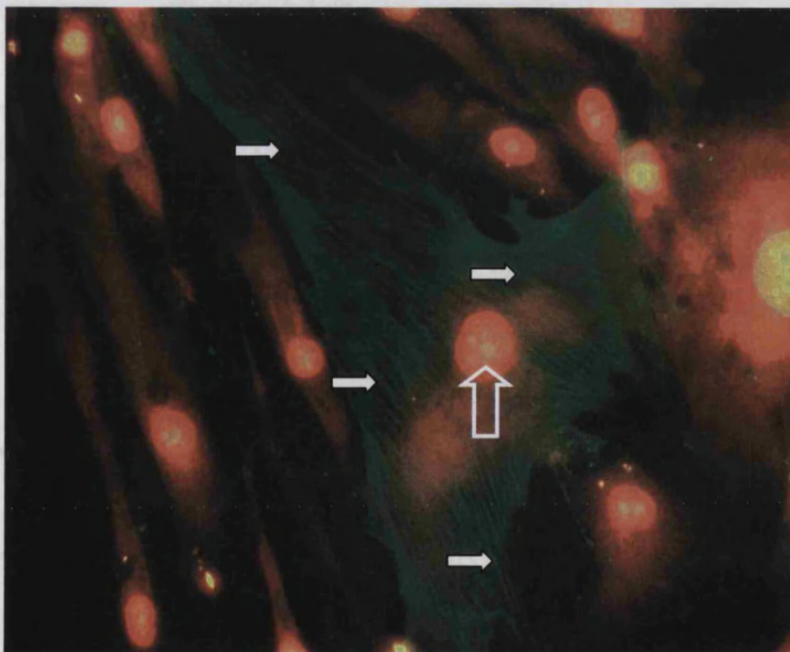
Figure 3.3.1. A myofibroblast at x 400 magnification. Staining demonstrates numerous fine intracellular microfilaments staining positively (green) for alpha-smooth muscle actin (solid arrow). The nucleus is counterstained (red) with propidium iodide (open arrow).
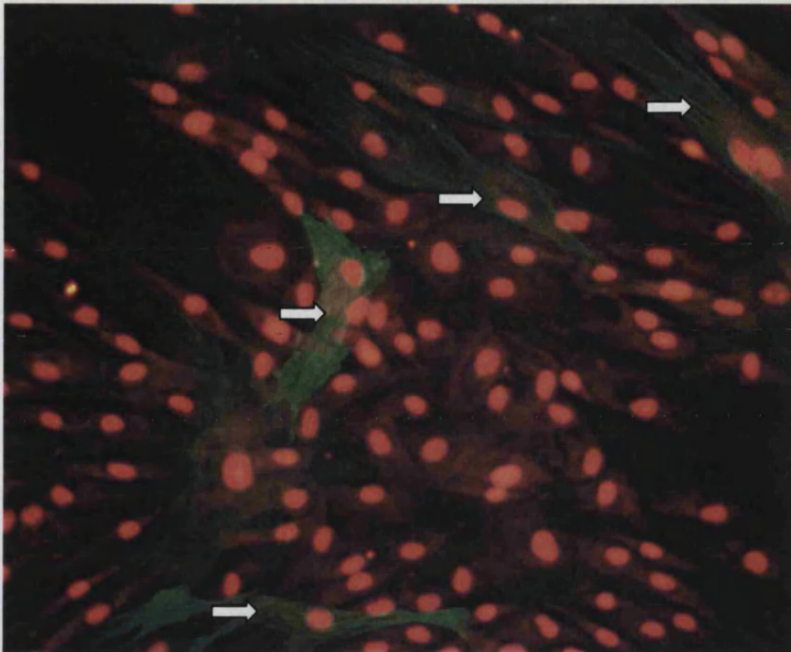
Figure 3.3.2. Cells in culture derived from Dupuytren's nodule at x 200 magnification stained for α-smooth muscle actin and counterstained with propidium iodide. Cells with green cytoplasmic filaments are positive (arrows). Note the high proportion of positive staining cells (mean 9.65%) compared with figure 3.3.3.
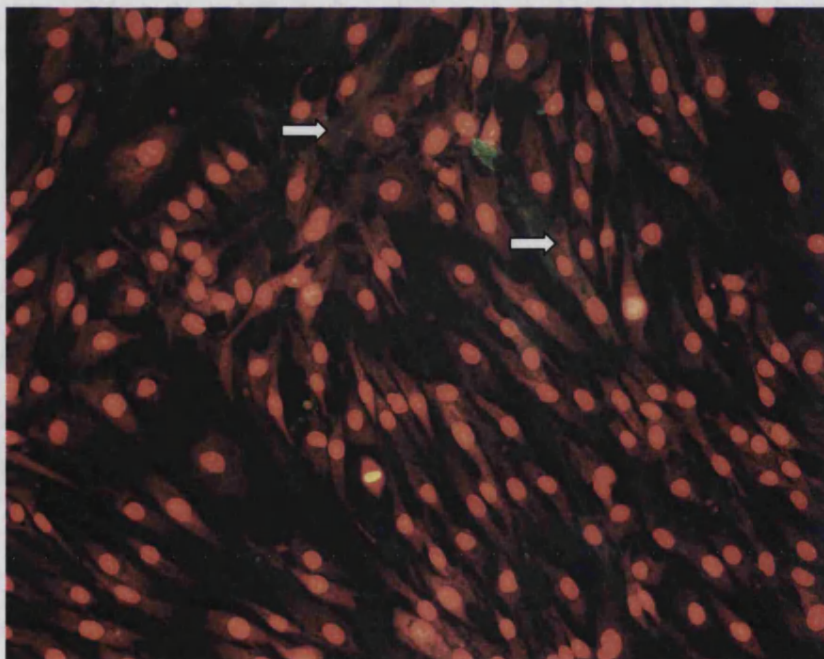
Figure 3.3.3. Cells in culture derived from Dupuytren's cord at x 200 magnification stained for α-smooth muscle actin and counterstained with propidium iodide. Cells with green cytoplasmic filaments are positive (arrows). Note the lower percentage of positive staining cells (mean 2.74%) compared with figure 3.3.2. above.
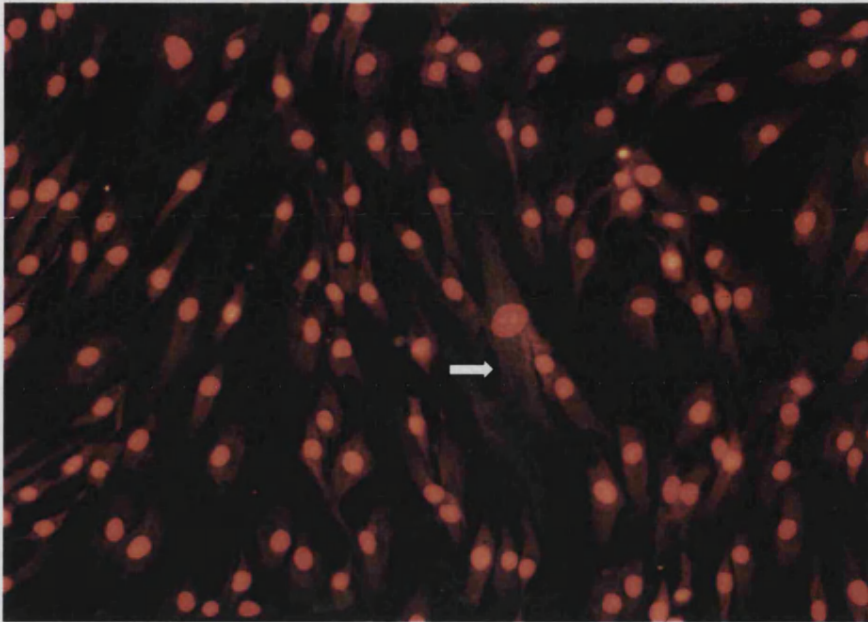
Figure 3.3.4. Cells in culture derived from control carpal ligament at x 200 magnification stained for α-smooth muscle actin and counterstained with propidium iodide. In this field there is only a single, weakly positive cell with green cytoplasmic filaments centrally (arrow).

Figure 3.2.5 is a histogram indicating the mean proportion, expressed as a percentage of the total cell number, of myofibroblasts present in nodule, cord and carpal ligament cell cultures. The percentages are low, however nodule contains three times as many positively stained cells at 9.65% (SD ± 4.48, n=9) compared with cord cell cultures at 2.74% (SD ± 1.50, n=10) the difference being statistically significant, $p < 0.001$. Carpal ligament cell cultures contained even fewer myofibroblasts at 1.3% (SD ± 1.89, n=4), again being significantly different from nodule ($p < 0.01$) but not from cord (p= 0.16).
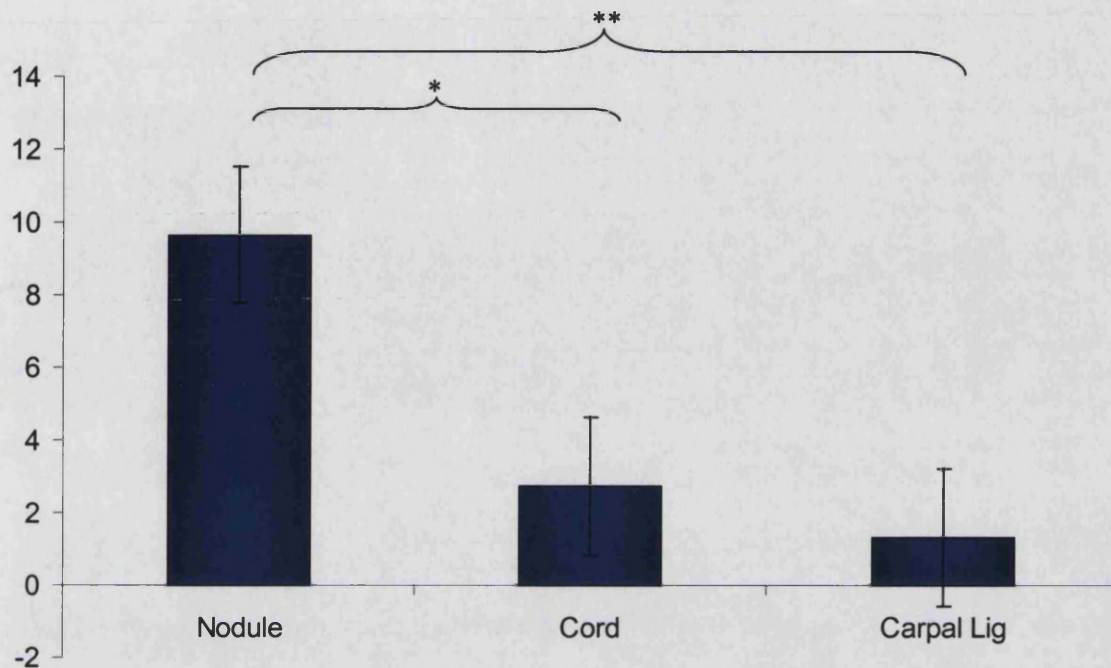
Figure 3.3.5. The mean percentage of myofibroblasts in cell cultures derived from Dupuytren's nodule (n=7), Dupuytren's cord (n=8) and control carpal ligament tissue (n=4). The error bars represent standard deviations. There was a significant difference between nodule and cord *, $p<0.001$, and nodule and carpal ligament **, $p<0.01$, but not between cord and carpal ligament.

3.3.5. <u>Discussion</u>

Within these two dimensional fibroblast cultures, significant differences in the presence of myofibroblasts between the cell types studied have been demonstrated. In keeping with previous studies by Vandeberg *et al* (1984) these results have shown the persistence of the myofibroblast phenotype from the *in vivo* tissue of nodules to fibroblasts cultured specifically from these areas. Vandeberg *et al* used electron microscopy to study the ultrastructural features allowing myofibroblast identification. Here by the use of α-SMA staining it has been possible to quantify the actual number of cells within a population of cultured fibroblasts that demonstrate the myofibroblast phenotype.

Despite finding very few myofibroblasts within only four of the sixteen cord tissue specimens examined (see section 3.2.), and many previous authors finding none (Vande

Berg *et al*, 1984; Badalamente *et al*, 1983), or few (Pasquali-Ronchetti *et al*, 1993), there were a small percentage present in all cord derived cell cultures. This was contrary to Vande Berg *et al*'s work and was also the case for carpal ligament specimens, a fact that has not been reported before.

There are several potential reasons for this difference between the *in vivo* and *in vitro* findings. Explant culture of fibroblasts inherently produces some degree of cellular heterogeneity and this may be additionally exacerbated by the nature of the tissue categorised as cord. It is occasionally observed on standard histology sections of cord (see 3.1.4.) that there are foci of increased cellular diseased tissue within the sparsely fibroblast populated, thick parallel collagen bundles. If these cell "nests" become incorporated into the explanted tissue, increased myofibroblasts numbers may result. Indeed it is these areas that contain positive cells when tissue sections are stained for α-SMA (Section 3.2.4.).

Secondly, culture of fibroblasts in 2 dimensions on the base of a tissue flask or glass coverslip provides a stiff environment for the cells to attach to and has been shown to stimulate stress fibre formation (Tomasek *et al* 2002). Some of the above reasons could be the explanation for the finding of some, all be it very small numbers of myofibroblasts in carpal ligament cultures. No evidence was found of myofibroblasts *in vivo* (Section 3.2) and their presence would not be in keeping with the general function of this tissue. This in part was the reason for choosing carpal ligament as an appropriate comparative tissue or control. It is a fascial tissue of the distal upper extremity but not involved in Dupuytren's disease, whilst functionally acting as a static sheath.

Dugina *et al* (2001) used Dupuytren's nodule fibroblasts in a study of focal adhesions in myofibroblasts. Using a similar immunohistochemical method to that presented here they found only 3% myofibroblasts in untreated cultures. This was however in serum free conditions whereas cultures here were incubated with 10% serum, which is likely to account for the higher basal level of expression.

Some authors have stated that nearly all cells within nodules are myofibroblasts (Vande Berg *et al*, 1984), however by determination of α-SMA positivity in our specimens this does not appear to be the case. Certainly there are areas of tissue in specimens where strong staining occurs and most of the cells within a region are positive. There are also several areas within all of the nodules observed where there is no staining evident (see figure 3.2.4.). This corresponds with the findings presented here in cultured nodule cells where despite the significantly increased levels of myofibroblasts above cord cells, there are still only 9.65% positively stained. It is possible that the nodules these authors studied showed particularly high myofibroblast populations, one might speculate that this could be the case in recurrent disease, whereas all of the specimens in this study were from primary procedures. It may also be that their use of ultrastructural observation demonstrated widespread intracellular microfilaments or stress fibres, many of which were not actually α-smooth muscle actin, but other isoforms (eg f-actin). Recently Tomasek *et al* (2002) have termed these cells proto-myofibroblasts with only true "differentiated myofibroblasts" expressing α-SMA.

The finding of higher basal myofibroblast percentages in nodule cultures compared with both cord and carpal ligament, suggests that specific regional cultures retain some of their *in vivo* characteristics at least in the early passages that have been used for these studies. It further supports the theory that it is the nodule and its resident cells that constitute the active stage of Dupuytren's disease as stated by several authors (Hueston, 1985, Moyer *et al*, 2002). Disease activity is implied by a spectrum of features including cellularity, proliferation, presence of myofibroblast phenotype, collagen production (specifically type III indicating turnover and new collagen) and contraction.

Strong links have been made between the myofibroblast and tissue contraction from the time it was first identified in granulation tissue (Gabbiani, 1971). Indeed subsequently, cellular contraction and myofibroblast or α-SMA content have been correlated (Tomasek and Rayan, 1995 and Hinz *et al* 2001). Because of the prevalence of myofibroblasts within nodules on electron microscopy but relative paucity or absence in cords it has been suggested that the nodules are the source of clinical contractures in Dupuytren's disease

(Moyer *et al*, 2002). The results here support the theory that nodule cells are more active than those derived from cords or indeed comparison carpal ligament fibroblasts if one accepts that myofibroblasts correlate with disease activity and contractile capacity.

Following from these results, should an appropriate non-surgical therapy become available, for example to inhibit myofibroblast proliferation or activity, the delivery of this would be of critical importance to its effectiveness. Certainly for a local or topical agent one would need to target the **nodular disease** tissue to ensure the desired effects, because this is where myofibroblasts are present (as demonstrated by results in chapter 3.2. and the persistence of this phenotype into specific cultures here). Cord tissue and cell behaviour may remain unchanged from the natural disease progression, there being much fewer myofibroblasts to target.

SUMMARY:-

- The percentage of α-SMA +ve staining myofibroblasts in nodule derived cell cultures is significantly higher than in cord derived cell cultures.
- Cord cell cultures are more like carpal ligament cultures in terms of the myofibroblast numbers.

These findings support the theory that the nodule is the active form of the disease.
The nodule should be targeted if a non-surgical therapy for Dupuytren's disease became available, as it is the active form.

In light of these results and the current understanding of cellular and tissue contraction, it was hypothesised that nodule derived fibroblasts would demonstrate increased contraction compared with cord or carpal ligament fibroblasts.

3.4. Baseline Contractility of Dupuytren's Nodule, Dupuytren's Cord and Control Carpal Ligament Derived Cell Cultures in 3 Dimensional Fibroblast Populated Collagen Lattices

3.4.1. Introduction

The nature of Dupuytren's disease as a fibrocontractive disorder has lead to a great deal of interest in the mechanism of diseased tissue contraction. Current theories suggest that the matrix physically shortens due to a combination of cell mediated contraction and matrix remodelling (Brickley-Parsons et al, 1981).

The main method of investigating cell mediated matrix contraction has been the study of fibroblast populated collagen lattices. Cell contraction of a 3D matrix has been shown to be serum dependent (Tomasek et al, 1992; Rayan and Tomasek, 1994, Brown et al, 2002) and related to the initial collagen concentration of the gels seeded (Bell et al, 1979; Zhu et al, 2001).

Several authors have compared Dupuytren's fibroblast contraction in circular lattices (usually choosing a stress-relaxed model) with other fibroblast types (Rayan and Tomasek, 1994; Tarpila, et al, 1996). Others have studied the effect of varying inhibitory or activating factors on the ability of Dupuytren's fibroblasts to reduce collagen gel diameter (Sanders et al, 1999; Rayan et al, 1996; Badalamente et al, 1988; Hurst et al, 1986). Tomasek and Rayan have also correlated the α-smooth muscle actin expression of Dupuytren's fibroblasts with the contraction of stress relaxed fibroblast populated collagen lattices. The mechanism of free-floating collagen lattice contraction, which is generally a slow sustained process, is believed to be based upon cell attachment to the matrix and migration or locomotion through it (Grinnell, 1994).

In contrast tethered collagen lattices develop isometric force as the resident cell population contracts against the fixed points. Myofibroblasts develop with the formation of α-smooth muscle actin and on release of the gel from its attachments a rapid contraction occurs proportional to the isometric force build up. All of the above studies employ a very

110

simple circular lattice model and this suffers from being only a semi-quantitative method of assessment based upon changes in lattice diameter. Furthermore, under no circumstances are cells *in vivo* ever suspended in a free-floating matrix, they are always under some degree of tension. Thus both models, free-floating and stress-relaxed, create an artificial environment to study cellular contraction.

The culture force monitor developed by Eastwood *et al*, (1994) has allowed the measurement of actual forces developed within a fibroblast populated collagen lattice in real time. This not only permits the measurement of a peak force generated but also the pattern of force development over time in the form of a contraction profile. Thus differences in the rate of force generation at various times can be observed so quantifying how cells attach to the matrix and go on to achieve tensional homeostasis. Contrary to the circular collagen gel models the FPCL remains under tension at all times thus representing a more accurate *in vivo* environment. There have been no published studies to date investigating Dupuytren's fibroblasts or carpal ligament fibroblasts using the culture force monitor model. Additionally there has only been one recently published study comparing contraction between nodule and cord derived fibroblasts. It appeared in print as this experimental work was drawing to a close but used a free-floating gel contraction assay, so providing only limited semi-quantitative data (Moyer *et al*, 2002).

Using the precise analysis possible with the culture force monitor model it was proposed to investigate the basic contraction profiles of Dupuytren's cord and nodule derived fibroblasts, comparing them with each other and carpal ligament cells. These carpal ligament fibroblasts are of a similar type of fascial tissue origin, in the upper limb as non diseased palmar fascia and have been used by previous authors as controls in contraction studies for Dupuytren's disease (Rayan and Tomasek, 1994; Tomasek and Rayan, 1996).

The increased cellularity, increased tissue myofibroblast phenotype and increased cell culture myofibroblast phenotype in Dupuytren's nodules demonstrated in the preceding chapters should theoretically result in increased cellular contraction by nodule fibroblasts.

3.4.2. Aim

To determine if Dupuytren's nodule derived fibroblasts had different basic contractile properties than fibroblasts derived from Dupuytren's cord, whilst comparing both to normal fascial fibroblasts.

3.4.3. Methods

Fibroblasts from nine Dupuytren's nodule cell lines, ten Dupuytren's cord cell lines and four carpal ligament cell lines were examined using the culture force monitor. As detailed in section 2.5, fibroblasts to be used were grown under standard conditions to near confluence in T225 tissue culture flasks. Five million cells were then seeded into a 5 ml collagen lattice, prepared between two floatation bars. The lattice was allowed to gelate in an incubator for 30 minutes before being floated and placed on the culture force monitor stage and attached to the force transducer.

The system was allowed to equilibrate in terms of temperature (37°C) and CO_2 (5%) levels for 5 minutes before recordings were commenced. Each gel was then left to contract over 20 hours with the computer taking real time measurements of the tension developed within the system at 1 second intervals. For each cell line run the data was converted to one minute data points by using a DOS Macro which determined the mean force for each minute from the 60 readings recorded. A contraction profile could then be plotted as seen in 3.4.1 for each cell line.

The mean contraction profiles along with standard deviations and standard errors for each cell type, nodule, cord and carpal ligament, were calculated by amalgamating the minute data points within Microsoft Excel spreadsheets. The mean force generated at 20 hours per 5 million cells for each fibroblast type was determined as were the gradients of the contraction profiles at two points in the contraction. The gradient of the early phase of contraction was calculated by dividing the difference in the force readings at 1 hour and 2 hours by 60 to give a value of rate of change of force in dynes per minute per five million cells. This was labelled the "2 hour" gradient, whilst the "20 hour" gradient was derived in the same way at the end of the experiment using the difference in force readings at 19.5 hours and 20.5 hours.

112

3.4.4. Results

The contraction profiles of the nine different Dupuytren's nodule cell lines are displayed in figure 3.4.1. There is a range of differences between cell lines and this is especially apparent early in contraction where some profiles show an early rapid contraction whilst others display a delay in the onset of contraction. Profiles 2 and 5 illustrate the extremes of these two patterns. Profile 2 shows a delay of some four hours during which time tension in the system even decreases before there is onset of contraction. This is then continuous to the end of the experiment with only a slight shallowing of the contraction profile and certainly no plateau. Profile 5 shows a rapid initial contraction, which climbs well above the other profiles but by 5 hours demonstrates some plateauing of force. This never stops climbing however, and by the end of the experiment the rate of increase of force has increased again. Between these two extremes the majority of profiles fall within a tighter range.
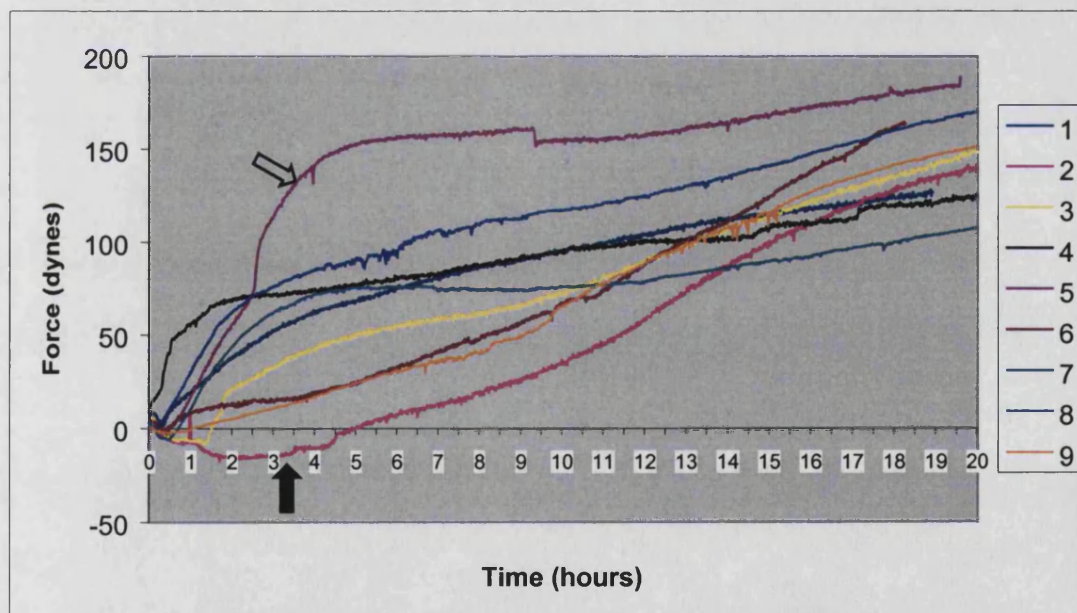
Figure 3.4.1. A graph showing all 9 of the Dupuytren's nodule fibroblast contraction profiles, with force generated by 5 million fibroblasts plotted against time. Note the variability in the early stages of contraction especially in series 2 where there is a delay in the onset of contraction (solid arrow) and series 5 where there is a sustained rapid early generation of force (open arrow).

The mean Dupuytren's nodule contraction profile illustrated in figure 3.4.2. shows the more typical overall contraction profile and despite inter cell line variation the standard errors of the means shown at hourly intervals along the contraction curve are not disproportionate. Figure 3.4.3. shows the mean contraction profiles with standard errors of the means for all three cell types investigated. Mean contraction by Dupuytren's nodule fibroblasts (n=9) is greater throughout the 20-hour period than cord derived fibroblast contraction (n=10). There is divergence of the contraction profiles by 2 hours, where nodule has reached 33 dynes but cord only 28 dynes. These become further separated as time progresses although the pattern of contraction remains similar in both cell types.
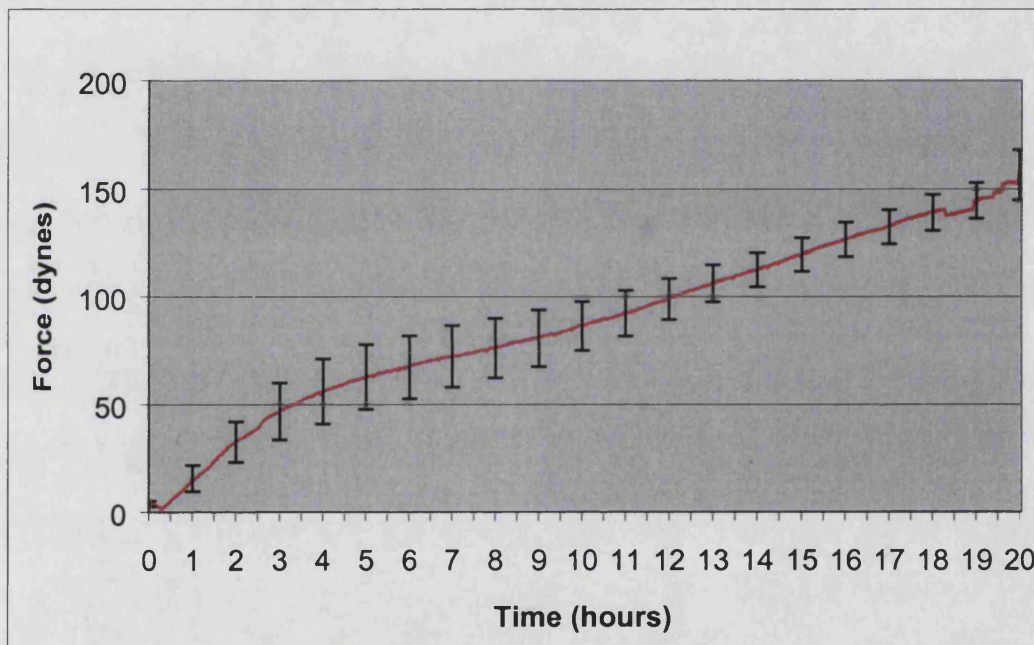
Figure 3.4.2. The mean contraction profile of n=9 Dupuytren's nodule fibroblast cell lines. The error bars represent the standard errors of the mean at hourly intervals.

114
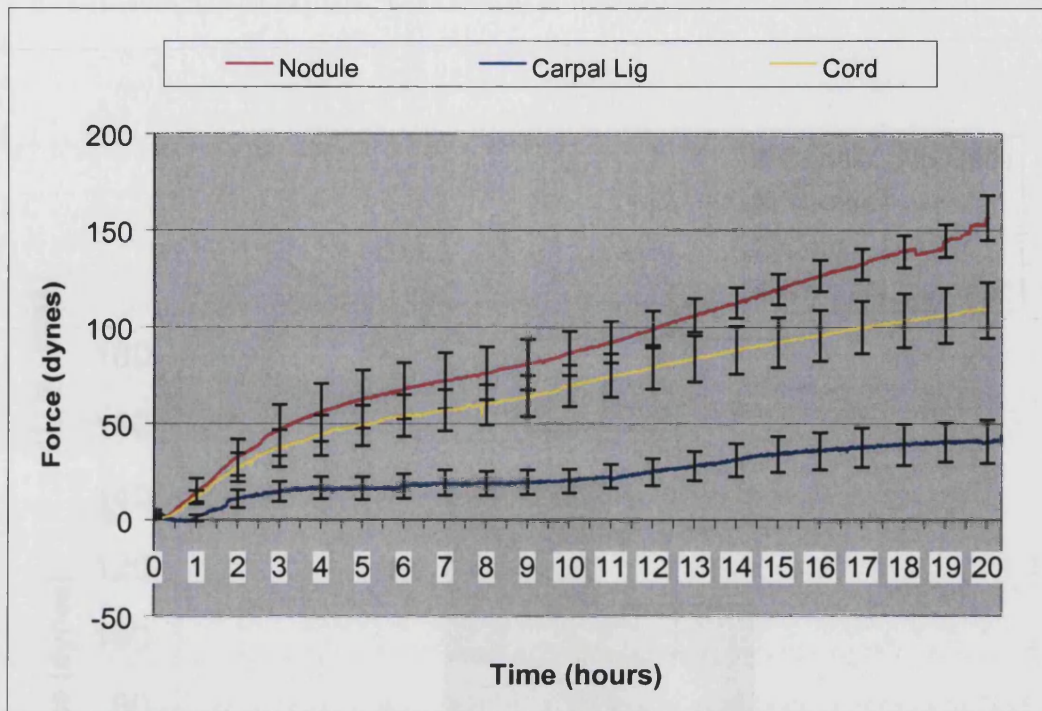
Figure 3.4.3. The mean contraction profiles of n=9 Dupuytren's nodule, n=10 Dupuytren's cord and n=4 carpal ligament fibroblast cell lines. The error bars represent the standard errors of the mean at hourly intervals.

The carpal ligament derived fibroblast, however demonstrate a very different profile. As noted already when assessing the reliability and reproducibility of the technique (Chapter 2.5.3), carpal ligament cells produce very little contractile force. There is an initial moderate increase in force to 15 dynes after about 2 hours with subsequent very gradual rises in force until 17 hours where the profile plateaus at only 40 dynes (range 36 to 68 dynes, SEM ± 13.1). When the mean force generated at 20 hours is compared between cell types as displayed graphically in figure 3.4.4., both nodule and cord cell lines generate significantly greater force than carpal ligament (p<0.001 and p<0.05 respectively).
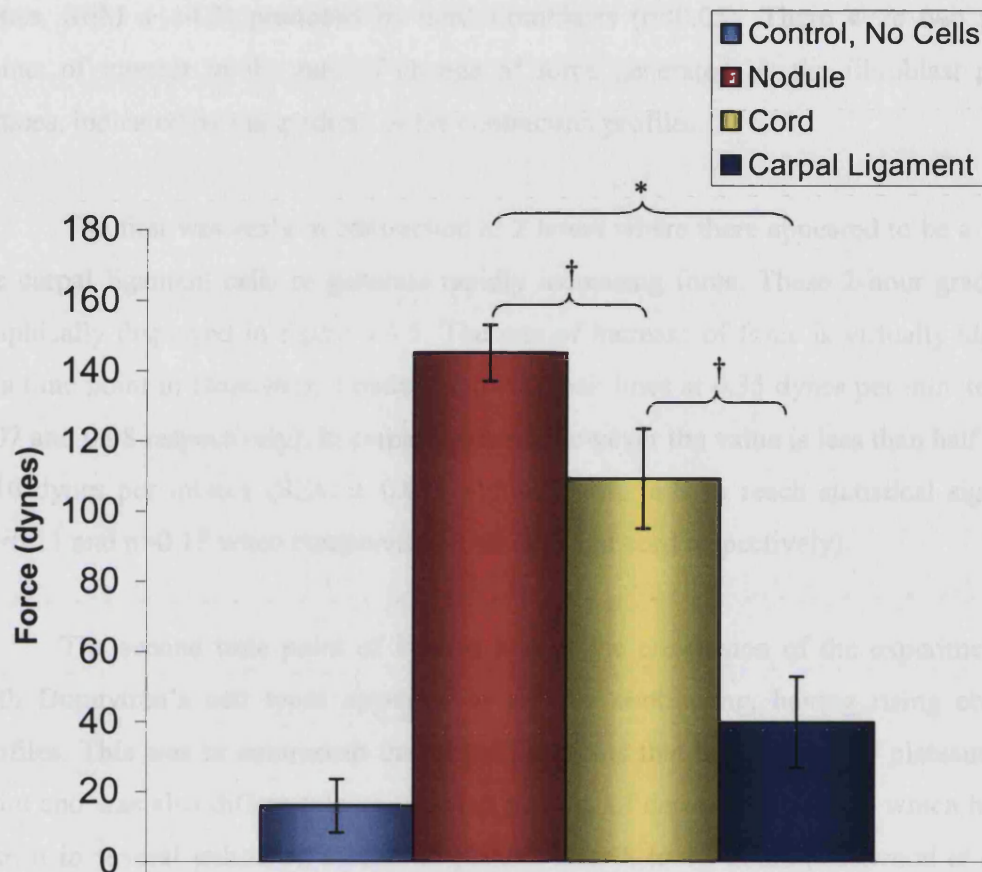
Figure 3.4.4. The mean force generated at 20 hours by Dupuytren's nodule (n=9), Dupuytren's cord (n=10) and carpal ligament (n=4) fibroblast cell lines. The error bars represent the standard errors of the mean at hourly intervals. Note the pale blue bar represents the force generated by control, acellular collagen gels (n=3) which do contract to a minimal degree. Nodule values are statistically significantly greater than both cord and carpal ligament, whilst cord is statistically significantly greater than carpal ligament.
* p<0.001
† p<0.05

The force generated at 20 hours by nodule fibroblasts of 145 dynes (range 106 to 184 dynes, SEM ± 7.9) is also significantly greater than the 109 dynes (range 52 to 192 dynes, SEM ± 14.2) produced by cord fibroblasts ($p<0.05$). There were two particular points of interest in the rate of change of force generated by the fibroblast populated lattices, indicated by the gradient of the contraction profiles.

The first was early in contraction at 2 hours where there appeared to be a failure of the carpal ligament cells to generate rapidly increasing force. These 2-hour gradients are graphically displayed in figure 3.4.5. The rate of increase of force is virtually identical at this time point in Dupuytren's nodule and cord cell lines at 0.35 dynes per minute (SEM ± 0.07 and 0.08 respectively). In carpal ligament, however the value is less than half of this at 0.16 dynes per minute (SEM ± 0.07), although this fails to reach statistical significance ($p=0.11$ and $p=0.15$ when compared with nodule and cord respectively).

The second time point of interest was at the conclusion of the experiment where both Dupuytren's cell types appeared to still be contracting, having rising contraction profiles. This was in contrast to the carpal ligaments that had essentially plateaued at this point and was also different to contraction profiles of dermal fibroblasts, which have been shown in several published studies to plateau after 8 to 12 hours (Eastwood et al, 1996, Brown et al, 1998). A histogram showing the mean gradients of the contraction profiles from each cell type is displayed in figure 3.4.6. The gradients of both the Dupuytren's nodule fibroblast profile, at 0.086 dynes per minute (SEM ± 0.02), and the Dupuytren's cord fibroblast profile, at 0.044 dynes per minute (SEM ± 0.01), are significantly greater ($p<0.05$) than the carpal ligament gradient of 0.004 dynes per minute (SEM ± 0.001). Additionally there is a strong trend for nodule fibroblasts to be contracting at a greater rate at 20 hours than cord, the mean profile climbing nearly twice as quickly, although this just fails to reach statistical significance ($p=0.068$).
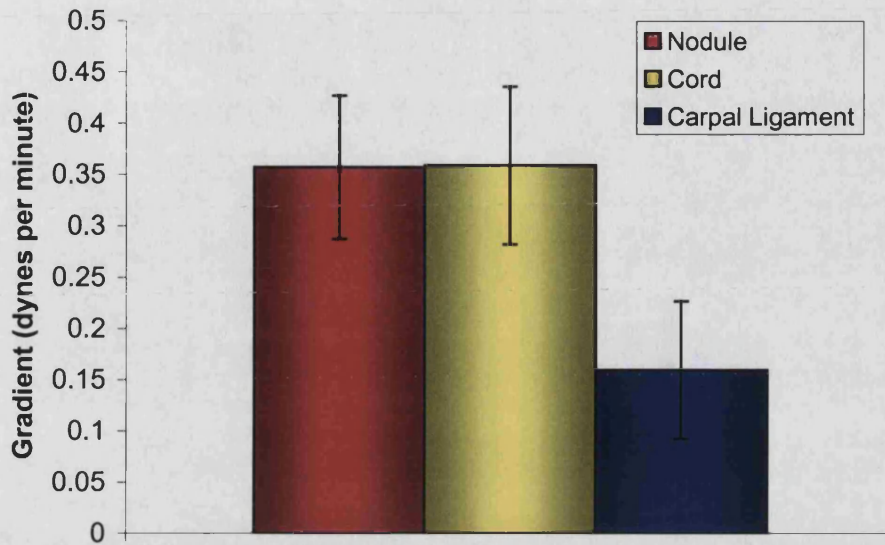
Figure 3.4.5. The mean contraction profile gradient at 2 hours in Dupuytren's nodule (n=9), Dupuytren's cord (n=10) and carpal ligament (n=4) fibroblast cell lines. The error bars represent the standard errors of the mean at hourly intervals. Differences just failed to reach statistical significance.
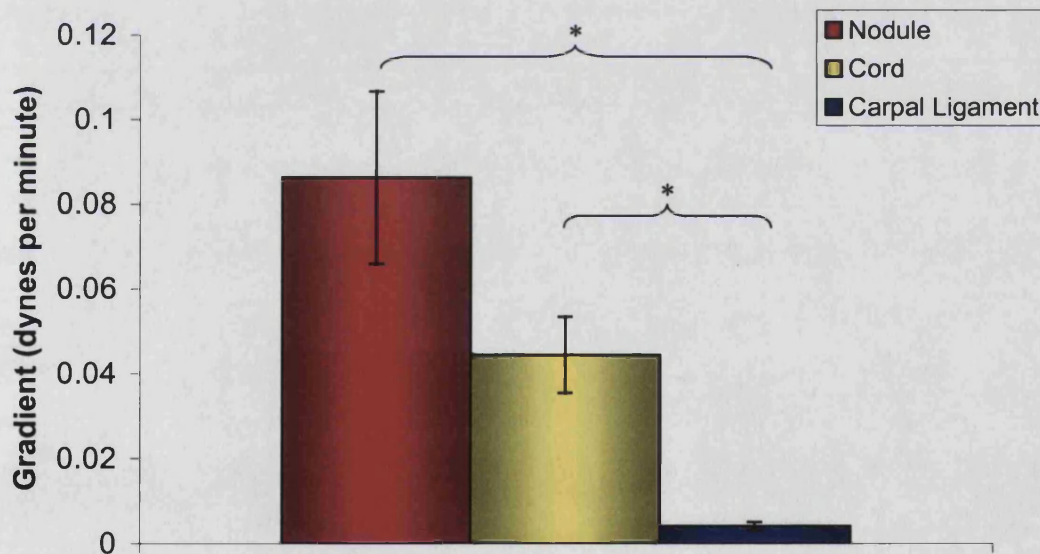
Figure 3.4.6. The mean contraction profile gradient at 20 hours in Dupuytren's nodule (n=9), Dupuytren's cord (n=10) and carpal ligament (n=4) fibroblast cell lines. The error bars represent the standard errors of the mean at hourly intervals. There was a statistically significant difference between both Dupuytren's cell lines and the carpal ligament cell lines, * $p<0.05$, but not between the nodule and cord cell lines themselves.

This failure of Dupuytren's fibroblast force generation to plateau in the first 20 hours is in contrast to previously studied cell types and control carpal ligament cells, and is **a new finding**. This may provide a fascinating insight into the development of diseased matrix contraction.

3.4.5. Discussion

The culture force monitor model allows accurate quantitative assessment of the cell-mediated effects of collagen matrix contraction (Eastwood *et al*, 1994). It is currently believed that this, in concert with continuous matrix remodelling is the mechanism behind physical shortening of affected fascia in Dupuytren's disease (Brickley-Parsons *et al*, 1981) Most of the published work using this model has concentrated on the contraction patterns of dermal fibroblasts, although other cell types are now beginning to be investigated.

Dermal fibroblasts have been described as having a three-phase contraction profile evident over the first 20 to 24 hours (Eastwood *et al*, 1996). Phase 1 is thought to be due to cellular attachment and locomotion through the matrix and is characterised by an early rapid contraction to around 8 hours. From this point on there is a plateauing of force generation in phase 2 and finally from 15 hours a steady state with balanced forces of cell contraction versus matrix tension becomes established.

Here the Dupuytren's fibroblasts of both nodule and cord origin differed from this typical pattern. There did appear to be an identifiable first phase in most cell lines where there was a rapid production of tension, although as shown in figure 5.5.1, some of the nodule cell lines displayed a delay before the onset of contraction and there was notable variability in this early phase of contraction. The reason for this is not clear, however, if the mechanism of this early generation of force is the attachment and spreading of cells through the newly formed matrix, one can speculate that there is a degree of heterogeneity in the ability of explanted fibroblasts to do this. Part of this may be natural inter-patient variability, whilst some heterogeneity may develop as a result of the explant process,

119

certain fibroblasts being better able to migrate from the tissue. Furthermore pieces of tissue selected for explantation may contain varying degrees of cellularity and fibroblast/myofibroblast activity as has already been demonstrated in chapters 3.1 and 3.2.

Subsequent to this first phase of contraction there is a failure of the Dupuytren's fibroblast contraction profiles to plateau in contrast to the pattern observed for dermal fibroblasts. There is a reduction of the rate of contraction but as demonstrated by the mean traces for both cord and nodule cell lines (figure 3.4.3.) this continues to rise at a steady rate from 8 hours onwards, until the termination of the experimental period at 20 hours. Both nodule and cord profiles are in stark contrast to that obtained by carpal ligament cells, however these also demonstrate a very different pattern from a classical dermal fibroblast, which has not been described before in the literature.

The mean force generated at 20 hours by Dupuytren's nodule cells of 145 dynes or 29 dynes per million cells, corresponds with values published for dermal fibroblasts, which vary between 22 and 60 dynes per million cells (Eastwood *et al*, 1996; Brown *et al*, 1998), all be it in the lower end of the range. Cord force generation falls below this, whilst carpal ligament cellular force generation is very much lower.

The study of cell viability at 24 hours (Chapter 2.5.3.) confirmed that the differences seen in contractile properties at this early stage were not due to differential cell death or proliferation within the collagen gels and hence altered cell numbers. This would have been an unlikely explanation as several authors have studied cell proliferation or apoptosis in 3D collagen gels. Although apoptosis has been described in a free-floating model (Fluck *et al*, 1998) or when tension is released (Grinnell *et al*, 1999) this is not the case in fixed or tethered gels analogous to this model. Kasugai *et al* (1990) found a small rise in cell number in dog periodontal fibroblasts over 24 hours although this increased dramatically by 5 days. Kolodney and Wysolmerski (1992) found no replication of fibroblasts within their collagen gels attached to an isometric force monitoring apparatus over 48 hours, whilst Greco and Ehrlich (1992) demonstrated that rat fibroblasts started

proliferating within 24 hours but human and gorilla fibroblasts failed to proliferate until day 3.

Interestingly when Eastwood et al (1996) examined rabbit endotendon fibroblasts, they only demonstrated a modest level of contraction to around 9 dynes per million cells at 24 hours. This level of tension is equivalent to that seen here with our carpal ligament cells although the onset of rabbit fibroblast contraction was delayed until 12 hours. The low force generation in both may reflect the original environment, being consistent with their function in vivo. These cell types surrounded by thick collagen matrix with little remodelling are stress shielded (Eastwood et al, 1998).

The only other study to investigate differences in contractile properties of nodule and cord derived fibroblasts was published as this thesis was in preparation (Moyer et al, 2002), also finding higher levels of contraction by nodule fibroblasts than cord. This was conducted using a free-floating collagen lattice model and the authors found that in late passage cells the differences disappeared, nodular contraction becoming more like that seen with early cord cells. They proposed this as further evidence for the theory that nodules progress to cords as the Dupuytren's fascia evolves over time.

Other authors have also compared contraction of carpal ligament fibroblasts to those derived from Dupuytren's disease. In contrast to our results Rayan and Tomasek (1994) found an equivalent contraction by carpal ligament fibroblasts to that developed by Dupuytren's nodule fibroblasts. They used a stress-relaxed circular gel contraction assay and lattices were left for 5 days before release. It is impossible to make direct comparisons with these other studies as the models used are different, although the culture force monitor provides a closer representation to the in vivo environment of the cells as discussed above in section 3.4.1.

In a subsequent study the same authors (Tomasek and Rayan, 1995) demonstrated a significant difference between carpal ligament and Dupuytren's nodule fibroblast contraction in a sub-population of nodule cells expressing high levels of α-SMA (>15%).

121

When one looks at figure 3.4.7a, which shows α-SMA expression (as determined in chapter 3.3) plotted against force generation, for those cell lines where data is available on both, the populations of carpal ligament fibroblasts is clearly separate from the Dupuytren's nodule cells. This is in complete agreement with Tomasek and Rayans second study, despite lesser α-SMA percentages. The picture is less clear when the data available for cord cell lines is included as in figure 3.4.7b. with this population merging with carpal ligament fibroblasts. Although there appears to be more of a continuum, the R^2 (linear regression coefficient) value for the data as a whole is only 0.25.

Tarpila *et al* (1996) compared contraction of dermal fibroblasts with Dupuytren's nodule cells using a free-floating circular lattice model. In their study there was a significantly greater contraction by dermal fibroblasts at 36 hours of 35% than the 19% diameter reduction by Dupuytren's cells. The findings presented here appear somewhat contrary to these, although no formal comparison with dermal fibroblasts has been made. The amounts of force generated by nodule fibroblasts are similar although at the lower end of the published range. The free-floating model however is not analogous to the culture force monitor.

Grinnell (1994) has suggested two basic models of cell mediated collagen gel contraction. In the free-floating model tension is developed within the matrix as cells attach to it and subsequently move through the substrate organising collagen fibres. Ehrlich and Rajaratnam (1990) also elegantly demonstrated these cell locomotion derived forces by observing gels with either a donut or wedge configuration.

The second model of tension development is the tethered fibroblast populated collagen lattice. Whilst tethered no physical contraction can take place and isometric tension builds up. This is believed to stimulate the formation of stress fibres and α-SMA as fibroblasts take on the myofibroblast phenotype (Tomasek *et al*, 2002). On release of the gel's attachments there is a rapid contraction in proportion to the amount of isometric force developed.
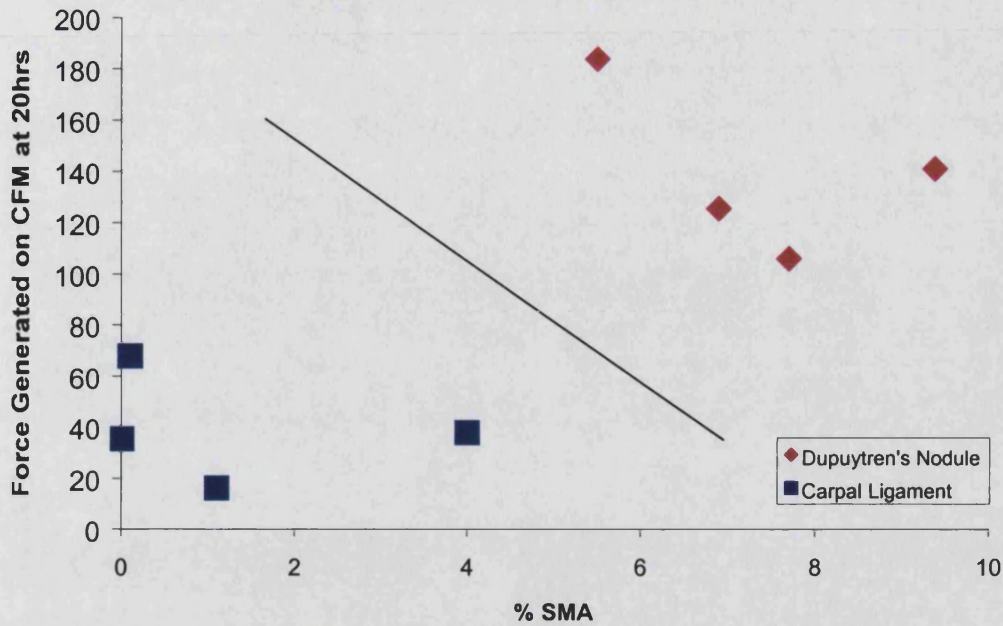
Figure 3.4.7a. Scatter plot of force generated by a particular cell line at 20 hours on the culture force monitor against the α-SMA content of the cell line determined by 2D immunoflourescence staining. The oblique line represents the division between the two populations.
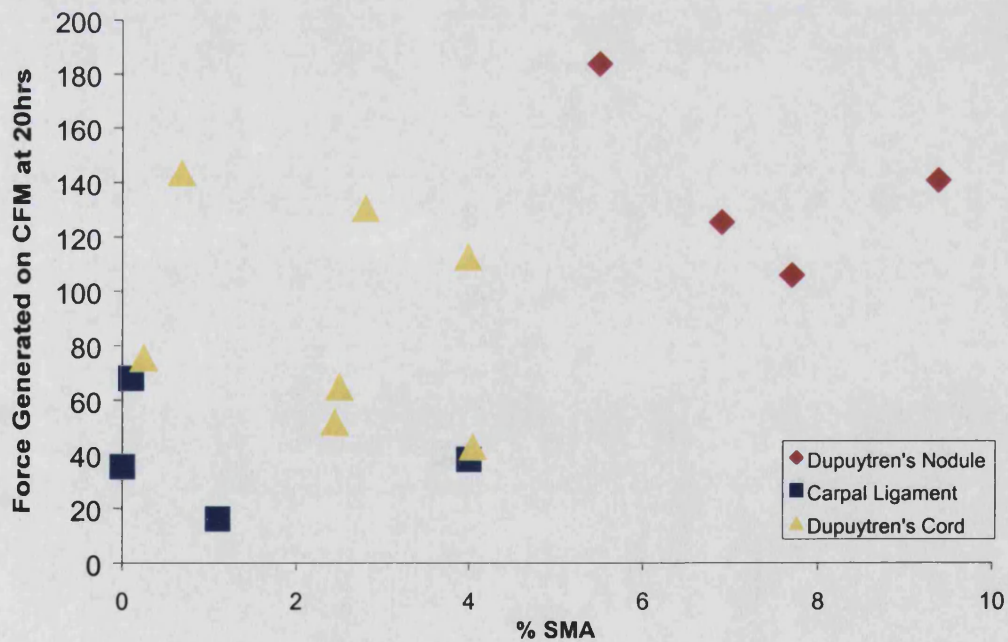
Figure 3.4.7b. Scatter plot of force generated by a particular cell line at 20 hours on the culture force monitor against the α-SMA content of the cell line now including Dupuytren's cord cell lines. There is no longer such a clear division with more of a continuation of points.

Although the early phase of contraction seen with the culture force monitor has been linked with cell attachment and locomotion (Eastwood *et al*, 1996) as in free floating gels, the later phases all occur within a tethered system, contraction occurring against the force transducer.

Part of the reason nodules cells here generated similar forces as quoted dermal fibroblast values may have been their tendency to continue contracting throughout the 20 hour period of the experiment. This continued contraction at 20 hours represented by the 20 hour gradient was also observed in cord fibroblast to a lesser extent but not in carpal ligament cells.

By 20 hours dermal fibroblasts have been shown to reach tensional homeostasis (Brown *et al*, 1998) where the forces generated by the cells are equal to the resistance of the force transducer. This plateau phase (phase 3) indicates the preferred level of tension at which the cells exist. Subsequent increases in tension within the system by mechanical load cause a cellular response with cells relaxing to take off this tension and return the force to the preferred level. Conversely decreases in force will cause cell contraction in an attempt to maintain equilibrium.

The continuing contraction of Dupuytren's cells at 20 hours may represent a delay in the acquisition of tensional homeostasis, which additionally might occur at a much greater force than seen here. This could only be clarified by a series of additional experiments, leaving the culture force monitor gels to contract over an extended period of time to determine if a plateau phase was attained. These experiments were beyond the scope of the current investigation. This delay in homeostasis does not occur in normal carpal ligament fascial fibroblasts and thus alterations in tensional homeostasis may be crucial to understanding the development of Dupuytren's disease.

Affected fibroblasts may have escaped normal tensional controls, preferentially existing within the diseased matrix at a higher level of tension than normal fascial fibroblasts. **This could cause an increase in the cell-mediated tension on the matrix resulting in slow but progressive tissue shortening and digital flexion deformities.**

SUMMARY:-

- Dupuytren's nodule fibroblasts generate significantly greater force than cord fibroblasts in the culture force monitor model. Both nodule and cord fibroblasts generate significantly greater force than normal carpal ligament fascial cells.

- The contraction profile shape of Dupuytren's cells is different to that of published dermal fibroblasts or carpal ligament controls, with significant continuing force generation at 20 hours.

- These differences indicate a delay in reaching tensional homeostasis, which occurs at a higher level of tension in Dupuytren's fibroblasts, and especially those derived from nodules.

Abnormalities in tensional homeostasis could go some way to explaining fibroblast behaviour in the formation of clinical contractures.

In order to investigate the tensional homeostasis of Dupuytren's disease fibroblasts further it was decided to observe the response of these cells to mechanical stimuli within the culture force monitor model.

3.5. The Response of Dupuytren's Nodule, Cord and Carpal Ligament Fibroblasts within Collagen Lattices to Mechanical Stimuli.

3.5.1. Introduction

Most cells *in vivo* exist in a dynamic environment, attached and embedded within a matrix. This often has constantly changing external stresses placed upon it and these cause changes in the tension or forces across the matrix. These forces are transmitted to the cells through cell matrix adhesion molecules such as integrins (Riikonen *et al*, 1995). Within the dermis vast alterations in tension can occur depending on whether the skin is stretched or relaxed, pressure is being applied or it is affected by gravity. It is in the cells of the dermal matrix, dermal fibroblasts, that the theory of tensional homeostasis has been elucidated (Brown *et al*, 1998).

Experimental data suggests that a basal "preferred level" of cell-matrix tension can only be maintained if cells react to changes in stress in the short term, relaxing to take off increases in tension across the matrix, and contracting when forces decrease. Longer periods of tensional change will in addition, undoubtedly result in tissue remodelling. Within a tissue such as the palmar fascia there are particularly rapid and continuous changes in matrix loading as hands are used for every day tasks and fingers flex and extend. In Dupuytren's disease the changes in loading may be exacerbated because of the matrix thickening and increased stiffness. Attempting to extend ones fingers against a tight band of diseased fascia will cause huge increases in external force, particularly as the extending force is aligned with the longitudinal direction of the fascia. In certain circumstances when an extending force is enhanced by continually increasing external splinting (Messina & Messina, 1993) this is sufficient to activate tissue remodelling (Bailey *et al*, 1994) and the shortened fascia can be elongated to allow extension of the digit. As soon as the splint is removed for any length of time, however the contracture returns, possibly at a more rapid rate than would normally be expected.

It has also been reported that patients with early disease who constantly stretch their fingers in fear of developing Dupuytren's contractures, actually rapidly acquire thick fibrous cords (Skoog, 1963). These observations suggest that mechanical stimuli
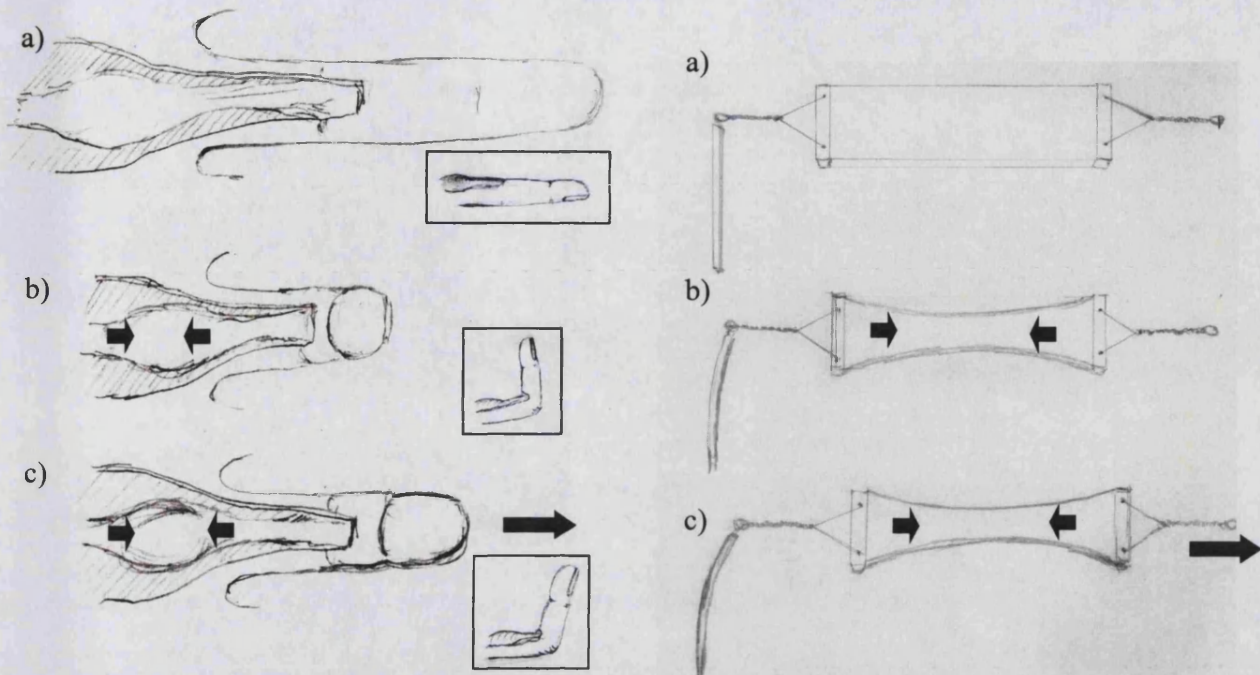
Figure 3.5.1. Diagram illustrating the applicability of the Culture Force Monitor model to Dupuytren's contracture. a) The newly set fibroblast populated collagen lattice is equivalent to non contracted Dupuytren's disease tissue. b) Dupuytren's disease with a shortened nodule/cord complex causing a digital flexion deformity is analogous to a fully contracted collagen gel on the CFM. c) Loading of the contracted collagen gel is equivalent to the clinical situation where attempts are made to extend a digital flexion deformity.

and abnormal responses of Dupuytren's fibroblasts to these, may play a role in the progression of disease. Having therefore proposed in the previous chapter that the acquisition and basal level of tensional homeostasis were altered in Dupuytren's fibroblasts, the work presented in this chapter investigates the responses of cells to a defined directional mechanical stimulus.

As alluded to above, the direction of the force being applied is a very important consideration and in the case of Dupuytren's disease these forces generally have a specific orientation. Cords and nodules are aligned longitudinally in the hand and fingers, causing contractures in this direction and hence forces are also concentrated along this axis. In this respect the culture force monitor provides an excellent model for investigating this type of force change. As illustrated in figure 3.5.1. the collagen lattice can be likened to the Dupuytren's disease tissue that shortens as cell mediated contraction progresses. This

generates a longitudinally orientated tension applied to the force transducer in a similar fashion as the Dupuytren's disease tissue would itself apply force to an affected digit. It is proposed that attempts to apply an extending force to the digit will transmit an increased uniaxial loading force to the diseased fascia, which is analogous to the uniaxial overloading one can apply to the culture force monitor. It is this type of mechanical stimulus that will be investigated in this chapter.

3.5.2. Aim

To test the effects of mechanical overloading on Dupuytren's nodule, cord and carpal ligament fibroblasts.

3.5.3. Methods

Contraction experiments were set up as described in chapter 3.4. At the conclusion of each experimental run on the culture force monitor at 20 hours a series of uniaxial tensional overloads were applied to the fibroblast populated collagen lattice. This was achieved by moving the culture force monitor mounting stage away from the force transducer as detailed in chapter 2.5.4. by manually turning the stage micrometer wheel through 30 micrometers. The culture force monitor was then left for 30 minutes to record the subsequent changes in force in this "post overload" period. A series of overloads were performed sequentially in exactly the same way and the post overload responses recorded for each as described in detail in chapter 2.5.4. Three acellular control gels were subjected to this pattern of serial overloads first and then nine Dupuytren's nodule, ten Dupuytren's cord and four control carpal ligament cell lines were investigated. The gradient of the contraction profile over the thirty minute post overload period was calculated as the rate of change in force in this 30 minutes.

3.5.4. Results

A typical control, acellular lattice contraction profile during the overloading sequences is displayed in figure 3.5.2. Each overload indicated by a block arrow is characterised by a sharp rise in the force being recorded through the transducer. In these control gels during each post overload period there is a steady decrease in force being recorded and the rate of this decrease (y) is constant in all four periods. There are no cells in these gels and therefore this response is a result of the elastic properties of the matrix/collagen gel. In other words the collagen lattices appear to have a degree of pliability and there is some relaxation in the gel after loading. This relaxation only appears to occur over the first 30 to 35 minutes after the loading as shown after the fourth
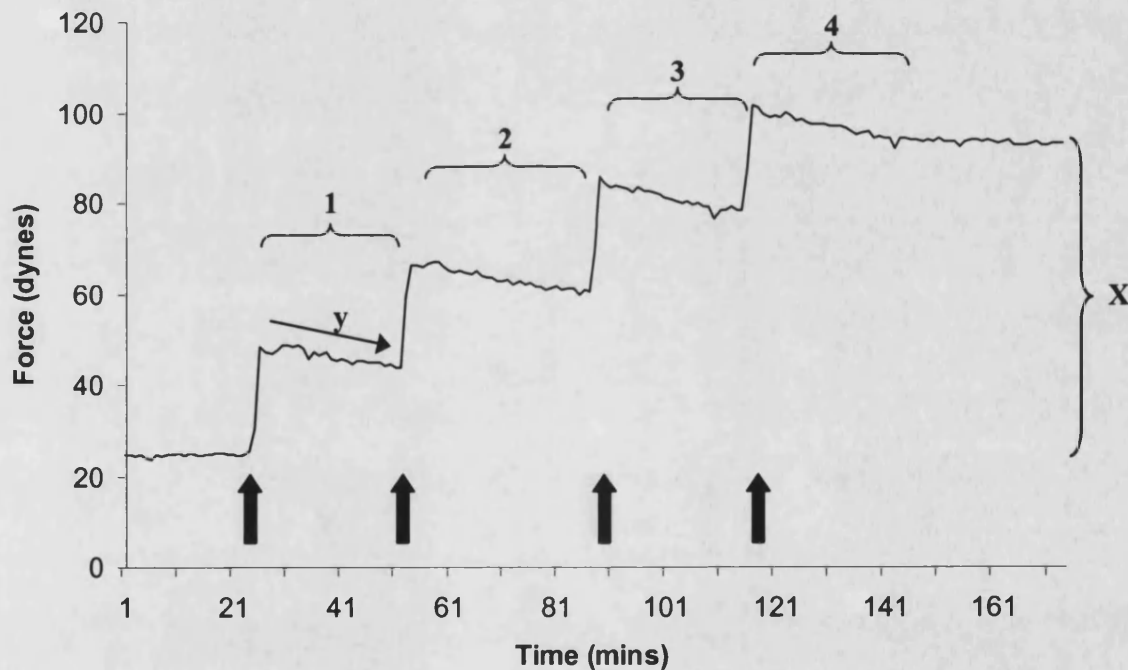
Figure 3.5.2. Contraction profile of a control acellular collagen lattice undergoing a series of four tensional overloads (arrows). The subsequent post overload periods are numbered 1 to 4. Note the uniform negative, downward gradient of each of these periods. X represents the increase in stiffness of the collagen matrix induced by the series of four overloads. The gradient of "relaxation" y, represents the elastic properties of the matrix.

129

overload in figure 3.6.2. where the gel was left for 60 minutes. The trace has plateaued after 35 minutes and there is no further change in force in the system. Following each overload the reduction in force because of the gels elastic properties, never fully returns to the pre loading level of tension, so that with each overload there is a stepwise increase in the underlying tension.

Recent unpublished observations from the same laboratory (M. Marensa personal communication, 2002) suggest that this increased tension corresponds to a rise in the stiffness of the collagen matrix. The point where the trace plateaus after relaxation represents the increased level of matrix stiffness, thus the overall change in force from the pre-loading state to the plateau following the fourth overload is equivalent to the increase in stiffness in the collagen matrix induced by the complete sequence of overloads (see X in figure 3.5.2).

The gradient of the control traces in each overload period (y in figure 3.5.2) is negative and the means of three runs are illustrated in figure 3.5.3.
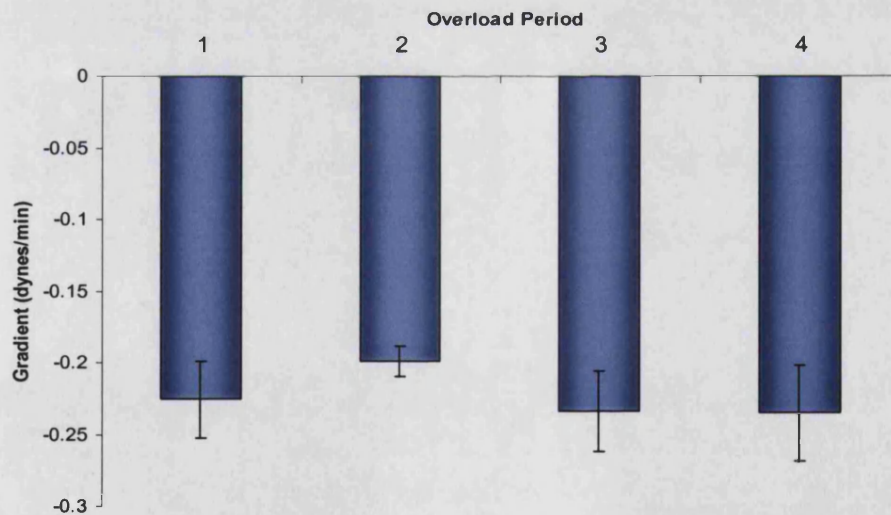
Figure 3.5.3. A histogram showing the mean post overload period gradients for control, acellular collagen lattices (n=3). Error bars represent standard errors of the means. Each period has a similar negative gradient.

130

In the first overload period the gradient was −0.23 dynes per minute (SEM ± 0.03) with subsequent overload periods being nearly identical at −0.20, −0.23 and −0.24 dynes per minute. There was no significant difference between these results.

When carpal ligament fibroblasts were seeded into the collagen lattices and the same overloading sequence was performed at 20 hours a very similar pattern to the acellular control was observed. Again gradients were negative in the post overload periods and the values of these did not differ significantly either between overloads 1 to 4 or from acellular control values. The mean results of four cell lines are displayed graphically along side the control data in figure 3.5.4.
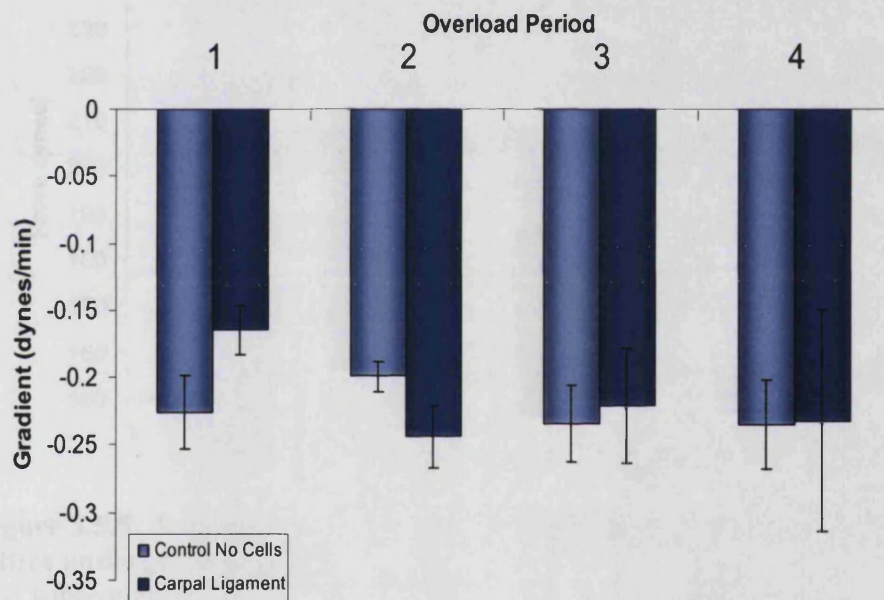
Figure 3.5.4. Histogram comparing the control and carpal ligament mean post overload gradients for periods 1 to 4. Error bars represent standard errors of the means. There is no significant difference between the two groups in any of the periods.

The mean first overload period gradient was −0.16 dynes per minute (SEM ± 0.02), slightly less than controls but not reaching statistical significance (p= 0.112). The mean second, third and fourth post overload period gradients were −0.24 dynes per minute (SEM ± 0.02), −0.22 dynes per minute (SEM ± 0.04) and −0.23 dynes per minute (SEM ± 0.08) respectively. This was not what we had expected as the theory of tensional homeostasis

would suggest that the cells, having undergone an increase in force would relax to take off this tension. The cells appeared to have no effect above that seen by the elastic properties of the control gel.

When Dupuytren's fibroblasts were seeded within the collagen gels results were even more unexpected. Unlike the control blank gels and carpal ligament fibroblast seeded gels, the gradient of the contraction profile in the first post overload period was, more often than not (6 out of 9 nodule and 6 out of 10 cords), positive as shown by a typical nodule trace in figure 3.5.5.
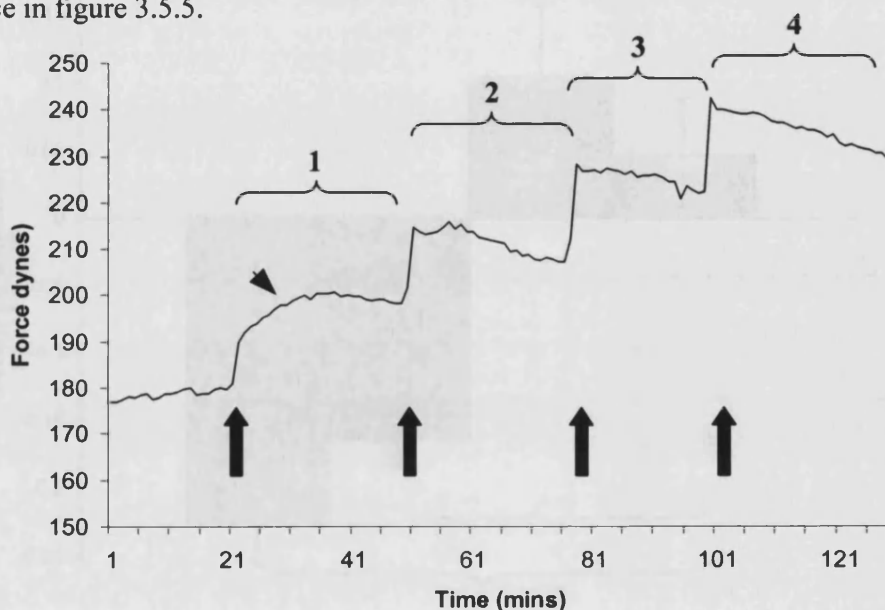
Figure 3.5.5. A typical contraction profile trace from a nodule cell line seeded collagen lattice undergoing a series of four tensional overloads (arrows).
The subsequent post overload periods are numbered 1 to 4. Note the very different pattern in the first period where there is actually contraction (arrow head) in response to the overload.

Even in those three nodule and four cord cell lines where the gradient was negative the values were far less than the controls, suggesting that in every case the Dupuytren's fibroblasts were responding to the increased load by increased cellular contraction. The nodule fibroblasts tended to contract to a greater degree than the cord fibroblasts and this is graphically represented in figure 3.5.6. where the relative mean gradients in the first post

132

overload period are displayed for each cell type and the control gels. The mean nodule gradient for this first post overload period was +0.1 dynes per minute (SEM ± 0.05) whilst for cord it was +0.05 (SEM ± 0.04). The differences seen between nodule and cord failed to reach statistical significance (p=0.4) however the nodule gradient was statistically significantly greater than both carpal ligament and controls in the first post overload period (p<0.01). This was also the case for Dupuytren's cord fibroblasts (p<0.01).
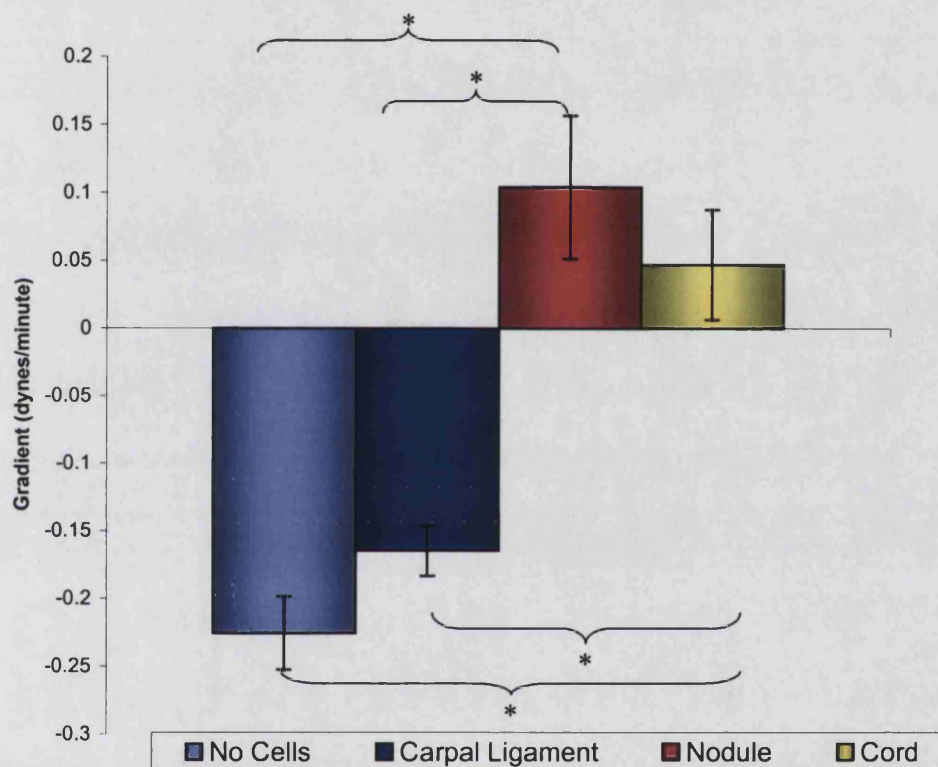
Figure 3.5.6. The mean gradients of the first post overload period for control gels (n=3) carpal ligament (n=4), Dupuytren's nodule (n=9) and Dupuytren's cord (n=10) fibroblast seeded collagen lattices. Error bars represent standard errors of the means. There are significant differences between both nodule and cord and the control and carpal ligament groups as indicated. * p<0.01.

In subsequent post overload periods the gradients recorded returned towards control and carpal ligament values. In the second period the mean nodule gradient was –0.21 dynes per minute (SEM ± 0.03) and the corresponding value for cord was –0.15 dynes per minute (SEM ± 0.04). Neither of these values was significantly different from each other or control and carpal ligament gradients. Values were similar for the gradients in post overload

133

periods three and four, again with no significant differences. This total mean data is shown in figure 3.5.7 where the mean gradients are shown for each of the post overload periods and all cell types.
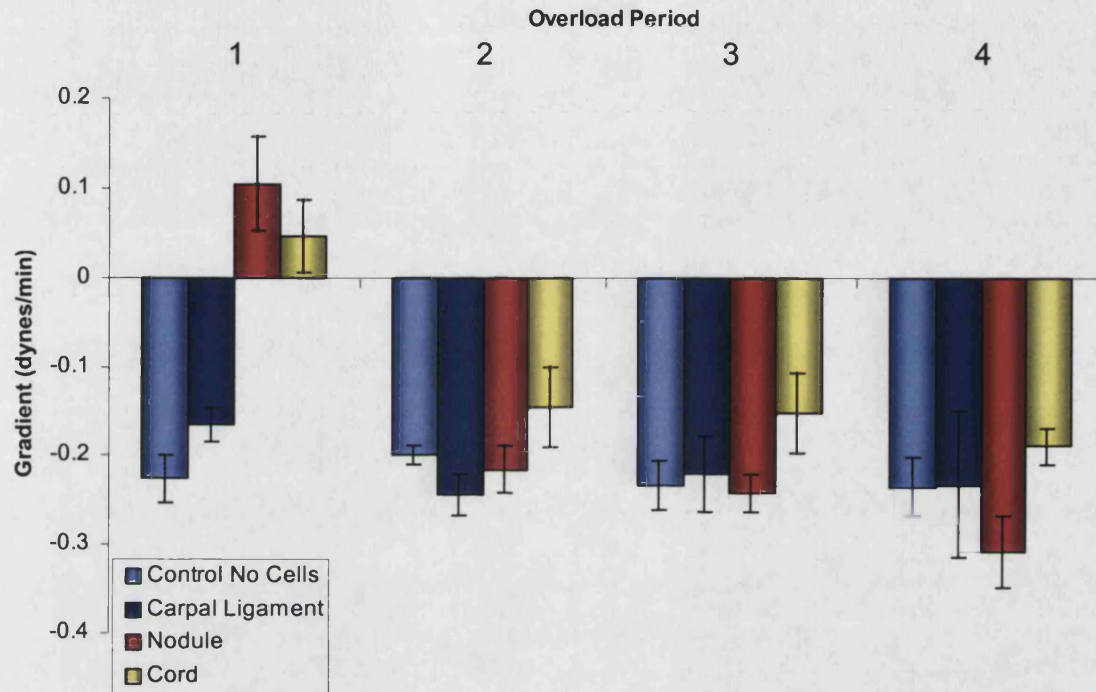
Figure 3.5.7. A histogram showing the mean gradients for control gels (n=3), carpal ligament (n=4), Dupuytren's nodule (n=9) and Dupuytren's cord (n=10) fibroblast seeded collagen lattices for all for of the post overload periods. Error bars represent standard errors of the means. There are no significant differences between the groups except in the first post overload period as shown already in figure 3.5.6.

3.5.5. Discussion

The culture force monitor model (Eastwood *et al*, 1994) or equivalent (Delvoye *et al*, 1991) is the only device that has the ability to monitor actual forces in real time within a fibroblast populated collagen lattice. Circular free floating or fixed released gels may give an indication of relative, overall contractile properties however they cannot provide a quantitative assessment as has been done here. Cellular responses to changes in tension or loading have therefore only recently begun to be investigated, despite this being an integral part of most fibroblasts behaviour.

Tensional homeostasis has been elucidated in dermal fibroblasts using the tensioning culture force monitor (tCFM) (Brown *et al*, 1998). These cells contract to reach a steady state equilibrium within a collagen lattice where the force remains constant over time. If, however, the collagen gel is subjected to an overloading force, the fibroblasts relax to take this tension off of the matrix returning the force in the system towards the preferred steady state. A reduction in force within the system by underloading the gel causes a contraction by resident cells, so increasing the force in the lattice and again returning to the equilibrium tension. Delvoye and co workers (1991) saw a similar phenomenon using their comparable model but did not expand on this observation.

In their study of tensional homeostasis Brown *et al* (1998) used the tCFM to overload FPCLs over 15 minutes studying subsequent cell mediated responses over a further 15 minutes. They did state that similar responses were observed when loading occurred over a shorter period of time. This chapter studies the effect of a very rapid overload (2 to 4 seconds) by manually moving the CFM mounting stage by a set distance with the micrometer wheel. In many ways this is more in keeping with the *in vivo* nature of tissue loading in the hand where fingers are flexed and extended in a matter of seconds rather than over many minutes. Fibroblasts therefore may also display rapid responses.

The reduction of force after loading of control acellular gels (gradient y in figure 3.5.2) has not been noted before but is thought to be due to elastic properties of the collagen lattice itself. After a rapid overload the compliance of the lattice allows a gradual

reduction of force in the system as a degree of relaxation occurs. This was probably not seen by Brown *et al* (1998), because their system of overloading was somewhat different to that used here, taking place using a mechanical motor gradually over 15 minutes. Compensation in the lattice compliance would have occurred **during** their slower overload. The relaxation appears to last for about 30 minutes (see figure 3.5.2) and does not return the gel to the level of tension prior to overloading but a new higher level is established. This higher level corresponds with matrix stiffening, as has recently been demonstrated in this laboratory, and is an important finding as a stiffer matrix will affect both the way resident fibroblasts generate force and they way in which changes in force are perceived by the cells.

This is the first study of the response by Dupuytren's cells or carpal ligament fibroblasts to changes in tension. Carpal ligament fibroblast seeded FPCLs demonstrated no significant difference in response to overloading forces when compared to control acellular gels. The reduction in force after each overload could therefore have been accounted for by the elastic properties of the gel alone. If these fibroblasts do exhibit tensional homeostasis the responses may be at such a low level after this rapid overloading, that in this experimental model they are indistinguishable from the initial elastic properties of the gel. Nevertheless, whether such cells would exhibit tensional homeostasis under the experimental conditions used by Brown *et al* (1998) is unknown. A low level of responsiveness could be in keeping with their poor overall contraction as demonstrated in section 3.5 and their *in vivo* properties. As discussed in 3.4.5, the surrounding dense collagen matrix with relatively low turnover or remodelling may provide a stress shielded environment (Eastwood *et al*, 1998) requiring little in the way of force generation or homeostatic control. An alternative explanation is that these fibroblasts are relatively "mechano-insensitive" and would require much greater changes in force to initiate a cell mediated response than the forces used in this model. Modified or different models would be required to investigate these hypotheses, allowing study of either very large or very small changes in forces.

The responses seen by both nodule and cord Dupuytren's derived fibroblasts after rapid uniaxial tensional overload were unexpected and contrary to the theory of tensional homeostasis. In general the increase in force of each overload was around 20% to 30% of the total developed force, which should have been sufficient to elicit a typical cell mediated homeostatic response (Brown *et al*, 1998). These cells exhibited a contractile response to the first overload, increasing the force still further and overcoming the elastic properties of the collagen gel. Nodule fibroblasts showed a greater response than cord in keeping with the emerging trend from this work of nodule cells being more active or contractile, although the difference failed to reach significance. This contraction in the first post overload period could be seen as highly abnormal in the context of tensional homeostasis and might be viewed as causing a positive feedback loop, where an increase in force causes cell mediated contraction of the matrix and a further increase in force.

This abnormal response however, disappears by the second post overload period and for this and the subsequent periods values do not differ significantly from control acellular gels. As with carpal ligament FPCLs this may be because tensional homeostasis is weak within Dupuytren's derived fibroblasts and indistinguishable from the forces caused by elastic changes within the gel. Alternatively it could be that tensional homeostasis does or would occur but could not cause a physical reduction in force at a greater rate than the elastic properties of the collagen gels (-0.2 to -0.3 dynes per minute). Had studies continued, to observe cell responses from 30 to 60 minutes it may have been apparent by a continued reduction in force that tensional homeostasis was occurring in an attempt to return the system to equilibrium. Contradicting this are the findings of several greater negative post overload gradients by Brown *et al* (1998), suggesting that collagen gel relaxation is not a rate-limiting factor. Different cell types are being investigated here, however, and as the interplay between gel elasticity, cell mediated contraction and responses to changes in tension are not yet understood it is difficult to draw a firm conclusion.

It is not clear why the abnormal response is observed in only the first post overload period. It may be linked to the continuing rise in force seen at the start of overloading in

Dupuytren's fibroblasts. If the cells have yet to reach tensional homeostasis and are still contracting they will continue to contract if the force of the overload is insufficient to attain the level of homeostasis. When the gradients at 20 hours (derived from data presented in chapter 3.4) are compared with the gradient of the first overload period as illustrated in figure 3.5.8. there is some correlation. As the gradient of the contraction profile at 20 hours increases, indicating a higher level of continuing contraction, there is an increasing gradient of the first post overload. The R^2 value for the resultant line of regression is 0.5.
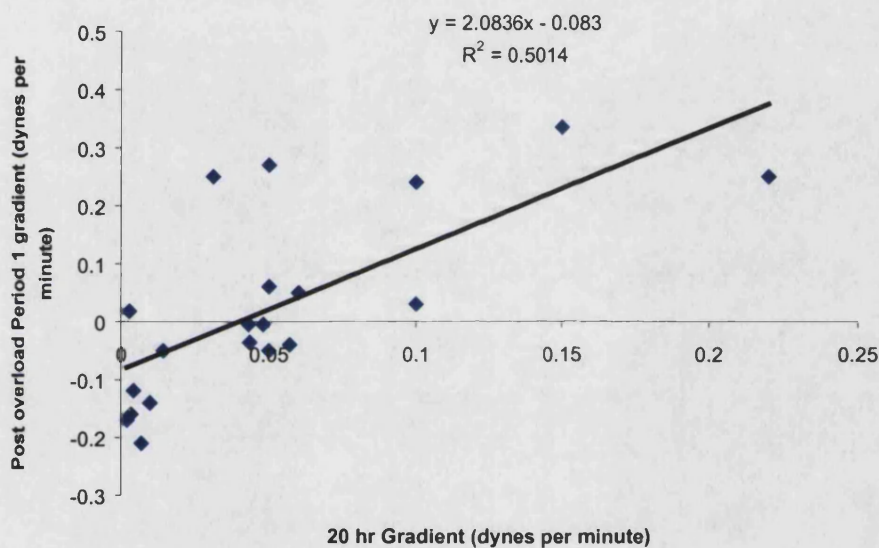
Figure 3.5.8. A scatter plot of the contraction profile gradients at 20 hours and the gradient of the corresponding first post overload period including nodule, cord and carpal ligament cell lines. Note the line of best fit indicating increasing post overload gradient as the 20 hr gradient increases.

It is conceivable that the second overload will increase the force to such a level that the homeostatic equilibrium is achieved and no further contraction need occur to attain this. This theory would suggest that the level of force at homeostatic equilibrium is between 1 and 2 overloads greater, or 30 to 40% more than the force generated by fibroblasts at 20 hours. Alternatively this contraction in response to applied load could be an inherent abnormal response from Dupuytren's cells and would act as a positive feedback loop causing further cell-mediated contraction.

In order to test this theory one would have had to leave the collagen gels until a steady state had been achieved and then undertake the overloading sequence in the same way. If the responses were the same it could be deduced that there was an inherent abnormality. There are potential difficulties with continuing experiments using the CFM for extended periods of time. The culture system is not strictly enclosed as there are openings in the lid for the "A" frame bars (see appendix III) and thus infection often occurs during long-term experimentation. There are additional practical issues regarding the use of limited equipment resources over long periods of time and therefore the above experiments were not performed.

A second alternative hypothesis as to why the abnormal contractile response is only observed in the first overload period, hinges on the matrix stiffening, which as described earlier is induced by loading of the matrix. One way of stiffening a matrix is by increasing the collagen concentration and this has been shown to alter the cell-mediated contraction (Bell *et al*, 1979; Zhu *et al*, 2001). A second way is by loading the matrix. The stiffer matrix transmits less force to resident cells; essentially stress shielding them, so that they perceive less of any additionally applied force. It is conceivable that in my experimental model the second and subsequent overloads increased matrix stiffness to such an extent that the resident cells were no longer able to perceive the change in tension. If they cannot detect the change they will not react to it and thus the only response to these overloads will be that relating to the elastic properties of the gel (see figure 3.5.9). The cells become mechano-unresponsive. Actually, the fact that there is an abnormal response by Dupuytren's fibroblasts to the first overload may be even more significant, given the increased matrix stiffness and thus decreased force perceived by the cells following even this first loading.

A possible third hypothesis to be considered as an explanation why a response is only seen following the first overload could be that this response, being an active cellular process, requires certain intracellular elements. Intracellular pools of these elements, be they for example ions (eg Calcium ion flux) or proteins linked to mechanotransduction, may be finite and therefore used up by the first response. Subsequent overloads were

applied relatively soon following each other and these elements may not have had sufficient time to reach the desired levels or even be manufactured once more. Thus the cells may have a refractory or latent period in a similar way that nerve and muscle cells have to electrical impulses and contraction (Guyton and Hall, 1996). The fibroblasts might only be able to react again once this refractory period is over.

In any of the three hypotheses presented here, an abnormal cellular contractile response to loading in Dupuytren's fibroblasts is an important finding and could suggest the basis by which flexion deformities of the digits occur and progress. Taking these results in context with those from 3.4 a clinical scenario could be envisaged where Dupuytren's cells are continually striving to reach tensional homeostasis but failing to attain it. Further external forces, as simple as finger extension would place increased tension on the resident cells within the diseased tissue, causing additional cellular contraction as seen here following the first overload. This positive feedback would exacerbate the condition.

Even these high cell mediated contractile forces produced would not be strong enough to overcome the extending force of the digital extensor tendons, however at times of rest rapid matrix turnover and remodelling could "set" the matrix at this new shortened length. The increased ratio of type III to type I collagen found in Dupuytren's tissue, especially nodules (Bazin et al, 1980; Brickley-Parsons et al, 1981) suggests the matrix being laid down is new and immature and there is also evidence of increased matrix turnover with higher levels of MMP expression when under tension (Tarlton et al, 1998; Bailey et al, 1994). Once this has occurred, resident cells might then relax and make new attachments to the matrix before the whole process repeats itself in a minutely stepwise but continuous, progressive fashion. Thus one can see how fibroblast contraction in combination with matrix remodelling could cause unchecked disease progression.

a) Unloaded collagen gel

b) Gel overloaded once

c) Gel overloaded twice
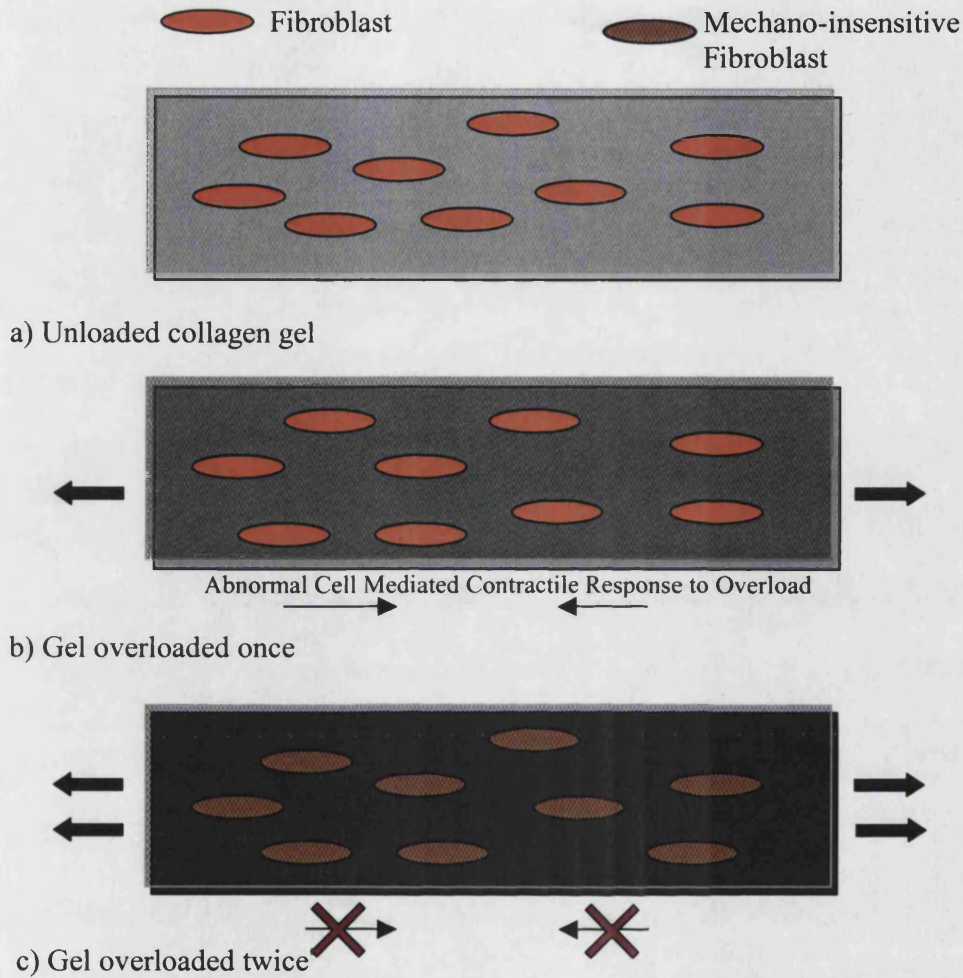
Figure 3.5.9. Diagram representing the proposed effect of collagen gel loading on fibroblast perception of force. Prior to loading cells are able to perceive force and respond to it. The first overload causes a stiffening of the matrix (Darker colour ▨) but the cells are still able to perceive the force. The second overload stiffens the matrix still further (Much darker colour ▪) which prevents the force being transmitted to and perceived by the fibroblasts(⬬), so they are unable to respond to it (◄✖).

141

This may also explain the observation that in patients who continually manually stretch their fingers in an attempt to overcome the disease, thick aponeurotic cords develop with rapid clinical contractures (Skoog, 1963; Flint and Poole, 1990 in Dupuytren's Disease). The regular extension would provide an external loading of the Dupuytren's cells causing not only additional collagen deposition but also further cell contraction. Similarly in patients who have undergone continuous elongation techniques (Messina and Messina, 1991) to extend severely contracted digits prior to surgery, it is noted that the contractures recur very quickly if the operation is delayed once traction is removed (Bailey et al, 1994). In this situation the external stretching or overloading force applied to the resident cells could be providing strong positive feedback and as soon as the external fixation is removed there is an aggressive cell mediated contraction combined with the high matrix remodelling that has been shown to exist during this procedure (Bailey et al, 1994).

SUMMARY:-

- Rapid overloading of acellular control collagen lattices causes a subsequent gradual reduction in force over 30 minutes because of the gel's elastic properties, which is highly reproducible in all four post overload periods.

- Overloading of lattices seeded with carpal ligament fibroblasts causes no significant differences in the 30 minute post overload periods when compared with acellular control gels.

- **Overloading of lattices seeded with Dupuytren's fibroblasts causes an abnormal contractile response during the first post overload period.**

This abnormal response and the altered level of tensional homeostasis in Dupuytren's fibroblasts found in chapter 3.4, could when combined with matrix remodelling, underlie the development of progressive flexion deformities clinically.

The next step would be to identify potential factors that cause or are key modulators of these abnormal responses, and establish their role in the processes that have been discovered. Transforming growth factor beta$_1$ is a likely candidate.

3.6. Myofibroblast Phenotype in Two-Dimensional Cell Cultures From Dupuytren's Nodules, Cords and Control Carpal Ligament Treated with TGF β_1

3.6.1. Introduction

Transforming growth factor beta$_1$ (TGF β_1) is a pleotropic polypeptide growth factor with wide and varied cellular effects. It has been linked in particular to the processes occurring in response to injury, healing and fibrosis (Border and Noble, 1994). It has been shown to both stimulate and inhibit cellular proliferation depending on circumstances and cell type (eg inducing proliferation of mesenchymal cells such as fibroblasts and inhibiting growth of ectodermal cells (Roberts *et al*, 1986). In addition ECM production and especially collagen synthesis is stimulated by TGF β (Roberts *et al*. 1986; Petrov *et al*, 2002; Serini and Gabbiani, 1999) and several studies have demonstrated the up regulation of fibroblast to myofibroblast transformation by it (Desmouliere *et al*, 1993; Desmouliere and Gabbiani, 1994). The myofibroblast itself has been proposed as the common denominator in fibrocontractive disorders (Ariyan *et al*, 1978) because of its prevalence in such conditions and this type of cells contractile phenotype. These facts make it likely that TGF β plays a key role in tissue fibrosis. Dupuytren's disease is a fibrotic pathology, where all of these are important. Indeed TGF β stimulation of cell proliferation (Badalamente *et al*, 1996), collagen production (Alioto *et* al, 1994; Bulstrode, MD Thesis 2001) and myofibroblast transformation (Jemec, MD Thesis 1999; Vaughan *et al*, 2000) have also been established in Dupuytren's disease.

It is unclear however if there is a different response to TGF β from cells originating in different regions of the Dupuytren's lesion such as nodule and cord, having already shown differences in the cell types in monolayer culture (Chapter 3.2). It was hypothesised, given the differing basal levels of myofibroblasts in nodule and cord cell cultures, that the response to TGF β_1 stimulation would be different between these two cell types.

Furthermore could responses and fibroblast behaviour such as contraction be simply due to the myofibroblast percentage and thus TGF β_1, or are there inherently altered responses? (Addressed in Chapters 3.7 and 3.8)

143

3.6.2. <u>Aim</u>

To determine the upregulation of the myofibroblast phenotype in fibroblast cell cultures obtained from Dupuytren's nodule, Dupuytren's cord or control carpal ligament when stimulated with TGF β_1.

3.6.3. <u>Material and Methods</u>

The same protocol was used as for section 3.3.3. however at 24 hours after seeding fibroblasts in the six well plates, the normal growth media was replaced by normal growth media supplemented with 2 ng per ml of TGF β_1. Cells were fixed on the cover slips 72 hours later and stained and counted as before. Seven nodule, seven cord and four carpal ligament cell lines were studied and differences between the groups analysed using the student's t test.

3.6.4. Results

Figure 3.6.1 illustrates the typical appearances of a Dupuytren's nodule cell line after three days treatment with TGF β_1 at 2 ng per ml. There is an obvious increase in the percentage of positively staining myofibroblasts when compared with figure 3.3.2, an untreated nodule.
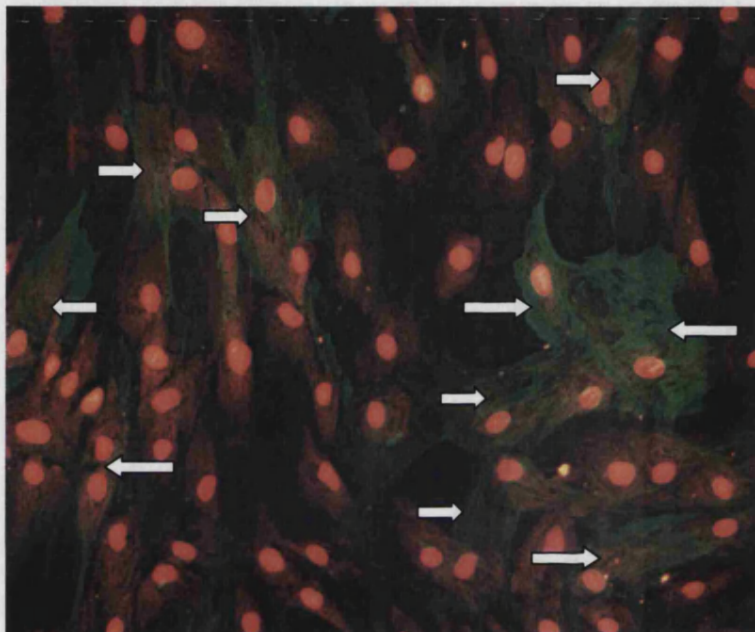
Figure 3.6.1. Cells in culture derived from Dupuytren's nodule at x 200 magnification stained for α-smooth muscle actin and counterstained with propidium iodide after stimulation with TGF β_1. Cells with green cytoplasmic filaments are positive (arrows). Note the significant increase in positively staining cells when this image is compared with figure 3.3.2.

This is even more striking in cord cell lines (figure 3.6.2) where the untreated cord contained few if any myofibroblasts (figure 3.3.3). Unexpectedly TGF β_1 treatment had little effect on the myofibroblast percentage in comparison carpal ligament cell lines where figure 3.3.4 illustrates the appearance of a typical cell line following stimulation.
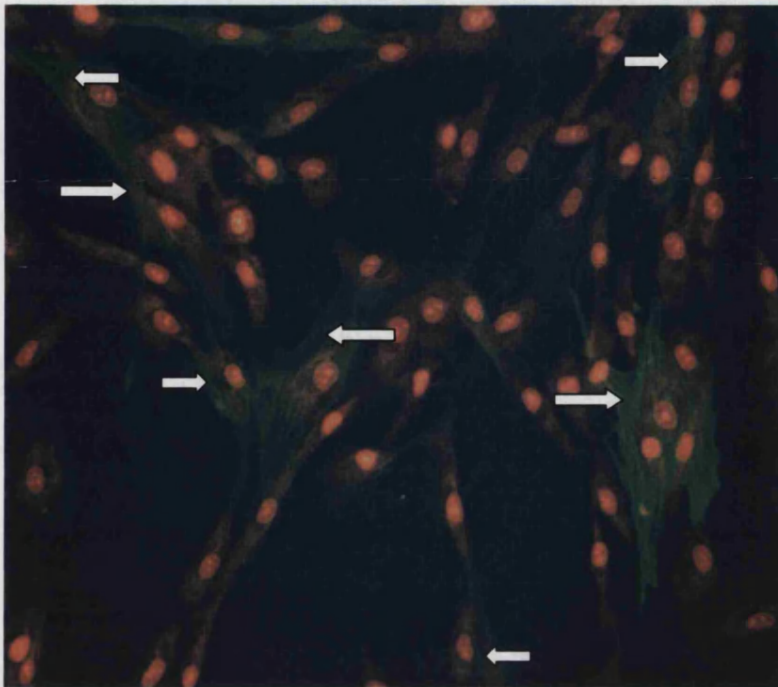
Figure 3.6.2. Cells in culture derived from Dupuytren's cord at x 200 magnification stained for α-smooth muscle actin and counterstained with propidium iodide after stimulation with TGF β$_1$. Cells with green cytoplasmic filaments are positive (arrows). Note the significant increase in positively staining cells when this image is compared with figure 3.3.3.
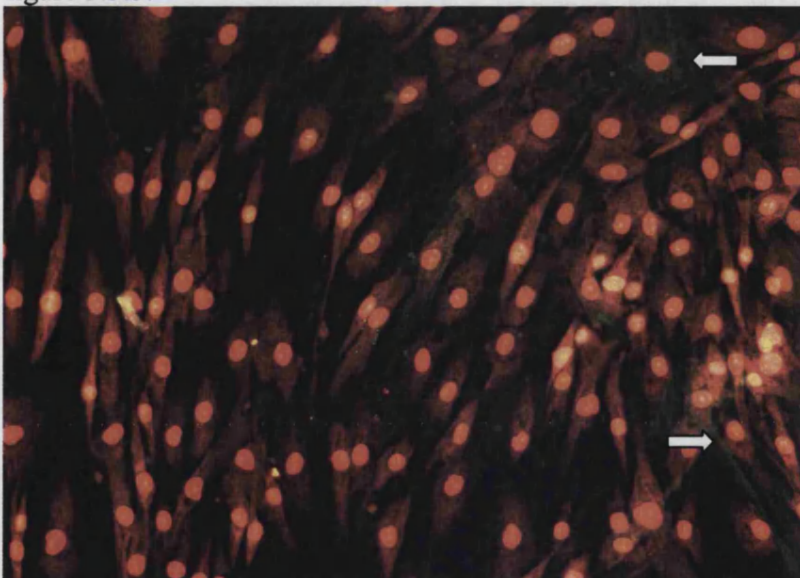
Figure 3.6.3. Cells in culture derived from control carpal ligament at x 200 magnification stained for α-smooth muscle actin and counterstained with propidium iodide after stimulation with TGF β$_1$. Note there is no significant increase in positively staining cells (arrows) when this image is compared with figure 3.3.4.

Overall the mean myofibroblast percentages are displayed in figure 3.6.4 along side of the untreated results from section 3.3. In nodule cell lines treated with TGF β_1 at a concentration of 2 ng per ml for three days myofibroblasts made up 25.4% (SD $\pm$ 5.5%, n=7) of the cell population. This was a significant rise over the non-treated levels of 9.7% with p<0.001. The mean myofibroblast percentage in cord cell lines after TGF β_1 treatment was 25.7% (SD $\pm$ 5.8%, n=7), which was again highly significant when compared with untreated levels of 2.7%, p<0.001. TGF β_1 treated nodule and cord cell lines were not significantly different from each other in terms of the myofibroblast phenotype, p=0.90. The mean myofibroblast percentage in TGF β_1 stimulated control carpal ligament cell cultures was 2.6% (SD $\pm$ 0.7%, n=4), which was not significantly different from untreated levels of 1.3% (p=0.23), however it was highly significant when compared with both stimulated nodule and stimulated cord cell lines (p<0.001). If one looks at the overall increase in myofibroblasts from unstimulated, basal levels, for each cell line the mean rise for nodules was 3 fold whereas the mean rise for cord was 11.6 fold. The individual percentage increases fail to fall within a normal distribution and thus a Mann-Whitney Rank Sum test was used to compare these differences, which just reached significance (p<0.05).
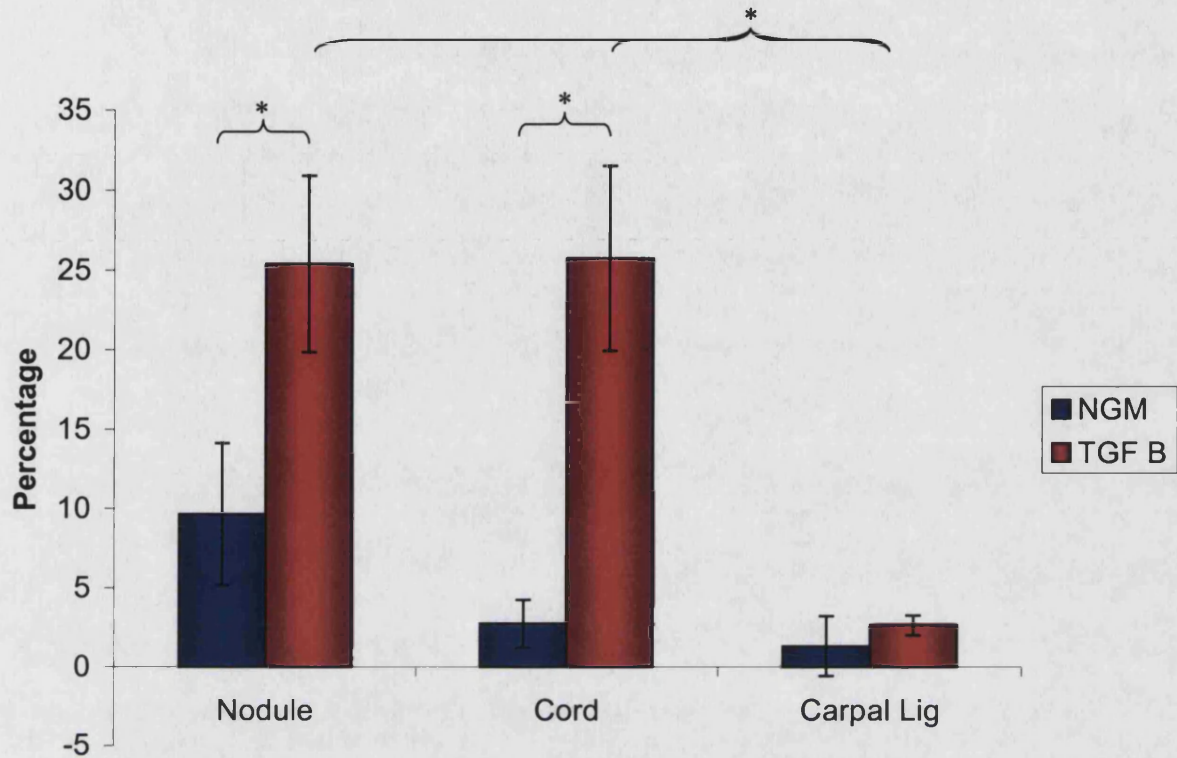
Figure 3.6.4. The mean percentage of myofibroblasts in cell cultures derived from Dupuytren's nodule (n=7), Dupuytren's cord (n=7) and control carpal ligament tissue (n=4) following stimulation with TGF-β_1 at 2 ng/ml for three days ■ . The error bars represent standard deviations. Shown along side are the corresponding unstimulated percentages ■ . There was a significant difference between treated and untreated percentages in both nodule and cord, * p<0.001, but not in carpal ligament. Both nodule and cord cultures when stimulated with TGF-β_1 were significantly different from stimulated carpal ligament values as shown.

3.6.5. Discussion

The transforming growth factors are part of a family of polypeptides, which play significant roles in cell signalling, activation and suppression within an array of physiological and pathological settings. Most interest within the group has been focused upon the transforming growth factor betas and in particular transforming growth factor-β_1. This has been shown to be important in wound healing, abnormal scarring and fibrotic diseases (Border and Noble, 1994).

The work in this chapter has demonstrated increased differentiation of the myofibroblast phenotype in Dupuytren's disease derived fibroblasts after stimulation with TGF-β_1. TGF-β_1 has been shown to induce myofibroblast transformation from fibroblasts in several studies (Desmoulière *et al*, 1993; Yokozeki *et al*, 1997; Vaughan *et al*, 2000). Currently it is believed that fibroblasts are stimulated to differentiate into proto-myofibroblasts and then "differentiated myofibroblasts" expressing α-smooth muscle actin by TGF-β_1 in addition to a range of other factors, which can act in concert (Tomasek *et al*, 2002). Desmoulière *et al* (1993) demonstrated an upregulation of myofibroblasts in a rat *in-vivo* model after subcutaneous injection of TGF-β_1 to granulating wounds. They subsequently found a corresponding increase in α-smooth muscle actin synthesis in cultured fibroblasts from both rat and humans using Western blot analysis. This occurred across a whole range of TGF-β_1 concentrations from 1ng/ml to 10ng/ml. In this study a concentration of 2ng/ml has been used, which is the standard concentration used in our laboratory for stimulation of myofibroblast differentiation, and falls within this range. The same concentration has been used by previous workers in this laboratory investgating Dupuytren's disease (Jemec MD Thesis, 1999; Bulstrode, N. MD Thesis, 2001).

Dugina *et al* (2001) used Dupuytren's nodule fibroblasts to study the formation of focal adhesions in myofibroblasts in response to TGF-β treatment. After TGF-β stimulation for 5 days they found an increase in myofibroblast numbers to 71% (from 3%), significantly more than encountered here. In the studies presented in this thesis however,

cultures were stimulated for three days. Additionally Dugina *et al* used TGF-β_2 rather than TGF-β_1 but did state that similar changes were observed with both growth factors, which has been found in other studies (Serini and Gabbiani, 1999). They also used a concentration of 5ng/ml, more than double the amount used here and this is most likely to account for the differences observed. Other authors (Vaughan *et al*, 2000) have determined myofibroblast percentages in stressed fibroblast populated collagen lattices by staining for α-smooth muscle actin. They used a maximum concentration of 1ng/ml of TGF-β_1, showing an increase from 7.9% to 23.4% after stimulation of Dupuytren's derived fibroblasts for 5 days.

Several groups have demonstrated the presence of TGF-β_1 in Dupuytren's tissue or Dupuytren's derived fibroblasts using a variety of techniques (Badalamente *et al*, 1996; Baird *et al*, 1993; Berndt *et al*, 1995; Zamora *et al*, 1994; Kloen *et al*, 1995) . Zamora *et al* (1994) only found TGF-β in early nodules whilst Bernt *et al* (1995) showed a greater intensity of staining for TGF-β_1 protein in proliferative nodules and co-localisation of TGF-β_1 synthesis and the myofibroblast phenotype to these regions.

The evidence in the literature therefore, combined with the proposed role of the myofibroblast, point to this growth factor playing a central function in the development and progression of Dupuytren's disease. Fibroblasts resident within cords of Dupuytren's tissue may be quiescent as indicated by the absence of myofibroblasts shown by previous histochemical studies, or the low levels demonstrated in section 3.2. These *in vivo* tissue differences were maintained in fibroblast culture as proved in section 3.3 by the basal, unstimulated results, however here when exposed to TGF-β_1 stimulus they became as equally differentiated as the traditionally active nodule cells. In fact, when one compares the overall increase in the myofibroblast phenotype, nodules demonstrate on average a three-fold rise whereas cord cultures had an eleven-fold rise. One can only speculate if this is a result of cord cells actually being more sensitive to TGF-β_1 however it is equally possible that cord simply has a lower basal expression of the myofibroblast phenotype within a population of similar diseased cells. Both nodule and cord fibroblasts would then respond to an equal degree following the same level of TGF-β_1 stimulation. This would

ultimately lead to a similar overall maximal upregulation of myofibroblasts leading to the result encountered here.

Carpal ligament cultures appeared completely insensitive to the stimulatory effects of TGF-β_1, showing no increase in myofibroblast phenotype. This is in keeping with previous unpublished work in our laboratory examining carpal ligament cells in this way (Jemec MD thesis, 1999). As discussed above all other fibroblast types investigated in the literature show some up regulation of myofibroblasts in response to TGF-β_1, this therefore is a significant finding. As with the poor contractile properties of carpal ligament cells, this lack of response to TGF-β_1 may reflect the nature and activity of these cells *in vivo*. The fact that Dupuytren's cells irrespective of their origin show highly significant differences to the control fascial tissue suggest there is a specific cellular abnormality of the diseased cells rather than being normal cells stimulated to behave aberrantly by external factors. This could be at the level of the cell membrane receptors, for example Kloen and co workers (1995) showed a different pattern of TGF-β_1 receptors in Dupuytren's fibroblasts compared with dermal fibroblasts.

The equal differentiation of the myofibroblasts phenotype in nodule and cord derived cells has important implications for clinical practice and could explain the high recurrence rate following treatment for Dupuytren's disease, other authors having correlated recurrence with presence of myofibroblasts (Gelberman *et al*, 1980). Any factors causing increased tissue levels of TGF-β_1 will lead to activation of Dupuytren's fibroblasts and an increase in the myofibroblast phenotype. Even the local trauma of surgical excision and the natural wound healing response will lead to release of large amounts of TGF-β_1 (Bennett and Schultz, 1993) and any residual tissue of nodule or cord origin will be susceptible to stimulation, myofibroblast transformation, cell proliferation, collagen deposition and the cycle of recurrent disease. Obvious nodules are of course usually excised during fasciectomy however small remnants of fibrous cord tissue are impossible to completely eradicate and are inevitably left within the wound bed. The results presented in this chapter suggest that recurrent disease could as equally develop from these remaining foci as from grossly diseased tissue.

SUMMARY:-

- Stimulation of fibroblast cultures with TGF-β_1 causes a significant up regulation of the myofibroblast phenotype in both nodule and cord derived cultures to the same level despite basal differences.

- Stimulation of carpal ligament derived fibroblast cultures with TGF-β_1 had no effect on the already low level of myofibroblasts present.

Dupuytren's fibroblasts appear to have a specific abnormal difference from control cells in their sensitivity to TGF-β_1 stimulation. This in itself could explain some of the pathological features of the disease. In addition the fact that cord cells are equally responsive to stimulation could be a key reason why there is such a high recurrence rate following any type of surgical treatment.

Having established the changes in 2 dimensional cell culture of the contractile cell phenotype, myofibroblasts, it was logical to see if there were corresponding changes in fibroblast contractility using the culture force monitor model.

3.7. The Contractility of Dupuytren,s Nodule, Cord and Carpal Ligament Derived Fibroblasts Following Stimulation with TGF-β_1.

3.7.1. Introduction

In addition to the increased cell proliferation, collagen production and myofibroblast differentiation that were discussed in 3.6.1., TGF-β_1 has been shown to increase cellular contraction. Using three dimensional fibroblast populated collagen lattices (FPCLs) several authors have demonstrated that TGF-β_1 induces an increase in contraction of both free-floating lattices (Montesano and Orci, 1988; Tingstrom *et al*, 1992; Reed *et al*, 1994; Riikonen *et al*, 1995; Arora *et al*, 1999) and of the stress-relaxed model (Arora *et al*, 1999) using dermal fibroblasts. Other workers have found similar responses by Dupuytren's fibroblasts (Vaughan *et al*, 2000). Once again these experimental models suffer from providing only semi-quantitative data. Brown *et al* (2002) have used the culture force monitor model providing actual measurements of the increased force generation by dermal fibroblasts in response to TGF-β_1 and TGF-β_3 stimulation. Many of these authors have investigated the effects of direct addition of TGF-β to the contraction assays however to maintain consistency within the work in this thesis it was decided to pre-treat fibroblasts with TGF-β_1 in exactly the same way, and using identical doses, as was done in chapter 3.6.

The levels of myofibroblasts and the degree of cell mediated collagen lattice contraction have been found to correlate (Tomasek, J. and Rayan, GM., 1995; Hinz, B. *et al*, 2001) and thus, having demonstrated an increase in the myofibroblast phenotype in Dupuytren's cell cultures when stimulated by TGF-β_1, it was hypothesised that FPCL contraction would be similarly enhanced in Dupuytren's cell lines but not in carpal ligaments.

3.7.2. Aim

To quantify the cell mediated contraction of collagen lattices seeded with fibroblasts from Dupuytren's nodule, cord and carpal ligament that had been stimulated with TGF-β_1 comparing them to untreated results from 3.4.

3.7.3. Methods

Fibroblast populated collagen lattices were prepared and set up on the culture force monitor in exactly the same way as described in section 3.4 and explained in detail in chapter 2.5. Prior to preparation however the fibroblasts had been stimulated with TGF-β_1. This was achieved by exchanging the normal growth media bathing the cells in T225 tissue culture flasks with a similar volume of normal growth media supplemented with 2ng/ml of TGF-β_1 three days prior to the experiment. This media change was carried out when flasks were approximately 60% confluent such that cells at the time of use would be around 90% confluent. Two T225 flasks were required to provide five million cells for each gel. The TGF-β_1 supplemented media was added only once and then the flasks incubated without further media changes in standard conditions (37°C and 5% CO_2) for the subsequent 3 days so matching the conditions used for myofibroblast determination in chapter 3.6.

Eight Dupuytren's nodule, eight Dupuytren's cord and four carpal ligament cell lines were investigated in this way with experiments once again left to contract over 20 hours after equilibration. The same mean contraction profiles and parameters were calculated as in chapter 3.4 so that direct comparisons could be made. Differences were analysed using the student's t test.

3.7.4. Results

Figure 3.7.1 illustrates the mean contraction profile of TGF-β_1 stimulated nodule derived cell lines plotted along side the untreated contraction profile from section 3.4. There was an early divergence of the traces with a statistically significant difference apparent even by 1 hour, $p<0.05$ (mean 1hr nodule force:- 15.6 dynes SEM $\pm$ 6.1; mean 1hr nodule + TGF-β_1 force:- 35.6 dynes SEM $\pm$ 7.1). The TGF-β_1 stimulated mean trace continued to climb rapidly until around 5.5 hours where there was a plateauing of the force at 228 dynes. Subsequently an interesting pattern was observed, not seen in un-stimulated cell lines, where there was actually a small gradual reduction in the force generated or the cells appeared to relax from 6 hours until 8 hours. Throughout this period the force

generated remained significantly higher in the stimulated fibroblasts than un-stimulated nodule cells (p<0.001). Finally from 11 hours onwards there was a continuous increase in the force generated up to the conclusion of the experiment at 20 hours. Overall, because of the reduction in the force at 6 to 8 hours the contraction profile took on a saddle shaped form. There was variability within individual cell lines, some demonstrating no saddle shape and others showing much more pronounced dips at similar time points.
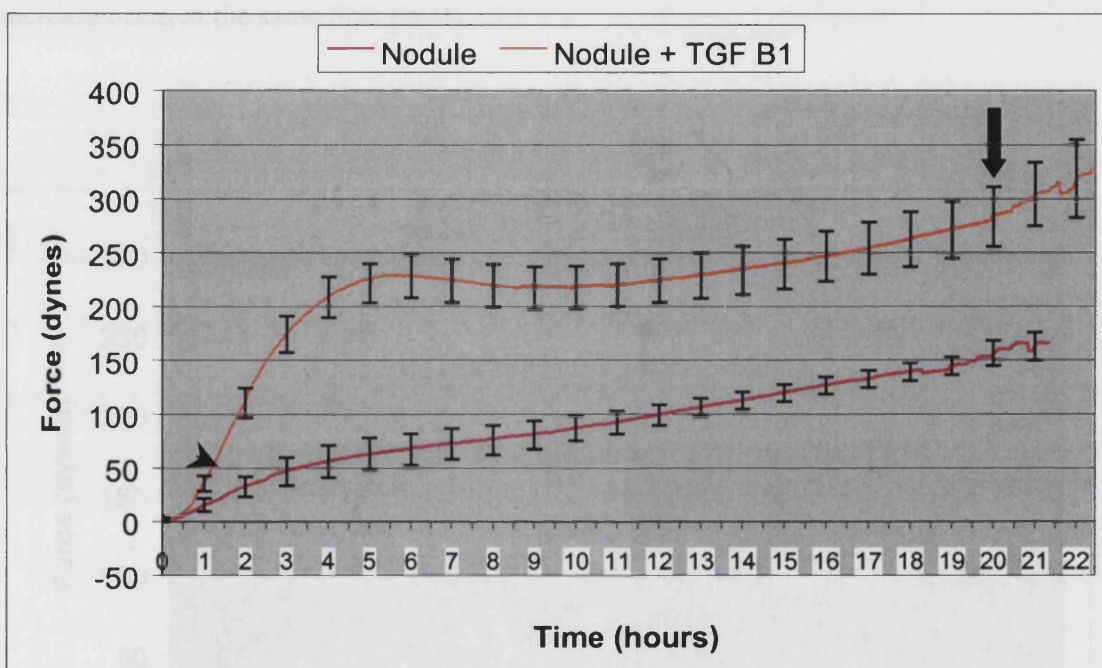
Figure 3.7.1. The mean contraction profile of TGF-β_1 stimulated Dupuytren's nodule fibroblasts (n=8) plotted along side the mean non-treated nodule fibroblast contraction profile (n=9). Error bars represent the standard errors of the means. Note the approximate doubling of the force generated by 20 hours (arrow) and the rapid force generation by stimulated fibroblasts (arrow head) in the first few hours causing an early significant divergence of the traces. The TGF-β_1 stimulated profile takes the form of a saddle shaped trace.

155

A similar graph is shown in figure 3.7.2. for Dupuytren's cord cell lines again comparing TGF-β_1 stimulated fibroblasts with non-treated. Exactly the same pattern is encountered here as with nodule cells. There is rapid early contraction by stimulated cells causing the traces to diverge and again leading to a significant difference by 1 hour, p<0.05 (mean 1hr cord force:- 11.8 dynes SEM ± 3.5; mean 1hr cord + TGF-β_1 force:- 27.9 dynes SEM ± 7.1). In TGF-β_1 stimulated cord cells the mean profile develops less of a pronounced saddle shape than nodules, although the plateauing of force and then further increase occur at the same time points.
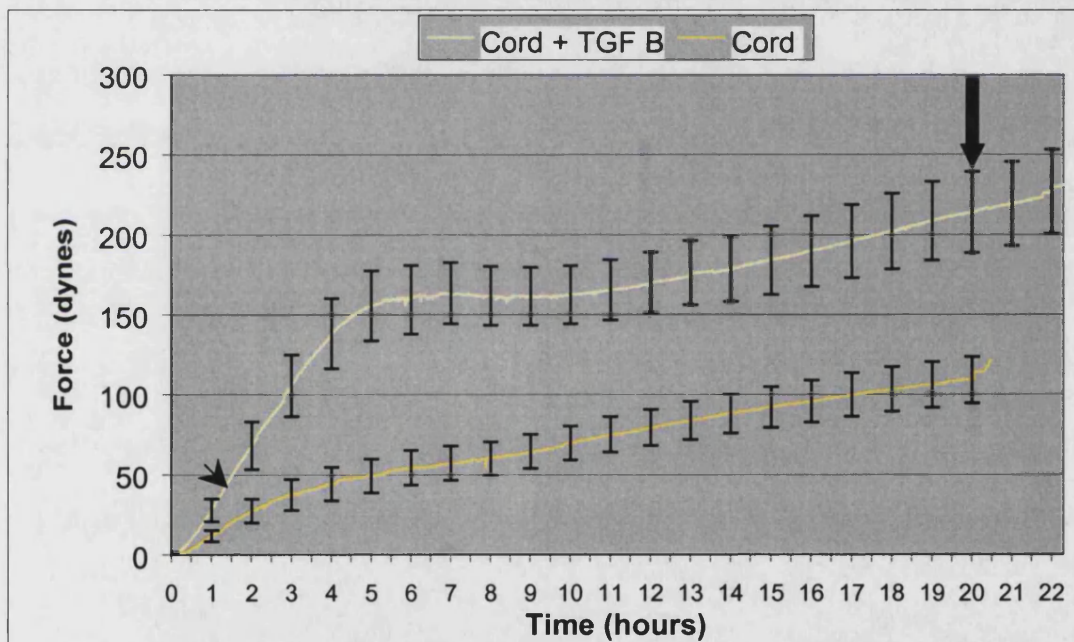
Figure 3.7.2. The mean contraction profile of TGF-β_1 stimulated Dupuytren's cord fibroblasts (n=8) plotted along side the mean non-treated cord fibroblast contraction profile (n=11). Error bars represent the standard errors of the means. Note the approximate doubling of the force generated by 20 hours (arrow) and the rapid early force generation by stimulated fibroblasts (arrow head). The TGF-β_1 stimulated profile has a less pronounced saddle shape than that of TGF-β_1 stimulated nodules (figure 3.7.1).

Interestingly carpal ligament cells when stimulated by TGF-β_1 showed a marked increase in contraction from the initial very poor force generation. This is illustrated in figure 3.7.3. where the mean contraction profiles of un-stimulated and TGF-β_1 stimulated fibroblasts are displayed together. As with both Dupuytren's cell types there was a more rapid generation of force by the stimulated fibroblasts, leading to significant differences in the generated force by one hour when compared with untreated carpal ligament fibroblasts, $p < 0.05$ (mean 1hr carpal ligament force:- 1.0 dynes SEM $\pm$ 1.5; mean 1hr carpal ligament + TGF-β_1 force:- 28.3 dynes SEM $\pm$ 9.1). There was a plateauing of this initial force generation between 6 and 8 hours at 131 dynes, about 1 hour later than the plateauing observed in Dupuytren's cell lines. There was then no significant relaxation of the tension before a gradual consistent increase in force occurred from 10.5 hours onwards. At the conclusion of the experiment the rate of increased force generation again appeared to be lower when compared to Dupuytren's cell lines.
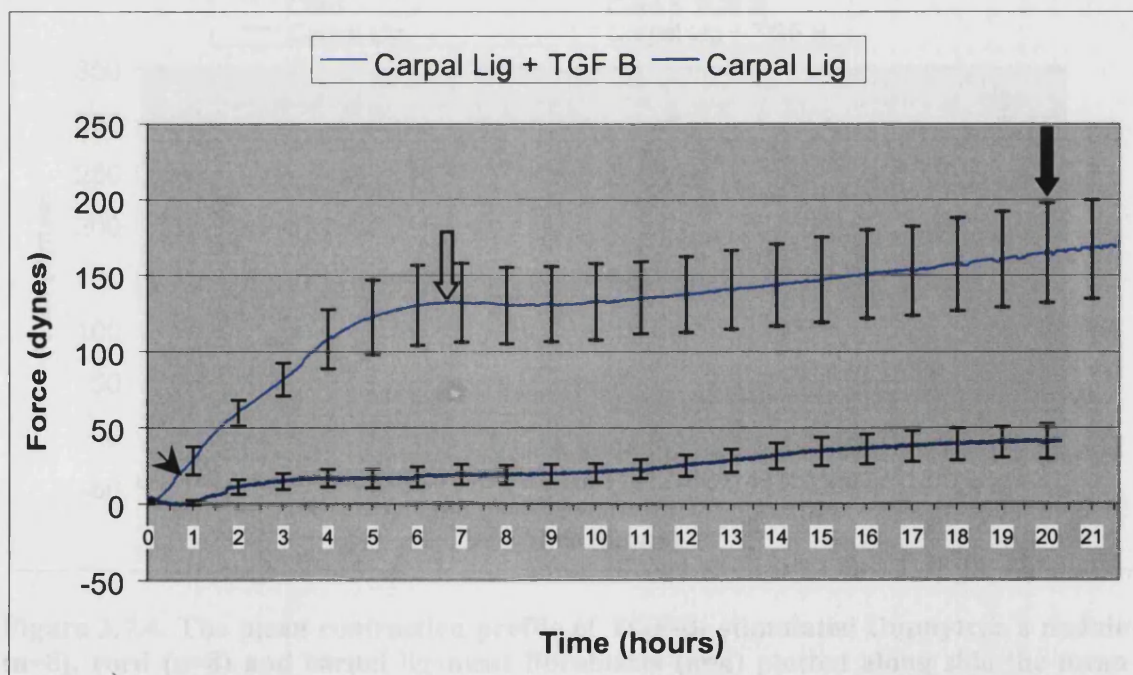
Figure 3.7.3. The mean contraction profile of TGF-β_1 stimulated carpal ligament fibroblasts (n=4) plotted along side the mean non-treated carpal ligament contraction profile (n=4). Error bars represent the standard errors of the means. Note the quadrupling of the force generated by 20 hours (arrow) and the rapid early force generation by stimulated fibroblasts (arrow head). The first plateau (open arrow) occurs later than in TGF-β_1 stimulated Dupuytren's cell lines.

157

In order to compare all of the contraction profiles of TGF-β_1 stimulated and un-stimulated Dupuytren's and carpal ligament fibroblasts the mean profiles presented above in figures 3.7.1 to 3.7.3 have been plotted together in figure 3.7.4. As with the untreated curves stimulated Dupuytren's nodule cells display a greater generation of force than both cord or carpal ligament cells and the cord profile falls between the two. With all of the profiles viewed together it becomes clear that not only are there significant differences in the overall force generated at 20 hours, but that this appears to be due to the differences in the rate of early contraction, indicated by the 2 hour gradient (arrow). These parameters are important as they provide clues as to when and how the fibroblasts are generating force by both attachment to the matrix and cell mediated contraction of it. They will now therefore be analysed in detail.
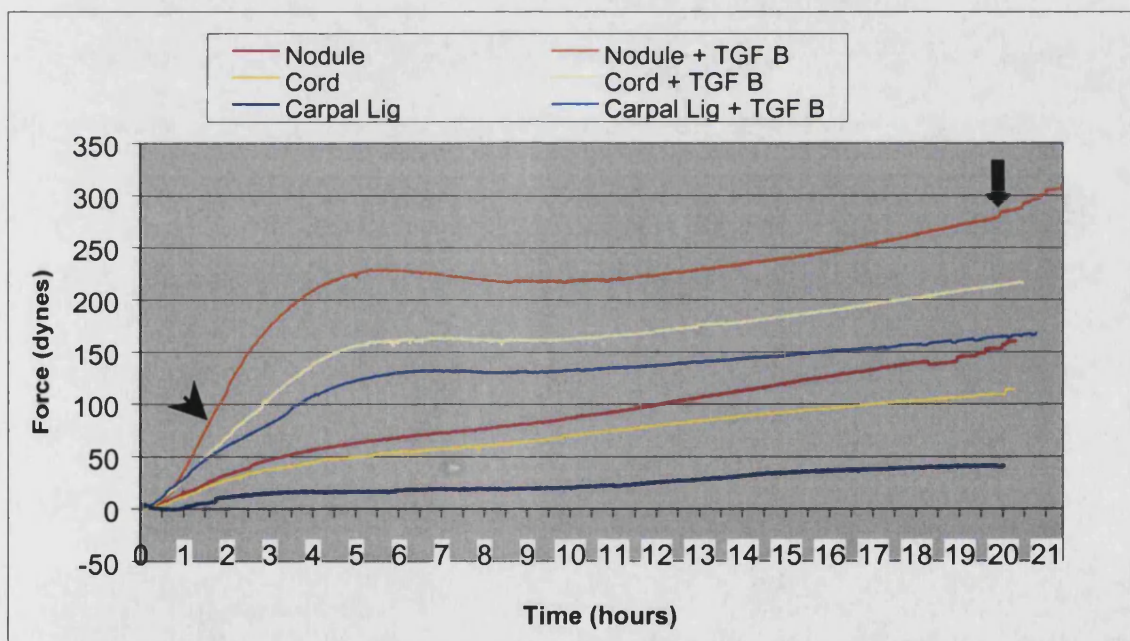
Figure 3.7.4. The mean contraction profile of TGF-β_1 stimulated Dupuytren's nodule (n=8), cord (n=8) and carpal ligament fibroblasts (n=4) plotted along side the mean non-treated Dupuytren's nodule (n=9), cord (n=10) and carpal ligament (n=4) contraction profiles. The differences in mean force generated at 20 hours (arrow) appear to be largely due to the rate of early contraction (arrow head).

The mean force generated at 20 hours for each cell type following TGF-β_1 stimulation is displayed in figure 3.7.5 along side the untreated values from section 3.4. TGF-β_1 stimulated nodule fibroblasts generated 280 dynes (range 180 to 373 dynes, SEM ± 27.1), significantly more than similarly treated carpal ligament at 165 dynes (range 80 to 239 dynes, SEM ±32.7), p<0.05. TGF-β_1 stimulated Dupuytren's cord fibroblasts generated a mean force at 20 hours of 214 dynes (range 113 to 292 dynes, SEM ±25.4) which although corresponding with the general trend for cord cells to contract less than nodules and more than carpal ligaments, differences with both of these groups just failed to reach statistical significance (p=0.097 and p=0.277 respectively). In all three cell types the increased mean force generation after TGF-β_1 stimulation was significant when compared with the untreated values (Nodule 145 dynes, p<0.01; Cord 109 dynes, p<0.01; Carpal ligament 40 dynes, p<0.05).
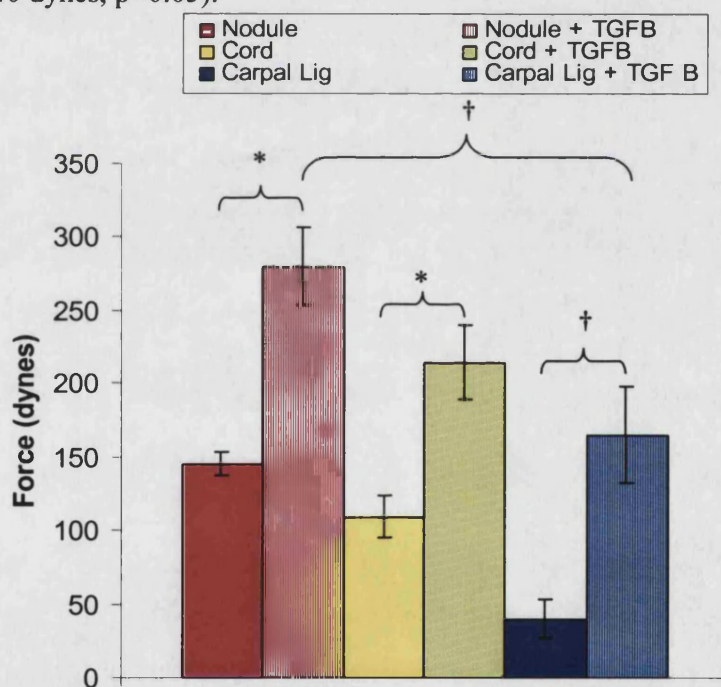
Figure 3.7.5. The mean force generated at 20 hours by TGF-β_1 stimulated Dupuytren's nodule (n=8), cord (n=8) and carpal ligament fibroblasts (n=4) plotted along side the mean non-treated values. Mean non-treated 20 hour forces are from Dupuytren's nodule (n=9), cord (n=10) and carpal ligament (n=4). There is a significant increase in force generated by TGF-β_1 stimulated cells when compared to untreated values as shown. Stimulated nodule fibroblasts generate significantly more force than stimulated carpal ligament fibroblasts but the differences between these and stimulated cord cells do not reach statistical significance. * = p<0.01;   † =p<0.05

159

The relative increase in force generation at 20 hours was then compared for each cell type after TGF-β_1 stimulation by calculating the percentage increase in 20 hour forces in treated experiments from matched untreated cell lines. The mean percentage increases in 20 hour force generation following TGF-β_1 stimulation are shown in figure 3.7.6. Dupuytren's nodule and cord cell lines showed a similar percentage rise following TGF-β_1 stimulation (91% SEM ±16.2% and 79% SEM ±15.3% respectively) however the corresponding rise in carpal ligaments was 344% (SEM ±35.4%). This was highly significantly different from both Dupuytren's fibroblast types (p<0.001).
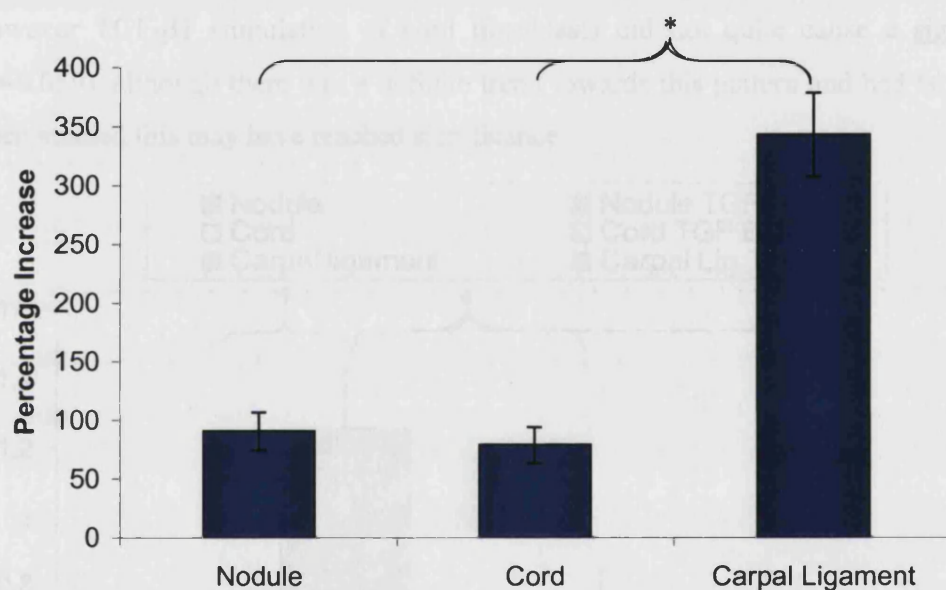
Figure 3.7.6. The mean percentage increase in 20 hour force following TGF-β_1 stimulation of cell cultures compared with un-stimulated values for nodule (n=8), cord (n=8) and carpal ligament (n=4). Error bars represent the standard errors of the means. The percentage increase in force generation by stimulated carpal ligament cells is significantly greater than both nodule and cord. * p<0.001.

Figure 3.7.7 displays the early rate of force generation, the 2 hour gradients, that appear to be of importance in the overall generation of force after stimulation with TGF-β_1. This was calculated as outlined in chapter 3.4 by dividing the difference in the force readings at 1 hour and 2 hours by 60 to give a value of rate of change of force in dynes per minute per five million cells. The stimulated nodule, mean 2 hour gradient of 1.25 dynes per minute (SEM ±0.16) was significantly (p<0.05) greater than stimulated cord values of 0.69 dynes per minute (SEM ±0.15) and stimulated carpal ligament values (0.52 dynes per

minute SEM ±0.10). This was in contrast to un-stimulated cells where nodule and cord 2 hour gradients were identical. The difference between stimulated cord fibroblasts and stimulated carpal ligament fibroblasts failed to reach statistical significance (p=0.153).

When the effect of TGF-β1 stimulation is studied for each cell type by comparison with un-stimulated values (section 3.4) the most notable difference was in nodules where there was a four-fold increase in the early rate of force increase or 2 hour gradient, p<0.001. Differences in carpal ligament were also statistically significant (p<0.05), however TGF-β1 stimulation of cord fibroblasts did not quite cause a significant rise (p=0.059), although there was a definite trend towards this pattern and had larger numbers been studied this may have reached significance.
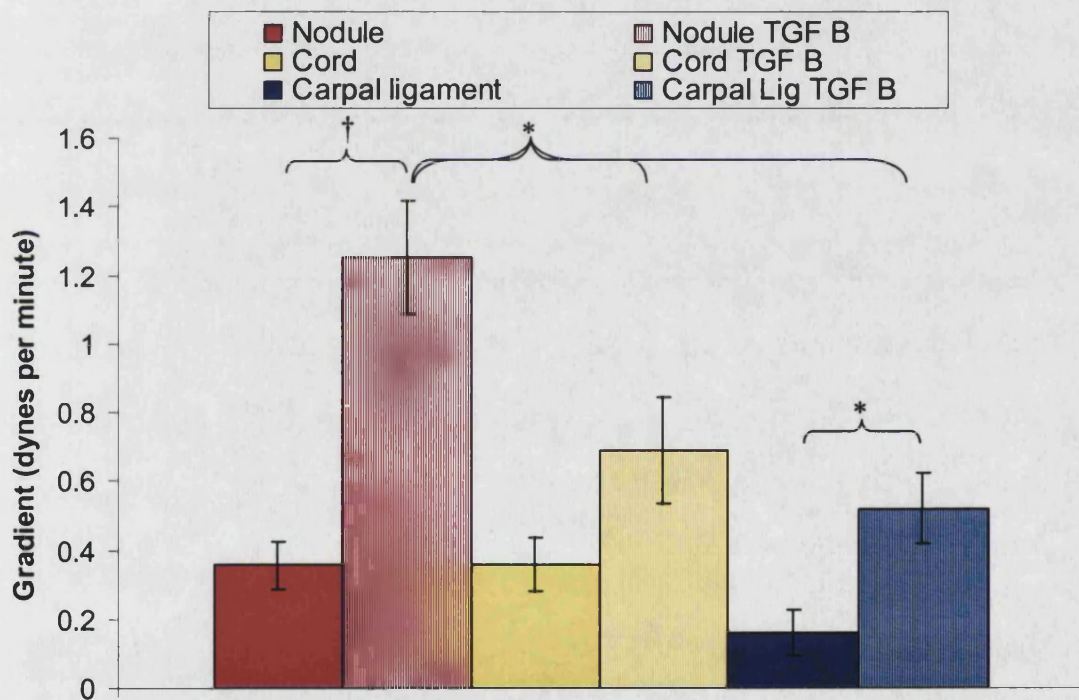
Figure 3.7.7. Histogram displaying the effect of TGF-β₁ stimulation on the 2 hour contraction profile gradient for Dupuytren's nodule (n=8), Dupuytren's cord (n=8) and carpal ligament (n=4) fibroblasts. Note the large increase in nodule cells following treatment. Statistical differences are indicated. * =p<0.05; † =p<0.001.

The final parameter that was used for comparison was the rate of continued force generation at the conclusion of each experiment, the late or 20 hour gradient. This was calculated as outlined in chapter 3.4 by dividing the difference in the force readings at 19.5 hours and 20.5 hours by 60 to give a value of rate of change of force in dynes per minute per five million cells. Figure 3.7.8 illustrates these values for both TGF-β_1 stimulated and un-stimulated fibroblasts of each type. Following TGF-β_1 stimulation there was a rise in all of the mean 20 hour gradients when compared to un-stimulated values (chapter 3.4). In nodule cell lines the mean gradient increased from 0.086 to 0.147 dynes per minute (SEM ±0.04), cord increased from 0.044 to 0.093 dynes per minute (SEM ±0.02) and carpal ligament increased from 0.004 to 0.063 dynes per minute (SEM ±0.016). The increases seen in cord and carpal ligament are both significant ($p<0.05$), however the increased nodule 20 hour gradient following TGF-β_1 stimulation failed to reach statistical significance ($p=0.18$). Despite the trend for the nodule 20 hour gradient to be greater than cord, and this in turn to be greater than carpal ligament, none of the TGF-β_1 stimulated mean 20 hour gradients was significantly different from the others.
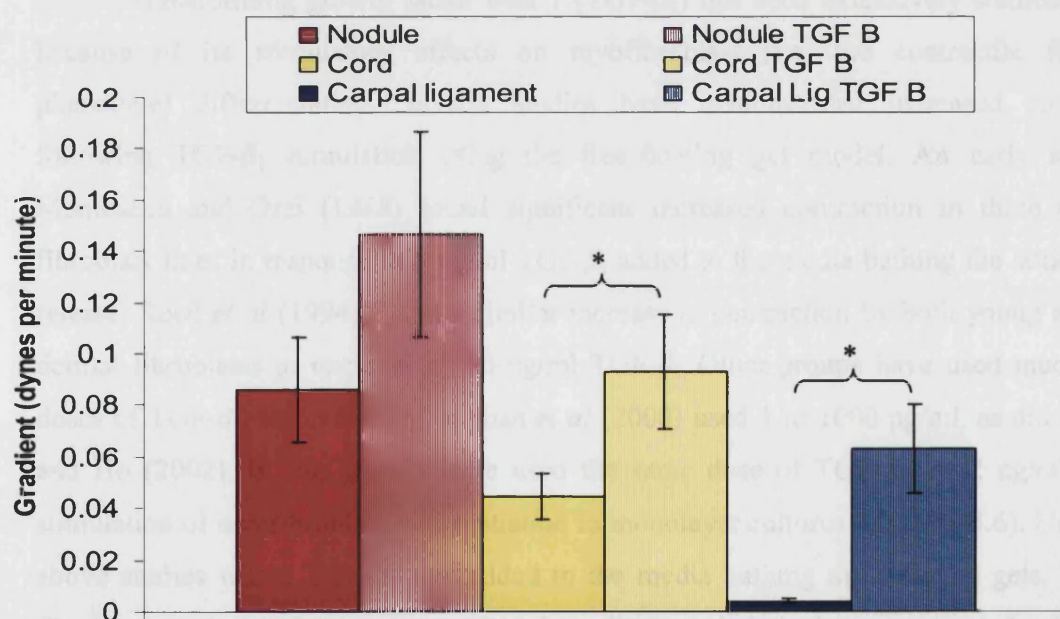
Figure 3.7.8. Histogram displaying the effect of TGF-β_1 stimulation on the 20 hour contraction profile gradient for Dupuytren's nodule (n=8), Dupuytren's cord (n=8) and carpal ligament (n=4) fibroblasts. Note the increased gradient in all cell types following TGF-β_1 stimulation and the continuing trend of nodule>cord>carpal ligament. * = p<0.05.

3.7.5. Discussion

The studies of three dimensional fibroblast populated collagen lattice contraction have provided fascinating insights into cell motility and force generation. The findings have been related to both pathological processes such as wound contraction (Grinnell *et al*, 1999) and physiological processes such as tooth eruption (Bellows *et al*, 1981). In the last ten years factors that influence the cell-mediated contraction have begun to be elucidated using the same models. Lysophosphatidic acid (LPA) has been shown to stimulate contraction, as has platelet derived growth factor (PDGF) (Grinnell *et al*, 1999; Tingström *et al*, 1992). In Dupuytren's disease Rayan *et al* (1996) studied a range of factors, finding LPA, Angiotensin II, serotonin and prostaglandin $F_{2\alpha}$ to be agonists of fibroblast contraction and that prostaglandins E_1 and E_2, nifedipine and verapamil antagonised the effects of LPA. Sanders *et al* (1999) found that interferon-α_{2b} reduced contraction in both control and Dupuytren's fibroblasts.

Transforming growth factor beta 1 (TGF-β_1) has been extensively studied, in part because of its stimulatory effects on myofibroblast (i.e. the contractile fibroblast phenotype) differentiation. Several studies have demonstrated increased contraction following TGF-β_1 stimulation using the free-floating gel model. An early study by Montesano and Orci (1988) found significant increased contraction in three different fibroblast lines in response to 5 ng/ml TGF-β_1 added to the media bathing the lattices after release. Reed *et al* (1994) found a similar increase in contraction by both young and aged dermal fibroblasts in response to 10 ng/ml TGF-β_1. Other groups have used much lower doses of TGF-β_1, for example Vaughan *et al* (2000) used 1 to 1000 pg/ml, as did Grinnell and Ho (2002). In this work I have used the same dose of TGF-β_1, of 2 ng/ml, as for stimulation of myofibroblast differentiation in monolayer cultures (Chapter 3.6). Unlike the above studies where TGF-β_1 was added to the media bathing the collagen gels, here the fibroblasts to be used in seeding within the collagen gels have been pre-treated, whilst still in monolayer culture. This would cause in increase in the myofibroblast phenotype in the population of cells to be investigated, whereas simple addition of TGF-β_1 to the bathing media of floating unstressed assays does not achieve this for two reasons. Firstly it has been

shown that fibroblast to myofibroblast differentiation takes time with optimal stimulation only occurring between 3 and 5 days (Arora *et al*, 1999; Grinnell and Ho, 2002). The experiments within this study are only run over 24 hours. Secondly it has been shown that in free-floating lattices differentiated myofibroblasts fail to appear, only occurring in stressed gels (Vaughan *et al*, 2000; Arora *et al*, 1999).

Although Vaughan *et al* (2000) used Dupuytren's fibroblasts in their work, there have been no specific studies to date comparing the effects of TGF-β_1 stimulated contraction of collagen gels from Dupuytren's and control fibroblasts, or of Dupuytren's fibroblast from different stages of disease such as nodule and cord. This work has addressed both of these gaps in our knowledge and additionally by using the culture force monitor, has used the most realistic tissue environment model currently available. There has only been one other study published looking at the effects of TGF-β stimulation on dermal fibroblast contraction using the culture force monitor (Brown *et al*, 2002). The other models, free-floating and stress-relaxed, as discussed earlier are far from physiological, although can be useful to answer specific questions, whereas the set up of the culture force monitor allows the development of balanced cell-mediated / matrix forces which can be measured in real time. Thus the patterns of contraction and differences in the way that fibroblasts develop force can be studied in detail. This has been particularly interesting in this study where not only has the overall force generation increased following TGF-β_1 stimulation but also the shape of the contraction profile leading to the development of this tension was altered. This allows one to hypothesise as to the reasons for the greater contractile ability, furthermore it has been demonstrated that TGF-β_1 has an important role in the very early stages of fibroblast attachment and contraction, which cannot be shown using other experimental models.

The finding here of increased force generation after TGF-β_1 stimulation corresponds with all of the previous studies where TGF-β_1 consistently causes increased contraction irrespective of the method or time of growth factor delivery. In particular, they correspond with a number of studies that have now examined pre-incubation of fibroblasts with TGF-β_1, where their subsequent contractility is increased (Arora *et al*, 1999; Grinnell and Ho,

2002; Liu *et al*, 2001; Wen *et al*, 2001; Yokozeki *et al*, 1997). Several authors have also correlated the level of α-smooth muscle actin in fibroblast cultures with the increased degree of contractility. Tomasek and Rayan, (1995) compared increased monolayer myofibroblasts with stress-relaxed collagen gel contraction whilst Arora, *et al* (1999), Vaughan *et al* (2000) and Grinnell and Ho (2002) used Western blotting of cells extracted from the FPCLs to determine α-smooth muscle actin content. Here it has not been possible to quantify α-smooth muscle actin content of the cells as the gels were fixed and stained and technical limitations made accurate assessment impossible (see chapter 3.9). If however one compares the force generated on the CFM with the monolayer myofibroblast percentages following TGF-β_1 stimulation, some interesting differences are observed.

Firstly myofibroblast percentages increased to the same level in monolayer nodule and cord fibroblast cultures, however there was still a trend for the CFM force generated by nodule fibroblasts to be greater than cord at 20 hours, despite this not reaching significance. Similarly the shape of the contraction profile was altered with significant differences in the 2-hour gradient between nodule and cord cells. Secondly the carpal ligament fibroblasts did not show any increase in the myofibroblast percentages in response to TGF-β_1 stimulation of monolayer cultures, however there was a highly significant increase in force generation by these cells on the CFM, which actually exceeded the basal level of nodule fibroblast contraction. This means that when one compares the percentage of myofibroblasts in cultures with the force generated after TGF-β_1 stimulation as shown in figure 3.7.9 there is no identifiable trend as was seen in un-stimulated fibroblasts (figure 3.4.7).

In terms of the α-smooth muscle actin expression and force generation the population of nodule and cord cells where data is available for both, overlap to some extent, however the carpel ligament population of cells are separated due to their lack of myofibroblasts despite force generation of up to 246 dynes. When results for both TGF-β_1 stimulated and un-stimulated fibroblast cell lines are combined (figure 3.7.10.) there is a general but weak trend for increasing myofibroblast percentages to correlate with greater force production however the R^2 coefficient is only 0.38. The group of TGF-β_1 stimulated Dupuytren's fibroblasts (both nodule and cord) is distinct from all the other cell lines

including TGF-β_1 stimulated carpal ligaments. A virtually identical trend with a weak correlation is encountered when earlier time point force generation, at 2hours, is plotted against the myofibroblast percentages (figure 3.7.11.; R^2= 0.39).
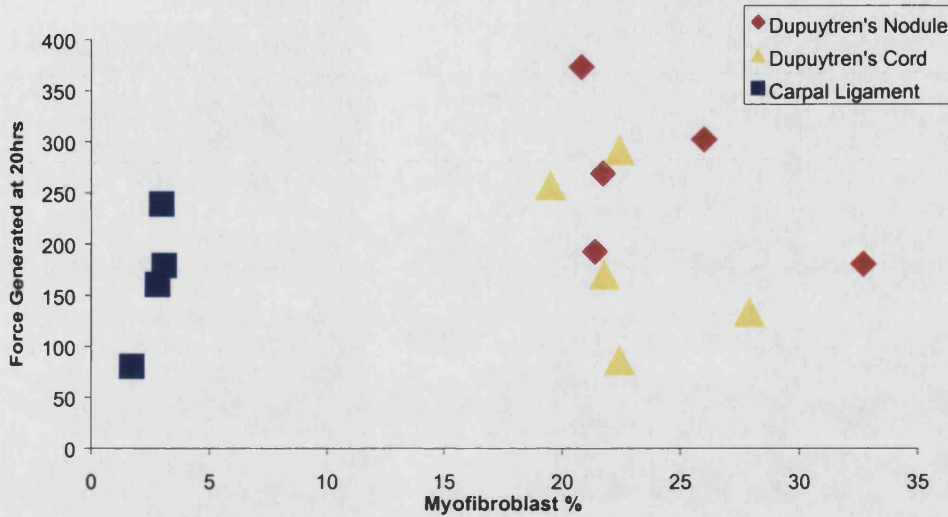
Figure 3.7.9. A scatter plot comparing the percentage of myofibroblasts in monolayer cultures after stimulation with TGF-β_1 with the force generated by corresponding cell lines that were stimulated with TGF-β_1 before seeding into collagen gels. Note that there is <u>no</u> trend apparent of increasing force with increasing myofibroblasts, however the carpal ligament cells appear to make up a separate population.
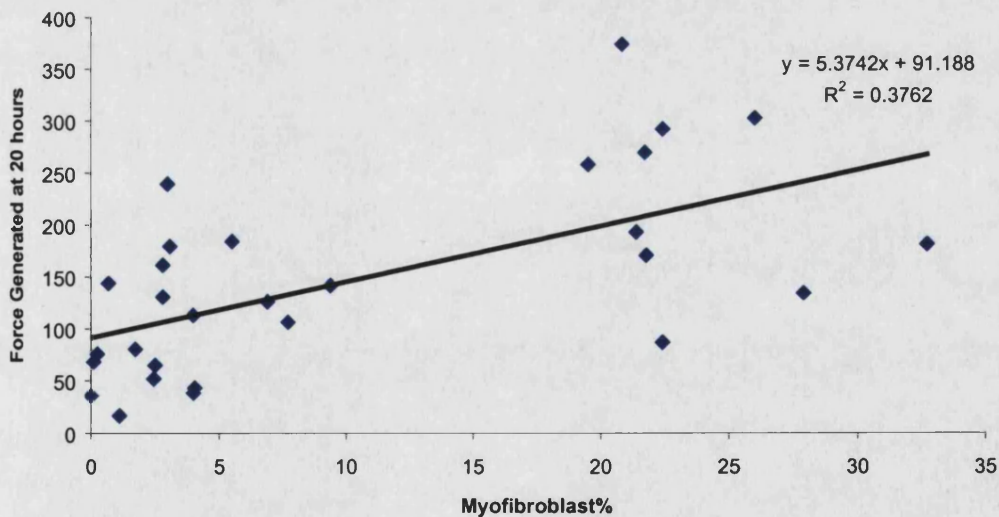
Figure 3.7.10. A scatter plot of all TGF-β_1 stimulated and un-stimulated cell lines from nodule, cord and carpal ligament origin, comparing myofibroblast percentages and the force generated at 20 hours on the CFM. There is a weak correlation of the two parameters.

166
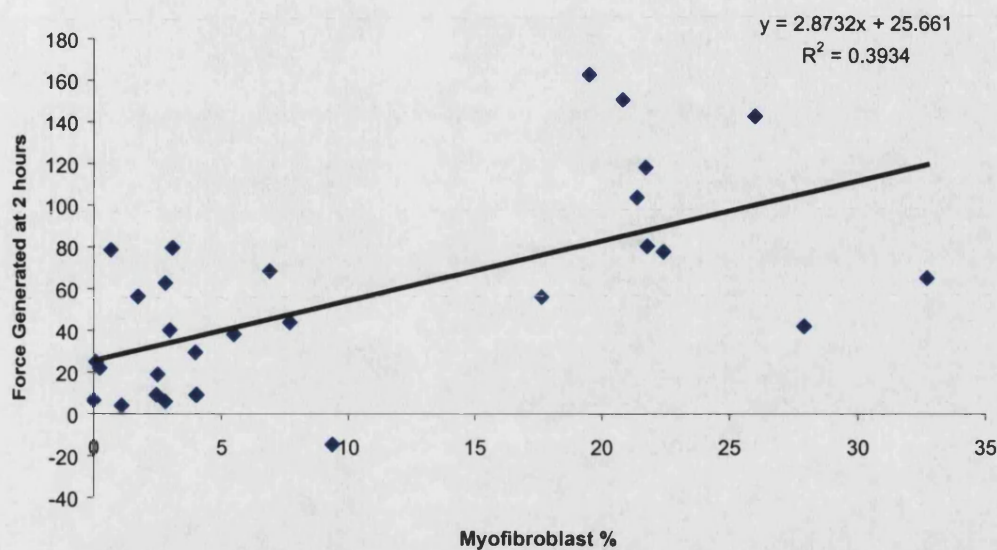
Figure 3.7.11. A scatter plot of all TGF-β_1 stimulated and un-stimulated cell lines from nodule, cord and carpal ligament origin, comparing myofibroblast percentages and the force generated at 2 hours on the CFM. There is a weak correlation of the two parameters.

Pre-treatment with TGF-β_1 certainly up regulates myofibroblasts in Dupuytren's fibroblast cultures. The subtle differences, however, in contraction profile shape between nodules and cords as well as the up regulation of carpal ligament force production without myofibroblast phenotype increase, indicate that cell mediated contraction in the culture force monitor model is **not merely a function of α-smooth muscle actin expression**. One can speculate from the changes in contraction profile shapes and the highly significant changes in 2 hour gradients, that TGF-β_1 stimulation enhances the early phase of contraction. This is consistent with studies by Grinnell and Ho (2002) where TGF-β_1 stimulation mediated enhanced contraction of collagen lattices by elevated myofibroblast levels but also appeared to act as a direct agonist of collagen lattice contraction in free floating models where no myofibroblast differentiation had occurred.

This direct agonist effect may be of additional significance given the fact that TGF-β_1 has been shown to induce it's own expression in several studies (Yokozeki *et al*, 1997; Van *et al*, 1988).

Eastwood *et al* (1996) have suggested that early force generation on the CFM is a result of cell attachment to the matrix and locomotion of cells and their processes as they

167

spread to form a network from their initially rounded state. A number of groups have shown an increase in integrin expression following TGF-β_1 stimulation of fibroblasts (Riikonen *et al*, 1995, Dugina *et al*, 2001, Brown *et al*, 2002). These cell surface receptors are a family of molecules, which enable matrix to cell binding, thus allowing cell mediated force transmission to the matrix (For review see Hynes, 1992). The differences observed here between nodule and cord would fit with a different pattern or increased expression of these integrins. If this was the case, the fact that 2 hour gradients were identical in non TGF-β_1 stimulated nodule and cord cell lines would further suggest that there are inherent differences between nodule and cord cells in the way they respond to TGF-β_1 stimulation, nodule fibroblasts being more sensitive.

Brown *et al* (2002) also used the culture force monitor when they investigated the effects of TGF-β_1 and TGF-β_3 stimulation of dermal fibroblasts. Not only did they use a different cell type than those studied here but they only added TGF-β to the bathing media and did not pre-treat cultured cells as has been done in this thesis. Similar increases in force generation were however observed with an early rapid rise in contraction, although this plateaued without further contraction. This is consistent with the dermal fibroblasts reaching tensional homeostasis and is in contrast to the findings here in Dupuytren's cells where tensional homeostasis appears even more delayed after TGF-β_1 stimulation. Brown and co-workers, however also demonstrated an inconsistent temporal relationship between the increased expression of integrin receptors and the generation of force, concluding that this was not the means by which TGF-β caused enhanced early force generation. They suggested instead that this was a direct effect of TGF-β on cytoskeletal force output during cell traction. Integrin up regulation cannot be ruled out as a cause of the increased early force generation in the model used in this work, as pre-treatment by TGF-β_1 would allow sufficient time for stimulated expression of these molecules. Of course, defining a single change as the cause of altered force generation may be a highly simplistic view as it is likely that there is a more complex interplay of multiple factors, which may include increased integrin expression, direct stimulation of cytoskeletal forces and responses to the matrix itself.

Whatever the actual effect of TGF-β_1 on the cell population that cause the observed changes, from the results presented here, it is clear that the fibroblasts have some "memory" of the stimulation or undergo an at least semi-permanent modification. The differences were apparent after direct stimulation was withdrawn and the cells had been merely pre-treated and then trypsinised and reseeded into collagen lattices, where there was no additional TGF-β_1 present.

Having stated that the early phase of contraction in the culture force monitor model is due to cell-matrix attachment, so called traction forces (Brown et al, 2002; Eastwood et al. 1996; Ehrlich and Rajaratnam, 1990), the later stages of contraction, for example after 10 hours, have been seen as a function of the active cellular contraction of fibroblasts within the matrix. This is when tensional homeostasis becomes important and it is here that the role of myofibroblasts may be more apparent. In the results presented in this chapter, the mean 20 hour gradients were all increased following TGF-β_1 stimulation although this failed to reach significance in nodule cell lines. This failure of force generation to plateau may, as discussed in chapter 3.4, represent a delay in acquiring tensional homeostasis.

Thus, TGF-β_1 appears to exacerbate further this delay, or cause cells to have an even higher "preferred" tensional force where equilibrium is maintained. Furthermore, control carpal ligament fibroblasts begin to demonstrate this delay. As with the total force generation there is no strict correlation of the 20 hour gradients with myofibroblast percentages in monolayer culture following stimulation with TGF-β_1. This is confounded once again by increases in carpal ligament 20 hour gradients but not in myofibroblast numbers, and similarly by equal levels of myofibroblasts in nodule and cord cultures stimulated with TGF-β_1 but apparent differences in the CFM model. Despite the hypothesis that this latter profile of force generation is myofibroblast dependent this may not represent the complete mechanism. It may be that the three dimensional nature of the CFM model or the cell-matrix interactions plays a role. It has been shown that the nature of the matrix influences cell behaviour within it (Arora et al, 1999; Grinnell and Ho, 2002; Bell et al, 1979; Zhu et al, 2001) and one could speculate that the combination of TGF-β_1 stimulation and the collagen gel environment bring about further alterations in myofibroblast

169

phenotype expression, above those seen in two dimensions. To establish this would require further analysis of α-smooth muscle actin content of the collagen gels following CFM runs, which was beyond the capacity of the current work.

SUMMARY:-

- TGF-β_1 stimulation of fibroblasts caused a significant increase in the mean generation of force in all cell types at 20 hours, which was accompanied by a change in the shape of the contraction profile in Dupuytren's cells.

- The increased force was due largely to a rapid early rate of contraction indicated by the increase in 2-hour gradients. This was particularly significant in nodule-derived fibroblasts.

- There was a further delay in reaching tensional homeostasis following TGF-β_1 stimulation of Dupuytren's cell lines, indicated by increased 20 hour gradients. Carpal ligament fibroblasts also began to demonstrate this continuing contraction throughout the experimental periods.

This stimulation of increased force generation and additional alterations in tensional homeostasis of Dupuytren's cells by TGF-β_1 may imply a role for this growth factor in the progression of clinical contractures in Dupuytren's disease. As with the stimulation of myofibroblast differentiation, demonstrated in chapter 3.6., factors which cause release of TGF-β_1 such as trauma or surgery and the subsequent wound healing process, will exacerbate the abnormal contractile properties of Dupuytren's fibroblasts. This could trigger rapid disease progression following trauma as has been reported (McFarlane and Shum, 1990; Hueston and Seyfer, 1991) or fluctuating basal levels of TGF-β_1 could underlie the slower but insidious natural disease progression.

Having demonstrated that fibroblast contractility and tensional homeostasis were altered by TGF-β_1 stimulation the next chapter addresses the response of stimulated cells to mechanical loading, which is in keeping with the *in-vivo* environment of these cell types where the system is not static and forces are constantly changing.

3.8. The Response of Dupuytren's Nodule, Cord and Carpal Ligament Fibroblasts within Collagen Lattices to Mechanical Loading Following TGF-β_1 Stimulation.

3.8.1. <u>Introduction</u>

An inherent feature of maintaining tensional homeostasis (Brown *et al*, 1998) is the ability of fibroblasts to respond to external stresses; altering the amount of force they generate to preserve the equilibrium. In chapters 3.4. and 3.5. it was demonstrated that tensional homeostasis was delayed and the initial responses to overloading were abnormal in Dupuytren's fibroblasts. In the preceding chapter it has been shown that TGF-β_1 stimulation of fibroblasts altered further the tensional homeostasis and thus it was logical to next determine the combined effects of TGF-β_1 stimulation and mechanical loading. Although there are several published studies of collagen gel contraction and the effects of TGF-β_1 the only one to use the culture force monitor was by Brown *et al*, (2002) and did not look at effects of changes in mechanical load. The culture force monitor or equivalent device is the only experimental model that allows measurement of real time cellular responses to mechanical changes, thus none of the other studies which use free floating or stress-relaxed models, have been able to asses this. The work presented here is therefore unique at the current time.

TGF-β_1 is believed to play a central role in the development and progression of Dupuytren's disease (Kloen, 1999) and here it has been shown that it acts consistently to exacerbate the abnormal features of Dupuytren's fibroblasts in culture. It follows therefore that TGF-β_1 stimulation of fibroblasts may also cause additional abnormal responses to mechanical loads.

3.8.2. <u>Aim</u>

To determine the responses of Dupuytren's nodule, Dupuytren's cord and carpal ligament fibroblasts to mechanical loading using the culture force monitor, after stimulation with TGF-β_1.

3.8.3. Methods

As already described in chapter 3.5.3. at the conclusion of each CFM experiment the gels, this time populated with TGF-β_1 stimulated fibroblasts, underwent a series of uniaxial tensional overloads. The method of overload was identical. The culture force monitor was then left for 30 minutes to record the subsequent changes in force in this "post overload" period. A second, third and fourth overloads were then performed in exactly the same way and the post overload responses recorded for each as described in detail in chapter 2.5.4. Eight Dupuytren's nodule, eight Dupuytren's cord and four control carpal ligament cell lines were investigated and the post overload period gradients were calculated as before.

3.8.4. Results

The contraction profile obtained during overloading of a TGF-β_1 stimulated Dupuytren's nodule fibroblast cell line is displayed in figure 3.8.1. As with similar overloading traces shown in figures 3.5.2. and 3.5.5. the rapid rises in force indicated by arrows are the points when each uniaxial overload was applied and this is followed by a post overload period during which the responses of the cells are measured. Here there is a particularly profound contractile response in the first post overload period, with an increase in force by 30 dynes following the first overload. Although all TGF-β_1 stimulated nodule fibroblasts demonstrated a contraction in response to the first overload this was the most dramatic reaction that was encountered.

In un-stimulated nodule cells this abnormal contraction following tensional loading was only seen in the first post overload period (figure 3.5.5.), however as can be seen in figure 3.8.1. there is also a further increase in force generated by nodule cells after the second and third overloads. Even in the fourth post overload period there is only a levelling of force rather than the consistent decrease seen in blank control gels (figure 3.5.2.). This pattern of abnormal contractile responses persisting into the second, third and even fourth post overload periods was typical of the traces obtained from TGF-β_1 stimulated nodule fibroblasts.

172
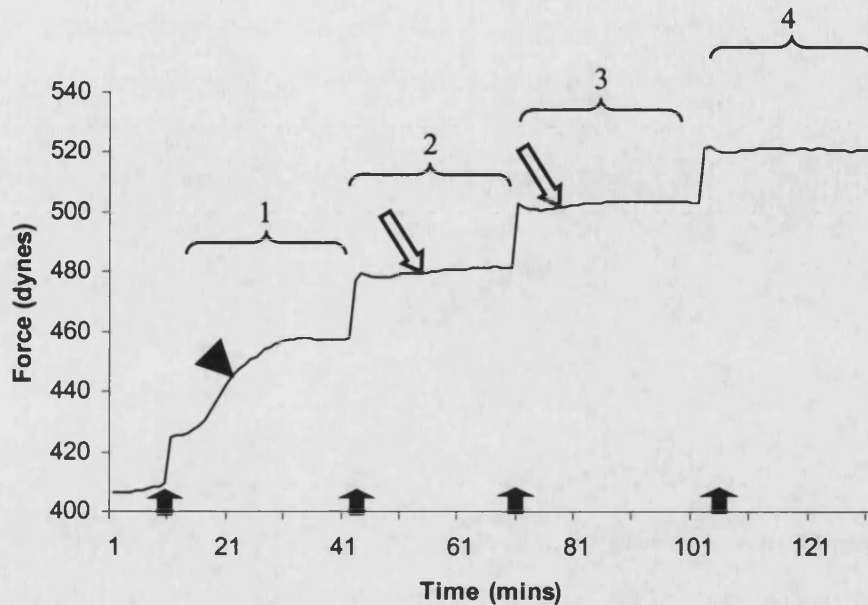
Figure 3.8.1. A contraction profile trace from a collagen lattice seeded with TGF-β_1 stimulated nodule fibroblasts undergoing a series of four tensional overloads (arrows). The subsequent post overload periods are numbered 1 to 4. Note the very large increase in force during the first period (arrow head). There is also contraction in response to the second and third overloads (open arrows), whilst even in the fourth period there is only a level trace rather than the decrease in force seen in control blank gels (figure 3.5.2.).

A similar overloading profile is shown in figure 3.8.2. this time from a typical cord fibroblast populated lattice after TGF-β_1 stimulation. There is once again contraction in response to the first overload (arrow head) and, in contrast to the results from chapter 3.5., this abnormal contractile response is also seen in the second post overload period. By the third period there is a more characteristic decline in force although not to the same extent as in control blank gels (figure 3.5.2.). This rate of reduction in force is only approached in the fourth post overload period.

TGF-β_1 stimulation also caused carpal ligament fibroblasts to demonstrate a contractile response to the first overload, which was in marked contrast to their mechano-insensitivity when not previously stimulated with TGF-β_1. Unlike Dupuytren's cells however this new abnormal response did not persist into subsequent post overload periods.
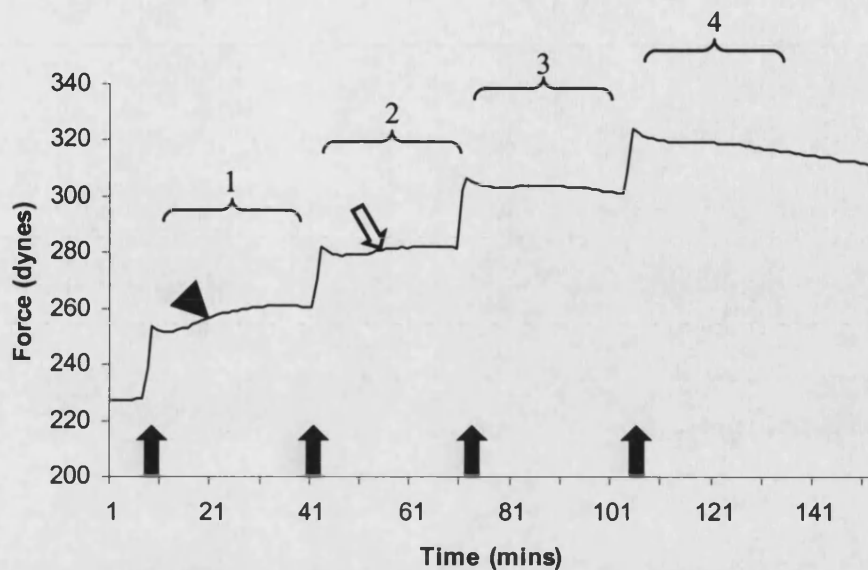
Figure 3.8.2. A contraction profile trace from a collagen lattice seeded with TGF-β_1 stimulated cord fibroblasts undergoing a series of four tensional overloads (arrows). The subsequent post overload periods are numbered 1 to 4. Note the increase in force during the first period (arrow head), which is also seen in response to the second overload (open arrow). By the third post overload period the trace shows a reduction of force that by the fourth period is similar to that encountered in blank control gels (figure 3.5.2.).
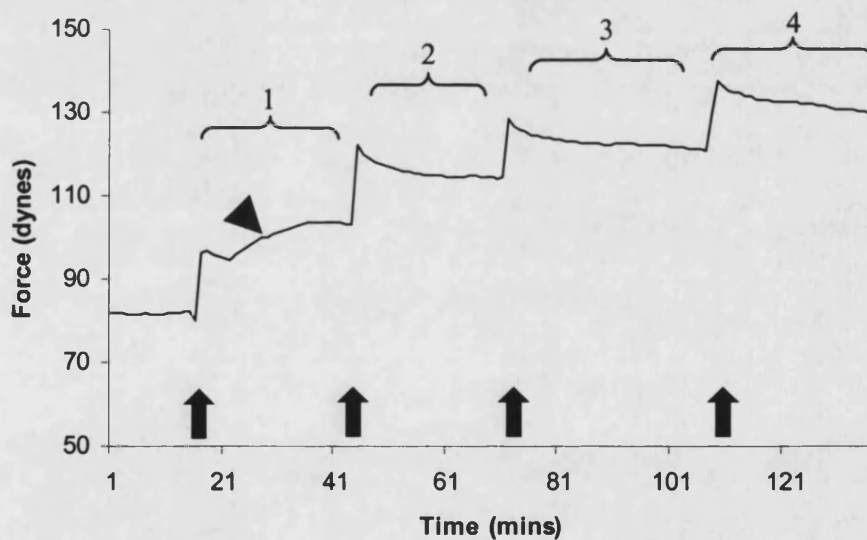
Figure 3.8.3. A contraction profile trace from a collagen lattice seeded with TGF-β_1 stimulated carpal ligament fibroblasts undergoing a series of four tensional overloads (arrows). The subsequent post overload periods are numbered 1 to 4. Note the increase in force during the first period (arrow head), which disappears by the second, third and fourth post overload periods where here the changes are similar to that encountered in blank control gels or un-stimulated carpal ligament fibroblast gels.

174

As in chapter 3.5. the post overload responses were quantified by calculating the gradients of each post overload period for each cell line, expressed as the rate of change of force in dynes per minute. A positive value represented an increase in force over the period whilst a negative value represented a relaxation of the tension across the system. The mean gradients were then determined for each cell type, Dupuytren's nodule, Dupuytren's cord and carpal ligament fibroblasts. The TGF-β_1 stimulated fibroblast results are graphically displayed along side of the unstimulated values in figure 3.8.4.

In the first post overload period the mean gradient for TGF-β_1 stimulated nodule fibroblasts was +0.27 dynes per minute (SEM ± 0.12), which did not reach statistical significance when compared with the un-stimulated result (+0.1dynes per minute, p=0.2). It was also not significantly different from the mean gradient of the first post overload period in TGF-β_1 stimulated cord fibroblasts of +0.19 dynes per minute (SEM ± 0.06)(p=0.39) or that of TGF-β_1 stimulated carpal ligament fibroblasts of + 0.14 (SEM ± 0.06)(p=0.70). All of the TGF-β_1 stimulated mean first post overload gradients were, however, significantly greater than the blank control gel gradient (-0.23 dynes per minute, p<0.005) and the un-stimulated carpal ligament gradient (-0.16 dynes per minute, p<0.05). The mean first post overload gradient for TGF-β_1 stimulated cord fibroblasts was +0.19 dynes per minute (SEM ± 0.07), which only just failed to reach statistical significance when compared with the un-stimulated result (+0.05 dynes per minute, p=0.06).

The trend in the second post overload period was for there to be a reduction in the mean gradients however this only returned to control blank gel or un-stimulated values in TGF-β_1 stimulated carpal ligament fibroblasts (-0.26 dynes per minute, SEM ± 0.05). The nodule fibroblasts gradient was +0.07 dynes per minute (SEM ± 0.04), not significantly different from the first post overload gradients but highly significantly increased (p<0.001) when compared to un-stimulated nodule second post overload period gradients. This was not the case for TGF-β_1 stimulated cord fibroblasts at –0.05 dynes per minute (SEM ± 0.04; p= 0.173).

The abnormal contractile responses persisted in the third post overload period for both nodule and cord Dupuytren's fibroblasts at 0.0 dynes per minute (SEM ± 0.06) and –

0.01 dynes per minute (SEM ± 0.04) respectively. These values were significantly greater than corresponding third post overload period results in un-stimulated nodule and cord fibroblasts (p<0.01 and p<0.05 respectively). Only by the fourth post overload period were mean gradients in TGF-β_1 stimulated Dupuytren's fibroblasts similar to the control blank gel, or un-stimulated gradients although even here nodule fibroblasts showed a significant difference (p<0.01) following TGF-β_1 stimulation at –0.14 dynes per minute (SEM ± 0.04) when compared with un-stimulated period four gradients (-0.3 dynes per minute). Other results did not differ significantly from the non-stimulated or control values.
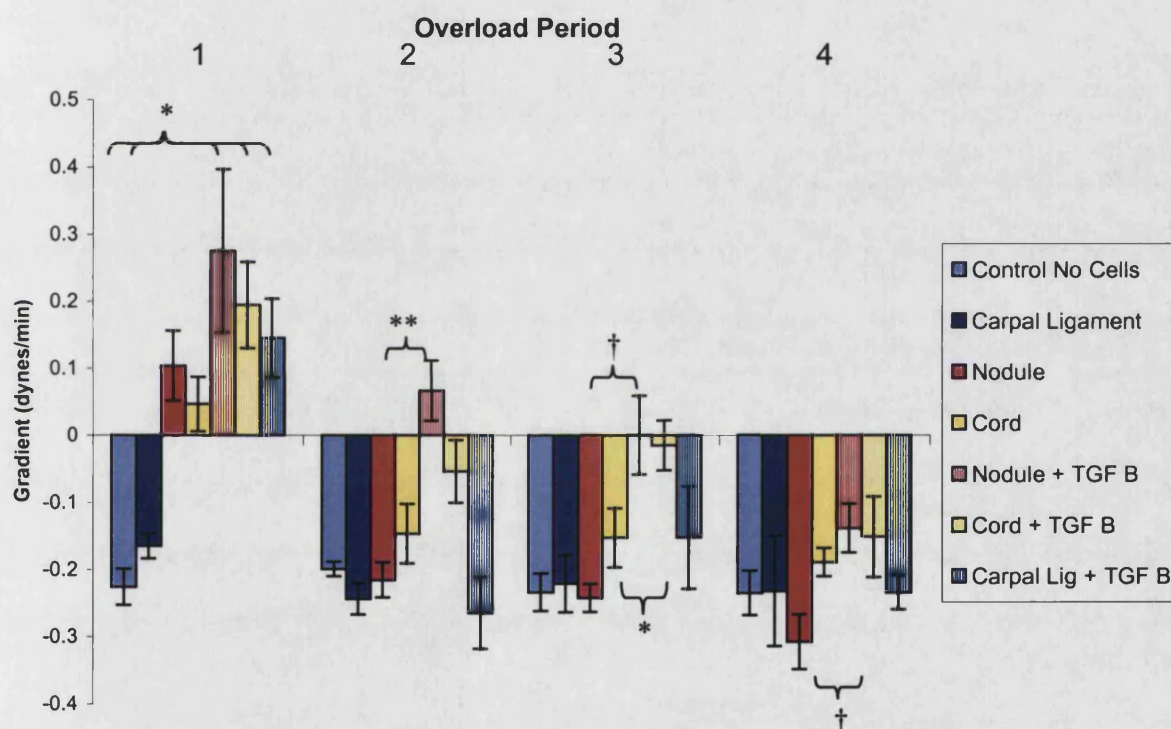
Figure 3.8.4. A histogram comparing the mean post overload gradients with and without TGF-β_1 stimulation. Control gels (n=3), carpal ligament (n=4), Dupuytren's nodule (n=9) and Dupuytren's cord (n=10) are compared with TGF-β_1 stimulated Dupuytren's nodule (n=8), TGF-β_1 stimulated Dupuytren's cord (n=8) and TGF-β_1 stimulated carpal ligament (n=4) fibroblast seeded collagen lattices for all for of the post overload periods. Error bars represent standard errors of the means. The trend for first post overload period gradients to be greater following TGF-β_1 stimulation is only significant in carpal ligament cells. Note also the persisting abnormal response to loading in Dupuytren's fibroblasts into periods two and three following TGF-β_1 stimulation.
* = p<0.05 ; † = p<0.01 ; ** = p<0.001

176

3.8.5. Discussion

The work contained in this section is unique for several reasons. Firstly in order to study the real time responses to mechanical stimulation a device such as the culture force monitor (Eastwood *et al*, 1994) or equivalent is required. Previously circular collagen gels were used to study fibroblast behaviour in three dimensions, however these provide only semi-quantitative and intermittent data. The recent development of the CFM overcomes these problems and is also ideally suited to investigate both the early stages of cell contraction and responses to changes in the tensional environment. Secondly the effects of TGF-β_1 pre-stimulation have been investigated rather than the addition during the experimental procedures. This stimulation causes fibroblast differentiation prior to seeding into the collagen lattices. As demonstrated in chapter 3.7., despite the lack of continued stimulation the fibroblast population remains altered, evidenced by their changed basic contractile properties. This suggests a permanent or semi-permanent alteration of the fibroblasts or a "memory" of the stimulation provided. Finally no authors to date have looked at the combined effects of changes in mechanical load **and** TGF-β_1 stimulation on the cell mediated contractile responses.

In contrast to the serial loading experiments in un-stimulated fibroblast populated collagen lattices (section 3.5) where there was contraction only in the first period, here the abnormal contractile response in Dupuytren's fibroblasts persists into subsequent post overload periods. In fact a statistically significant difference in the response of TGF-β_1 stimulated Dupuytren's nodule fibroblasts is still found in the fourth post overload period when compared with un-stimulated nodule cells. There is also a trend for the contractile response in the first post overload period to be greater following TGF-β_1 stimulation. This is only significant in the carpal ligament fibroblast seeded lattices, however following stimulation the pattern of responses to serial overloading in these cells becomes almost identical to those exhibited by un-stimulated nodule cells.

If the lines of discussion brought out in chapter 3.5. are continued, the reasons for the changes in response to increased tension as each overloading is performed remain

speculative. As was seen from observation of the TGF-β_1 stimulated contraction profiles there are increases in overall force generation and a trend to increasing 20 hour gradients. This may suggest an even higher level of tensional homeostasis, which would take longer to attain. One reason proposed in chapter 3.5.5. for the abnormal response of Dupuytrens fibroblasts only being initially observed in the first overload period was that the equilibrium of tensional homeostasis was attained during the second overload after which the cells acted like controls, becoming relatively mechano-insensitive. This theory could also hold true with the TGF-β_1 stimulated fibroblasts here, but the proposed higher level of tensional homeostasis following stimulation would mean the equilibrium is only attained around the fourth overload. Obviously there will be inter cell line variability, and being over a wider range of forces following TGF-β_1 stimulation, this would explain the stepwise reduction in mean post overload gradients as is seen in each subsequent period.

The second theory proposed for the differences observed in response with progressing overloads was that of matrix stiffening. The stiffer matrix produced with increasing applied forces caused less force to be perceived by the cells. This reduced the abnormal contractile response of Dupuytren's disease fibroblasts subsequent to the first post overload period (figure 3.5.9.). Following TGF-β_1 stimulation the overall tension in the collagen gels is much greater and it follows that the matrix stiffness will also be significantly increased with cells perceiving less overall force, however the abnormal contractile responses to loading are still encountered. TGF-β_1 may therefore greatly enhance the sensitivity of fibroblasts to changes in mechanical force. From the data presented here this seems to be especially so in Dupuytren's fibroblasts but also occurs in control carpal ligament fibroblasts in the first post overload period. With each overload the matrix stiffness increases again, although at the higher levels of force with TGF-β_1 stimulation, the proportional increase in stiffness with each overload will be less than in un-stimulated gels. It might be a combination of this and the increased sensitivity of fibroblasts to mechanical stimuli (see figure 3.8.6 for explanation) that cause abnormal contractile responses to persist into later post overload periods, despite the fact that they may be perceiving less transmitted force each time the matrix stiffness increases.

a) Unloaded collagen gel

b) Gel overloaded once

c) Gel overloaded twice

d) Gel overloaded twice seeded with TGF-β_1 stimulated fibroblasts
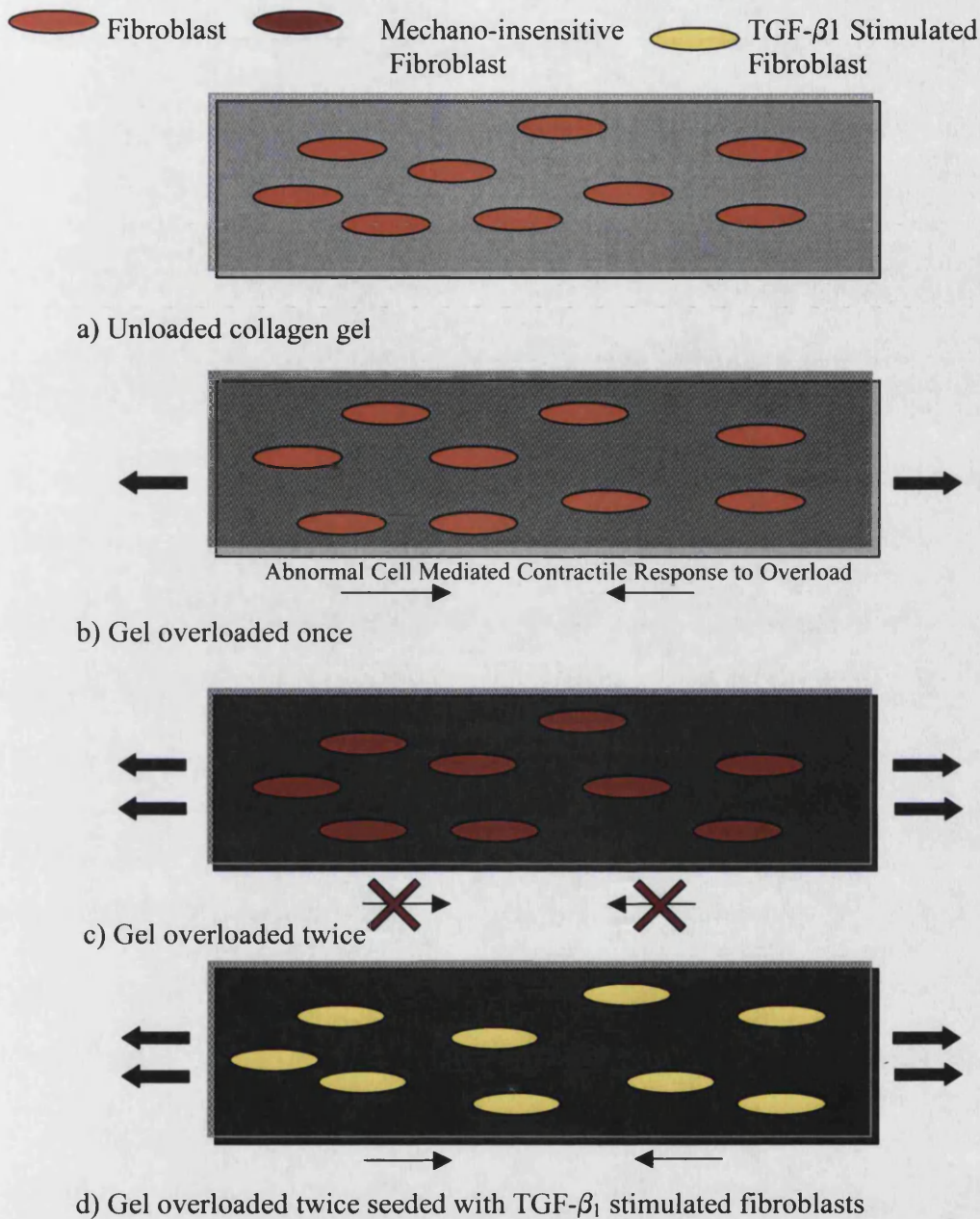
Figure 3.8.5. Diagram representing the proposed effect of collagen gel loading on fibroblast perception of force and the result of TGF-β_1 stimulation. Prior to loading and cells are able to perceive force and respond to it. The first overload causes a stiffening of the matrix (Darker colour 🔲) but the cells are still able to perceive the force. The second overload stiffens the matrix still further (Much darker colour ⬛) which prevents the force being transmitted to and perceived by the fibroblasts, so they are unable to respond to it (◀✖—) and become mechano-insensitive (⬭).Following TGF- β_1 stimulation, however the fibroblasts are more sensitive to applied mechanical forces (indicated by their brighter colour ⬭) and despite the stiffer matrix they are still able to perceive and react to the increased force of the overload.

179

The third hypothesis put forward in chapter 3.5.5. to explain the loss of abnormal response to loading after the first overload was that of a refractory period. Here TGF-β_1 stimulation could be inducing the build up of increased intracellular stores of the factors (ions or proteins) that may be used up during cell-mediated contraction, or causing modification of the fibroblasts to manufacture more rapid and increased amounts of these factors. Thus, in stimulated fibroblasts the refractory period might initially be shorter or delayed so that the abnormal contractile response only diminishes following the third or fourth overload.

The mechanism by which TGF-β_1 stimulation of fibroblasts could increase sensitivity to external mechanical stimuli is also not addressed by these experiments. Upregulation of cell/matrix interaction molecules such as integrins (Ingotz and Massague, 1986) could occur along with an increase in cell process extension. Brown et al (2002) proposed that TGF-β_1 caused a direct effect on the cytoskeletal motor with enhanced integrin expression occurring later. An enhanced intracellular cytoskeleton, as is seen with differentiated myofibroblasts, could also improve perception of mechanical forces. Alternatively TGF-β_1 could upregulate any of the aspects of intracellular mechanotransduction pathways (Addario et al, 2001), which are thought to be involved in the way cells recognize and react to external forces.

As with the initial loading experiments in chapter 3.5. an important finding is the fact that these fibroblasts are contracting in response to an increased load. This again contradicts the theory of tensional homeostasis and is seen as an abnormal response to the elevated tension. Here it is demonstrated that TGF-β_1 stimulation causes exacerbation of these abnormal responses, which not only occur at a higher level of tension and to a greater degree, but also persist into subsequent post overload periods. TGF-β_1 is thus implicated once more in triggering or progression of Dupuytren's contractures by acting in synergy with a mechanical stimulus to cause more rapid or prolonged fibroblast contraction. If combined with rapid and continuous matrix remodelling the diseased tissue would, in theory shorten more rapidly than with non TGF-β_1 stimulated fibroblasts.

The clinical scenario is clearly a much more complex milieu of interacting factors and forces however the findings here may have clinical implications. For example the patients who Skoog described (1963) as continuously extending fingers to try and overcome their Dupuytren's disease would be particularly susceptible to rapid disease progression if there were also high levels of TGF-β_1 within the hand. An injury or repetitive minor trauma could cause release of this, or even as some authors have suggested hypoxia from microvascular occlusion (Murrell, 1992). A small increase in TGF-β_1 locally in susceptible individuals could be sufficient to reach a threshold where myofibroblasts differentiate, fibroblasts contract excessively and respond abnormally to external mechanical stimuli and Dupuytren's disease would rapidly progress.

The question arises; should patients who have established Dupuytren's disease and suffer hand trauma, or undergo surgery for other reasons, have vigorous physiotherapy? In this scenario there will be high levels of TGF-β_1 present and continuous passive or active finger extension will constantly load the Dupuytren's tissue. It is conceivable, given the results here, that this will cause an exaggerated abnormal contractile response from the resident Dupuytren's disease fibroblasts, which in combination with remodelling will lead to rapid disease progression. This is not infrequently encountered in clinical practice with several reports of single injuries causing exuberant evolution of Dupuytren's disease (reviewed by Hueston and Seyfer, 1991).

Of course these patients present challenging management problems and sensible judgement must be employed to maintain a balance of doing the most good for least harm. In hand injuries it is usually preferable to strive for the best range of movement possible, dealing with potential Dupuytren's contractures later.

In operations for Dupuytren's disease itself, TGF-β_1 has already been proposed as a possible culprit for disease recurrence by reactivating residual cord tissue (Chapter3.6). Its synergistic role with mechanical stimuli may not be as directly involved here, as in most procedures the diseased matrix is divided or excised. Thus post operative physiotherapy

although stretching the fingers in extension will not apply this force to the Dupuytrens's fibroblasts. This would only be the case if a tissue gap were later bridged, for example by scar tissue or if the diseased tissue was incompletely released.

SUMMARY:-

- TGF-β_1 stimulation of fibroblasts caused a trend for the abnormal contractile responses in the first post overload period to be increased, which was significant in carpal ligament cells.
- TGF-β_1 stimulation of Dupuytren's fibroblasts caused their abnormal contractile responses to loading to persist into subsequent post overload periods in contrast to the pattern seen in un-stimulated fibroblasts.

Once again TGF-β_1 stimulation has been shown to exacerbate the features of Dupuytren's fibroblasts that may underlie the fascial tissue shortening which leads to clinical contractures. Here by increasing the sensitivity of fibroblasts to mechanical stimuli and exacerbating the abnormal contraction in response to loading, in disagreement with theories of tensional homeostasis, it could accelerate disease progression. TGF-β_1's role in the matrix biology of Dupuytren's disease could, however, be turned to the surgeons advantage by acting as a potential therapeutic target. By locally blocking or reducing the effects of TGF-β_1 the abnormal contraction, alterations in tensional homeostasis and abnormal responses to mechanical stimuli could be abrogated.

3.9. The Cellular Morphology of Dupuytren's Nodule, Dupuytren's Cord and Carpal Ligament Fibroblasts Within Collagen Lattices.

3.9.1. Introduction

At the conclusion of experimental runs on the culture force monitor the collagen lattices were processed as detailed in chapter 2.5.6. Half of the gel was used for morphological studies; the resident cells being stained using two techniques (chapter 2.5.7. and 2.5.8).

Several techniques have been developed to observe cells seeded within three-dimensional lattices in order that morphological changes could be studied. These generally require fixation of the collagen gel and subsequent staining of the resident cells. Eastwood *et al* (1996 and 1998) have simply stained the lattices using 1% Toluidine blue which will turn the cells a deep blue, easily identified using light microscopy. Others have used fluorescent stains such as phalloidin or phallacidin, which stains all actin filaments (Tarpila *et al*, 1996, Rayan and Tomasek, 1994, Tomasek *et al*, 1992). Vaughan *et al* (2000) have selectively stained for α-smooth muscle actin, identifying myofibroblasts within the collagen gels.

These techniques of visualising fibroblasts within collagen lattices under varying conditions or at differing time points have allowed researchers to gain important insights into cellular contractile function by relating the observed morphology to gel contraction. For example Eastwood *et al* (1996) found that most of the early contractile force generated by dermal fibroblasts on the CFM occurred whilst fibroblasts were extending cell processes and filopodia, concluding that this tension was actually the result of tractional remodelling. Staining for α-smooth muscle actin has demonstrated that the myofibroblast phenotype only occurs after a period of time in a tethered system (Tomasek *et al* 2002), thus in the culture force monitor model this is likely to be later once balanced forces are attained.

Importantly Eastwood *et al* (1998) also showed that fibroblasts align themselves along the lines of isometric tension in a low aspect ratio gel such as the one I have used here. Lattices can be described as having a high or low aspect ratio depending on the orientation of the rectangular gel and the forces across these two alternatives vary. A low

aspect ratio gel is attached to the floatation bars along the long sides of the rectangle and force changes across the gel are minimal and more evenly distributed. High aspect ratio gels are arranged longitudinally with the floatation bars attached to the short sides and force gradients are much greater. Eastwood *et al*'s findings indicates that cells can both perceive loads and the direction that they occur in, and reacting accordingly by altering their cytoskeleten to change alignment.

On observing the collagen lattices that had been fixed and stained following CFM experiments in the studies presented here, it was noted that nodule fibroblasts appeared to display a high degree of orientation along the long axis of the collagen gel. Conversely the carpal ligament fibroblasts appeared much less organised, often stellate in appearance. This difference in orientation was fascinating as it broadly corresponded with the force that the fibroblasts generated.

It was of interest therefore to next quantify these differences in cellular orientation.

3.9.2. Aim

To quantify the degree of alignment of fibroblasts within collagen lattices following contraction and loading, comparing each cell type, with and without TGF-β_1 stimulation.

3.9.3. Methods

The method was developed as detailed in chapters 2.5.8 and 2.5.9. Collagen lattices were stained by two techniques following fixation in 10% formal saline. 1% Toluidine blue staining allowed reasonable assessment of the gross appearances (see figure 3.9.1.) of cells within the gels. It was felt however that immunohistochemical staining for α-SMA with a counter stain allowed better overall visualisation of the fibroblasts, their cytoskeleton in relation to the nuclei, and the particular orientation of cells (figure 3.9.2 illustrates a high power view of a myofibroblasts within a collagen lattice).

For an initial comparison the mean cell body heights at 90° to the long axis of the collagen gel were measured for nodule and carpal ligament fibroblast populated collagen

lattices. This was compared with the mean angle of deviation from the long axis of the collagen gel of the bipolar fibroblasts that were in focus in a random 2D micrograph. After consideration, the later method was believed to be superior and this was then applied to random fields at 400 x magnification to a sample of all other cell types. The reasoning behind this decision was based upon several factors. Firstly by measuring the cell body height, at no point was the actual direction of orientation of the fibroblast determined. The measurement was simply an indirect way of attempting to assess this based on the hypothesis that fibroblasts orientated along the long axis would have smaller cell body heights in this direction. The second method at least made a direct measurement of the orientation of the cells, all be it subjective in nature. In addition it was observed that there was not uniformity of cell body height within cells displaying similar orientation. Thus the mean angle of deviation from the long axis of the gel of all fibroblast types with and without TGF-β_1 stimulation was obtained.

The results were compared and statistical analysis performed using the student's t test (Sigma Stat, Jandel Corps.)

3.9.4. Results

Figure 3.9.1 illustrates a typical nodule fibroblast seeded collagen gel observed under 200 x magnification following staining with 1% Toluidine blue. This field is from a central area of the collagen gel (see figure 2.14) and longitudinal alignment of the fibroblasts can be observed. There is however little definition of the intracellular cytoskeleton. In contrast the high power image of a similar region of collagen gel stained using the immunohistochemical method shown in figure 3.9.2, illustrates well the cell processes, cytoskeleton and thus the true orientation of each cell in focus, or the cell body height can be better determined.

$\longleftrightarrow$

Long axis of collagen gel
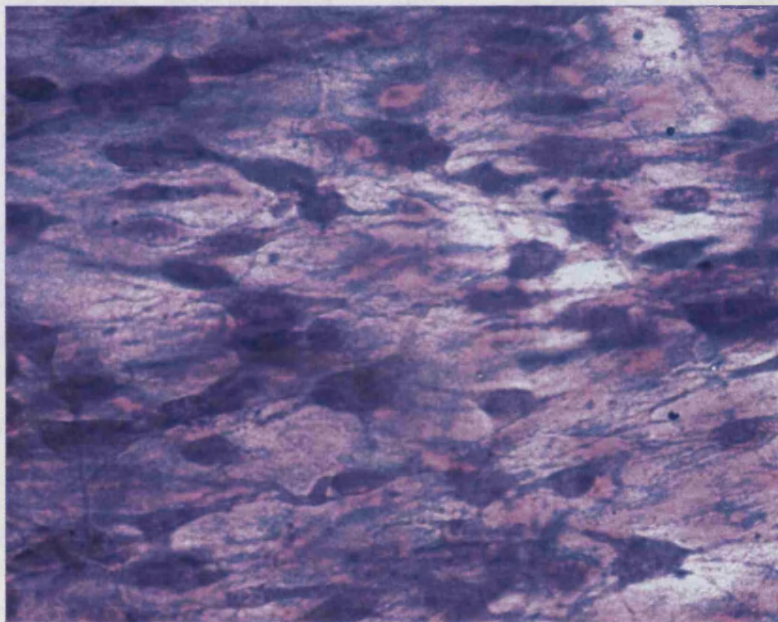
Figure 3.9.1. Micrograph of collagen gel seeded with nodule fibroblasts (x400 magnification). At the conclusion of the experimental run on the culture force monitor the gel was fixed in formal saline and then stained using 1% toluidine blue. A general trend in the fibroblast orientation can be observed in the direction of the long axis of the collagen gel.

Long axis of
collagen gel
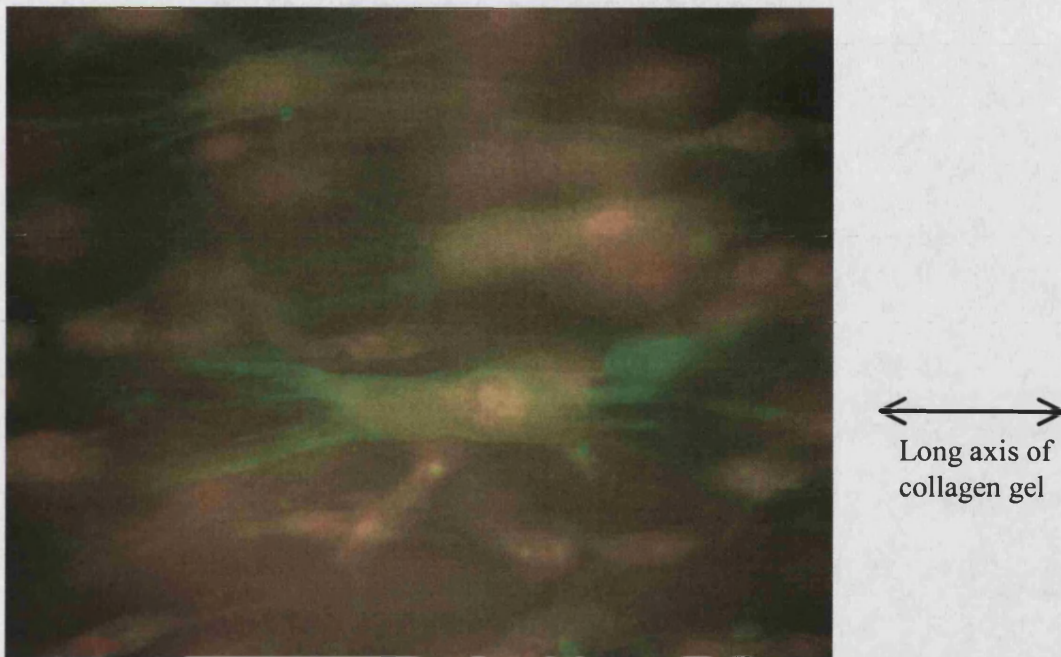
Figure 3.9.2. Photomicrograph of collagen gel seeded with nodule fibroblasts (x400 magnification). At the conclusion of the experimental run on the culture force monitor the gel was fixed in formal saline and then stained using the immunoflourescence technique described above. Once again alignment along the long axis of the collagen gel can be seen, however more cellular detail is visible using this method

Lower power immunohistochemical images of both nodule and carpal ligament fibroblasts within collagen lattices are displayed in figures 3.9.3. and 3.9.4., where there are observable differences in the degree and direction of alignment of these two fibroblast types. These differences were quantified using the methods outlined above.

The mean cell body height for the initial groups of Dupuytren's nodules and carpal ligament fibroblasts within collagen lattices on removal from the CFM is charted in figure 3.9.5. This was measured in arbitrary length units by using image analysis software (UTHSCSA Image tool) applied to images of random fields at a uniform magnification for 6 nodule cell lines and 6 carpal ligament cell lines (four different cell lines, 2 repeated).
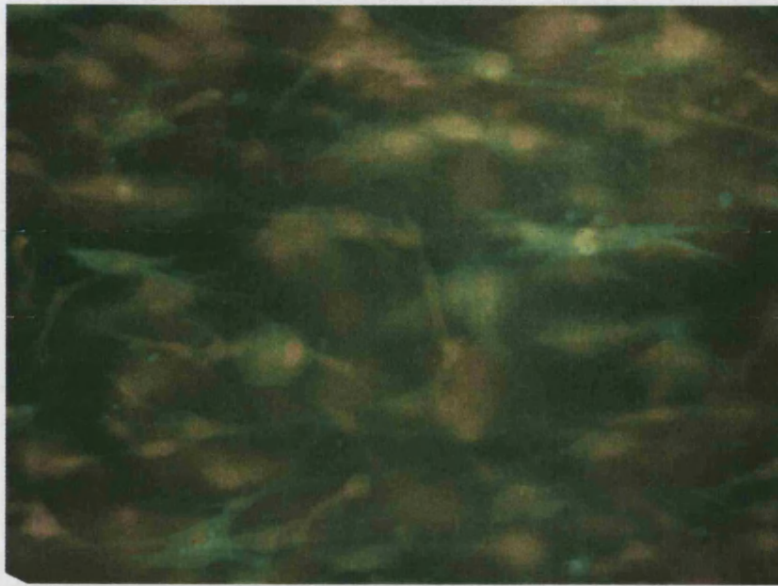
Long axis of
collagen gel

Figure 3.9.3. Dupuytren's nodule fibroblasts within collagen lattice at the end of a culture force monitor experiment, stained for α-SMA (x 200 magnification). Note that there appears to be a general orientation along the line of the long axis of the collagen gel, which is represented at the side of the micrograph.

Long axis of
collagen gel

Figure 3.9.4. Carpal ligament fibroblasts within collagen lattice at the end of a culture force monitor experiment, stained for α-SMA (x 200 magnification). Note that in contrast to the previous figure, there is no discernable principal orientation in relation to the line of the long axis of the collagen gel, which is represented at the side of the micrograph.

The mean cell body height for nodule fibroblasts was 91.6 units (SD ± 13.1 units), whilst the mean cell body height in carpal ligament fibroblasts was 72.5 units (SD ± 15.3 units). The difference between these two values does just reach statistical significance (p<0.05) however the difference is not as striking as that seen when the mean angles of deviation from the gel long axis are compared for the same set of images (figure 3.9.6).
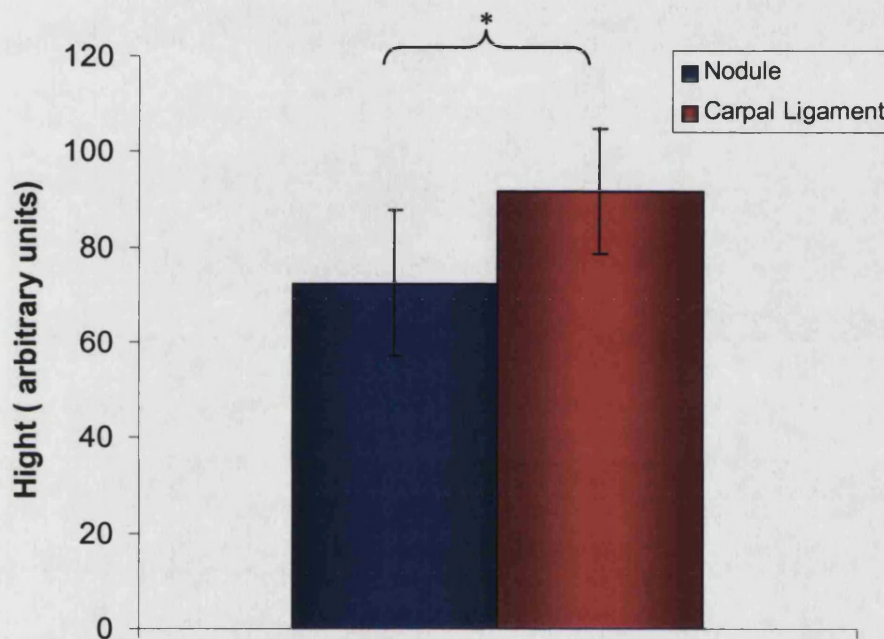
Figure 3.9.5. The mean cell body height of Dupuytren's nodule fibroblasts (n=6) compared with carpal ligament fibroblasts (n=6) within 3D collagen lattices at the end of experimental runs on the culture force monitor. Error bars represent the standard deviations of the values, which are measured in arbitrary units using image analysis software. * p<0.05

Here the mean angle of deviation of Dupuytren's nodule cells from the gel long axis is 12.9°, (SD ± 6.6 °) compared to a value of 38.9 ° (SD ± 4.4 °) for carpel ligament fibroblasts. This value is highly significant (p<0.001) and indicates that the Dupuytren's fibroblasts display a much closer alignment to the long axis of the collagen gels than is seen in carpal ligament fibroblasts. This reflected in a quantitative manner, what were apparent observable differences in the stained collagen gels.
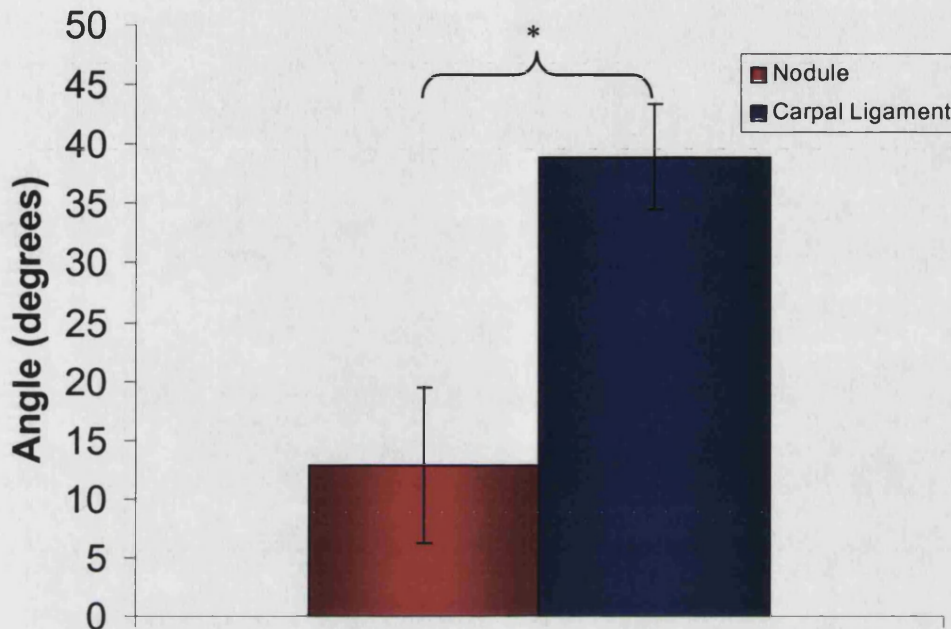
Figure 3.9.6. The mean angle of deviation from the long axis of 3D collagen lattices of Dupuytren's nodule fibroblasts (n=6) and carpal ligament fibroblasts (n=6) at the end of experimental runs on the culture force monitor. Error bars represent the standard deviations of the values. * p<0.001

Subsequently this technique of quantifying cellular alignment was used for all fibroblasts types, with and without TGF-β_1 stimulation the results of which are displayed in figure 3.9.7. As detailed above in section 3.9.3 and is discussed further in the following section (3.9.5) this second technique was not selected because of the greater statistical significance but because of the appropriateness to the question being raised. Further to the data already obtained for nodule and carpal ligament fibroblasts, the mean deviation of cord fibroblasts was calculated as 28.9 ° (SD ± 8.0°), which was significantly less than carpal ligament (p<0.05) and greater then nodule (p<0.01).

Following TGF-β_1 stimulation of fibroblasts seeded in CFM collagen gels, the mean deviation from the gel long axis was 7.8 ° (SD ± 1.9°) for nodule fibroblasts, 14.7° (SD ± 6.1 °) for cord fibroblasts and 15.8° (SD ± 6.5°) for carpal ligament fibroblasts. Both cord and carpal ligament values were significantly less than the un-stimulated values ($p<0.01$ and $p<0.001$ respectively) although a similar comparison between nodule and TGF-β_1 stimulated nodule fibroblasts just failed to reach significance ($p=0.08$). Additionally the differences between alignment of both cord and carpal ligament fibroblasts following stimulation were significantly different from TGF-β_1 stimulated nodule fibroblasts ($p<0.05$).
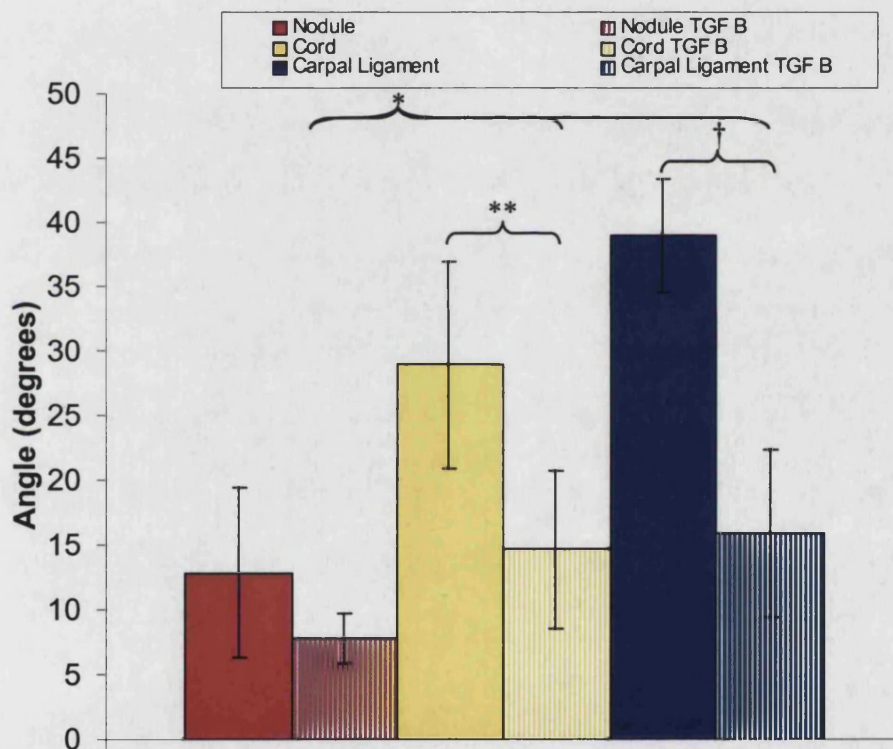
Figure 3.9.7. The mean angle of deviation from the long axis of 3D collagen lattices of all fibroblast types, with and without TGF-β_1 stimulation. Error bars represent standard deviations. Significant differences are shown. * $p<0.05$; ** $p<0.01$; † $p<0.001$

3.9.5. Discussion

Cellular morphology is able to provide many clues as to the functional aspects of behaviour. As such microscopic examination of fibroblast structure has frequently been undertaken in collagen lattice studies. In some of the first culture force monitor experiments performed by Eastwood *et al* (1996), staining of fibroblasts within the collagen gels at set time points from the beginning of experiments, allowed the authors to conclude that the early phase of contraction was due to tractional remodelling. The rapid generation of force correlated well with fibroblasts changing shape from rounded cells to a more elongated or bipolar shape and additionally the spreading of cellular processes. Importantly the same group (Eastwood *et al*, 1998) also demonstrated that dermal fibroblasts within CFM collagen gels responded to the lines of mechanical stress that are exerted across the gel. In low aspect ratio gels where lines of stress were poorly pronounced, fibroblasts showed no specific orientation. By contrast, in high aspect ratio gels, such as those used in this study, where high strain gradients are present the fibroblasts demonstrated a bipolar shape, aligned parallel to the principle iso-strain lines. These results in high aspect ratio gels correspond with the findings here in Dupuytren's nodule fibroblasts. As can be seen from figures 3.9.2. and 3.9.3. there is a clearly observable alignment of the fibroblasts within the central areas of the collagen lattices. This was not the case in carpal ligament fibroblast populated collagen lattices where a much more random cellular orientation was observed, often with stellate rather than bipolar fibroblasts. This correlated with the appearances of fibroblasts observed by Eastwood *et al* (1998) in low aspect ratio gels.

The work here has gone one step further than them, however, and a method of quantifying the cellular alignment of fibroblasts within the collagen lattices has been developed. The second method tested, on reflection was more appropriate to apply to the study of cellular alignment and was therefore used for all subsequent quantification, although both techniques have flaws. In both methods it is necessary to select a random field from the stained collagen gel and then apply the image analysis to fibroblasts that appear in focus within a slice of the collagen gel. Therefore a 2 dimensional sample

population of the cells in a 3D collagen gel are used to determine alignment. In the first method, measuring of cell body height at right angles to the collagen gel long axis, the value may be variable upon other factors than cell orientation. For example larger cells will clearly have a larger cell body and hence a greater cell body height irrespective of orientation. Myofibroblasts, for instance are generally larger cells than standard fibroblasts and therefore if a gel contains more myofibroblasts, such as may be the case in nodule cells, then the mean cell body height will be artificially elevated. This picture may be further complicated by the fact that stellate cells with no particular orientation often have larger cell bodies.

The second method of defining a longitudinal axis of each in focus cell within the selected field relies on the subjective assessment of the observer to define that axis. In many fibroblasts this is straightforward, however some such as stellate cells, have a much more difficult axis to define, so introducing observer error. Other authors have quantified alignment of cells, for example Umeno and Ueno (2002) observing cell orientation caused by magnetic fields derived a figure between 1 and 0, relating the direction of the cells of interest to the mean direction of the total cells observed. A value of 1 suggested complete orientation, whereas a value of 0 represented a random orientation. Harding *et al* (2000) used a similar method to the one developed here, constructing a line through bipolar fibroblasts and measuring the deviation of this line from the axis of fibronectin cables.

The alignment of fibroblasts in this work correlated with the amount of overall force generation, with the most consistently aligned nodule fibroblasts generating most force, followed by cord, whilst carpal ligament fibroblasts generated least force and were more randomly oriented. It is impossible from these studies to determine if the significant differences observed in the alignment of carpal ligament fibroblasts and both nodule and cord fibroblasts was cause or effect. From the results obtained by Eastwood *et al* (1998) referred to above it is conceivable that the fibroblasts, in generating more force, also therefore perceived this increased force and were stimulated to become orientated along these lines of stress. One cannot rule out, however, the possibility that the very reason that more force was generated was because of the enhanced ability of the resident cells to align

parallel to the gels long axis. It could be hypothesised that Dupuytren's fibroblasts attach to the matrix in a superior way (with tighter or multiple adhesion sites) to carpal ligament fibroblasts. They therefore would be both better at perceiving tensional forces across the gel (thus developing alignment) and transmitting their own cytoskeletal contractile forces to the matrix, so generating increased contractile force.

The results of the alignment studies presented here also showed that TGF-β_1 stimulated fibroblasts were better oriented along the long axis of the collagen gels than non-stimulated fibroblasts. This correlated with the tendency to generate increased force in all cell types following TGF-β_1 stimulation and therefore fits in with the above discussion. To date there has been no published literature demonstrating increased alignment of fibroblasts following TGF-β_1 stimulation.

It was not possible to quantify the presence of myofibroblast phenotype cells within the 3D collagen gels, despite satisfactory staining for α-SMA. The fibroblast density in CFM gels is very high compared with that used in other lattice models (Rayan and Tomasek, 1994; Tarpila et al, 1996; Vaughan et al, 2000) this makes separation of individual fibroblasts difficult especially in slices of three dimensional gels where background staining of other cells can obscure or blur clear margins. This makes differentiation between negative staining red cells and positive staining green cells impossible unless the individual fibroblast is brought into direct focus. One method of achieving a quantification of α-SMA in the collagen gels would have been cellular extraction and subsequent Western blotting for the protein in question. This technique has been used by other authors (Grinnell et al, 1999; Vaughan et al, 2000) but was beyond the scope of the current investigation. In subsequent studies however, it would be interesting to compare α-SMA in the 3D model between cell types comparing them with the results obtained in monolayer culture (Chapters 3.3 and 3.6). Interestingly Tomasek and Rayan (1995) correlated contraction of stress-relaxed circular FPCLs with monolayer α-SMA expression in Dupuytren's fibroblasts, but only after dividing cultures into low (<10% α-SMA +ive cells) and high (>15% α-SMA +ive cells). Later the same group (Vaughan et al, 2000) correlated increased 3D α-SMA positivity with fixed released lattice contraction.

In their study of strain pattern and fibroblast alignment using high and low aspect ratio gels, Eastwood *et al* (1998) also demonstrated an area in high aspect ratio lattices close to the floatation bars where there was a very low strain gradient. In this so-called delta zone fibroblasts were randomly oriented, often stellate. The same pattern was observed with our Dupuytren's fibroblast seeded collagen lattices when areas of delta zone (figure 2.13.) were stained and observed as shown in figure 3.9.8.

Long axis of collagen gel
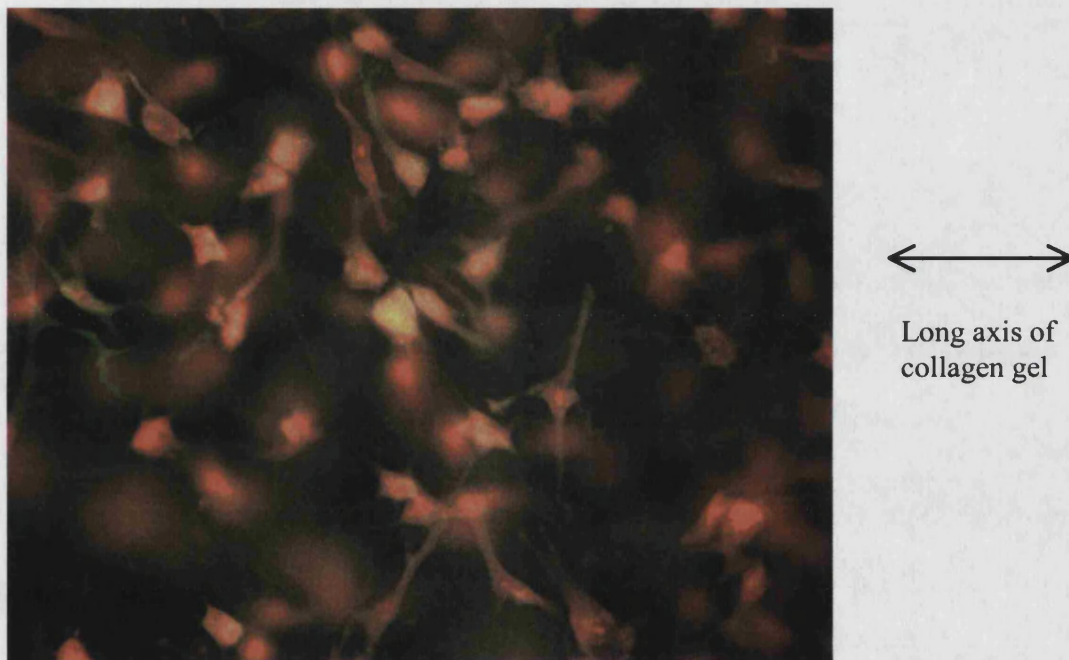
Figure 3.9.8. An area of delta zone from a nodule fibroblast populated collagen lattice stained for α-SMA. (viewed at 400x magnification). Note the random orientation of fibroblasts compared with the long axis of the gel and the stellate nature of many.

SUMMARY:-

- Observed differences in the degree of alignment of fibroblasts within lattices were quantified and it was determined that the nodule fibroblasts demonstrated significantly closer alignment to the line of the long axis of the collagen gels than the cord or carpal ligament fibroblasts.

- **Degree of alignment corresponded with the degree of contraction measured.**

- Stimulation of fibroblasts with TGF-β_1 caused a significant increase in the mean alignment of fibroblasts within collagen gels in cord and carpal ligament cell types.

Chapter 4

General Discussion

4. <u>General Discussion</u>

4.1. Background

In this thesis a series of experiments have been undertaken in order to understand the cellular mechanisms behind the development of the most disabling aspect of Dupuytren's disease, the digital flexion deformities. Following an extensive review of the literature and evaluation of the current theories regarding contracture formation, it is apparent that digital flexion deformities occur as a result of physical shortening of the Dupuytren's fascial fabric (Brickley Parsons *et al*, 1981). This is a consequence of two simultaneous processes. Firstly cell mediated contraction of the matrix and secondly matrix remodelling which fixes the matrix in the shortened position. The continuous stepwise progression of these process results in a shorter piece of fascia, which contracts the digits of the involved rays and prevents extension.

The study has focussed on the aspect of cell-mediated contraction whilst additionally addressing the hypothesis that nodule and cord derived fibroblasts may exhibit different phenotypes and behaviours and thus show differential matrix shortening properties. This may lead on to allow a better understanding both of the natural history of disease progression and of the relative contribution nodules and cords play in the pathogenesis of Dupuytren's disease.

4.2. Experimental Evidence

Tissue cellularity has been quantified (Section 3.1) in those regions of Dupuytren's fascia specifically defined as nodule or cord. Significant differences were established with nodule being three times more cellular than areas of cord. It was thus possible to be confident that tissue separation for explant cultures on the basis of gross morphology was valid.

The investigation into cell-mediated contraction began by assessment of the myofibroblast phenotype, firstly in tissue specimens of nodule, cord and carpal ligament. The myofibroblast, because of its morphological features and the presence of an α-SMA cytoskeletal network has been proposed as the contractile cell of

197

Dupuytren's contracture since it was first identified in the diseased fascia by Gabbiani and Majno in 1972.

By staining tissue sections for α-SMA it was demonstrated that the myofibroblast phenotype was prevalent in nodules, however it was also possible to established that myofibroblasts could be identified in 20% of cords examined; a previously unreported finding. Furthermore the myofibroblasts that were present in cords tended to be in defined areas or foci of hypercellularity. Luck (1959) proposed that nodules progress to dormant fibrotic cords as the natural history of Dupuytren's disease, in which case these areas may be old nodules that are in the final stage of regression. Alternatively they may be small foci of re-activated Dupuytren's disease within previously dormant cords. Fibroblasts, stimulated by local factors may have begun to proliferate, as well as differentiate into myofibroblasts. In either case the presence of this contractile phenotype in cords suggests they may play at least some role in the cell mediated contraction, all be it to a lesser extent than nodules. In comparison to Dupuytren's tissue no myofibroblasts were observed in carpal ligament tissue.

Results then demonstrated that these *in-vivo* findings of myofibroblast phenotype are **maintained into populations of cultured fibroblasts** from the specific regions (Section 3.3.). Such differences in the phenotype of fibroblast cultures from nodules and cords have not been previously shown, indeed many authors who have studied myofibroblasts in cultured cells have either used undefined tissue (Murrell *et al*, 1991) or only nodular tissue (Hurst *et al*, 1986; Rayan *et al*, 1996; Tarpila *et al*, 1996). Once more the prevalence of the myofibroblast phenotype in nodules suggests they may have a greater role to play in the eventual pathogenesis of contracted tissue. One could hypothesise that the active, myofibroblast rich nodule acts almost as a motor, pulling on the cord, creating a nodule-cord contractile unit. **Thus the nodule might be a prime target for any future non-surgical therapy.**

Having proved that there was a significant difference in the contractile cell phenotype between nodule and cord cultures, and indeed a significantly increased percentage in nodule cultures than non-diseased carpal ligament cultures, the subsequent experiments examined the actual cell-mediated contractile properties of these fibroblast types.

In chapter 3.4 Dupuytren's nodule fibroblasts were demonstrated to possess enhanced force generation over both cord and carpal ligament fibroblasts using the culture force monitor model. Cord fibroblasts were also more contractile than carpal ligament fibroblasts, however of even greater interest was the alteration in the typical CFM contraction profile (described in dermal fibroblasts by Eastwood *et al*, 1994), which was observed in both types of Dupuytren's fibroblasts. As discussed in 3.4.5. this represents a delay in achieving the level of tensional homeostasis which may be encountered at a much higher level of tension. This finding alone is significant as it suggests Dupuytren's fibroblasts have altered tensional homeostasis and may explain why these abnormal cells could continue to contract in an effort to reach this higher level when normal fibroblasts would not. This could underlie the progressive irreversible nature of clinical contractures. Further to this however, it was also shown in the subsequent loading experiments (Chapter 3.5) that the responses to increases in mechanical stimulation are not what would be expected given the theory of tensional homeostasis.

Dupuytren's nodule fibroblasts, and to a lesser extent cord fibroblasts, in collagen gels contracted following a uniaxial loading stimulus. Clearly in the clinical setting this contraction would create an undesirable positive feedback, serving only to exacerbate the problem of cell-mediated contraction. This finding may also explain the anecdotal reports of excessive or rapid disease progression in patients who manually try to overcome the condition by continuous stretching (Skoog, 1963), as well as the observation that following continuous elongation techniques, if fasciectomy is not performed contractures redevelop very rapidly (Messina and Messina, 1993).

The growth factor Transforming Growth Factor beta one (TGF-β_1) has been widely studied for its pro-fibrotic effects and its ability to cause fibroblast to myofibroblast differentiation (Tomasek *et al*, 2002). The differential effects of TGF-β_1 stimulation on nodule and cord fibroblast cultures have, however not been previously studied.

The rise in the percentage of the myofibroblast phenotype in nodule cultures corresponded with previous studies (Dugina *et al*, 2001; Vaughan *et al*, 2000) although, notably, cord fibroblasts were stimulated to differentiate into myofibroblasts at an equal percentage, whereas this was not the case with comparison carpal ligament fibroblasts. These results are proposed to indicate cord fibroblasts remain susceptible to activation

or re-activation given an appropriate stimulus, even though they may appear quiescent. TGF-β_1 can be released in a variety of scenarios and it is well accepted that levels are increased locally following trauma and in wound healing (Bennett and Schultz, 1993). The results presented here therefore, could offer an explanation for disease progression or onset following trauma (Hueston and Seyfer, 1991) where dormant fibroblasts could become activated and hyper-contractile, but furthermore, they may provide the reason why disease recurrence is so high in this condition. Even the simple wound healing response following procedures for the Dupuytren's disease itself would provide an increase in local factors such as TGF-β_1 causing activation of residual fibroblasts and early recurrence.

Following studies of the effects of TGF-β_1 on the contractile cell phenotype, the model of actual contraction was revisited (Section 3.7). The effects of simple pre-stimulation of fibroblasts with TGF-β_1 were striking. Overall contractile force generation was increased across all fibroblast types with a trend to increased 20 hour gradients on the CFM. This indicated increased abnormalities of tensional homeostasis with greater fibroblast contractility. The changes observed in the shape of the contraction profile, with rapid early contraction, also challenge the purity of the myofibroblasts role in this enhanced contraction. **TGF-β_1 may be working at several levels to bring about up-regulated contraction of collagen lattices; as a direct agonist of contraction, by enhancing cell matrix interaction and by inducing myofibroblast differentiation.**

Finally the responses to uniaxial loading of fibroblasts in collagen gels (Chapter 3.8) lends further evidence to the role of TGF-β_1 in abnormal Dupuytren's fibroblast behaviour. Stimulated Dupuytren's fibroblasts showed both enhanced and persisting abnormalities in their response to a loading force when compared with un-stimulated fibroblasts. As before these were at odds with the theory of tensional homeostasis and would serve only to exacerbate the unwanted abnormal cellular responses that appear to be taking place in Dupuytren's fibroblasts. Clinically this might declare itself by rapid contracture development following splinting for an injury.

4.3. Unifying Theory of Contracture Development

In the light of the results from the experimental work presented here, combined with current knowledge of Dupuytren's disease an attempt has been made to formulate an overall theory of the mechanism of clinical contracture development. This is illustrated in figure 4.1 with numbers indicating where findings of this current study fit in to the framework. It is proposed that the nodule or nests of such nodular like tissue are responsible for most of the disease features. However, although there may be a progression from nodule to dormant cord tissue this could be reactivated by factors that induce TGF-β_1 such as trauma, and wound healing. This reactivation could cause recurrent disease after surgery or rapid progression in previously indolent disease. A proportion of fibroblasts would differentiate into myofibroblasts causing a period of active disease.

Resident cells, especially those within nodules would apply force to the surrounding matrix in an attempt to achieve a new higher level of tensional homeostasis. Cell contraction could be exacerbated by positive feedback from external forces as was seen in the overloading studies. Factors such as rapid, continuous matrix remodelling could have a duel effect by preventing the acquisition of homeostasis and causing physical tissue shortening leading to unchecked fascial shortening and resulting in clinical digital flexion deformities.

Figure 4.1. Theory of Dupuytrens Contracture Development
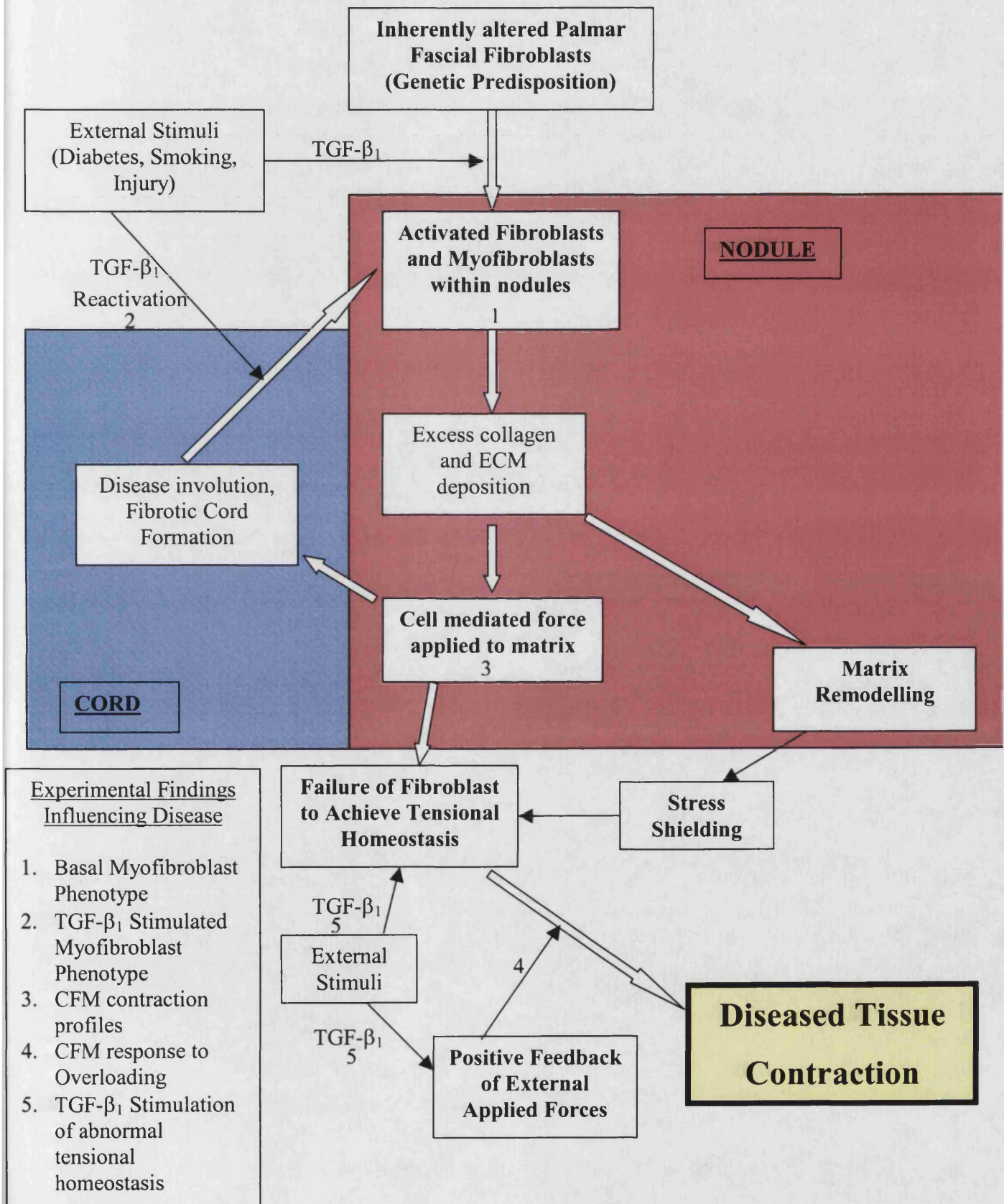
The investigations in this thesis have concentrated on the relative properties of nodule and cord derived cells and how these may be involved in the natural history of Dupuytren's contracture. Studies of the contractile properties of Dupuytren's fibroblasts and their response to tensional stimuli have provided a fascinating insight into how cells within the diseased matrix may behave to cause contracture development and progression. With further work to identify the interplay between these new features of abnormal fibroblast behaviour and the process of matrix remodelling, a clear understanding of why Dupuytren's disease occurs and progresses could emerge.

Looking to the future, it may become possible to target the process of cellular contraction or even the more basic function of cell-matrix interaction. If the abnormalities of tensional homeostasis that have been elucidated here could be reversed or blocked there may be hope of developing therapies for this challenging and enigmatic condition to halt contracture advancement.

4.4. Conclusions

- Quantification of cellularity in Dupuytren's disease tissue determined that areas defined as nodule displayed significantly greater cellularity than areas of cord.

- The Myofibroblast phenotype was present in a greater number of nodule tissue specimens than cord and at a higher density.

- Differences in the myofibroblast phenotype were maintained into differential cultures of Dupuytren's nodule, Dupuytren's cord and carpal ligament cells.

- The myofibroblast phenotype in cultures as a percentage of total cell number was three times higher in nodules than cords.

- Dupuytren's nodule fibroblasts generated significantly greater force than cord fibroblasts in the culture force monitor model. Both nodule and cord fibroblasts generated significantly greater force than normal carpal ligament fascial cells.

- Overloading of lattices seeded with Dupuytren's fibroblasts caused an abnormal contractile response during the first post overload period.

- Stimulation of fibroblast cultures with TGF-β_1 caused a significant up regulation of the myofibroblast phenotype in both nodule and cord derived cultures to the same level despite basal differences.

- TGF-β_1 stimulation of fibroblasts caused a significant increase in the mean generation of force in all cell types at 20 hours, which was accompanied by a change in the shape of the contraction profile in Dupuytren's cells.

- TGF-β_1 stimulation of Dupuytren's fibroblasts caused their abnormal contractile responses to loading to persist into subsequent post overload periods in contrast to the pattern seen in un-stimulated fibroblasts.

- Degree of fibroblast alignment within FPCLs removed from the culture force monitor corresponded with the degree of contraction measured.

4.5. Future Direction

There is potentially interesting work within the current investigation which has not been undertaken due to constraints of time. For example α-smooth muscle actin content of the snap frozen stored CFM gels could be analysed by protein extraction and Western blotting. It might then be possible to relate this more directly to contractile force and draw comparisons with the α-smooth muscle actin content seen here in monolayer cultures. Differences might highlight the role of the environment that the cells exist within.

In addition, whilst the effect of an overloading stimulus has been examined it would also be of interest to study the effects of an equivalent underloading. Cells may also respond in an unexpected way to this stimulus, which might be analogous to the clinical setting of fasciotomy where tension is suddenly released from the matrix.

There are then two possible avenues to follow for the subsequent focus of the main research.

One main aim would be to try and find a means of reducing Dupuytren's fibroblast contractility, either nodule, cord or both. This brings the current investigation back round towards it's therapeutic goals.

One method of doing this might be to investigate the use of an anti-TGF-β_1 antibody. As has been shown in this thesis TGF-β_1 appears to have a stimulatory role for the abnormalities that have been elucidated in contraction and tensional homeostasis, as well as its known role in the differentiation of myofibroblasts. By blocking TGF-β_1 these abnormalities within the Dupuytren's fibroblast population may be reduced thus diminishing the potential for contracture formation.

A second alternative could be to investigate the matrix changes brought about by the contracting cells. Dupuytren's disease, as has been stated several times within this thesis, is a combination of cellular contractile forces coupled with constant matrix remodelling. This causes the permanent shortening of the diseased tissue and fixed contractures. Degree of matrix remodelling by contracting fibroblasts could be

examined by the addition of cytoskeletal disrupting agents such as cytochalasin D. This would cause the release all cell mediated contraction and forces held by the cellular cytoskeleton, leaving only the gel shortening that had occurred due to collagen remodelling over the time course of the experiments. Using the culture force monitor this residual level of tension could be measured and comparisons made once more between nodule, cord and carpal ligament fibroblasts. Again the role of TGF-β_1 could be examined. This may provide evidence that Dupuytren's fibroblasts, and possibly nodule fibroblasts in particular, are more adept at remodelling the matrix they reside within. Having investigated cell mediated contraction in this thesis, such an investigation of matrix remodelling could complete the picture of the cell biology of contracture formation.

Appendix

APPENDIX I: List of Dupuytren's and control fibroblast cell lines.

Dupuytren's cell lines				
Patient	Sex	Age/yrs	Hand	Digit
1	M	49	L	Little
2	M	45	L	Ring
3	F	65	R	Ring
4	M	72	L	Ring
5	M	62	R	Ring
6	M	70	L	Ring & Little
7	M	55	L	Little
8	M	70	R	Ring
9	M	65	L	Little
10	M	27	R	Ring
11	M	71	L	Ring & Little
12	M	75	R	Ring & Little
13	M	62	L	Middle
14	M	66	L	Ring
15	F	79	L	Ring & Little
16	F	71	R	Little

Table I. The age of the patient, hand and ray that the Dupuytren's scar was excised from.

Control Carpal Ligament cell lines			
Patient	Sex	Age/yrs	Hand
1	F	55	L
2	M	72	R
3	M	73	R
4	F	62	R

Table II. The age of the patient and hand that the carpal ligament originated from.

APPENDIX II: Recipes and Formulations of Solutions Used

Normal Fibroblast Growth Media (NGM 10% FCS)

Dulbecco's Modified Eagles Media Gibco	500ml
Foetal Calf Serum No. 10106-169 Gibco	50ml
Pen/Strep No. 1540-122, Gibco	5ml
L-Glutamine 200MM (100x) No. 250030-024, Gibco	5ml
Hepes Buffer (1M pH8)	3.5ml

Trypsin : Versene Solution (1:10)

Trypsin (2.5%) No. 15090-046, Gibco	2ml
Versene No. 15040-033, Gibco	18ml

Bufffered Formal Saline

Formaldehyde No. 284216N, BDH	1litre
Sodium Dihydrogen Phosphate (dihydrate)	45g
Di-sodium hydrogen phosphate (anhydrous)	65g
Made up to a total of 10 litre with distilled water	

Tris Buffered Saline + Tween (100mM Tris and 150mM NaCL, pH 7.6)

Distilled Water	950ml
Tris	12.11g
NaCl	8.75g
HCL	Dropwise to reach a pH of 7.6
Made up to a total of 1 litre with distilled water	

Phosphate Buffered Saline without magnesium and calcium (PBS)

Distilled Water	1000ml	
KCl	0.2g	2.685mM
NaCl	8.0g	0.13M
KH_2PO_4	0.2g	1.47mM
$Na_2HPO_4.2H_2O$	1.435g	8.06mM

DABCO Mixture – Anti Fade Agent for Immunofluorescence

14-Diazodicyclo 2,2,2 Octane (Sigma Aldrych D2, 780-2)	1g
PBS (As made up above)	4ml
Glycerol	36ml
Stored at 4°C, wrapped in silver foil	

APPENDIX III: The Culture Force Monitor

Mould Composition

Silicone Elastomer Kit,	
Sylgard 186: 63417 5U Dow Corning, USA	200g
Sylgard 186: 63417 7W Dow Corning, USA	20g

The above quantities of elastomer gel mix are combined in a beaker to form a smooth thick paste.

The resulting liquid mix is poured into 10cm Nalgene petri dishes (No. 8-0402, Nalgene, Nalge Company, Rochester, New York) around a standard sized, machined metal bar placed in the center of the dish where the well is to be. This is then placed in a vacuum cylinder and negative pressure applied until no further bubbles are evacuated from the gel (around 20 minutes). Bubbles on the surface of the gel are burst with a sterile needle and the mould is placed in the vacuum for a further 15 minutes again until no further bubbles are evacuated. Finally it is placed in an incubator at 37^0C overnight to solidify. Once set the bar is removed leaving the mould ready for use after autoclaving.

Dimensions of Mould

7.5 cm

2.5 cm

10 cm
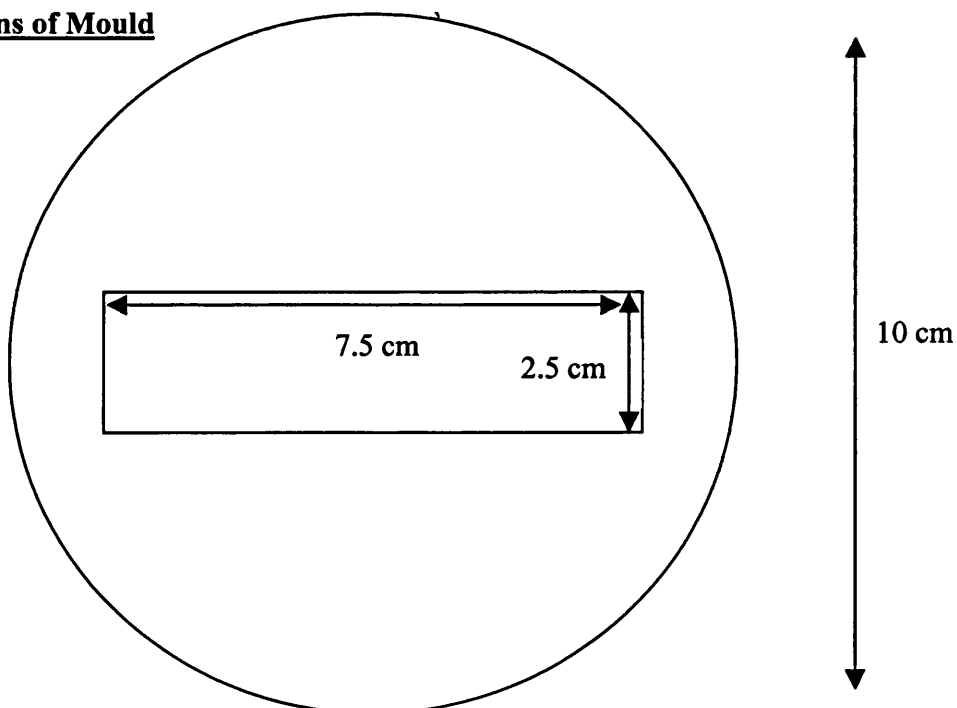
Dimensions and Composition of Floatation Bars and A Frames

0.3 cm

3.5 cm

2.5 cm
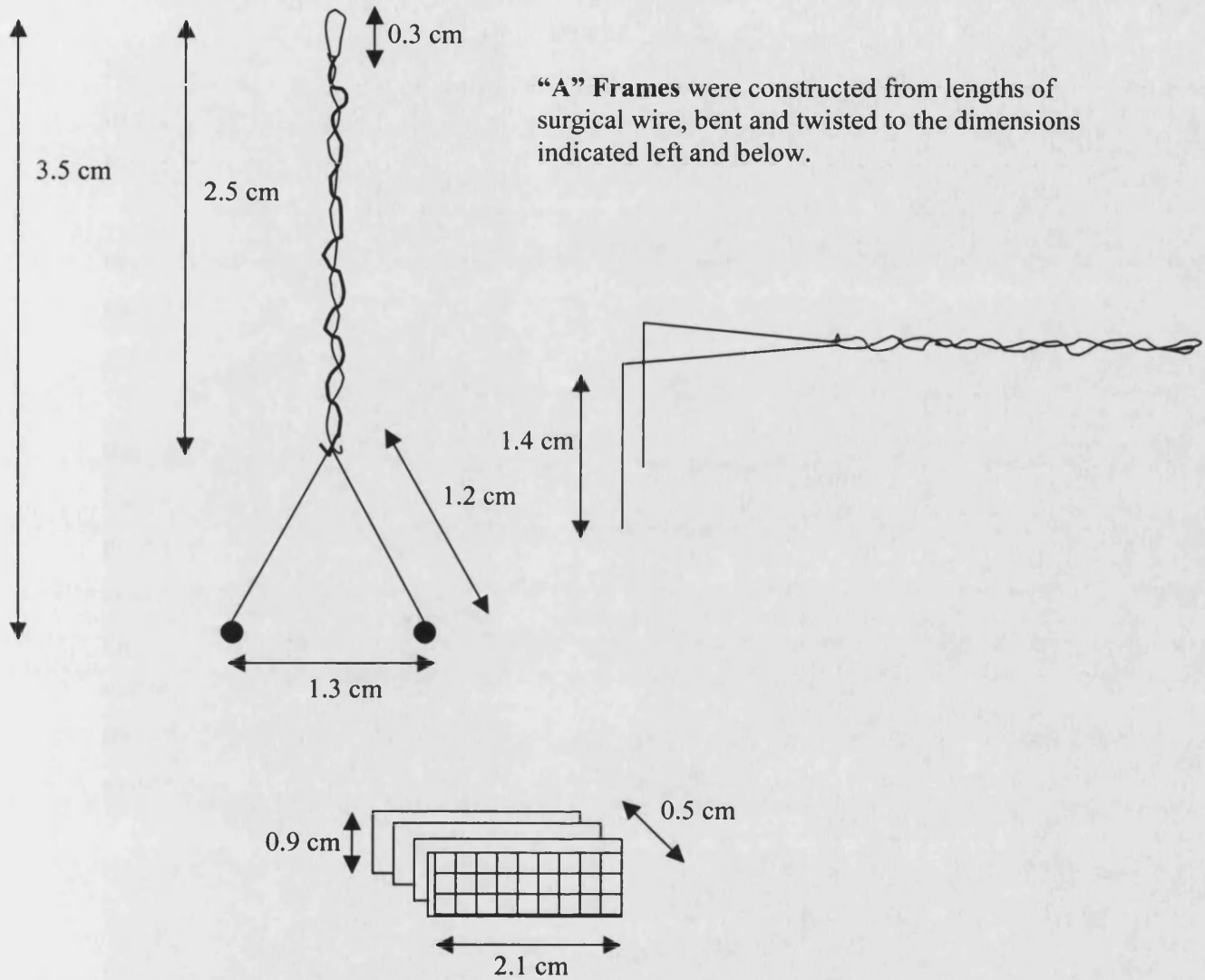
"A" Frames were constructed from lengths of surgical wire, bent and twisted to the dimensions indicated left and below.

1.4 cm

1.2 cm

1.3 cm

0.9 cm

0.5 cm

2.1 cm

Floatation Bars were constructed from No. 10 Clear Mesh (Cat No. 33030-1, John Lewis Department Store, Haberdashery Dept.)
Four 8 x 3 square rectangles are joined together to form the floatation bars using nylon thread.

APPENDIX IV: Calibrating The Culture Force Monitor

In order to ensure the continuing accuracy of the readings obtained on the culture force monitor, the force transducer needs to be calibrated. This is done on a monthly basis to obtain a calibration factor, which is entered into the appropriate box in the LabVIEW VI, Program (National Instruments).

The calibration is carried out using a series of precise weights, which are placed in turn onto the force transducer. This is mounted using its clamp so that the weights will pull the force transducer vertically down in the same direction as a contracting collagen lattice would pull the lever arm if it were orientated horizontally.

Starting with no weight on the force transducer (0) the incubator door is closed and the system allowed to equilibrate for temperature and CO_2 levels. The calibration factor in LabVIEW VI is set to 1 and a one minute recording is made of the force measured. At this point the first in the series of weights is carefully placed onto the force transducer. This causes a deflection and an increase in the force reading. Once again the incubator door is closed and the system allowed to equilibrate, before a second one minute recording is made. This process is repeated for each weight in turn. For each one minute force recording the software will record 60 readings of force and the mean of these 60 readings is calculated to provide a relative mean force transducer reading for each weight.

This data is then tabulated against the weight used and the force in dynes that this weight corresponds to (1 dyne = 10^{-5} newtons). A sample table is shown below and from this a scatter plot of each computer reading and the equivalent standard force applied is generated. A best-fit line is drawn and providing the correlation coefficient (R^2) is good, the slope of the graph corresponds to the calibration factor, which should be entered into the software (ie. the value the actual reading of the force transducer needs to be multiplied by to convert the figure to dynes). A sample graph and the relevant calculations are shown below the table.

Weight Number	Actual Weight (g)	Corresponding Force in Dynes	Mean Force Transducer Reading	Mean Force Transducer Reading – 0 Reading
0		0	-0.06154	0
1	0.03	29.4	15.18333	15.24487
2	0.05	49	27.91803	27.97957
3	0.2	196	108.7419	108.8035
4	0.3	294	162.9885	162.7501
5	0.5	490	270.2121	270.2737

Table showing actual weight used to calibrate the CFM force transducer, the corresponding force in dynes that this relates to and sample readings from a calibration run. The final column of mean force transducer readings for each weight with the zero value subtracted is then used to generate the scatter plot below.

NB. Force = Mass x Acceleration so here

The force (in Newtons) = Weight (kg) x Gravity (9.8)

And Dynes = 10^{-5} Newtons
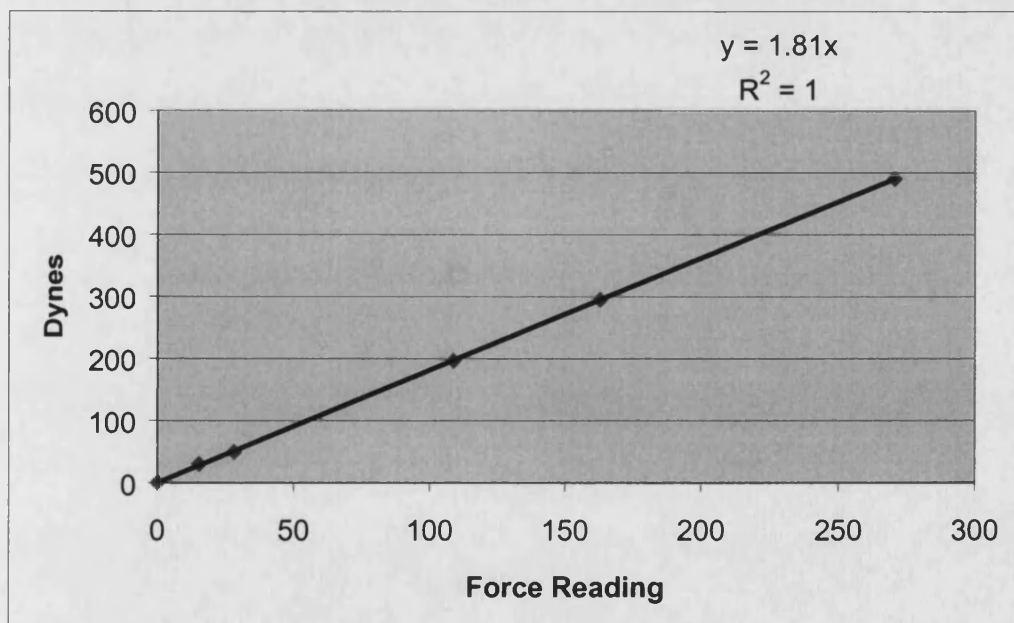
Scatter Plot of Calibrating force in Dynes plotted against the CFM force transducer reading. Here the linear correlation is ideal ($R^2 = 1$) and the slope of this line gives the calibration factor to be used. In this case it is 1.81.

215

Bibliography

Abbott K, Denney J, Burke F, al e. A review of the attitudes to splintage in Dupuytren's contracture. *J Hand Surg [Br]* 1987;**12**:326-8.

Adam RF,.Loynes RD. Prognosis in Dupuytren's disease. *J Hand Surg [Am]* 1992;**17**:312-7.

Alioto RJ, Rosier RN, Burton RI, Puzas JE. Comparative effects of growth factors on fibroblasts of Dupuytren's tissue and normal palmar fascia. *J Hand Surg [Am]* 1994;**19**:442-52.

An HS, Southworth SR, Jackson WT, Russ B. Cigarette smoking and Dupuytren's contracture of the hand. *J Hand Surg [Am]* 1988;**13**:872-4.

Andrew JG,.Kay NR. Segmental aponeurectomy for Dupuytren's disease: a prospective study. *J Hand Surg [Br]* 1991;**16**:255-7.

Arafa M, Noble J, Royle SG, Trail IA, Allen J. Dupuytren's and epilepsy revisited. *J Hand Surg [Br]* 1992;**17**:221-4.

Arafa M, Steingold RF, Noble J. The incidence of Dupuytren's disease in patients with rheumatoid arthritis. *J Hand Surg [Br]* 1984;**9**:165-6.

Ariyan S, Enriquez R, Krizek TJ. Wound contraction and fibrocontractive disorders. *Arch Surg* 1978;**113**:1034-46.

Arkkila PE, Kantola IM, Viikari JS, Ronnemaa T, Vahatalo MA. Dupuytren's disease in type 1 diabetic patients: a five-year prospective study. *Clin Exp Rheumatol* 1996;**14**:59-65.

Arora PD, Bibby KJ, McCulloch CA. Slow ocillations of free intracellular calcium ion concentration in human fibroblasts responding to mechanical stretch. *J Cell Physiol* 1994;**161**:187-200.

Arora PD, Narani N, McCulloch CA. The compliance of collagen gels regulates transforming growth factor- beta induction of alpha-smooth muscle actin in fibroblasts. *Am J Pathol* 1999;**154**:871-82.

Attali P, Ink O, Pelletier G, al e. Dupuytren's contracture, alcohol consumption, and chronic liver disease. *Arch Int Med* 1987;**147**:1065-7.

Badalamente MA,.Hurst LC. Enzyme injection as nonsurgical treatment of Dupuytren's disease. *J Hand Surg [Am]* 2000;**25**:629-36.

Badalamente MA, Hurst LC, Grandia SK, Sampson SP. Platelet-derived growth factor in Dupuytren's disease. *J Hand Surg [Am]* 1992;**17**:317-23.

Badalamente MA, Hurst LC, Sampson SP. Prostaglandins influence myofibroblast contractility in Dupuytren's disease. *J Hand Surg [Am]* 1988;**13**:867-71.

Badalamente MA, Sampson SP, Hurst LC, Dowd A, Miyasaka K. The role of transforming growth factor beta in Dupuytren's disease. *J Hand Surg [Am]* 1996;**21**:210-5.

Badalamente MA, Stern L, Hurst LC. The pathogenesis of Dupuytren's contracture: contractile mechanisms of the myofibroblasts. *J Hand Surg [Am]* 1983;**8**:235-43.

Bailey AJ, Sims TJ, Gabbiani G, Bazin S, LeLous M. Collagen of Dupuytren's disease. *Clin Sci Mol Med* 1977;**53**:499-502.

Bailey AJ, Tarlton JF, Van der Stappen J, Sims TJ, Messina A. The continuous elongation technique for severe Dupuytren's disease. A biochemical mechanism. *J Hand Surg [Br]* 1994;**19**:522-7.

Baird KS, Crossan JF, Ralston SH. Abnormal growth factor and cytokine expression in Dupuytren's contracture. *J Clin Pathol* 1993;**46**:425-8.

Bazin S, Le Lous M, Duance VC, Sims TJ, Bailey AJ, Gabbiani G *et al*. Biochemistry and histology of the connective tissue of Dupuytren's disease lesions. *Eur J Clin Invest* 1980;**10**:9-16.

Bell E, Ivarsson B, Merrill C. Production of a tissue-like structure by contraction of collagen lattices by human fibroblasts of different proliferative potential in vitro. *Proc Natl Acad Sci U S A* 1979;**76**:1274-8.

Bennett NT,.Schultz GS. Growth factors and wound healing: biochemical properties of growth factors and their receptors. *Am J Surg* 1993;**165**:728-37.

Benzonana G, Skalli O, Gabbiani G. Correlation between the distribution of smooth muscle or non muscle myosins and alpha-smooth muscle actin in normal and pathological soft tissues. *Cell Motil Cytoskeleton* 1988;**11**:260-74.

Berndt A, Kosmehl H, Katenkamp D, Tauchmann V. Appearance of the myofibroblastic phenotype in Dupuytren's disease is associated with a fibronectin, laminin, collagen type IV and tenascin extracellular matrix. *Pathobiology* 1994;**62**:55-8.

Berndt A, Kosmehl H, Mandel U, Gabler U, Luo X, Celeda D *et al*. TGF beta and bFGF synthesis and localization in Dupuytren's disease (nodular palmar fibromatosis) relative to cellular activity, myofibroblast phenotype and oncofetal variants of fibronectin. *Histochem J* 1995;**27**:1014-20.

Border WA,.Noble NA. Transforming growth factor beta in tissue fibrosis. *N Engl J Med* 1994;**331**:1286-92.

Brandes G, Messina A, Reale E. The palmar fascia after treatment by the continuous extension technique for Dupuytren's contracture. *J Hand Surg [Br]* 1994;**19**:528-33.

Brickley-Parsons D, Glimcher MJ, Smith RJ, Albin R, Adams JP. Biochemical changes in the collagen of the palmar fascia in patients with Dupuytren's disease. *J Bone Joint Surg [Am]* 1981;**63**:787-97.

Brotherston TM, Balakrishnan C, Milner RH, Brown HG. Long term follow-up of dermofasciectomy for Dupuytren's contracture. *Br J Plast Surg* 1994;47:440-3.

Brown RA, Prajapati R, McGrouther DA, Yannas IV, Eastwood M. Tensional homeostasis in dermal fibroblasts: mechanical responses to mechanical loading in three-dimensional substrates. *J Cell Physiol* 1998;175:323-32.

Brown RA, Sethi KK, Gwanmesia I, Raemdonck D, Eastwood M, Mudera V. Enhanced fibroblast contraction of 3D collagen lattices and integrin expression by TGF-beta1 and -beta3: mechanoregulatory growth factors? *Exp Cell Res* 2002;274:310-22.

Brown RA, Talas G, Porter RA, McGrouther DA, Eastwood M. Balanced mechanical forces and microtubule contribution to fibroblast contraction. *J Cell Physiol* 1996;169:439-47.

Bryan AS,.Ghorbal MS. The long-term results of closed palmar fasciotomy in the management of Dupuytren's contracture. *J Hand Surg [Br]* 1988;13:254-6.

Bulstrode, N. Dupuytren's disease of the hand. Potential for reducing fibrosis using 5 - fluorouracil.   237.   2001.   University   of   London. Ref Type: Thesis/Dissertation

Burge P. Genetics of Dupuytren's disease. *Hand Clin* 1999;15:63-71.

Burge P, Hoy G, Regan P, Milne R. Smoking, alcohol and the risk of Dupuytren's contracture. *J Bone Joint Surg Br* 1997;79:206-10.

Burridge K. Are stress fibres contractile? *Nature* 1981;294:691-2.

Carson J,.Clarke C. Dupuytren's contracture im pensioners at the Royal Hospital Chelsea. *Journal of the Royal College of Physicians of London* 1993;27:25-7.

Caughell KA, McFarlane RM. The development of the palmar fascia. In McFarlane RM, McGrouther DA and Flint MH, eds. *Dupuytren's Disease: Biology and Treatment*, pp 119-26. Edinburgh, London, Melbourne and New York: Churchill Livingstone, 1990.

Chiquet-Ehrismann R, Tannheimer M, Koch M, Brunner A, Spring J, Martin D *et al.* Tenascin-C expression by fibroblasts is elevated in stressed collagen gels. *J Cell Biol* 1994;127:2093-101.

Citron N,.Messina JC. The use of skeletal traction in the treatment of severe primary Dupuytren's disease. *J Bone Joint Surg Br* 1998;80:126-9.

Clarkson P. The aetiology of Dupuytren's disease. *Guy Hosp Rep* 1961;110:52-62.

D'Addario M, Arora PD, Fan J, Ganss B, Ellen RP, McCulloch CA. Cytoprotection against mechanical forces delivered through beta 1 integrins requires induction of filamin A. *J Biol Chem* 2001;276:31969-77.

Darby I, Skalli O, Gabbiani G. Alpha-smooth muscle actin is transiently expressed by myofibroblasts during experimental wound healing. *Lab Invest* 1990;63:21-9.

Delbruck A,.Schroder H. Metabolism and proliferation of cultured fibroblasts from specimens of human palmar fascia and Dupuytren's contracture. The pathobiochemistry of connective tissue proliferation, II. *J Clin Chem Clin Biochem* 1983;**21**:11-7.

Delbruck AF, Gurr E. Proteoglycans and glycosaminoglycans. In McFarlane RM, McGrouther DA and Flint MH, eds. *Dupuytren's Disease: Biology and Treatment*, pp 48-57. Edinburgh, London, Melbourne and New York: Churchill Livingstone, 1990.

Delvoye P, Wiliquet P, Leveque JL, Nusgens BV, Lapiere CM. Measurement of mechanical forces generated by skin fibroblasts embedded in a three-dimensional collagen gel. *J Invest Dermatol* 1991;**97**:898-902.

Desmouliere A,.Gabbiani G. Modulation of fibroblastic cytoskeletal features during pathological situations: the role of extracellular matrix and cytokines. *Cell Motil Cytoskeleton* 1994;**29**:195-203.

Desmouliere A, Geinoz A, Gabbiani F, Gabbiani G. Transforming growth factor-beta 1 induces alpha-smooth muscle actin expression in granulation tissue myofibroblasts and in quiescent and growing cultured fibroblasts. *J Cell Biol* 1993;**122**:103-11.

Dugina V, Fontao L, Chaponnier C, Vasiliev J, Gabbiani G. Focal adhesion features during myofibroblastic differentiation are controlled by intracellular and extracellular factors. *J Cell Sci* 2001;**114**:3285-96.

Early PF. Population studies in Dupuytren's contracture. *J.Bone Joint Surg [Br]* 1962;**44B**:602-13.

Eastwood M, McGrouther DA, Brown RA. A culture force monitor for measurement of contraction forces generated in human dermal fibroblast cultures: evidence for cell-matrix mechanical signalling. *Biochim Biophys Acta* 1994;**1201**:186-92.

Eastwood M, McGrouther DA, Brown RA. Fibroblast responses to mechanical forces. *Proc Inst Mech Eng [H]* 1998;**212**:85-92.

Eastwood M, Mudera VC, McGrouther DA, Brown RA. Effect of precise mechanical loading on fibroblast populated collagen lattices: morphological changes. *Cell Motil Cytoskeleton* 1998;**40**:13-21.

Eastwood M, Porter R, Khan U, McGrouther G, Brown R. Quantitative analysis of collagen gel contractile forces generated by dermal fibroblasts and the relationship to cell morphology. *J Cell Physiol* 1996;**166**:33-42.

Egawa T, Senrui H, Horiki A, Egawa M. Epidemiology of the oriental patient. In McFarlane RM, McGrouther DA and Flint MH, eds. *Dupuytren's Disease: Biology and Treatment*, pp 239-45. Edinburgh, London, Melbourne and New York: Churchill Livingstone, 1990.

Ehrlich HP,.Rajaratnam JB. Cell locomotion forces versus cell contraction forces for collagen lattice contraction: an in vitro model of wound contraction. *Tissue Cell* 1990;**22**:407-17.

Elliot D. The early history of contracture of the palmar fascia. Part 1: The origin of the disease: the curse of the MacCrimmons: the hand of benediction: Cline's contracture. *J Hand Surg [Br]* 1988;13:246-53.

Elliot D. The early history of contracture of the palmar fascia. Part 2: The revolution in Paris: Guillaume Dupuytren: Dupuytren's disease. *J Hand Surg [Br]* 1988;13:371-8.

Elliot D. Pre-1900 literature on Dupuytren's disease. *Hand Clin* 1999;15:175-81.

Elliot D. The early history of Dupuytren's disease. *Hand Clin* 1999;15:1-19.

Elsdale T,.Bard J. Collagen substrata for studies on cell behavior. *J Cell Biol* 1972;54:626-37.

Enzinger FM, Weiss SW. Fibromatoses. In Enzinger FM, Weiss SW, eds. *Soft Tissue Tumours*, p 206. St. Louis, Missouri: Mosby, 1995.

Flint MH. Connective Tissue Biology. In McFarlane RM, McGrouther DA and Flint MH, eds. *Dupuytren's Disease: Biology and Treatment*, pp 13-24. Edinburgh, London, Melbourne and New York: Churchill Livingstone, 1990.

Flint MH, Gillard GC, Reilly HC. The glycosaminoglycans of Dupuytren's disease. *Connect Tissue Res* 1982;9:173-9.

Flint MH, Poole CA. Contraction and contracture. In McFarlane RM, McGrouther DA and Flint MH, eds. *Dupuytren's Disease: Biology and Treatment*, pp 104-16. Edinburgh, London, Melbourne and New York: Churchill Livingstone, 1990.

Fluck J, Querfeld C, Cremer A, Niland S, Krieg T, Sollberg S. Normal human primary fibroblasts undergo apoptosis in three-dimensional contractile collagen gels. *J Invest Dermatol* 1998;110:153-7.

Foo IH, Naylor IL, Timmons MJ, Trejdosiewicz LK. Intracellular actin as a marker for myofibroblasts in vitro. *Laboratory Investigation* 1992;67:727-33.

Fraser-Moodie A. Dupuytren's contracture and cigarette smoking. *Br J Plast Surg* 1976;29:214-5.

Gabbiani G,.Majno G. Dupuytren's contracture: fibroblast contraction? An ultrastructural study. *Am J Pathol* 1972;66:131-46.

Gabbiani G, Ryan GB, Majno G. Presence of modified fibroblasts in granulation tissue and their possible role in wound contraction. *Experientia* 1971;27:549-50.

Gelberman RH, Amiel D, Rudolph RM, Vance RM. Dupuytren's contracture. An electron microscopic, biochemical, and clinical correlative study. *J Bone Joint Surg Am* 1980;62:425-32.

Glimcher MJ, Peabody HM. Collagen. In McFarlane RM, McGrouther DA and Flint MH, eds. *Dupuytren's Disease: Biology and Treatment*, pp 72-85. Edinburgh, London, Melbourne and New York: Churchill Livingstone, 1990.

Gonzalez AM, Buscaglia M, Fox R, Isacchi A, Sarmientos P, Farris J et al. Basic fibroblast growth factor in Dupuytren's contracture. Am J Pathol 1992;141:661-71.

Gonzalez MH, Sobeski J, Grindel S, Chunprapaph B, Weinzweig N. Dupuytren's disease in African-Americans. J Hand Surg [Br] 1998;23:306-7.

Gordon S,.Anderson W. Dupuytren's contracture following injury. Br J Plast Surg 1961;14:129-31.

Greco RM,.Ehrlich HP. Differences in cell division and thymidine incorporation with rat and primate fibroblasts in collagen lattices. Tissue Cell 1992;24:843-51.

Grinnell F. Fibroblasts, myofibroblasts, and wound contraction. J Cell Biol 1994;124:401-4.

Grinnell F. Fibroblast-collagen-matrix contraction: growth-factor signalling and mechanical loading. Trends Cell Biol 2000;10:362-5.

Grinnell F,.Ho CH. Transforming growth factor beta stimulates fibroblast-collagen matrix contraction by different mechanisms in mechanically loaded and unloaded matrices. Exp Cell Res 2002;273:248-55.

Grinnell F, Ho CH, Lin YC, Skuta G. Differences in the regulation of fibroblast contraction of floating versus stressed collagen matrices. J Biol Chem 1999;274:918-23.

Grinnell F, Zhu M, Carlson MA, Abrams JM. Release of mechanical tension triggers apoptosis of human fibroblasts in a model of regressing granulation tissue. Exp Cell Res 1999;248:608-19.

Gudmundsson KG, Arngrimsson R, Sigfusson N, Bjornsson A, Jonsson T. Epidemiology of Dupuytren's disease: clinical, serological, and social assessment. The Reykjavik Study. J Clin Epidemiol 2000;53:291-6.

Guyton AC, Hall JE. Contraction and Excitation of Smooth Muscle. In Guyton AC, Hall JE, eds. Textbook of Medical Physiology, pp 95-103. Philadelphia: W. B. Saunders Co., 1996.

Haeseker B. Dupuytren's disease and the sickle-cell trait in a female black patient. Br J Plast Surg 1981;34:438-40.

Halliday NL, Rayan GM, Zardi L, Tomasek JJ. Distribution of ED-A and ED-B containing fibronectin isoforms in Dupuytren's disease. J Hand Surg [Am] 1994;19:428-34.

Harding SI, Underwood S, Brown RA, Dunnill P. Assessment of cell alignment by fibronectin multi-fibre cables capable of large scale production. Bioprocess Engineering 2000;22:159-64.

Harris AK, Stopak D, Wild P. Fibroblast traction as a mechanism for collagen morphogenesis. Nature 1981;290:249-51.

He Y,.Grinnell F. Stress relaxation of fibroblasts activates a cyclic AMP signaling pathway. *J Cell Biol* 1994; **126**:457-64.

Heathcote JG, Cohen H, Noble J. Dupuytren's disease and diabetes mellitus. *Lancet* 1981;**1**:1420.

Hinz B, Celetta G, Tomasek JJ, Gabbiani G, Chaponnier C. Alpha-smooth muscle actin expression upregulates fibroblast contractile activity. *Mol Biol Cell* 2001;**12**:2730-41.

Hodgkinson PD. The use of skeletal traction to correct the flexed PIP joint in Dupuytren's disease. A pilot study to assess the use of the Pipster. *J Hand Surg [Br]* 1994;**19**:534-7.

Houghton S, Holdstock G, Cockerell R, Wright R. Dupuytren's contracture, chronic liver disease and IgA immune complexes. *Liver* 1983;**3**:220-4.

Hueston J. The role of the skin in Dupuytren's disease. *Ann R Coll Surg Engl* 1985;**67**:372-5.

Hueston JT. Overview of Etiology and Pathology . In Hueston JT, Tubiana R, eds. *Dupuytren's Disease*, Edinburgh: Churchill Livingston, 1985.

Hueston JT. Further studies on the incidence of Dupuytren's contracture. *Med.J.Aust.* 1962;**1**:586-8.

Hueston JT. 'Firebreak' grafts in Dupuytren's contracture. *Aust N Z J Surg* 1984;**54**:277-81.

Hueston JT,.Seyfer AE. Some medicolegal aspects of Dupuytren's contracture. *Hand Clin* 1991;**7**:617-32.

Hueston JT. Dupuytren diathesis. In McFarlane RM, McGrouther DA and Flint MH, eds. *Dupuytren's Disease: Biology and Treatment*, pp 246-52. Edinburgh, London, Melbourne and New York: Churchill Livingstone, 1990.

Hurst LC, Badalamente MA, Makowski J. The pathobiology of Dupuytren's contracture: effects of prostaglandins on myofibroblasts. *J Hand Surg [Am]* 1986;**11**:18-23.

Hynes RO. Integrins: versatility, modulation, and signaling in cell adhesion. *Cell* 1992;**69**:11-25.

Ignotz RA,.Massague J. Transforming growth factor-beta stimulates the expression of fibronectin and collagen and their incorporation into the extracellular matrix. *J Biol Chem* 1986;**261**:4337-45.

Jabaley ME. Surgical treatment of Dupuytren's disease. *Hand Clin* 1999;**15**:109-26.

Jemec, B. Proliferation and the action of an anti-proliferative agent in Dupuytren's fibroblast cultures. 190. 1999. University of London. Ref Type: Thesis/Dissertation

Jemec B, Linge C, Grobbelaar AO, Smith PJ, Sanders R, McGrouther DA. The effect of 5-fluorouracil on Dupuytren fibroblast proliferation and differentiation. *Chir Main* 2000;**19**:15-22.

Kasugai S, Suzuki S, Shibata S, Yasui S, Amano H, Ogura H. Measurements of the isometric contractile forces generated by dog periodontal ligament fibroblasts in vitro. *Arch Oral Biol* 1990;**35**:597-601.

Keilholz L, Seegenschmiedt MH, Sauer R. Radiotherapy for prevention of disease progression in early-stage Dupuytren's contracture: initial and long-term results. *Int J Radiat Oncol Biol Phys* 1996;**36**:891-7.

Kelly C,.Varian J. Dermofasciectomy: a long term review. *Ann Chir Main Memb Super* 1992;**11**:381-2.

Kelly SA, Burke FD, Elliot D. Injury to the distal radius as a trigger to the onset of Dupuytren's disease. *J Hand Surg [Br]* 1992;**17**:225-9.

Ketchum LD. Dupuytren's contracture - triamcinolone injection. *American Soc Surg Hand Newsletter* 1983;**2**.

Khan U, Occleston NL, Khaw PT, McGrouther DA. Differences in proliferative rate and collagen lattice contraction between endotenon and synovial fibroblasts. *J Hand Surg [Am]* 1998;**23**:266-73.

Kivirikko KI. Collagens and their abnormalities in a wide spectrum of diseases. *Ann Med* 1993;**25**:113-26.

Kloen P. New insights in the development of Dupuytren's contracture: a review. *Br J Plast Surg* 1999;**52**:629-35.

Kloen P, Jennings CL, Gebhardt MC, Springfield DS, Mankin HJ. Transforming growth factor-beta: possible roles in Dupuytren's contracture. *J Hand Surg [Am]* 1995;**20**:101-8.

Kolodney MS,.Wysolmerski RB. Isometric contraction by fibroblasts and endothelial cells in tissue culture: a quantitative study. *J Cell Biol* 1992;**117**:73-82.

Lappi DA, Martineau D, Maher PA, Florkiewicz RZ, Buscaglia M, Gonzalez AM *et al.* Basic fibroblast growth factor in cells derived from Dupuytren's contracture: synthesis, presence, and implications for treatment of the disease. *J Hand Surg [Am]* 1992;**17**:324-32.

Larkin JG,.Frier BM. Limited joint mobility and Dupuytren's contracture in diabetic, hypertensive, and normal populations. *Br Med J (Clin Res Ed)* 1986;**292**:1494.

Larson RD, Takagishi N, Posch JL. The Pathogenesis of Duypuytren's Contracture: Experimental and further clinical observations. *Journal of Bone and Joint Surgery* 1960;**42 (A)**:993-1007.

Leclercq C. Associated Conditions. In Tubiana R, Leclercq C, Hurst LC, Badalamente MA, Mackin EJ, eds. *Dupuytren's Disease*, pp 108-16. London: Martin Dunitz, 2000.

Leclercq C. Clinical Presentation. In Tubiana R, Leclercq C, Hurst LC, Badalamente MA, Mackin EJ, eds. *Dupuytren's Disease*, pp 79-96. London: Martin Dunitz, 2000.

Leclercq C. Results of Surgical Treatment. In Tubiana R, Leclercq C, Hurst LC, Badalamente MA, Mackin EJ, eds. *Dupuytren's Disease*, pp 239-50. London: Martin Dunitz, 2000.

Leclercq C, Hurst LC, Badalamente MA. Non-Surgical Treatment. In Tubiana R, Leclercq C, Hurst LC, Badalamente MA, Mackin EJ, eds. *Dupuytren's Disease*, pp 121-31. London: Martin Dunitz, 2000.

Lennox IA, Murali SR, Porter R. A study of the repeatability of the diagnosis of Dupuytren's contracture and its prevalence in the grampian region. *J Hand Surg [Br]* 1993;18:258-61.

Levinson H, Peled Z, Liu W, Longaker MT, Allison GM, Ehrlich HP. Fetal rat amniotic fluid: transforming growth factor beta and fibroblast collagen lattice contraction. *J Surg Res* 2001;100:205-10.

Ling RSM. The genetic factors in Dupuytren's disease. *J.Bone and Joint Surg.* 1963;45(B):709-18.

Liu XD, Umino T, Ertl R, Veys T, Skold CM, Takigawa K *et al*. Persistence of TGF-beta1 induction of increased fibroblast contractility. *In Vitro Cell Dev Biol Anim* 2001;37:193-201.

Luck JV. Dupuytren's Contracture - A New Concept of the Pathogenesis Correlated with the Surgical Management. *J.Bone and Joint Surgery{Am}* 1959;41:635-64.

Lund M. Dupuytren's contracture and epilepsy. *Acta Psych Neurol Scand* 1941;16:465-8.

MacCallum P,.Hueston JT. The pathology of Dupuytren's contracture. *Aust N Z J Surg* 1962;31:241-53.

Machtey I. Dupuytren's disease and diabetes mellitus. *J Rheumatol* 1997;24:2489-90.

Magro G, Lanzafame S, Micali G. Co-ordinate expression of alpha 5 beta 1 integrin and fibronectin in Dupuytren's disease. *Acta Histochem* 1995;97:229-33.

McCann BG, Logan A, Belcher H, Warn A, Warn RM. The presence of myofibroblasts in the dermis of patients with Dupuytren's contracture. A possible source for recurrence. *J Hand Surg [Br]* 1993;18:656-61.

McCash CR. The open palm technique in Dupuytren's contracture. *Br J Plast Surg* 1964;17:271-80.

McFarlane RM. Patterns of the diseased fascia in the fingers in Dupuytren's contracture. Displacement of the neurovascular bundle. *Plast Reconstr Surg* 1974;54:31-44.

McFarlane RM. Progress in Dupuytren's disease. *J Hand Surg [Br]* 1991;16:237-9.

McFarlane RM, Shum DT. A single injury to the hand. In McFarlane RM, McGrouther DA and Flint MH, eds. *Dupuytren's Disease: Biology and Treatment*, pp 265-73. Edinburgh, London, Melbourne and New York: Churchill Livingstone, 1990.

McGrouther DA. The microanatomy of Dupuytren's contracture. *Hand* 1982;14:215-36.

McGrouther DA. Dupuytren's Disease. In Watson N, Smith RJ, eds. *Methods and Concepts in Hand Surgery*, pp 75-96. Butterworths, 1986.

Meek RM, McLellan S, Crossan JF. Dupuytren's disease. A model for the mechanism of fibrosis and its modulation by steroids [published erratum appears in J Bone Joint Surg Br 1999 Sep;81(5):938]. *J Bone Joint Surg Br* 1999;81:732-8.

Menzel EJ, Piza H, Zielinski C, Endler AT, Steffen C, Millesi H. Collagen types and anticollagen-antibodies in Dupuytren's disease. *Hand* 1979;11:243-8.

Messina A,.Messina J. The continuous elongation treatment by the TEC device for severe Dupuytren's contracture of the fingers. *Plast Reconstr Surg* 1993;92:84-90.

Meyerding HW, Black JR, Broders AC. The etiology and pathology of Dupuytren's contracture. *Surg Gynecol Obstet* 1941;72:582-90.

Mikkelsen OA. The prevalence of Dupuytren's disease in Norway. A study in a representative population sample of the municipality of Haugesund. *Acta Chir Scand* 1972;138:695-700.

Mikkelsen OA. Epidemiology of a Norwegian population. In McFarlane RM, McGrouther DA and Flint MH, eds. *Dupuytren's Disease: Biology and Treatment*, pp 191-200. Edinburgh, London, Melbourne and New York: Churchill Livingstone, 1990.

Mio T, Adachi Y, Romberger DJ, Ertl RF, Rennard SI. Regulation of fibroblast proliferation in three-dimensional collagen gel matrix. *In Vitro Cell Dev Biol Anim* 1996;32:427-33.

Mitra A,.Goldstein RY. Dupuytren's contracture in the black population: a review. *Ann Plast Surg* 1994;32:619-22.

Moermans JP. Segmental aponeurectomy in Dupuytren's disease. *J Hand Surg [Br]* 1991;16:243-54.

Montesano R,.Orci L. Transforming growth factor beta stimulates collagen-matrix contraction by fibroblasts: implications for wound healing. *Proc Natl Acad Sci U S A* 1988;85:4894-7.

Moyer KE, Banducci DR, Graham WP, Ehrlich HP. Dupuytren's Disease: Physiologic Changes in Nodule and Cord Fibroblasts through Aging in Vitro. *Plast Reconstr Surg* 2002;110:187-93.

Murrell GA. An insight into Dupuytren's contracture. *Ann R Coll Surg Engl* 1992;74:156-60.

Murrell GA, Francis MJ, Bromley L. The collagen changes of Dupuytren's contracture. *J Hand Surg [Br]* 1991;**16**:263-6.

Murrell GA, Francis MJ, Howlett CR. Dupuytren's contracture. Fine structure in relation to aetiology. *J Bone Joint Surg Br* 1989;**71**:367-73.

Noble J, Heathcote JG, Cohen H. Diabetes mellitus in the aetiology of Dupuytren's disease. *J Bone Joint Surg Br* 1984;**66**:322-5.

Norotte G, Apoil A, Travers V. A ten years follow-up of the results of surgery for Dupuytren's disease. A study of fifty-eight cases. *Ann Chir Main* 1988;**7**:277-81.

Pal B, Griffiths ID, Anderson J, Dick WC. Association of limited joint mobility with Dupuytren's contracture in diabetes mellitus. *J Rheumatol* 1987;**14**:582-5.

Pasquali-Ronchetti I, Guerra D, Baccarani-Contri M, Fornieri C, Mori G, Marcuzzi A *et al*. A clinical, ultrastructural and immunochemical study of Dupuytren's disease. *J Hand Surg [Br]* 1993;**18**:262-9.

Petrov VV, Fagard RH, Lijnen PJ. Stimulation of collagen production by transforming growth factor-beta1 during differentiation of cardiac fibroblasts to myofibroblasts. *Hypertension* 2002;**39**:258-63.

Prajapati RT, Chavally-Mis B, Herbage D, Eastwood M, Brown RA. Mechanical loading regulates protease production by fibroblasts in three-dimensional collagen substrates. *Wound Repair Regen* 2000;**8**:226-37.

Prockop DJ,.Kivirikko KI. Collagens: molecular biology, diseases, and potentials for therapy. *Annu Rev Biochem* 1995;**64**:403-34.

Rafter D, Kenny R, Gilmore M, Walsh CH. Dupuytren's contracture--a survey of a hospital population. *Ir Med J* 1980;**73**:227-8.

Ragoowansi RH,.Britto JA. Genetic and epigenetic influences on the pathogenesis of Dupuytren's disease. *J Hand Surg [Am]* 2001;**26**:1157-8.

Rayan GM. Clinical presentation and types of Dupuytren's disease. *Hand Clin* 1999;**15**:87-96.

Rayan GM. Palmar fascial complex anatomy and pathology in Dupuytren's disease. *Hand Clin* 1999;**15**:73-86.

Rayan GM, Parizi M, Tomasek JJ. Pharmacologic regulation of Dupuytren's fibroblast contraction in vitro. *J Hand Surg [Am]* 1996;**21**:1065-70.

Rayan GM,.Tomasek JJ. Generation of contractile force by cultured Dupuytren's disease and normal palmar fibroblasts. *Tissue Cell* 1994;**26**:747-56.

Reed MJ, Vernon RB, Abrass IB, Sage EH. TGF-beta 1 induces the expression of type I collagen and SPARC, and enhances contraction of collagen gels, by fibroblasts from young and aged donors. *J Cell Physiol* 1994;**158**:169-79.

Richard H. Dupuytren's contracture treated with vitamin E. *BMJ* 1952;376-83.

Riikonen T, Koivisto L, Vihinen P, Heino J. Transforming growth factor-beta regulates collagen gel contraction by increasing alpha 2 beta 1 integrin expression in osteogenic cells. *J Biol Chem* 1995;**270**:376-82.

Roberts AB, Sporn MB, Assoian RK, Smith JM, Roche NS, Wakefield LM et al. Transforming growth factor type beta: rapid induction of fibrosis and angiogenesis in vivo and stimulation of collagen formation in vitro. *Proc Natl Acad Sci U S A* 1986; **83**:4167-71.

Sanders JL, Dodd C, Ghahary A, Scott PG, Tredget EE. The effect of interferon-alpha2b on an in vitro model Dupuytren's contracture. *J Hand Surg [Am]* 1999;**24**:578-85.

Schneider LH, Hankin FM, Eisenberg T. Surgery of Dupuytren's disease: a review of the open palm method. *J Hand Surg [Am]* 1986;**11**:23-7.

Schultz RJ, Tomasek JJ. Dupuytren diathesis. In McFarlane RM, McGrouther DA and Flint MH, eds. *Dupuytren's Disease: Biology and Treatment*, pp 86-98. Edinburgh, London, Melbourne and New York: Churchill Livingstone, 1990.

Schurch W, Seemayer TA, Lagace R, Gabbiani G. The intermediate filament cytoskeleton of myofibroblasts: an immunofluorescence and ultrastructural study. *Virchows Arch A Pathol Anat Histopathol* 1984;**403**:323-36.

Schurch W, Skalli O, Lagace R, Seemayer TA, Gabbiani G. Intermediate filament proteins and actin isoforms as markers for soft- tissue tumor differentiation and origin. III. Hemangiopericytomas and glomus tumors. *Am J Pathol* 1990;**136**:771-86.

Serini G,.Gabbiani G. Mechanisms of myofibroblast activity and phenotypic modulation. *Exp Cell Res* 1999;**250**:273-83.

Shreiber DI, Enever PA, Tranquillo RT. Effects of pdgf-bb on rat dermal fibroblast behavior in mechanically stressed and unstressed collagen and fibrin gels. *Exp Cell Res* 2001;**266**:155-66.

Shum DT. Histopathology. In McFarlane RMDFMH, ed. *Dupuytren's Disease: Biology and Treatment*, pp 25-30. Edinburgh, London, Melbourne and New York: Churchill Livingstone, 1990.

Skalli O, Ropraz P, Trzeciak A, Benzonana G, Gillessen D, Gabbiani G. A monoclonal antibody against alpha-smooth muscle actin: a new probe for smooth muscle differentiation. *J Cell Biol* 1986;**103**:2787-96.

Skoog T. Dupuytren's contracture with special reference to aetiology and improved surgical treatment. Its occurence in epileptics - Note on knuckle pads. *Acta Chir Scand* 1948;**96 (suppl 139)**:109-34.

Skoog T. The pathogenesis and etiology of Dupuytren's contracture. *PRS* 1963;**31**:258-67.

Srivastava S, Nancarrow JD, Cort DF. Dupuytren's disease in patients from the Indian sub-continent: Report of 10 cases. *J Hand Surg [Br]* 1989;**14**:32-4.

Stewart HD, Innes AR, Burke FD. The hand complications of Colles' fractures. *J Hand Surg [Br]* 1985;**10**:103-6.

Stopak D,.Harris AK. Connective tissue morphogenesis by fibroblast traction. I. Tissue culture observations. *Dev Biol* 1982;**90**:383-98.

Su CK,.Patek AJ, Jr. Dupuytren's contracture. Its association with alcoholism and cirrhosis. *Arch Intern Med* 1970;**126**:278-81.

Tarlton JF, Meagher P, Brown RA, McGrouther DA, Bailey AJ, Afoke A. Mechanical stress in vitro induces increased expression of MMPs 2 and 9 in excised Dupuytren's disease tissue [comment]. *J Hand Surg [Br]* 1998;**23**:297-302.

Tarpila E, Ghassemifar MR, Wingren S, Agren M, Franzen L. Contraction of collagen lattices by cells from Dupuytren's nodules. *J Hand Surg [Br]* 1996;**21**:801-5.

Tingstrom A, Heldin CH, Rubin K. Regulation of fibroblast-mediated collagen gel contraction by platelet- derived growth factor, interleukin-1 alpha and transforming growth factor-beta 1. *J Cell Sci* 1992;**102**:315-22.

Tomasek J,.Rayan GM. Correlation of alpha-smooth muscle actin expression and contraction in Dupuytren's disease fibroblasts. *J Hand Surg [Am]* 1995;**20**:450-5.

Tomasek JJ, Gabbiani G, Hinz B, Chaponnier C, Brown RA. Myofibroblasts and mechano-regulation of connective tissue remodelling. *Nat Rev Mol Cell Biol* 2002;**3**:349-63.

Tomasek JJ,.Haaksma CJ. Fibronectin filaments and actin microfilaments are organized into a fibronexus in Dupuytren's diseased tissue. *Anat Rec* 1991;**230**:175-82.

Tomasek JJ, Haaksma CJ, Eddy RJ, Vaughan MB. Fibroblast contraction occurs on release of tension in attached collagen lattices: dependency on an organized actin cytoskeleton and serum. *Anat Rec* 1992;**232**:359-68.

Tomasek JJ,.Hay ED. Analysis of the role of microfilaments and microtubules in acquisition of bipolarity and elongation of fibroblasts in hydrated collagen gels. *J Cell Biol* 1984;**99**:536-49.

Tomasek JJ, Vaughan MB, Haaksma CJ. Cellular structure and biology of Dupuytren's disease. *Hand Clin* 1999;**15**:21-34.

Tubiana R. Anatomy. In Tubiana R, Leclercq C, Hurst LC, Badalamente MA, Mackin EJ, eds. *Dupuytren's Disease*, pp 13-51. London: Martin Dunitz, 2000.

Umeno A,.Ueno S. Quantitative analysis of adherent cell orientation influenced by strong magnetic fields. *IEEE Trans Magn* 2002;**38**:67-8.

Van O, Schilling E, Roche NS, Flanders KC, Sporn MB, Roberts AB. *J.Biol.Chem.* 1988;**263**:7741-6.

Vande Berg JS, Gelberman RH, Rudolph R, Johnson D, Sicurello P. Dupuytren's disease: comparative growth dynamics and morphology between cultured myofibroblasts (nodule) and fibroblasts (cord). *J Orthop Res* 1984;**2**:247-56.

VandeBerg JS, Rudolph R, Gelberman R, Woodward MR. Ultrastructural relationship of skin to nodule and cord in Dupuytren's contracture. *Plast Reconstr Surg* 1982;**69**:835-44.

Vaughan MB, Howard EW, Tomasek JJ. Transforming growth factor-beta1 promotes the morphological and functional differentiation of the myofibroblast. *Exp Cell Res* 2000;**257**:180-9.

Walker GA, Guerrero IA, Leinwand LA. Myofibroblasts: molecular crossdressers. *Curr Top Dev Biol* 2001;**51**:91-107.

Weinzierl G, Flugel M, Geldmacher J. [Lack of effectiveness of alternative non-surgical treatment procedures of Dupuytren contracture]. *Chirurg* 1993;**64**:492-4.

Wen FQ, Skold CM, Liu XD, Ertl RF, Zhu YK, Kohyama T *et al.* Glucocorticoids and TGF-beta1 synergize in augmenting fibroblast mediated contraction of collagen gels. *Inflammation* 2001;**25**:109-17.

Wolfe SJ, Summerskill WJM, Davidson CS. Thickening and contraction of the palmar fascia (Dupuytren's contracture) associated with alcoholism and hepatic cirrhosis. *New England Journal of Medicine* 1956;**235**:559-63.

Wrobel LK, Fray TR, Molloy JE, Adams JJ, Armitage MP, Sparrow JC. Contractility of single human dermal myofibroblasts and fibroblasts. *Cell Motil Cytoskeleton* 2002;**52**:82-90.

Yokozeki M, Moriyama K, Shimokawa H, Kuroda T. Transforming growth factor-beta 1 modulates myofibroblastic phenotype of rat palatal fibroblasts in vitro. *Exp Cell Res* 1997;**231**:328-36.

Yost J, Winters T, Fett HC. Dupuytren's contracture: A statistical study. *Am.J.Surgery* 1955;**90**:568-72.

Zamora RL, Heights R, Kraemer BA, Erlich HP, Groner JP. Presence of growth factors in palmar and plantar fibromatoses. *J Hand Surg [Am]* 1994;**19**:435-41.

Zaworski RE,.Mann RJ. Dupuytren's contractures in a black patient. *Plast Reconstr Surg* 1979;**63**:122-4.

Zhu YK, Umino T, Liu XD, Wang HJ, Romberger DJ, Spurzem JR *et al.* Contraction of fibroblast-containing collagen gels: initial collagen concentration regulates the degree of contraction and cell survival. *In Vitro Cell Dev Biol Anim* 2001;**37**:10-6.